Synthesis of monomers for the biochemical investigation of plant polyesters

Martinez San Segundo, Ignacio

Publication date:
2018

Document Version
Publisher's PDF, also known as Version of record

Synthesis of monomers for the biochemical investigation of plant polyesters

Ignacio Martínez San Segundo

February 2018

“Experience is the teacher of all things”

– Julius Caesar, *Commentarii de Bello Civili*.

Preface

The present thesis condenses the research carried at the Technical University of Denmark (DTU) from December 2014 to January 2018 as part of the Danish program to obtain a PhD degree under the supervision of Professor Mads H. Clausen. As part of the program, a four months external stay was performed at the Rensselaer Polytechnic Institute (RPI), in Troy, NY, USA, under the supervision of Professor Richard Gross.

Chapter one provides a brief introduction to cutin and suberin, including their respective location, physiological role, composition and biosynthesis. Chapter two describes the synthesis of isotopically labelled 2-MHG and its use in enzymatic assays with. Chapter three summarizes the synthesis of three suberin monomers and their respective enzymatic assays with CUS1. Chapter four describes the synthesis and enzymatic assays of four 2-MHG derivatives, which was conducted by the master student Sara Britta Pedersen. Chapter five provides a summary of the two projects carried during the stay at RPI, regarding enzymatic polymerizations. Chapter six contains the experimental protocols and compound characterisation. Chapter seven shows the list of references consulted during the creation of the thesis.

A manuscript describing one of the projects performed at RPI has been submitted and is pendant of approval. Manuscripts describing the work presented in chapters 2–4 will be written and submitted.

Acknowledgements

"No man is an island entire of itself; every man is a piece of the continent, a part of the main" (John Donne, 1624). The truth contained within that sentence becomes very clear by looking back and reflecting on my time as a PhD student. The present work would have been impossible without the contribution of many people.

First and foremost, I would like to sincerely express my gratitude to Prof. Mads Clausen for accepting me in his group as a PhD student. Despite my lack of experience in organic synthesis, he believed that I could do it, and showed invaluable support and guidance during the whole PhD. He is a wonderful mentor who cares for his students and shows that chemistry is compatible with good humour and fun. It has been an honour to form part of his group for the last three years.

I would also like to thank all the present and former members of the Clausen´s group for creating such a fantastic work environment, in which inspiring chemistry discussions are intertwined with friendly conversations about the most various topics and unforgettable funny moments. I would like to thank specially Geana Min and Carlos Azevedo, for making the laboratory and the office a much better place to spend time in, and Jorge Peiró for being such a friendly person and talented chemist, always willing to help and provide interesting ideas. I would also thank Christine Kinnaert, Kim T. Mortensen, Viola Previtali, Cecilia Romanó and Faranak Nami for helping me correcting the thesis.

Of course, I could not forget mentioning Gauthier M. Scavée. Very rarely one encounters someone so willing to help regardless of the circumstances, so friendly, funny, and why not saying it, geeky. The majority of the best moments of the PhD, either in Denmark, the USA or Hungary, have been thanks to him. The PhD has been a perilous journey for the both of us, but I could not have wished to have a better partner during these years.

The whole technical staff of the chemistry department cannot be appreciated enough. I would like to thank specially Brian Brylle Dideriksen, Phillip Charlie Johansen, Anne Hector, Tina Gustafsson, Ea Judith Larsen and Lars Egede Bruhn. Without their superb work, the day-to-day work would inevitably sink into chaos.

I would also like to thank Prof. Richard Gross for welcoming me in his group at RPI. The time spent there was very interesting and fruitful. I would like to thank the members of his group for creating a welcoming environment, and specially Hubert Casajus for the countless hours we spent in the lab talking about the most diverse topics while cleaning the inside of an extruder of sticky polymeric materials.

I have been immensely fortunate for counting with the best family and friends anyone could hope for. I would like to thank specially Albert Fernández de la Peña and Douglas Milne, with whom I shared the experience of moving to Denmark, and whose friendship will accompany me for the rest of my life. I am extremely grateful to my parents, Inmaculada and Francisco, and to my sister, Laura, for their constant support and love during these years. None of my accomplishments would have been possible without their care, love and the excellent education they provided.

And thank you too, Paula, my love. Thank you for your patience, for your care and your love. I cannot express how much your support has meant for me. I will never be able to repay everything you have done during these years. If I am being able to finish this PhD is greatly thanks to you.

Abstract

Cutin and suberin are some of the most abundant polyesters on Earth, as they are found in all land plants. Both polymers form barriers that protect plants from desiccation and other environmental stresses and present a similar aliphatic composition, in which hydroxy fatty acids, α,ω-dicarboxylic fatty acids and glycerol are the main components. The mechanism of the biosynthesis of cutin and suberin has remained elusive for decades. However, a shred of light was recently cast upon the subject when the CUS family of enzymes was discovered. The essential role of glycerol-3-phosphate acyltransferases (GPAT) in cutin and suberin biosynthesis had previously been established. GPATs which selectively produce 2-monoacylglyceryl esters (2-MAGs) of fatty acid monomers. The most abundant monomer in tomato fruit (*Solanum lycopersicum*) cutin is 10,16-dihydroxyhexadecanoic acid. Its correspondent 2-MAG, 2-mono(10,16-dihydroxyhexadecanoyl)glycerol (2-MHG) was found in the soluble surface lipids of fruits carrying the *cutin deficient 1* (*cd1*) mutation, which reduces (>95%) the amount of polymerized cutin severely. The *cd1* mutation suppresses the formation of the extracellular CUS1. Furthermore, CUS1 have shown *in vitro* activity towards the polymerization of 2-MHG, further strengthening the hypothesis that cutin biosynthesis is extracellular and occurs through a series of transesterification reactions releasing glycerol. However, some questions remain unanswered, such as the selectivity of CUS1 towards the 2-MAGs of other common cutin or suberin monomers, and whether CUS1 is capable of accepting fatty acid esters other than 2-MAGs as substrates.

In the present work, three projects involving the synthesis of cutin and suberin monomer derivatives and their subsequent *in vitro* oligomerization catalyzed by CUS1 are presented. In the first project, both deuterium and tritium-labelled 2-MHG were successfully synthesized. The deuterium-labelled molecule was used in oligomerization assays together with 9-hydroxy 2-MHG to study the specificity of CUS1 towards the position of the mid-chain hydroxy group. CUS1 showed equal activity towards both monomers, suggesting that CUS1 is likely to participate in the incorporation of both monomers in cutin. Tritium-labelled 2-MHG could potentially be used to monitor transport and location of the monomer *in planta*. The second project consisted on the synthesis and enzymatic oligomerization of 2-MAG derivatives of three fatty acids commonly found in suberin: behenic acid, ω-hydroxy oleic acid and octadecanedioic acid. The three compounds were successfully synthesized and used as CUS1 substrates in enzymatic assays. CUS1 showed a very limited activity towards the octadecanedioic and ω-hydroxy oleic acid derivatives, and no activity towards the behenic acid 2-MAG. These results suggest that enzymes from the CUS or another similar family could be involved in the biosynthesis of suberin. The third project involved the synthesis of four 2-MHG derivatives, in which the *sn*-2 glyceryl moiety was substituted by other small alcohols. The subsequent enzymatic assays showed that CUS1 present activity towards fatty acid esters different than 2-MAGs including the product of the migration of the glyceryl moiety to one of the primary hydroxyls, 1-MHG.

Additionally, work conducted during my external stay at Rensselar Polytechnic Institute (RPI), USA, is presented. Two different projects, involving the synthesis of polyesters with the enzyme *Candida Antarctica* Lipase B (CALB) were conducted during that time. The first one consisted on the synthesis of polypentadecalactone (PPDL) by enzymatic reactive extrusion (eREX) for its use as scaffold to direct axonal extension in spinal cord injury models, whereas the second one consisted in the synthesis of branched polyol polyesters with pendant alkyne groups, which allow further modifications by copper-catalysed azide-alkyne cycloadditions ("click" chemistry).

Resumé

Kutin og suberin er nogle af de mest alment forekommende polyestere på jorden, da de findes i alle landplanter. Begge polymerer danner barrierer der beskytter planter fra udtørring og andre miljømæssigt stress, og udgør en lignende alifatisk sammensætning, hvor hydroxyfedtsyrer, α,ω-dicarboxylfedtsyrer og glycerol er hovedkomponenter. Mekanismen for biosyntesen af kutin og suberin er har været ukendt i årtier. Dog blev der kastet en smule lys over emnet da enzymerne fra CUS familien blev opdaget. Glycerol-3-phosphat acyltransferasers (GPAT) essentielle rolle i biosyntesen af kutin og suberin er tidligere blevet fastslået, der selektivt danner 2-monoacylglyceryl estere (2-MAGs) af fedtsyre monomerer. Den mest alment forekommende monomer i tomaten (*Solanum lycopersicum*) kutin er 10,16-dihydroxyhexadecan syre. Dens korresponderende 2-MAG, 2-mono(10,16-dihydroxyhexadecanoyl)glycerol (2-MHG), blev fundet i de opløselige overfladelipider af tomaten i *cutin deficient 1 (cd1)* mutationen, hvilket markant reducerede (>95%) mængden af polymeriseret kutin. Mutationen i *cd1* undertrykker dannelsen af ekstracellulært CUS1. Endvidere har CUS1 vist *in vitro* aktivitet mod polymerisering af 2-MHG, hvilket yderligere forstærker hypotesen om at biosyntesen af kutin er ekstracellulært og sker gennem en serie af transesterificerings reaktioner med udskillelse af glycerol katalyseret af CUS enzymer. Dog er der stadig ubesvarede spørgsmål angående selektivitet af CUS1 overfor 2-MAGs af andre kutin og suberin monomerer og om CUS1 er i stand til at acceptere andre fedtsyre-estere end 2-MAGs som substrater.

I denne afhandling præsenteres syntesen af forskellige 2-MAG fedtsyre monomerer fundet i kutin og suberin såvel som syntesen af isotopmærket 2-MHG og deres efterfølgende *in vitro* polymeriseringsstudier med CUS1 som katalysator. Desuden er fire estere af 10,16-dihydroxypalmitinsyre med forskellige alkoholer syntetiseret og brugt som substrater i polymeriseringsstudier med CUS1.

Yderligere, er arbejdet udført på mit eksternt ophold på Rensselaer Polytechnic Institute (RPI), USA, præsenteret. To forskellige projekter der involverer syntesen af polyestere med enzymet *Candida Antarctica* Lipase B (CALB) blev udført under opholdet. Det første bestod i syntesen af polypentadecalacton (PPDL) ved enzymatisk reaktiv ekstrudering (eREX) som scaffold til direkte axonal extension i modeller for rygmarvsskader. Det andet bestod i syntesen af forgrenede polyol polyestere med alkyn grupper, hvilket tillader yderligere modifikationer ved kobberkatalyseret azid-alkyn cykloaddition (”click” kemi).

List of abbreviations

1-MHG	1-Mono-(10,16-dihydroxyhexadecanoyl)glycerol
2-MAG	2-Mono-acylglyceryl ester
2-MHG	2-Mono-(10,16-dihydroxyhexadecanoyl)glycerol
ABC	ATP binding cassette
Ac	Acetyl
AIBN	2,2'-Azobis(2-methylpropionitrile)
ATP	Adenosine triphosphate
BAHD	*B*EAT, *A*HCT, *H*CBT1, *D*AT (BAHD)
BDG	BODYGUARD
Bn	Benzyl
br.	Broad
CALB	*Candida antarctica* Lipase B
CD	Cutin deficient
CoA	Coenzyme A
CSA	Camphorsulfonic acid
CUS	Cutin synthase-like
D	Doublet
d	Deuterated
Đ	Polydispersity index
DAISY	Docosanoic acid synthase
DCF	DEFICIENT IN CUTIN FERULATE
DCR	DEFECTIVE IN CUTICULAR RIDGES
dd	Doublet of doublets
DDDA	Dodecanedioic acid
DDQ	2,3-Dichloro-5,6-dicyano-*p*-benzoquinone
DHB	2,5-dihydroxy benzoic acid
DMAP	4-(Dimethylamino)pyridine

DMF	*N*,*N*'-Dimethylformamide
DMP	Dess-Martin periodinane
DMSO	Dimethyl sulfoxide
DSC	Differential scanning calorimetry
dt	Doublet of triplets
DTU	Technical University of Denmark
EDCl	*N*-(3-Dimethylaminopropyl)-*N*'-ethylcarbodiimide hydrochloride
ELS	Evaporative light scattering
EM	Enzyme-activated monomer
ER	Endoplasmic reticulum
eREX	Enzymatic reactive extrusion
ESI	Electrospray ionization
Et	Ethyl
FAE	Fatty acid elongation
GC-MS	Gas chromatography mass spectrometry
GDSL	Gly-Asp-Ser-Leu-motif lipase esterase
GPAT	Glycerol-3-phosphate acyltransferase
HA	5-Hexynoic acid
HD	1,6-Hexanediol
HDPE	High-density polyethylene
HPLC	High-performance liquid chromatography
HRMS	High-resolution mass spectrometry
J	Coupling constant
KCS	B-ketoacyl-CoA
LACS	Long-chain acyl CoA
LDPE	Low-density polyethylene
LTP	Lipid-tranfer proteins
m	Multiplet
m.p.	Melting point
MALDI-TOF	Matrix assisted laser desorption/ionization time-of-flight
MAS	Magic angle spinning

Me	Methyl
M_n	Number-average molecular weight
MS	Mass spectrometry
MSNT	1-(2-Mesitylenesulfonyl)-3-nitro-1H-1,2,3-triazole
N435	Novozyme 435
NAP	2-Napththalene
Naphth	2-Naphthylidene
n-Bu	*n*-Butyl
NMR	Nuclear magnetic resonance
p	Pentet
PDL	Pentadecalactone
PE	Polyester
PG	Protective group
Ph	Phenyl
PLLA	Poly-L-lactic acid
PMP	*p*-Methoxyphenyl
PPDL	Poly(pentadecalactone)
ppm	Part per million
PPP	Phenylpropanoids pathway
PS	Polystyrene
p-TSA	*p*-Toluenesulfonic acid
PVC	Polyvinyl chloride
q	Quadruplet
REX	Reactive extrusion
R_f	Retention factor
ROP	Ring opening polymerization
RPI	Rensselaer Polytechnic Institute
rpm	Revolutions per minute
s	Singlet
t	Triplet
TBAF	Tetra-*n*-butylammonium fluoride

TBS	*tert*-Butyldimethylsilyl
t-Bu	tert-Butyl
T_c	Crystallization temperature
TCDI	1,1'-Thiocarbonyldiimidazole
td	Triplet of doublets
TEM	Transmission electron microspray
TEMPO	2,2',6,6'-Tetramethylpiperidine-1-oxyl
FT-IR	Fourier-transform infrared spectroscopy
T_g	Glass-transition temperature
THF	Tetrahydrofuran
TLC	Thin-layer chromatography
T_m	Melting temperature
TMEDA	*N,N,N',N'*-Tetramethylethylenediamine
Ts	Tosyl
tt	Triplet of triplets
UHPLC	Ultra-high-performance liquid chromatography
UV	Ultra violet
δ	Chemical shift
ΔQ	Heat of fusion

Table of Contents

1. Introduction

Plants started the colonization of earth around 400 million years ago,[1] and became the dominant species in most ecosystems. Since the dawn of our history, the survival of humanity has been dependent on plants. Whether as a building element, an energy source, a raw material for the constructions of tools and commodities or simply as food, plants impregnate every aspect of our lives. This dependency explains the interest plants have always had as a subject of study. A very early taxonomical classification and systematic study of plants was done by Aristotle and continued by his disciple Theophrastus in his *Enquiry into plants* (Greek: *Περὶ φυτῶν ἱστορία, Peri phyton historia*) in the 4th century BC. The study of plants continued, but it was not until the 18th and 19th centuries that it was stablished as a scientific field.

The study of plant biology not only broadens our understanding of the world, but it can also help us to solve some of the main problems that modern society faces, such as global warming and the depletion of natural resources. Plants are a sustainable alternative to oil, both as an energy source and as raw resource for the production of polymeric materials.[2] Most plastics being produced are not recycled or incinerated at the end of their product life time and are instead discarded.[3] None of the most common plastics in use are biodegradable, and thus they pose a near permanent threat to the natural environment. Plants naturally produce a range of polymers, like polysaccharides and polyesters that have been considered as a source of plastic materials. Aliphatic polyesters are of special interest due to their mechanical properties and biorecyclabe nature.[4] Cutin, an aliphatic polyester found in the plant cuticle, is particularly attractive due to its abundance, its mechanical and thermal properties, its low water permeability and its biodegradability.[5]

All living organisms are covered by a layer of polymeric structural components, which defines their boundaries and serves as a barrier between them and their environment. Plants need organs with an extensive surface area to interact with their surroundings, both above and below ground. Those interfaces must protect the plant against infection by pathogens while allowing the exchange of gas and nutrients.[6] In the case of higher plants, two polyesters take that function: cutin, located in the cuticle, which is found in the aerial parts of the plant, and suberin, in the underground parts and wound surfaces.[7] The ubiquity of these polymers suggests that they played a key role in the adaptation of plants to land environments, about 450 million years ago.[8] This adaptation is considered one of the most important events in the history of biological evolution.[1,9]

For decades, most of the studies about cutin and suberin were mere comparative surveys about the monomeric composition in different species, despite their ubiquity and importance. Moreover, little advance was made towards the understanding of cutin and suberin structure and biosynthesis.[10] However, this trend is changing, and the last decade has seen significant progress in understanding the biological mechanisms for the synthesis of cutin and suberin monomeric units, as well as their assembly in the final polymer.[11] Nonetheless, there are a number of unanswered questions regarding those issues, and a complete understanding of cutin and suberin biosynthesis, from the monomers synthesis and transport to the polymerization site, has not yet been achieved.

Plant biology is a complex topic, and a multidisciplinary approach is necessary to achieve comprehension of the intricate processes involved in the biosynthesis of these natural polymers. In the present work, we follow a synthetic chemist's approach to understand the biosynthesis of cutin and suberin, two of the most abundant natural polyesters on Earth, by synthesizing some of their monomers and studying their enzymatic polymerization *in vitro*.

1.1 The plant cell wall

One of the defining characteristic of plants is the presence of a cell wall that encloses and limits the movement of the cell. Cell walls present a considerable diversity, not only between species, but between plants, cell types and cell wall microdomains.[12] However, they share the same structural principles. Plant cell walls are mainly composed of three polysaccharide polymers: cellulose, hemicellulose and pectin. Cellulose is a linear polymer consisting on β(1→4) linked d-glucose units. As is represented in Figure 1.1, cellulose fibres are interconnected by hemicellulose molecules that are hydrogen-bonded to their surfaces.[13] Hemicellulose has a more complex structure, and is composed of different glycans. The most abundant of them is xyloglucan, which consists on a backbone of β(1→4) linked D-glucose units with side chains of xylose, galactose, fructose, arabinose or glucoronate. Pectin, like hemicellulose, is composed of a heterogeneous group of polysaccharides. It forms a matrix in which the other components of the cell wall are embedded.[13] The cellulose-hemicellulose network resists tension, while pectin provides resistance towards compression and shearing forces.[13] Pectin is also found in the middle lamella between cell walls, where it binds cells together.

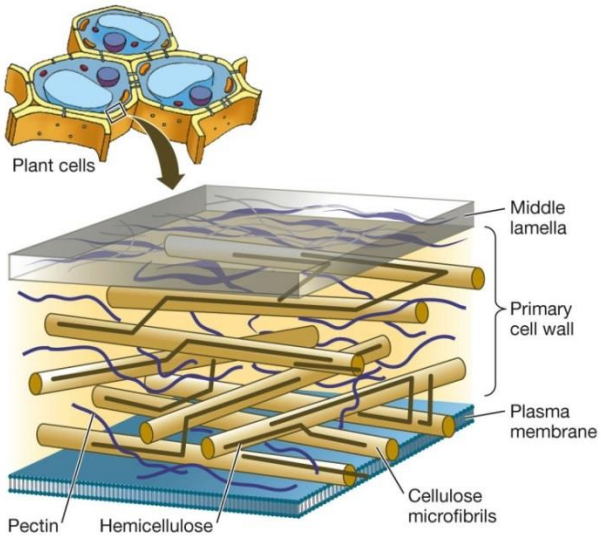

Figure 1.1. Schematic representation of the primary plant cell wall[14]

Cell walls are often classified as primary and secondary, although this distinction is sometimes considered reductive and oversimplistic. The primary cell wall is the first one to be formed during cell development. It is thin, between 50 and 200 nm, and is capable of sustaining cell expansion, increasing its area in the process.[13] The secondary cell wall, on the other hand, is normally formed in cells that have completed their expansion, and start adding successive layers in the inner section of the primary cell wall. The composition of the secondary cell wall is similar to the primary, but it tends to present a lower proportion of pectin and a higher proportion of cellulose. Additionally, lignin, a complex phenolic polymer that provides mechanical support and water impermeability, is often found in secondary cell walls.[13]

Cells walls can develop specialized modifications depending on their location within the plant. Thus, cells on the epidermis, the outermost part of the plant, develop a thick and waterproof layer in their outer surface, called the cuticle, which protects plants against desiccation and other environmental stresses. The innermost cell layer in the cortex of roots, called the endodermis, also develops a modification. The cell walls of that region are impregnated with a dense, cross-linked set of polymers called suberin.[13]

1.2 Cutin:

1.2.1 The plant cuticle and its biological role

The aerial organs of all land plants, such as leaves, fruits and non woody stems are covered by a lipophilic extracellular membrane called the cuticle or cuticular membrane.[15–20] The main components of the cuticle are a series of organic solvent soluble compounds collectively known as waxes and an insoluble polymer composed primarily of C16 and C18 ω-hydroxy fatty acids called cutin.[21–24] Trace amounts of polysaccharides and phenols can also be found in the cuticle.[25] The analysis of cuticules from various plant species has found a non-soluble solid residue resistant to alkaline hydrolysis that remains after the waxes and cutin have been removed.[6,26] This residue has received the name of cutan, and is believed to be an aliphatic polymer consistent on cutin monomers[17] held together by non-ester bonds, although their exact nature remain controversial.[27] Cutan was believed to be ubiquitous, since it appears in a large number of fossilized cuticules, coals and terrestrial sediments covering a large portion of the geological past.[25] However, further research showed that cutan is much less widespread than it was previously thought, and it might be restricted to a relatively small number of species.[28] A representation of the different parts in the cuticle can be found in Figure 1.2.

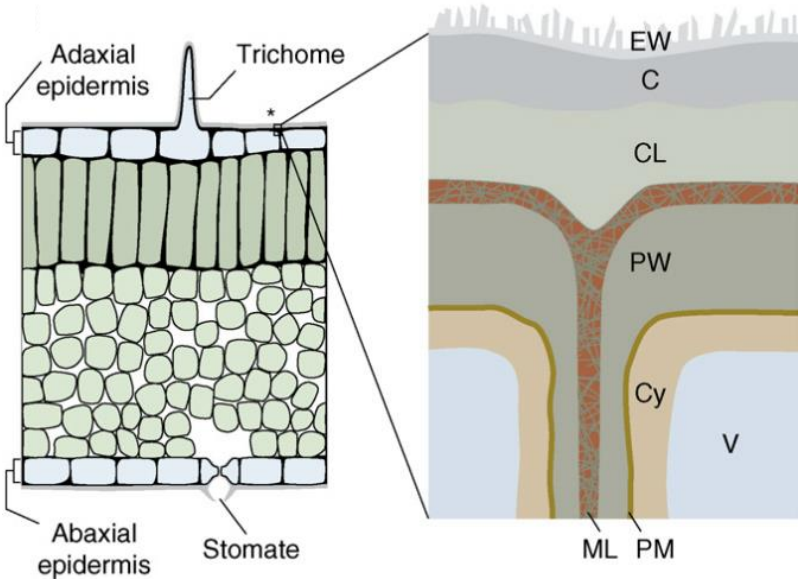

Figure 1.2. Schematic representation of the different layers of the cuticle and its location in a leaf. EW, epicuticular waxes; C, cuticle proper; CL, cuticular layer; PW, primary cell wall; Cy, cytoplasm; V, vacuole[23]

The composition of the cuticle is heterogeneous and can be divided in different layers. The outermost layer is composed by epicuticular waxes, which form crystals on the surface of the plant. Epicuticular waxes confer distinct macroscopic surface properties, such as the glossy appearance of common leaves

and fruits,[11] and determine the wettability of plant surfaces.[15] The layer underneath is known as the cuticle proper, which consists of a matrix of cutin embedded with intracuticular waxes. In the innermost part of the cuticle is found the "cuticular layer", which is less abundant in waxes but rich in polysaccharides from the cell wall, with both cellulose and pectin.[23,29] In fact, there is a strong interaction between this layer of the cuticle and the cell wall underneath, to the point that the cuticle can be considered as a lipidic modification of the cell wall, in a similar manner as lignification is a modification of the plant secondary cell walls.[11,19,30] A schematic representation of the location of the cuticle in the plant and its different parts can be found in Figure 1.2**.**

Despite those general traits, cuticles offer an enormous architectural and compositional diversity. There is a substantial difference in the proportion of waxes and cutin in different plant species. For example, the cuticle of tomato fruit (*Solanum lycopersicum*) is composed of 60–70% cutin and 2–10% waxes,[31] while the values in persimmon fruit (*Diospyros kaki*) are 48% and 35% respectively.[32,33] The amount of cutan and polysaccharides is also extremely variable. The proportion of cutan ranges from non-detectable levels in tomato to more than 90% in bilberry (*Vaccinium myrtillus*).[34] This diversity does not only occur between species, but also between organs in the same plant. For instance the cutin of apple (*Malus pumila*) leaves present greater amounts of C16 monomers and lower levels of unsaturated compounds than that of apple fruit.[35] It is also well known the case of *Arabidopsis thaliana*, whose leaves and stems present a cutin with exceptional levels of dicarboxylic acids, unlike that of its flowers.[6,36] These differences not only affect the composition, but the architecture of the cuticle as well. The thickness of the cuticle ranges from around 20 nm to more than 10000 nm.[37] In general, the cuticle from fruits is thicker than the one from other vegetative organs. For instance, the cuticle of mature tomato fruit (*Lycopersicon esculentum*) is significantly thick, of about 2000–9000 nm. However, a thick cuticle is not exclusive of fruits, as is showed by the drought tolerant bush *Hakea suaveolens*, with a leaf cuticle with a reported thickness 11500 nm.[37] There are also significant changes in cuticle composition and coverage through the plant ontogeny.[33,38] It has been reported that apple fruits experiment an increment in the deposition of cuticular waxes during ripening.[39] Cuticle deposition also changes throughout fruit growth, which is different in different species. For example, in tomatoes "Moneymaker" the total amount of cuticle increases during the whole growing and ripening period[18] and the ratio of cutin:polysaccharide increases during development. In contrast, in cherry tomatoes the cuticle is only accumulated in early stages of development, and a constant amount is maintained and no significant change in the cutin:polysaccharide ratio is observed for the remaining of the fruit life.[31] In addition, significant variations in cuticle composition have been reported between cultivars of a single species, particularly regarding cuticular waxes.[32,33,40]

The main role of the cuticle is to provide a barrier to avoid desiccation, allowing the plant to control water loss and gas exchange through the stomata –pores found in the epidermis of leaves and other organs that facilitate gas exchange.[11,29,33] Nevertheless, it has evolved to fulfil a number of different functions which are consistent with its location in the outermost layer of the plant. Some of these

functions include the protection against pathogens and pests, the prevention of organ fusion by establishing organ boundaries and protection against excessive UV radiation. The cuticle also provides mechanical support and a self-cleaning surface.[11,33] Figure 1.3 provides a summary of the cuticle functions. Although the cuticle is an effective barrier against water loss, it also allows certain degree of transpiration.[41] This is evident in case of mature fleshy fruits with few functioning stomata, in which transpiration through the cuticle is the main mode of water loss.[42,43] Counterintuitively, there is not a direct correlation between the thickness of the cuticle and its water permeability.[42,44] In fact, the rate of water loss in fruits is higher than the one in leaves, despite of the thicker cuticle of the former.[42,45] The rate of water loss is greater during the early stages of fruit growth. This is consistent with the needs of the growing fruit, as it depends on the nutrients carried by the transpiration stream.[42,45,46] Interestingly, there is also no correlation between water permeability and the amount of either waxes or cutin. A study with three tomato fruit cutin deficient (*cd1-cd3*) mutants with a dramatic reduction in cutin content (95–98%) showed no significant augment in water permeability. In fact, the mutant with the highest content in cutin presented the highest water loss rate.[10] Water permeability shows an inverse correlation with the amount of specific waxes, but not with the total amount of wax. A model was proposed in which waxes are organized in two domains: crystalline and amorphous.[47,48] Certain types of waxes, such as triterpenoids, would accumulate in the amorphous matrix, while other, as alkanes, would be localized in the crystalline domains. Hence, water would be forced to diffuse through the amorphous regions. Therefore, an increase in triterpenoids, together with a decrease in the amount of alkanes, would result in an increase in the amount of amorphous regions compared to the crystalline domains, leading to higher water permeability.[10,47] In this model, cutin does not function as a hydrophobic barrier *per se*, but it rather provides a framework in which intracuticular waxes can be deposited, and thus contributes to the creation of an impermeable barrier.[10]

The cuticle also functions as a barrier against pathogen attacks. It has been reported a correlation between susceptibility to fungal colonization and cuticle thickness in several species.[49,50] There are indications that cutin, rather than waxes, is mainly responsible for plant protection against pathogens.[33] This idea is supported by the fact that most fungal pathogens secrete cutinases that hydrolyse the ester bonds and release free monomers.[51,52] However, cutin does not only act as a passive barrier.[33] The free monomers that are released by the fungal attack can function as elicitors to activate plant defences, such as the production of hydrogen peroxide.[53,54] The mechanism of plant identification of free cutin monomers is still unknown.[55] This defence mechanism explains the enhanced plant defensive response towards fungal attack in some cutin-deficient mutants of *Arabidopsis*, as the increased cuticular permeability of those mutants enhances the diffusion of elicitors that induce the production of antifungal compounds.[56] The cuticle also offers protection against UV radiation due to the epicuticular waxes. Isolated cuticles have been found to provide effective screening of the UV- spectrum, while offering high transmittance in photosynthetically active wavelengths.[57] Epicuticular wax crystals can also reflect light to some extent,[58–60] although there is a trade-off between limiting damaging UV radiation by reflection and achieving photosynthetic efficiency.[11]

In addition to its protective functions, the cuticle has also shown to provide mechanical support[61] and to play an important role in defining organ boundaries during development. The majority of mutants showing post-genital organ fusions also exhibit defects in the cuticle.[62] This has been observed in different *Arabidopsis* mutants with abnormal cuticles[63–65] and in wax-deficient tomato mutants.[66] However, the specific contributions of cutin and waxes in the prevention of organ fusion have not been established to date.[62] Finally, the cuticle also participates in a self-cleaning mechanism known as the "lotus effect", which consists on the accumulation of droplets of water that roll to the grown, collecting particles on the leaf surface in the process. This effect has been correlated with the abundance of epicuticular wax crystals,[67] which repel water and allow the formation of an air pocket beneath the droplets. This effect could play an important role in washing away pathogen spores before they can germinate.[11]

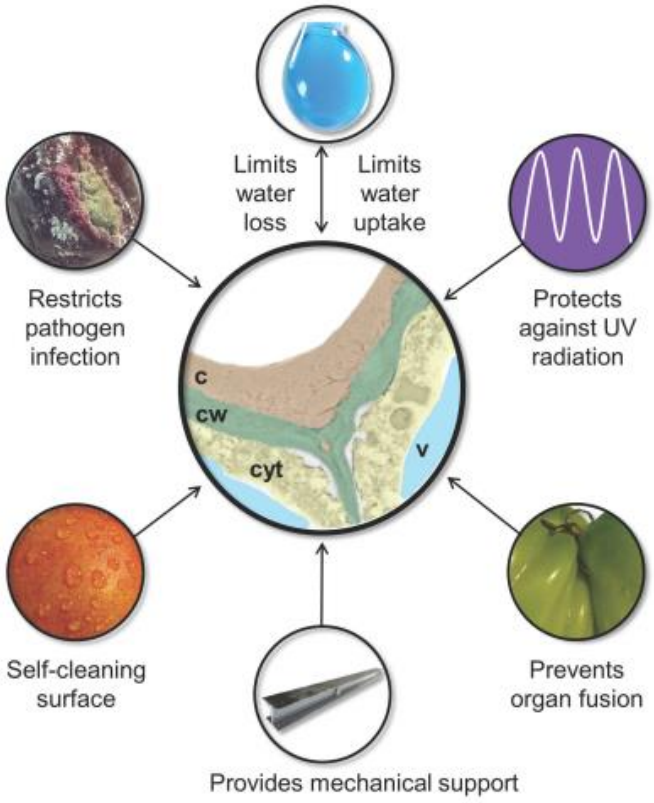

Figure 1.3. A summary of fruit cuticle functions. The central figure shows a colorized transmission electron microscopy image of the cuticle and underlying structures of a green tomato fruit. C, cuticle; CW, cell wall; Cyt, cytoplasm; V, vacuole.[33]

Wild tomato fruit (*Solanum lycopersicum*) presents an excellent model to study the complex relation between the cuticle synthesis, structure and functions.[68] Tomato fruit cuticle has a substantial amount

of cutin, and it presents a relatively simple composition of both waxes and cutin. The thick cuticular layer of tomato fruits enables detailed morphological analysis by optical microscopy as well as isolation of an intact membrane, which facilitates both biomechanical and chemical analysis.[69] Furthermore, the fruit epidermis does not have stomata, making it much easier to conduct permeability essays.

1.2.2 Cutin monomeric composition

Cutin is a polyester composed mainly by ω-hydroxy and mid-chain substituted fatty acids. The monomeric composition of cutin changes significantly among species, organs and with ontogeny. Despite of this variety, three main types of cutin have been identified to date based on their composition.[68] The two most common cutin types are a C16-type, which is rich in dihydroxyhexadecanoic acids, particularly 9(10),16-dihydroxyhexadecanoic acid, and a C18-type, rich on 9,10-epoxy-18-hydroxyoctadecanoic acid and 9,10,18-trihydroxyoctadecanoic acid.[24] A third type of cutin was identified more recently in the leaves of *Arabidopsis*, which presents a surprisingly high content of C18 dicarboxylic acids.[6]

The most common method to analyse cutin composition was developed by P.E. Kolattukudy.[70] In general terms, it consists on the extraction of waxes by washes with organic solvents, followed by the rupture of the ester bonds by hydrogenolysis with $LiAlH_4$ or methanolysis with BF_3/MeOH or HCl/MeOH. The resulting monomers are derivatized with TMS groups and analysed by GC/MS. A careful analysis of the mass spectra is needed to disclose the fragmentation patterns of the different polymers. The use of $LiAlH_4$ to break down the polymer chain results in the reduction of epoxy and carbonyl groups to hydroxyl groups, which cannot be distinguished from the naturally occurring hydroxyl groups. This problem can be overcome by the use of $LiAlD_4$ in the reduction.

Table 1.1 displays a summary of the main monomers and a range of their relative composition as a percentage in weight. The monomeric composition of C16 and C18 cutin is given as a range from various plant species and different organs.[10,34,70–77] It is important to note that the various studies use different methods for the depolymerization of cutin, and they report the results in various degrees of detail. Thus, some publications report the amount of the different monomers in detail, while others merely report the composition of monomer types (e.g. ω-hydroxylated fatty acid). Therefore, the purpose of the table is to provide an insight into the typical range in which the most common monomers appear in the different cutin types. It is also worth noting that most of those studies do not intend to classify the cuticles in one of those three types, and merely provide a list of monomeric composition. However, the differences between C16 and C18 cutin types are striking, and it is generally not difficult to classify a specific cutin in either type by comparing the relative amounts of C16 and C18 mid-chain oxygenated fatty acids.

Table 1.1. Summary of the monomeric composition of the three cutin types. All values are given as a percentage in weight. C16 and C18 type cutin monomeric composition are given as a percentage range from various plant species found in several publications. *Arabidopsis* monomer composition was taken from Franke *et al.*[6]

	C16-type cutin	**C18-type cutin**	***Arabidopsis thaliana* leaf cutin**
1-Alkanoic acids	1–23	0–2	8
Palmitic acid (C16:0)	1–18	<1	1.3
Oleic acid (C18:1)	-	<1	<1
Tetracosanoic acid (C24:0)	-	<1	2.6
ω-Hydroxy fatty acids	3–11	6–38	7
16-hydroxy-hexadecanoic acid (C16:0)	1–10	1–2	1.6
18-hydroxy-octadecanoic acid (C18:0)	0–4	0–1.5	<1
18-hydroxy-9-octadecenoic acid (C18:1)	0–9	3–33	<1
18-hydroxyoctadecanedienoic acid (C18:2)	0–4	0–1.5	2.4
α,ω-Dicarboxylic acids	0.5–3.5	0–8	40.9
Hexadecane-1,16-dioic acid (C16:0)	-	0–1	10.6
Octadecane-1,18-dioic acid (C18:0)	-	-	2.7
Octadecene-1,18-dioic acid (C18:1)	-	0–2.6	6.6
Octadecanedien-1,18-dioic acid (C18:2)	-	-	21.0
Mid-chain oxygenated fatty acids	46–93	60–91	8.6
Dihydroxyhexadecanoic acid* (C16:0)	34–89	2–31	1.2
9,10,18-trihydroxyoctadecanoic acid (C18:0)	1–11	4–25	-
9,10,18-trihydroxyoctadecenoic acid (C18:1)	-	0–23	
9,10-epoxy-18-hydroxyoctadecanoic acid (C18:0)	0.5–8	10–49	-
2-Hydroxyacids	0–1	0–1	13.9
2-hydroxytetracosanoic acid	-	-	4.5
Fatty alcohols	0–6	0–2	1.6
Aromatic compounds	0–3	-	-
Glycerol	1–14	2–5	-

*Mixture of various positional isomers

In both C16 and C18 cutin types, mid-chain oxygenated fatty acids comprise the most common family of monomers. In the case of C16 cutins, this family is dominated by various positional isomers of dihydroxyhexadecanoic acid. Those isomers are not separable by normal chromatographic methods, and most reports do not differentiate them. Moreover, it has been reported that the most common dihydroxyhexadecanoate isomer of tomato fruit and various organs of grape fruit (*Citrus paradise*) is 10,16-dihydroxyhexadecanoic acid, followed by its 9,16-dihydroxy isomer.[70,78] These two isomers represent 61–79% and 16–33% of the total amount of dihydroxypalmitate, respectively. Minor amounts of the 8,16- and 7,17- palmitic isomers were also identified in both plants. The monomer found in larger amounts in C18 cutins is 9,10-epoxy-18-hydroxyoctadecanoic acid, followed by 9,10,18-trihydroxyoctadecanoic acid. The inner bran of common wheat (*Triticum aestivum*) grains presents a very high amount of 18-hydroxyoctadecenoic acid, although it does not seem to be representative of this type of cutins. All the C18-type cutins analysed have a very low (0–2%) content of unsubstituted fatty acids. C16-type cutins tend to have a slightly higher amount of this class of monomers, with the exception of strawberry (*Fragaria x ananassa*), whose total content of unsubstituted fatty acids reaches almost 23%.[77] The leaf cutin of *Arabidopsis* presents a particular monomeric composition. Franke *et al.* performed an extensive characterization of cutin composition of *Arabidopsis*, finding α,ω-diacids as the major depolymerization products of its leaf cuticle.[6] In fact, C16 and C18 diacids comprise more than 40% of the cutin monomers. *Arabidopsis* leaf cutin also presents relatively high amounts of other uncommon monomers, such as 2-hydroxytetracosanoic acid (4.5%) and tetracosanoic acid (2.6%). It has been suggested that the high amount of diacids combined with the very low content of mid-chain hydroxyl fatty acids would lead to a polymer with a mostly linear structure, which would allow the polymer chains to align in closely parallel patterns of high density, thus allowing the cuticle to be much thinner without compromising its properties.[6]

Cutin composition also changes during growth, as it is shown in a study by Riederer and Schönherr, in which the composition of cutin at different positions in the leafs of *Clivia miniata*, which corresponds to different stages of development, was analysed.[71] *Clivia minata* presents a typical C18 cutin, with 9,10-epoxy-18-hydroxyoctadecanoic acid as the most abundant monomer in all stages of development. It was found that there is a high proportion of unsubstituted fatty acids in the younger cutin, which is dramatically reduced shortly after. The proportion of some monomers, namely 9,10-epoxy-18-hydroxyoctadecanoic acid, dihydroxyhexadecanoic acid and 18-hydroxy-9-octadecenoic acid increased rapidly in the first stages of development and then reached a plateau. 9,10,18-trihydroxyoctadecanoic acid on the other hand showed a small but continuous increment, not reaching a plateau. It is believed that it is formed by enzymatic hydration of the epoxy group.[71]

Despite the fact that cutins tend to fall into one of those three categories, that is not always the case. For instance, the cutin of crowberry (*Empetrum nigrum*), presents a composition that lays in between the C16 and C18 types, with 34% of 9,10-epoxy-18-hydroxyoctadecanoic acid, 29% of dihydroxyhexadecanoic acid and an amount of unsubstituted fatty acids that falls in the high end for C18 cutins.[77] This shows that although the classification between cutin types could be useful, it is also

arbitrary, and given the enormous variety in cutin composition among species and organs, it is likely that several cutins would not fall clearly in any of them.

1.2.3 Cutin biosynthesis

Several advances have been made in the previous decade to elucidate the complete biosynthesis of cutin. It follows a complex pathway, from the monomer biosynthesis and transport to the subsequent polymerization, which is still not fully understood.

1.2.3.1 Monomer biosynthesis

As it was discussed in the previous section, the most common cutin monomers are ω-hydroxylated fatty acids with either hydroxyl or epoxy functionalities in the middle of the chain. The first steps in the synthesis of cutin monomers begin in the endoplasmic reticulum (ER). There, unsubstituted fatty acids, previously synthesized in the plastid, experiment ω-hydroxylation, mid-chain hydroxylation or epoxidation and acylation to coenzyme A (CoA).[27] The order in which these steps proceed is not clearly understood, but there are some indications. It has been reported that an ω-hydroxylase enzyme from the same subfamily as the cutin ω-hydroxylases presents a much higher *in vitro* activity with acyl-CoA substrates than with free fatty acids.[79] Furthermore, it has also been reported that the enzyme identified as responsible for mid-chain hydroxylation for cutin monomers in *Arabidopsis* petals presents activity solely towards ω-hydroxylated fatty acids.[80] Thus, the most likely order in which these steps proceed is first acylation with CoA, followed by ω-hydroxylation and finally mid-chain oxidation.

The long-chain acyl-CoA synthetase (LACS) family of enzymes catalyzes the acetylation of cutin monomers with CoA. In particular, LACS1 and LACS2 seem to be responsible for the acetylation of C16 cutin monomers, although they also present overlapping functions with wax biosynthesis.[81] The oxidation reactions in cutin monomers biosynthesis are catalyzed by cytochrome P450 enzymes. Particularly, the CYP86A family catalyzes the ω-hydroxylation[64,79] and the CYP77A family catalyzes the mid-chain oxidations, as is represented in Figure 1.4.[82] To support this idea, it has been reported that an *Arabidopsis cyp86a2* mutant presents a lower cutin content and altered cutin composition[83] and *Arabidopsis cyp77a6-1* and *cyp77a6-2* knock-out mutants present a complete absence of 10,16-dihydroxypalmitic acid.[80] The closely related CYP77A4 enzyme catalyzes the epoxidation of oleic acid *in vitro*, but there is no further evidence that it performs this reaction in cutin synthesis.[27,82] Further oxidation of the terminal hydroxyl group to its correspondent carboxylic acid leads to the diacids found in *Arabidopsis*. *Cyp86a2* mutants show a significant reduction in the content of dicarboxylic acids while the content of 18-hydroxyoctadecenoate remains unaltered.[84] The content of diacids in *Arabidopsis* is also significantly reduced in *hothead* mutants, suggesting that CYP86A2 and HOTHEAD play a role in the oxidation of the terminal alcohol.[85]

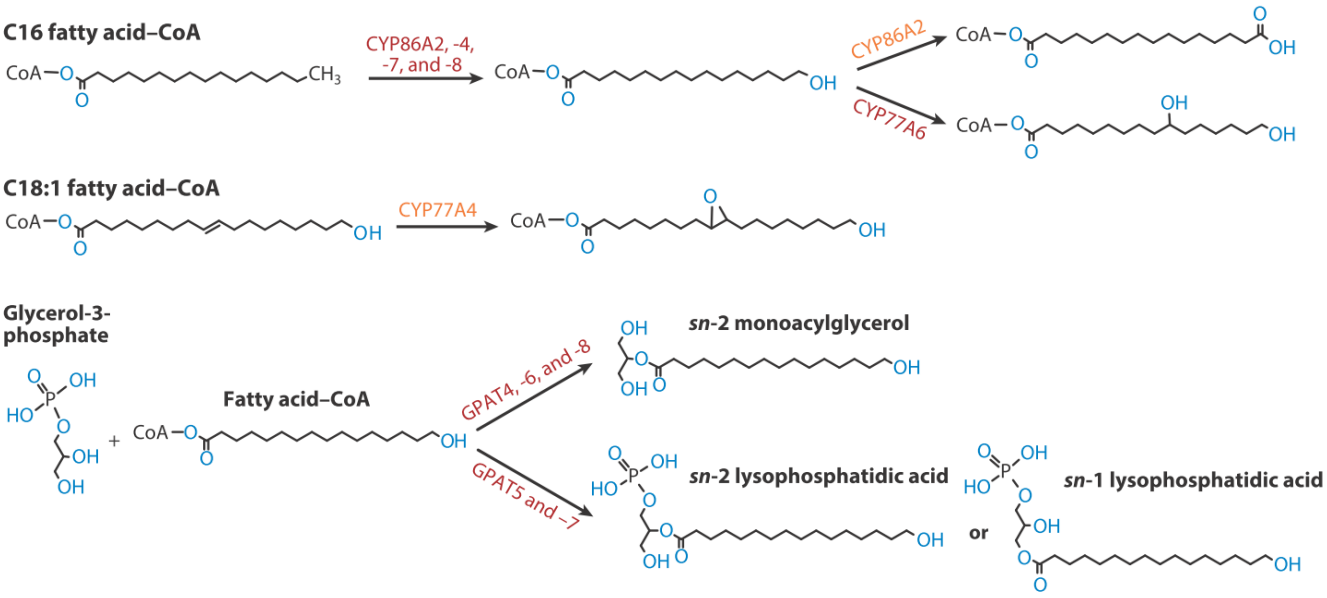

Figure 1.4. Role of cytochrome P450 and GPAT enzymes in the synthesis of cutin monomers. Names shown in red denote proved enzymatic functions, while names in orange denote speculative functions.[27]

A family of glycerol-3-phosphate acyltransferases (GPAT) involved in the synthesis of cutin and suberin monomers has recently been described.[86] This family comprises eight members in *Arabidopsis*. GPAT4 and GPAT6 are redundant in function, and are both required for the production of leaf and stem cutin. *In vitro* studies showed that those two enzymes present glycerol-acyltransferase activity towards C16 and C18 ω-oxidised CoA substrates with a strong preference towards the *sn-2* position. In addition, they also show phosphatase activity, leaving 2-monoacylglyceryl esters (2-MAGs) as the major products, as is represented in Figure 1.4.[86,87] GPAT6 is required in the synthesis of floral cutin in *Arabidopsis*, and it also shows specific *sn-2* acyltransferase activity together with phosphatase activity. GPAT5 and GPAT7 are related to suberin synthesis, and their activity will be discussed in Section 1.2.4.

The *sn-2* specificity of those enzymes differentiates them from other GPATs involved in the synthesis of membrane and storage glycerolipids. This class of *sn-2* specific GPATs is exclusive to land plants and it could be one of the evolutionary changes that allowed plants to develop a cuticle and adapt to their new environment.[86] 2-MAG products are thermodynamically less stable than their *sn-1* isoforms. This suggests that the formation of 2-MAGs is necessary for cutin biosynthesis.[87]

1.2.3.2 Monomer transport

The transport mechanism of cutin monomers to the cuticle is largely unknown. The monomers are synthesized in the ER and therefore must be exported across the plasma membrane and travel through the polysaccharide cell wall. It has been reported that wax transport to the cuticle depends on a subfamily of ATP binding cassette (ABC) transporters, known as ABCG. Some ABCG family members are half-transporters, and must dimerize to form fully functional ABC transporters. Among these half-transporters are ABCG11 and ABCG12, which have been found to be necessary for wax transport in *Arabidopsis*. ABCG11 is also involved in the transport of cutin monomers.[88,89] This was shown in an ABCG11 deficient *Arabidopsis* mutant, which showed a large reduction in the amount of a particular wax, nonacosane (C29), together with a significant reduction in almost all cutin monomers.[89] Although is known that ABC transporters are capable of accepting a wide range of substrates, it is unclear how ABCG11 can discriminate between fairly similar waxes, while still accepting a variety of structurally different cutin monomers. ABCG11 also showed the ability to form homodimers or ABCG11/ABCG12 heterodimers, while ABCG12 is only capable of forming dimers with ABCG11 in epidermal cells.[90] A full ABC transporter related to cutin precursors to the cuticle, ABCG32, was also identified in *Arabidopsis*.[91] *Abcg32* mutants present a 40% reduction in the amount of ω-hydroxylated fatty acids in cutin of flowers, and they show a higher water permeability and organ fusion between leaves and petioles. The transport of cutin monomers through the polysaccharide cell wall might be aided by lipid transfer proteins (LTPs). These proteins have shown to bind lipid substrates *in vitro*[92] and play a role in the deposition of cuticular waxes,[93] but their participation in the transport of cutin monomers have not yet been demonstrated. A summary of the different routes for the the synthesis and transport of cutin monomers can be found in Figure 1.5

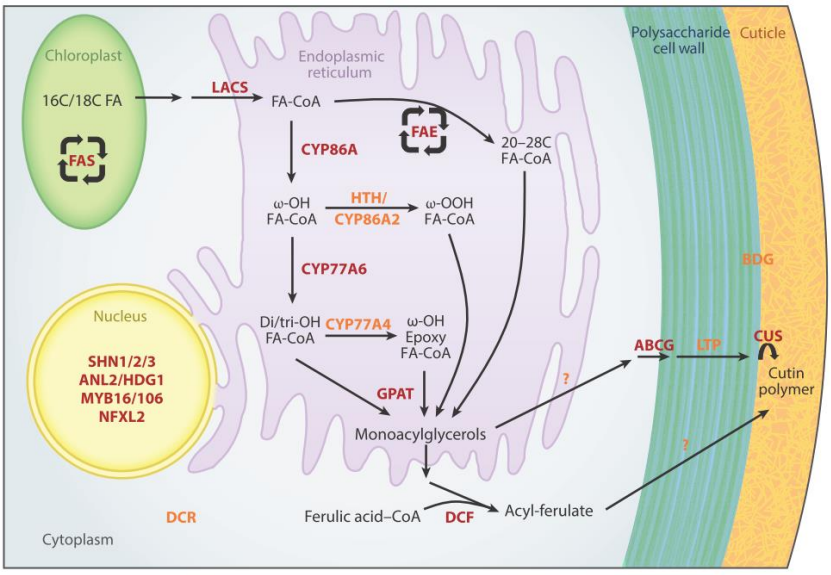

Figure 1.5. Possible biosynthetic routes for the synthesis and transport of cutin monomers.[27]

1.2.3.3 Cutin polymerization

The mechanism of cutin biopolymerization remained a mystery for decades after the discovery of this polyester. The difficulty to find an enzyme involved in the polymerization of cutin monomers led to the hypothesis of spontaneous monomer self-assembly.[94] Heredia *et al.* showed that 9,16-dihydroxypalmitic acid is capable of forming lipid vesicles *in vitro* called cutinsomes in aqueous media, and then suffer a series of spontaneous esterification reactions with their neighbors.[95,96] The self-esterification of cutin monomers without enzymatic participation have not been proven *in planta*, and since the postulation of this hypothesis some enzymes related to cutin biosynthesis have been described.

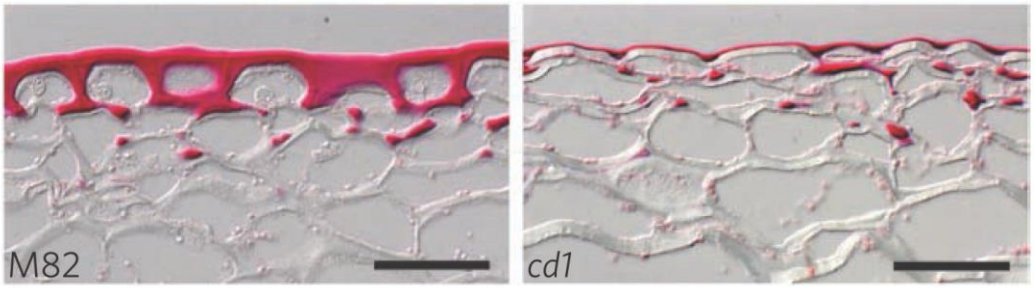

In recent years, an important breakthrough in the understanding of cutin biosynthesis took place when two research groups identified independently a member of the Gly-Asp-Ser-Leu-motif lipase/esterase (GDSL) family in the epidermis of developing tomato fruits, which functions as a cutin synthase.[27,97] Girard *et al.* used RNA interference to silence the *GDSL1* gene, which leads to reductions in monomer content and cutin thickness, as well as the appearance of nanopores in tomato cutin.[98] Additionally, trough fine mapping of the *cutin deficient 1* (*cd1*) tomato mutant, which presents a severe reduction of cutin content (90–95%), Yeats *et al.* identified the enzyme Cutin Deficient 1 (CD1) as responsible for cutin biopolymerization.[22] *cd1* mutants exhibit accumulation of 2-mono(10,16-dihydroxyhexadecanoyl) glycerol (2-MHG) in the soluble surface lipids, which is not present in wild-type tomato fruits. This confirms the importance of 2-MAGs as monomers in cutin polymerization, as it was suggested by the relevance of GPAT enzymes (See section 1.2.3.1). Furthermore, CD1 showed *in vitro* activity in the transesterification of 2-MHG, forming linear oligomers with terminal ester linkages.[99] It has been suggested that CD1 follows a ping-pong bi-bi mechanism in which the substrate *in vitro* is the same in the initial phase of the reaction.[99,100] CD1 would first react with a 2-MHG molecule to form an acyl-enzyme intermediate and release glycerol. This intermediate then reacts with

another 2-MHG molecule to form a dimer. 2-MHG dimer would act as a substrate in subsequent reactions, yielding to progressively larger products.

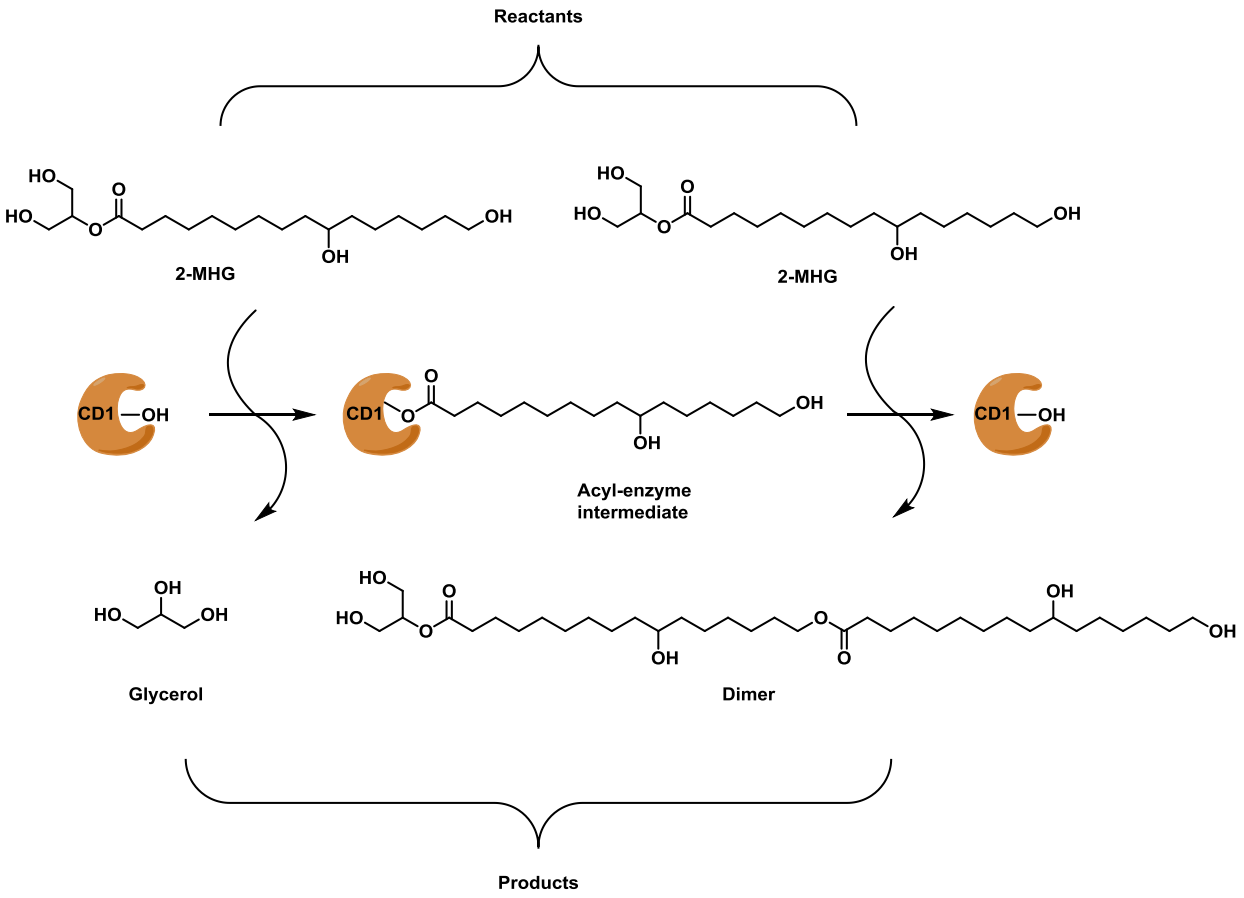

Figure 1.6. Proposed mechanism for the formation of 10,16 hexadecanoyl dimer from two molecules of 2-MHG. Figure adapted from ref 99

CD1was later identified as a member of a distinct clade of *GDSL* genes which encode an ancient family of cutin synthase-like (CUS) proteins, and herein renamed as CUS1. CUS enzymes present *in vitro* 2-MHG polymeric activity, although with various degrees of efficiency. These results suggest that other members of this family might act on other cutin monomers substrates.[99]

Other proteins, apart from the CUS family, have been found to be involved in cutin biosynthesis. One of them is BODYGUARD (BDG), an enzyme from the α/β-hydrolase family which is located exclusively in epidermal cells and accumulates in the outermost portion of the epidermal cell wall. Cutin of *Arabidopsis bdg* mutants presents a highly disorganized cuticle with similar defects to the ones observed in transgenic *Arabidopsis* plants that express a cutinase from the *Fusarium solani pisi* fungus.[65] Another important superfamily of enzymes with an important role in cutin formation is

*B*EAT, *A*HCT, *H*CBT1, *D*AT (BAHD). A member of this family, DEFICIENT IN CUTIN FERULATE (DCF) has been proven to be essential for the incorporation of ferulate, one of the few aromatic compounds of cutins.[101] A different member of the BAHD family, DEFECTIVE IN CUTICULAR RIDGES (DCR), also seems to play an important role in cutin synthesis. The cutin in *Arabidopsis* petals from a *dcr* mutant shows a complete reduction of 9(10),16-dihydroxypalmitic acid. However, both enzymes of the BAHD family are localized in the cytosol,[27,82] which is not consistent with a role in cutin biosynthesis.

1.2.4 Structure and properties

1.2.4.1 Molecular structure of cutin

The structure of the cutin matrix is partially determined by its monomeric composition. Monomers with a single hydroxyl group can only contribute to the formation of linear chains while monomers with a terminal and a mid-chain hydroxyl group are capable of forming dendritic structures. Thus, is expected that cutins with a higher content of ω-hydroxy fatty acids would present more linear structures. It has been found that the majority of terminal hydroxyl groups participate in ester bonds, while only half of the secondary hydroxyl groups do.[19,23,27] Consequently, the number of unesterified carboxyl groups is very small. The formation of cross-links between polymer chains and the incorporation of glycerol into the polymer matrix is only possible by the presence of dicarboxylic acids, which are only present in significant amounts in a very small number of cutins. Taken together, these data suggest that a dendrimer, shown in Figure 1.7, is likely the most common molecular structure of cutin. Glycerol is released during the polymerization of 2-MAG monomers by CUS enzymes and it could be trapped within the polymer structure, explaining its presence in isolated cutins.

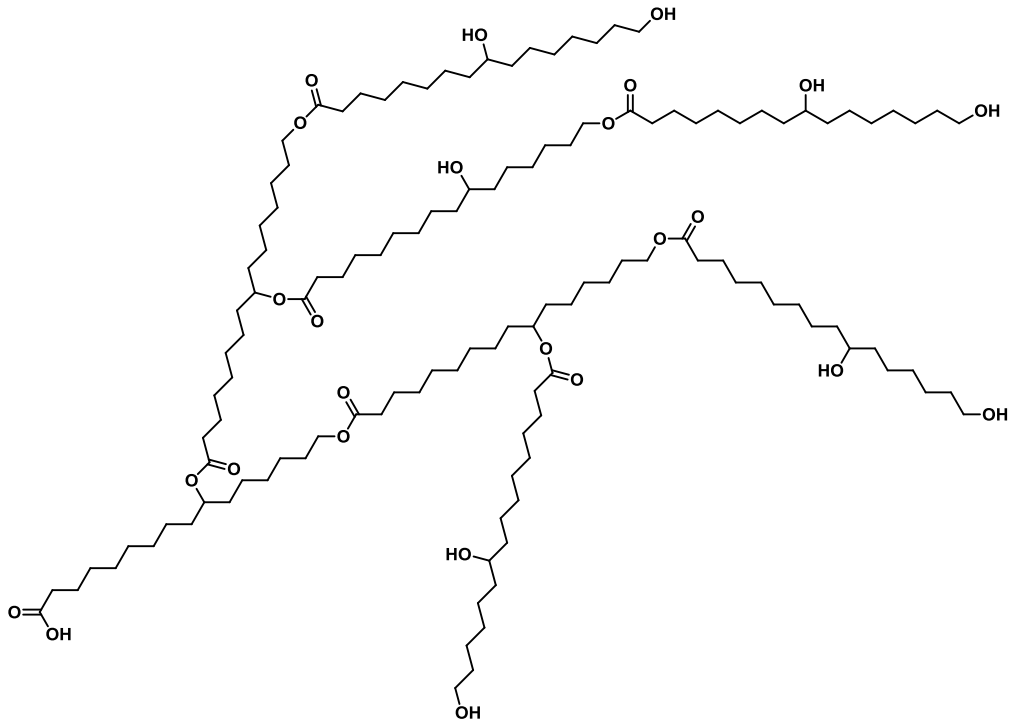

Figure 1.7. Possible dendritic molecular structure of cutin.

Despite the clues provided by the monomeric composition, the actual molecular structure of cutin remains unknown. Solid-state nuclear magnetic resonance (NMR) techniques have been employed to answer this question, each one with its own merits and limitations. Both direct-polarization and cross-polarization magic-angle spinning NMR (MAS NMR) have been used, but the overlap of signals with similar magnetic environment makes it difficult to differentiate between esterified and free hydroxyl groups[102]. Two-dimensional NMR analyses on gel-like samples swelled in dimethylsulfoxide provide enough resolution to distinguish these groups clearly, but their reliability is limited due to the reduced swelling capability of the highly crosslinked domains, thus biasing the analysis.[102]

1.2.4.2 Mechanical and thermal properties

Mechanical stress is higher on the surface of a body than in its interior. For this reason, is reasonable to assume that the cuticle plays an important role in providing mechanical support to the epidermal tissue of plants. The mechanical properties of tomato fruit cuticle and the contribution of its individual components have been described in several studies. To understand the mechanical properties of cutin is necessary first to clarify some concepts.

Whenever an external force is applied to a material it produces stresses that result in deformation. Ideal elastic materials experiment an instantaneous and constant strain during the duration of the applied stress, and the deformation is instantly reversed when the stress ceases.[103] The relationship between strain and stress is dominated by the elastic, or Young's modulus, which indicates the extent of the stiffness of the material. The other extreme of mechanical behaviour is found in ideal fluids, in which the strain increases constantly with time when a stress is applied, and remains constant when the force disappears. The cuticle of plants, as many polymeric materials, shows an intermediate, or viscoelastic, behaviour. The relationship between stress and strain in plant cuticles present two phases: at small stresses it presents an elastic behaviour where the deformation is instantaneous and fully reversible, whereas when higher stresses are applied, the cuticle shows a viscous behaviour and the deformation becomes irreversible.[19,104] López-Casado *et al.* showed that isolated tomato cutin does not present a biphasic behaviour, and its Young's modulus is significantly lower (92%) than the one of the cuticle. This suggests that the polysaccharide fraction of the cuticle is responsible for the elastic behaviour and high Young's modulus of the cuticle.[105] The mechanical properties of cutin are significantly affected by moisture and its development stage. Water disrupts hydrogen-bonded cross-links and diminishes methylene hydrophobic interactions, which results in a reduction of the elastic modulus.[25,105] Cutin from ripening tomatoes present a higher content in flavonoids, which increase its stiffness by providing strength in the elastic phase and reducing irreversible viscoelastic deformation.[31]

The specific heat value for cutin, that is, the amount of energy required to increase cutin temperature 1 °C, is around 2–2.5 $J\ K^{-1}\ g^{-1}$.[106] This is a significantly high value as compared, for instance, with cellulose, with a specific heat of 1.5 $J\ K^{-1}\ g^{-1}$.[107] This is consistent with the location of cutin in the outer layer of the epidermis, and suggests that cutin might play an important role as a thermoregulator between the plant and its environment.[19] Cutin presents a glass transition temperature (T_g) at around 23 °C, which is reduced to 16.3 °C upon sorption of water.[108] At temperatures below T_g, polymers show a glass-like state in which the polymer is more brittle, while above T_g, polymer molecules have a less restricted movement. The fact that cutin has a T_g in the range of ambient temperatures can have profound physiological implications, and it is related to cuticle permeability to small molecules, ions and water.[19]

Cutin has thermal and mechanical properties comparable to those of common plastics. Its young modulus and stress at break (maximum stress before the polymer breaks) are similar to those of low density polyethylene (LDPE), one of the most commonly used polymers.[5] Nonetheless, the elongation at break of cutin is much lower than the one of LDPE, and it is comparable to rigid polymers like polystyrene (PS). Cutin has an initial decomposition temperature of 200 °C, which is higher than polyvinyl chloride (PVC) and PS.[5] In addition, cutin is completely biodegradable, and can be fully hydrolysed by soil microorganisms in a period of three to eight months. These properties make cutin a very interesting candidate to substitute oil-based polymers in several functions, particularly in the packaging industry. Considering that an estimated 10^5–10^6 tons of cutin from tomatoes is deposed as an

agro-waste every year, the discovery of an industrial process to use this waste as raw material to produce a cutin-like polymer could have an enormous impact in the industry and in the long run reduce drastically the accumulation of plastics in the environment.

1.3 Suberin

Suberin is a modification of the cell wall found both in external and internal specialized tissues that is deposited during plant development or in response to microbial attack, wounding or abiotic stress.[23,109,110] Suberin is the most characteristic material of cork and comprises up to 50% of its dry weight.[111] In fact, the first observation of cell walls was performed by Robert Hooke in 1665 in cork tissue and he named the spaces between cell walls "cells" (see Figure 1.8).[13] The suberized layer of cell walls is composed of two distinct domains, aliphatic and aromatic. The aliphatic domain is a polyester constituted of long-chain fatty acid derivatives, mostly α,ω-diacids and ω-hydroxy acids, and glycerol, whereas the aromatic domain is composed mainly of phenylpropanoids, such as ferulic acid. The presence of those two distinct domains has led to a certain degree of confusion in the literature, in which sometimes suberin is referred solely as an aliphatic polyester which is associated with "suberin phenolics".[112] In the present thesis, we will refer to suberin as a macromolecule that contains both a polyaliphatic and a polyaromatic domain.

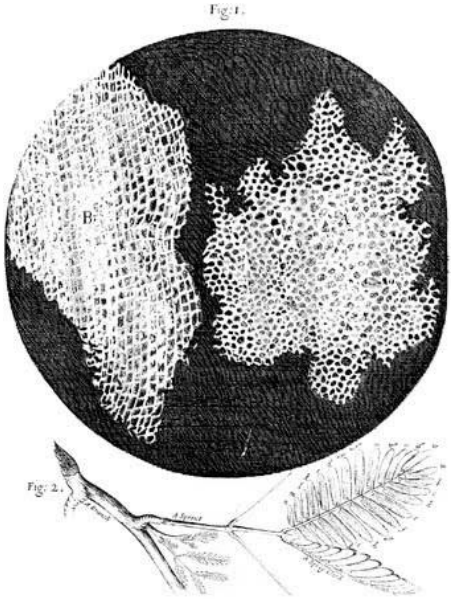

Figure 1.8. Micrograph of suberized cell walls in cork drawn by Robert Hooke. [113]

1.3.1 Suberin location and biological role

Suberized cell walls are found in different regions in the plant, such as the periderm, the hypodermis and endodermis of roots. The endodermis is an unicellular layer that separates the central cylinder of the root from the cortex, characterized by the presence of casparian strips (or bands), which are cell wall modifications composed mainly of lignin, and, to a lesser extent, suberin,[114] deposed in the radial and transverse cell walls of the endodermis of vascular plants which form a continuous cylindrical barrier within the root (Figure 1.9).[115] The hypodermis is a unicellular layer located directly underneath the rhizodermis, or root epidermis. By definition, a hypodermis that develops casparian strips is called exodermis.[116] After the casparian bands are mature in the exo- and endodermis, suberin is deposed in the inner face of primary cell walls in the form of sheets, known as suberin lamellae, which present a characteristic pattern of alternating dark and light bands in transmission electron microscopy (TEM), as seen in Figure 1.10.[110,112] Suberin may also be deposited in intermicrofibrillar spaces in the rhizodermis.[110] Some plant species do not develop any cell wall modifications after the deposition of suberized lamellae, but others grow another cell wall, which can be considered as a tertiary cell wall, composed mainly of polysaccharides and lignin. It is believed that this wall provide mechanical support in the root, although it has not been proven. Suberin is also produced as a response to wounds and environmental stresses, not only in previously suberized tissues, but also in organs normally protected by cutin.[117] This suggests that suberization is a universal response to wounding in all plant organs.[24] As a matter of fact, most of the studies about suberin have used skinned potato tubers as a model.[110,112]

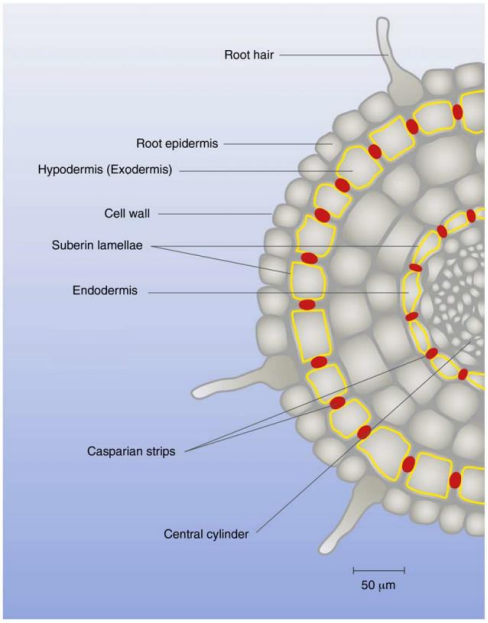

Figure 1.9. Transversal section of a root, showing the suberized exo- and endodermis cell walls as well as the casparian strips.[118]

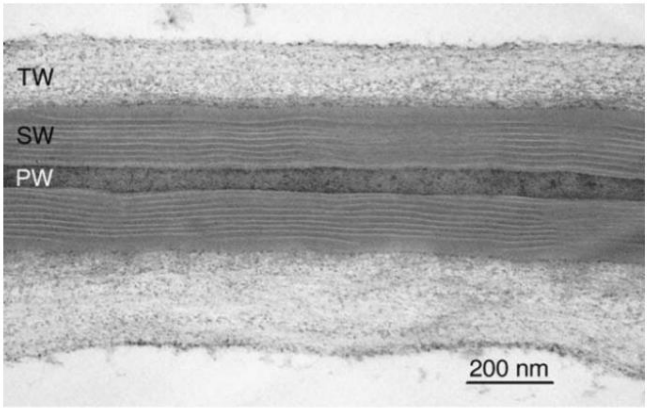

Figure 1.10. Transmission electron micrograph showing the lamellar structure of a suberized cell wall of potato tuber periderm. PW, primary cell wall; SW, secondary cell wall (suberin lamellae); TW, tertiary cell wall.[119]

The location and timing of suberin deposition speaks volumes about its physiological function. Suberin is deposited wherever the plant needs a barrier to prevent diffusion, whether it is between the plant and its environment or between different tissues within the plant.[110] The impregnation with suberin of unmodified cell walls significantly reduces the size of the intermicrofibrillar spaces and makes the walls much more hydrophobic, hence contributing to the regulation of apoplastic transport of water and solutes.

The plant root not only needs to take water and nutrients into the plant, but also have to block the entrance of toxic compounds and an excessive amount of water. The high hydrophobicity of the casparian bands suggests that they are a major barrier to control the movement of water to the stele. However, tests with maize (*Zea mays*) roots with injured endodermis did not show a significant increment in water flow through the endodermis, thus suggesting that an endodermis with just casparian bands (i.e. without suberized lamellae) does not act as a major water barrier, and needs the development of suberized lamellae to do so.[114] Exodermal suberized lamellae and casparian strips also restrict the movement of unwanted water, solutes and pathogens into the root. Plants can adjust the production of suberin in response to environmental stimuli, and thus regulate the apoplastic transport of water and solutes.[120] Casparian bands and suberized tissues have proven to be an affective barrier to ions, such as Hg^{2+},[121] Fe^{2+},[122] and Rb^{+}.[123] Plants are also capable of increasing the production of suberin as a response to salt stress. This was shown by ricinus (*Ricinus communis*), whose suberin content both in the exo- and endodermis was significantly increased by the presence of NaCl.[124] However, an unequal contribution of the casparian bands and the suberized lamellae as barrier against ions was found. Casparian strips seem to be fundamental to restrict Na^{+} ions in entering the shoot, while the suberized lamellae play a secondary, albeit useful, role in it.[125] Suberized cell walls are

capable of withstanding pathogen attack better than unmodified polysaccharide walls. Interestingly, there seems to be a difference in the antimicrobial features of the two domains of suberin. The aliphatic domain provides protection against fungus, while the aromatic domain offers a better protection against bacteria.[126]

Suberin not only restricts the entrance of undesired elements into the plant, but also impedes the backflow of water and solutes out of the stele,[110,116] allowing plants to build root pressure. Plants can respond to draught by increasing the production of suberin, which effectively reduces the amount of water loss.[127] Another important function of suberized tissues is the prevention of oxygen diffusion from the root to the anaerobic environment of the soil.[128,129] It was believed that both suberin and lignin were responsible of creating a barrier against oxygen diffusion, but a study with Amazonian wetland species showed a strong correlation between suberin content in the exodermis and the ability to prevent oxygen loss, while the amount of lignin did not appear to have any effect.[130]

1.3.2 Suberin monomeric composition

As it was stated previously, suberin is a complex polymer with two distinct domains: aliphatic and aromatic. The monomeric composition and the nature of the chemical linkages between them are radically different. Therefore, the challenges involved in the determination of their composition and the analytical tools used to overcome them are substantially different. The most common method to quantify the components of the polyaliphatic domain is similar to the one used to determine cutin composition. It consists on an organic solvent extraction to remove unpolymerized wax components, followed by hydrolysis of the ester bonds, whether by alkaline hydrolysis with NaOH, BF_3/MeOH transesterification or reduction with $LiAlH_4$, and GC-MS analysis of their TMS derivatives. The composition of the aliphatic domain of cutin varies widely between species, but it follows a recognisable pattern. The most common constituents of aliphatic suberin are long-chain α,ω-dicarboxylic acids and ω-hydroxy fatty acids, with a lesser amount of 1-alkanoic acids, fatty alcohols and glycerol. Suberin monomers vary in chain length from C16 up to C32[110], although the most common monomers belong to the C18 family. While the C16 and the very long fatty acid (≥ C20) monomers tend to be linear and unsaturated, C18 monomers are often unsaturated or mid-chain oxygenated. The stereochemistry of the double bond of one of the most abundant suberin monomers in a multitude of species, 18-hydroxy-octadec-9-enoic acid, remained elusive for decades. However, a careful analysis of Fourier transformation infra-red (FT-IR) spectroscopy and NMR of suberin monomers allowed to conclude that the totality of C18:1 acids in suberin have a *cis* configuration.[131] Table 1.1.2 provides a summary of the range of monomer content of aliphatic suberin found in a variety of species[6,109,132–138], as well as a specific example, the suberin of cork oak (*Quercus suber*). The different publications provide various degrees of detail when reporting the composition of suberin. While some disclose in detail the amount of each specific monomer, others simply report the composition of types of monomer (e.g. α,ω-dicarboxylic acid). Therefore, the purpose of the table is

merely to provide an insight of the range in which the most common suberin monomers appear in a variety of plants, together with the composition of a specific and well known suberin.

The chemical composition of the polyaromatic domain is more difficult to determine due to the nature of its chemical bonds and it has been a matter of debate for some time. The first attempts to analyse its components were done by cleaving the phenylpropanoids chains by alkaline nitrobenzene oxidation, which releases aromatic compounds representative of phenylpropanoids in the intact tissue, but that do not permit to confirm the identity of the parent compound.[112] More recent techniques for aromatic suberin degradation, including cupric oxide oxidation,[139] thioacidolysis[140] and derivatization followed by reductive cleavage,[141] have provided a better understanding of its composition.

Table 1.1.2. Range of aliphatic suberin monomers of various plants and suberin monomer composition of cork oak.[132] All values are given as a percentage (%) in weight.

	Suberin	***Q. Suber* peridermis suberin**
1-Alkanoic acids	0–11	1.1
Docosanoic acid (C22:0)	0–8	0.9
ω-Hydroxy fatty acids	13–61	16.8
16-Hydroxy-hexadecanoic acid (C16:0)	0–5	<1
18-Hydroxy-octadecanoic acid (C18:0)	0–3	<1
18-Hydroxy-9-octadecenoic acid (C18:1)	2–31	5.4
22-Hydroxy-docosanoic acid (C22:0)	0–8	7.9
α,ω-Dicarboxylic acids	2–46	45.5
Octadec-9-enedioic acid (C18:1)	4–15	6.2
9-Epoxyoctadecanedioic acid (C18:0)	0–23	22.9
9,10-Dihydroxyoctadecanedioic acid (C18:0)	0–17	7.7
Docosanedioic acid (C22:0)	1–5	4.5
Mid-chain oxygenated fatty acids	0–55	9.5
9,10,18-Trihydroxyoctadecanoic acid (C18:0)	0–29	2.2
9,10-Epoxy-18-hydroxyoctadecanoic acid (C18:0)	0–31	7.3
Fatty alcohols	0–11	0.4
Aromatic compounds	0–5	0.8
Glycerol	1–14	14.2

The polyaromatic domain of suberin is composed mainly of hydroxicinnamic acids with a smaller amount of monolignols. The relative amount of those two types of components changes in the different tissues of the root. The amount of monolignols increases when moving inwards from the rhizodermis, reaching almost 100% in the stele.[112]

1.2.4 Suberin biosynthesis

There have been significant advances in the understanding of suberin biosynthesis in the last decade, although many aspects of it remain obscure. Suberin is synthesized in specific tissues at certain stages of development or induced by external stimuli, and it follows an alternating pattern of aliphatic and aromatic domains. This suggest that its biosynthesis is tightly regulated, both at the cell and tissue level.[110] It has been revealed that the aromatic domain is deposited before the aliphatic domain,[126,142,143] which is supported by the earlier appearance of aromatic metabolites than long chain aliphatics in wound-healing potato tubers.[144]

Suberin monomers can be broadly classified in two groups: C18 ω-hydroxy and α,ω-dioic acid, and very long-chain (C20–C32) fatty acids derivatives. Therefore, it is expectable that ω-oxidation and chain elongation are the main features of their biosynthesis. In general terms, it follows the same pathway as cutin monomer biosynthesis (see section 1.2.3.1). Firstly, an enzyme of the LACS family catalyses the acylation of a fatty acid to CoA, which is then ω-hydroxylated and further oxidised to de corresponding diacids by cytochrome P450 enzymes, and finally is selectively acylated to the *sn*-2 position of glycerol by an enzyme of the GPAT family. There is controversy about the position of the chain elongation in this sequence, which can take place either before or after the ω-hydroxylation.[110]

Mutants of the cytochrome P450 monooxygenase CYP86A1 show a pronounced reduction in ω-hydroxylated C16 and C18 fatty acids, which in turn reduces significantly the total deposition of root suberin.[145–147] However, there was no appreciable reduction in the amount of very-long-chain (≥ 20) ω-hydroxylated and α,ω-diacids, suggesting the existence of specific enzymes responsible for their oxidation.[145,146,148] Chain elongation to produce very long chain fatty acids is regulated by components of the fatty acid elongation (FAE) complex, such as β-ketoacyl-CoA synthases (KCS). Very long fatty acids are synthesized by a series of FAE cycles to a pre-existing C18 fatty acid, each one of them consisting in four steps and resulting in the addition of two carbos, as is depicted in Figure 1.11. The FAE steps can be summarized as (i) condensation of malonyl-CoA with a long-chain acyl-CoA, (ii) reduction to β-hydroxyacyl-CoA, (iii) dehydration to enoyl-CoA, (iv) reduction; resulting in an elongated, reduced and saturated acyl-CoA.[149] The protein DAISY (Docosanoic AcId SYnthase) has also proven to be involved in the synthesis of C22 and C24 fatty acids in yeats.[150,151] *Arabidopsis daisy* and *kcs2* mutants are characterized by a reduction in C22 and C24 monomers in suberin, while C16, C18 and C20 monomers accumulate.[142] Furthermore, *DAISY* expression is co-localised in suberized tissues and is strongly induced by wounding, NaCl application and drought.[142] *DAISY/KCS2* is also expressed in other tissues, suggesting that suberization is not its only *in vivo* function. Another gene, *StKCS6* is involved in the elongation of fatty acid to produce C28 or higher suberin monomers. The suberin profile of tuber periderms in tomato plants downregulated in *StKCS6* presented a very pronounced reduction (50–95%) in C28 or higher monomers, while C26 or lower monomers accumulated.[119]

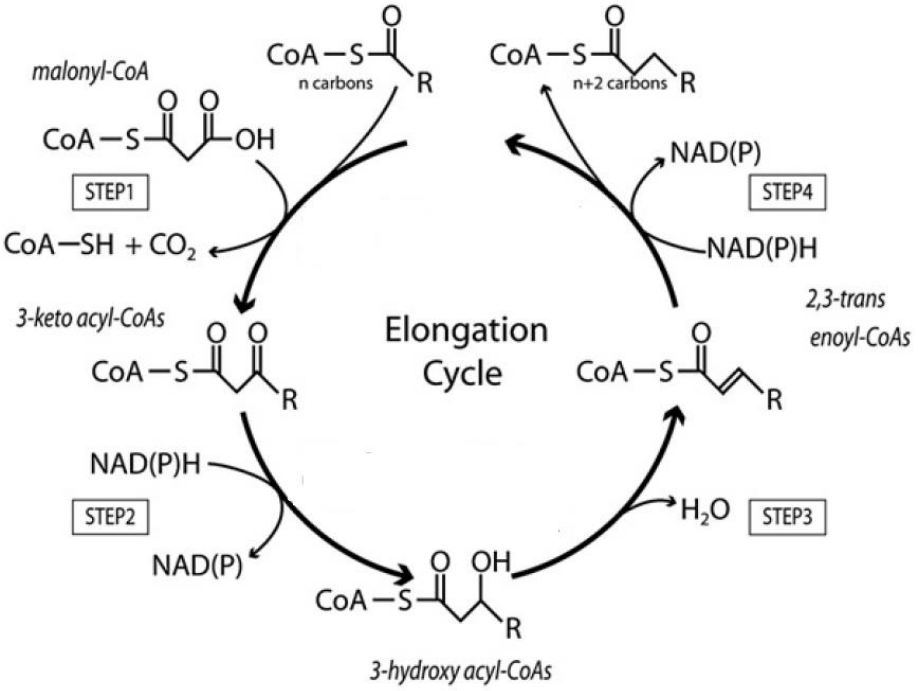

Figure 1.11. Fatty acid elongation cycle. Figure adapted from[152]

GPAT enzymes are necessary for the biosynthesis of suberin. As it was discussed previously (see section 1.2.3.1), this family of enzymes present glycerol-acyltransferase activity, generally with preference towards the *sn*-2 position, and some of them also present phosphatase activity. GPAT5 and GPAT7 have been proven to be involved in suberin biosynthesis and, unlike the GPATs associated with cutin biosynthesis, do not present phosphatase activity.[27] GPAT5 and -7 present a broad acyl-CoA specificity and are capable of accepting substrates ranging from C16 to C24 as well as ω-hydroxy, dicarboxylic and unsubstituted fatty acids, which contrasts with the specificity of GPAT4 and -6, which show a clear preference for C16 and C18 ω-hydroxy acyl-CoAs.[87] While GPAT5 have proven to be essential for suberin biosynthesis,[84,86,87] *gpat7* mutants did not reveal changes in the composition of suberin in *Arabidopsis* leafs, which suggests that GPAT7 might be more specialized in certain cells or as a response to wounding.[87]

The monomers from the aromatic domain are synthesized *via* the phenylpropanoids pathway (PPP), which is also responsible for lignin synthesis. Ferulic acid, a PPP intermediate, is thought to provide a link between the aromatic and the aliphatic domains. Enzymes of the BAHD family of acyltransferases are able to catalyse aliphatic feruloyzation using hydroxycinnamoyl-CoA esters as acyl donors, and are believed to be involved in suberin biosynthesis.[153] A gene from this family, *ASFT*, is highly upregulated in phellem tissue during seasonal cork growth periods, and mutants in *ASFT*/*AtHHT* present a complete absence of ferulic acid in the seed polyester.[154,155] Furthermore, the putative

orthologue FHT of potato have been proven to act as a ω-hydroxy fatty acid/fatty alcohol hydroxycinnamoyl transferase *in vitro*.[156]

The knowledge regarding monomer transport and suberin polymerization is very scarce. ABC transporters are likely responsible for aliphatic monomer transport to the polymerization site, as they are highly upregulated in the phellem tissue[157] and are co-expressed with suberin genes[155] One of those transporters, ABCG11 has been found to affect root suberin content.[158] The polymerization of the aliphatic domain is largely unknown, although it is likely that is a carefully controlled enzymatic process. The fact that GPAT proteins, which selectively produce 2-MAGs of very long fatty acids, are necessary for suberin biosynthesis, together with the recent discovery of the CUS family of enzymes, which are capable of polymerize extracellularly 2-MAGs of ω-hydroxy fatty acids, suggests that some enzymes of this family might be involved in suberin polymerization. However, GPAT5 and GPAT7 do not have phosphatase activity, which suggests that there might be other enzymes involved in the synthesis of 2-MAG derivatives or that the polymerization of suberin is due to a different family of enzymes.

1.2.5 Structure and Properties

Suberin presents a complex structure, whose molecular details remain largely unknown. At a macromolecular level, suberin presents a lamellar structure of alternating aliphatic and aromatic domains. One of the most recent models that explains suberin structure suggests that α,ω-diacids esterified to glycerol at both ends provides the basic backbone of the polymeric network.[109] ω-hydroxy fatty acids can be esterified simultaneously to glycerol and to ferulic acid, providing a link between the aromatic and the aliphatic domains (Figure 1.12).[133,159] $Ca(OH)_2$-catalysed methanolysis of cork periderm and subsequent elucidation of the obtained mono, di- and oligomeric units support this model. Some of the identified structures include glycerol esterified to ω-hydroxy and α,ω-dicarboxylic fatty acids, and ferulate esters of ω-hydroxy fatty acids.[160–162]

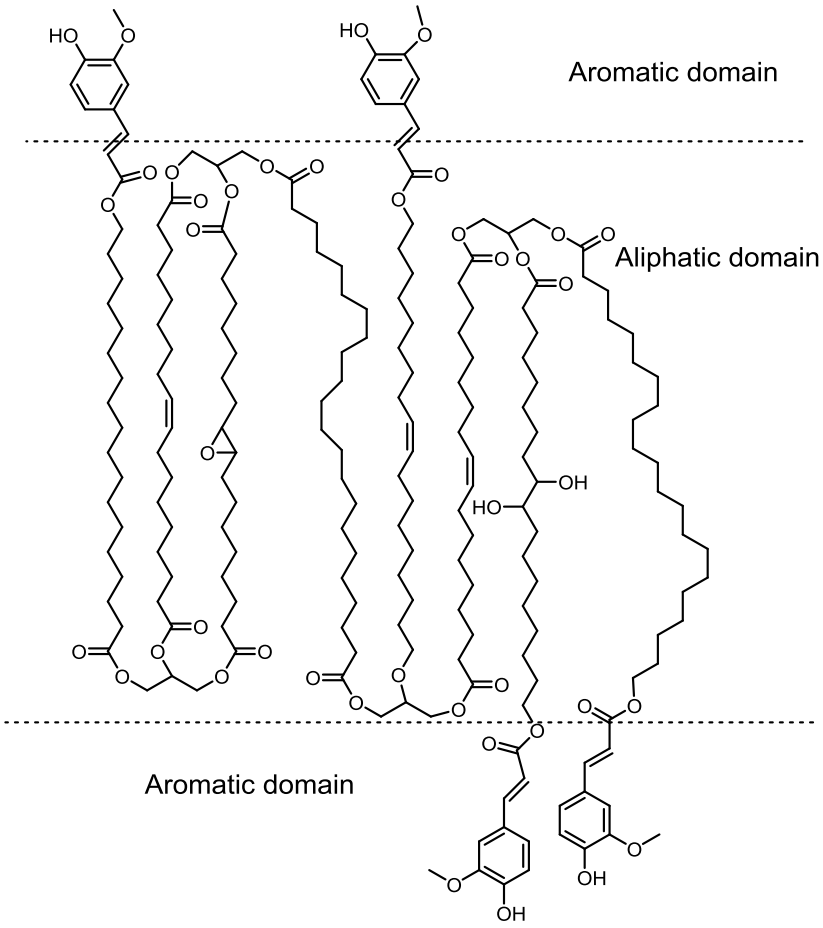

Figure 1.12. Macromolecular model for suberin lamella

The unique structure of suberin confers it the barrier properties discussed in Section 1.3.1. However, the mechanical and thermal properties of suberin are difficult to assess due to the difficulty of isolating intact suberin. Cordeiro *et al.* studied the properties of the oligomeric aliphatic remains of transesterified cork suberin after treatment with NaOMe.[163–165] This treatment breaks most of the ester linkages of suberin and removes the aromatic components, and therefore the results cannot be extrapolated to intact suberin. Differential Scanning Calorymetry (DSC) analysis of depolymerized suberin revealed the existence of a crystalline structure with a crystallization temperature (T_c) of 31 °C and a melting temperature (T_m) of 40 °C,[164] but no clear glass transition temperature was observed. This could indicate that the glass-liquid transition occurs in an interval of temperatures too wide to be detectable.[164] Rheological tests of depolymerized suberin are typical of a plastic response at room temperature due to the presence of crystalline domains, which is turned into a typical Newtonian behavior at 50 °C, when the crystals have melted.[164] Thermogravimetric analysis shows that depolymerized suberin has a good thermal stability up to approximately 270 °C,[166,167] which makes it

suitable to be used as an additive to commercial polymers by reactive extrusion. When added to high-density polyethylene (HDPE), depolymerized suberin acts as a plasticizer, improving the flexibility of the composite and reducing its stiffness.[166]

1.4 Comparison of cutin and suberin

Cutin and suberin present a series of evident similarities and are very often compared. Both polymers function as barriers to protect plants from external threats and desiccation, and present a similar aliphatic composition. Cutin and the aliphatic domain of suberin are hydrophobic polyesters composed mainly of hydroxy fatty acids, α,ω-dicarboxylic fatty acids and glycerol. Suberin fatty acids present a wider range of length, from C16 to C32, while the vast majority of cutin monomers are either C16 or C18. The presence of α,ω-dicarboxylic acids is scarce in most cutins, with the notable exception of *Arabidopsis* leaf cutin, but they are one of the major components of suberin. While glycerol is a component of both polymers, it is present in a higher degree in suberin and it is likely that it plays a more critical role there, due to the higher amount of dicarboxylic acids. These compositional differences, together with the existence of two distinct domains in suberin, affect the structure of the polymers, although the exact nature of their molecular structure is not well understood. Cutin is found exclusively as a component of the cuticle, located in the outermost layer of leaves, fruits and primary shoots. Suberin, on the other hand, can be found in different tissues, normally in the endo- and hypodermis of roots or the periderm, as well as in the wound periderm. Despite the differences in composition and location within the plant, cutin and suberin have a similar function and present comparable properties as barriers to prevent water and gas diffusion. A detailed comparison between cutinized and suberized cell walls can be found in Table 1.1.3.

Table 1.1.3. Similarities and differences between cutinized and suberized cell walls. Table adapted from[118]

	Cutinized cell wall	Suberized cell wall
Ocurrence	• Primary plant organs (leaves, fruits and primary shots)	• Primary plant organs: (endodermis and hypodermis of roots, bundle sheaths of leaves) • Secondary plant organs (shoot and root periderm) • Wound periderm
Anatomical structure	• Thin extracellular polymer layer	• Unicellular tissues (endodermis, hypodermis, bundle sheaths) • Multi-cellular tissues (periderm, hypodermis)
Polymer deposition	• Extracellular polymer layer of cutin deposited on the outer epidermal cell wall surface of leaves, fruits and primary shoots	• In the case of Casparian strips, suberin is deposited into the radial primary endodermal cell walls • Suberin lamellae are deposited as a polymer layer onto the inner surface of the primary cell wall, thus separating the cell wall from the plasma membrane (endodermis and hypodermis, peridermal cells, bundle sheaths)
Polymer chemistry	• Polymer of mostly saturated aliphatic oxygenated fatty acids with predominant chain lengths of C16 and C18	• Polymer composed of a poly-aliphatic domain (saturated and unsaturated aliphatic oxygenated fatty acids with chain lengths ranging from C16 to C32) and a poly-phenolic domain (monolignols, hydroxicinnamic acid and their derivatives)
Occurrence of waxes	• Linear long-chain aliphatic molecules belonging to different substance classes (e.g. alkanes, alcohols, acids, esters) and pentacyclic triterpenoids • Waxes are deposited into and onto the cutin polymer	• Present in periderms (e.g. potato periderm) facing the atmosphere with a pronounced water-vapour saturation deficit • Not present in suberized root tissues of primary roots (e.g. suberized endodermis and hypodermal cell walls) • Linear long-chain aliphatic molecules belonging to different substance classes (e.g. alkanes, alcohols, acids, esters) and alkyl ferulates • Waxes are deposited into the suberin polymer
Efficiency of the barrier	• In general, highly efficient barrier; however, not absolutely impermeable to water and gases • Barrier properties between different species can vary by a factor of 100-fold • Barrier properties are lost upon wax extraction	• Potato tuber periderm with wax deposition has barrier properties similar to the cuticle • Barrier properties are lost upon wax extraction • Suberized root cell walls without wax deposition have much higher permeabilities than cuticles and potato tuber periderm

2. Synthesis of isotopically labelled 10-hydroxy 2-MHG for the study of CUS1 specificity

2.1 Goals and scope of the project

The discovery of the CUS family of enzymes has been a major milestone in the understanding of cutin biosynthesis, but it opens new questions as much as it answers old ones. Two of the most abundant monomers in tomato cutin are 10,16- and 9,16-dihydroxyhexadecanoic acids, which only differ in the position of the secondary hydroxyl group. CUS1 has proven to polymerize the 2-MAG derivative of 10,16-dihydroxyhexadecanoic acid, 10-hydroxy 2-MHG, *in vitro*, but it is not known whether this enzyme is able to accept the other 2-MAG derivative, 9-hydroxy 2-MHG, as a substrate. In case 9-hydroxy 2-MHG acts as a substrate, it is not known whether CUS1 presents any preference towards one of the two monomers. Moreover, it is not possible to determine any substrate preference by performing a combined polymerization of 9- and 10-hydroxy 2-MHG and analysing the products by MALDI-TOF, because both monomers have exactly the same mass.

The goal of this project is to answer this question of specificity by the of synthesis deuterium-labelled 10-hydroxy 2-MHG and its further use as a substrate for CUS1, together with ordinary 9-hydroxy 2-MHG, to form combined oligomers and the assessment of their relative abundance by MALDI analyses. In order to assess any influence of the deuterium over the reactivity of CUS1, the inverse experiment, using ordinary 10-hydroxy 2-MHG and deuterium-labelled 9-hydroxy 2-MHG was also planned. The synthesis of the 9-hydroxy derivatives was performed by another PhD student working in the group, Gauthier Scavée, and the polymerization reactions were performed in collaboration with him.

Furthermore, the developed synthetic route for deuterium labelled 10-hydroxy 2-MHG was also used to synthesize tritium-labelled 10-hydroxy 2-MHG. The radioactivity of tritium would potentially enable monitoring transport/location of the monomer *in planta*, and thus it could provide invaluable aid to understand the transport of cutin monomers to their polymerization site.

2.2 Synthesis of isotopically labelled 10-hydroxy 2-MHG

One of the first steps in the synthesis of 10-hydroxy 2-MHG developed by Dr. Hélène Viart[22] consists of a coupling between the terminal alkyne **2** with the aldehyde resulting from the oxidation of the alcohol **1** by Swern oxidation, affording in the propargylic alcohol **3**, which is then protected with a *tert*-butyldimethylsilyl (TBS) group. Subsequent removal of the benzyl ether by hydrogenolysis also reduces the triple bond, and the synthesis continues with a linear alkane chain thereafter as is shown in Scheme 2.1.

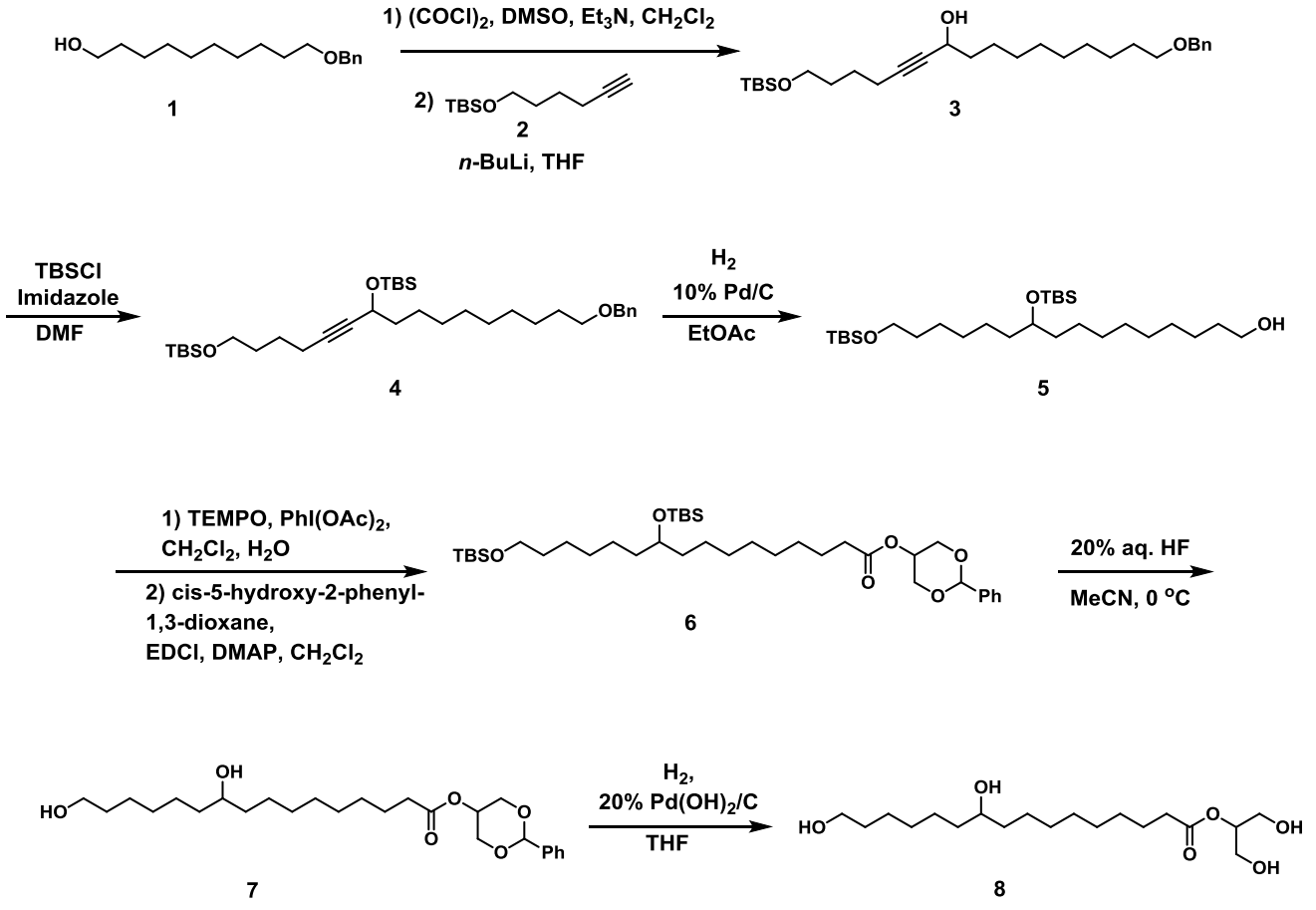

Scheme 2.1. Synthesis of 10-hydroxy 2-MHG. Scheme adapted from ref 22

The first synthetic strategy that was developed to produce isotopically labelled 10-hydroxy 2-MHG was inspired by this synthesis, and relied on maintaining the triple bond through the synthesis, which can be reduced from compound **11** with deuterium or tritium while simultaneously removing the benzylidene acetal, as is shown retrosynthetically in Scheme 2.2, resulting in the corresponding tritium or deuterium-labelled product **9** or **10**. This route requires the use of a different protecting group for the starting diol. This new protecting group must fulfil a series of conditions: it must be orthogonal to TBS, must withstand the basic conditions of the coupling with *n*-BuLi and must be removed without disturbing the triple bond. 2-Naphthalene ether (NAP) was the obvious choice as it has a similar reactivity to benzyl ether, but it can be removed oxidatively with DDQ.[168]

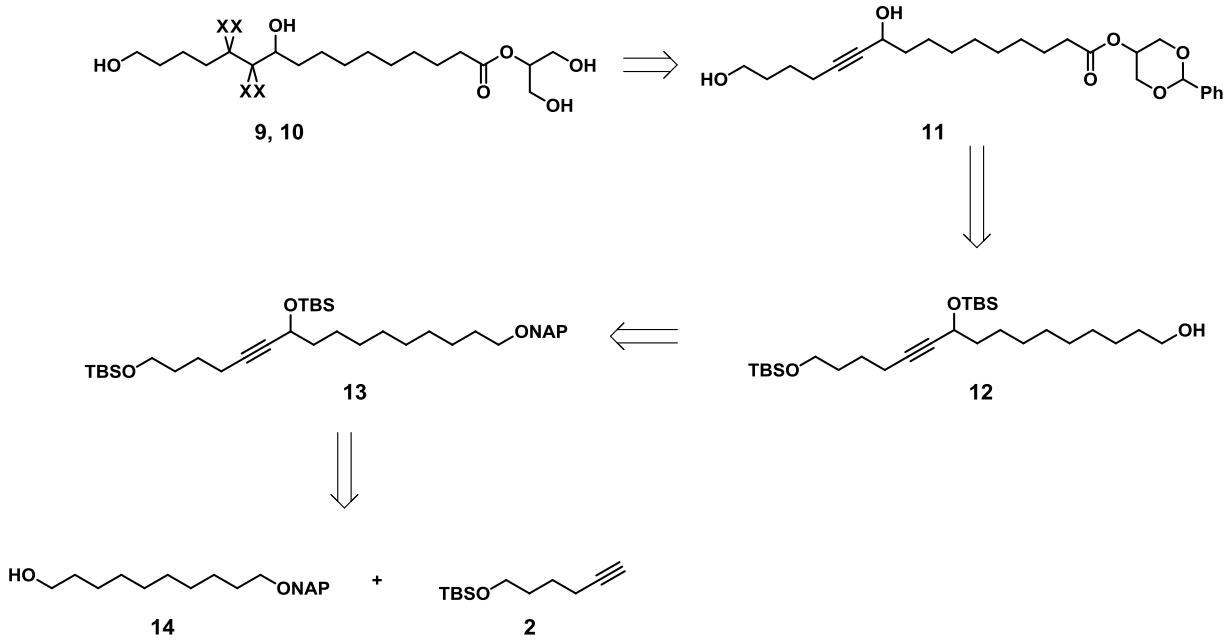

Scheme 2.2. Retrosynthetic analysis for isotopically labelled 10-hydroxy 2-MHG. **9**: X = D, **10**: X = T

Protection of one hydroxyl of 1,10-decanediol with NAP produced **14** in good yield. The other hydroxyl was oxidised to the aldehyde *via* Dess-Martin oxidation, which was preferred over the Swern oxidation used in the original synthesis due to its ease of preparation and excellent yield.[169] The resulting aldehyde was reacted with **2** and *n*-Buli in THF, producing in the propargylic alcohol **16** in good yield. The secondary alcohol was TBS-protected with TBSCl and imidazole to give **13** in 71% yield. The NAP group was then removed oxidatively with DDQ and H_2O to give the free primary alcohol **12**. The yield of this reaction turned out to be highly variable, ranging from 40% to 75% (Scheme 2.3). The cause of this fluctuation was not identified, but is suspected to arise from loss of material during the work-up.

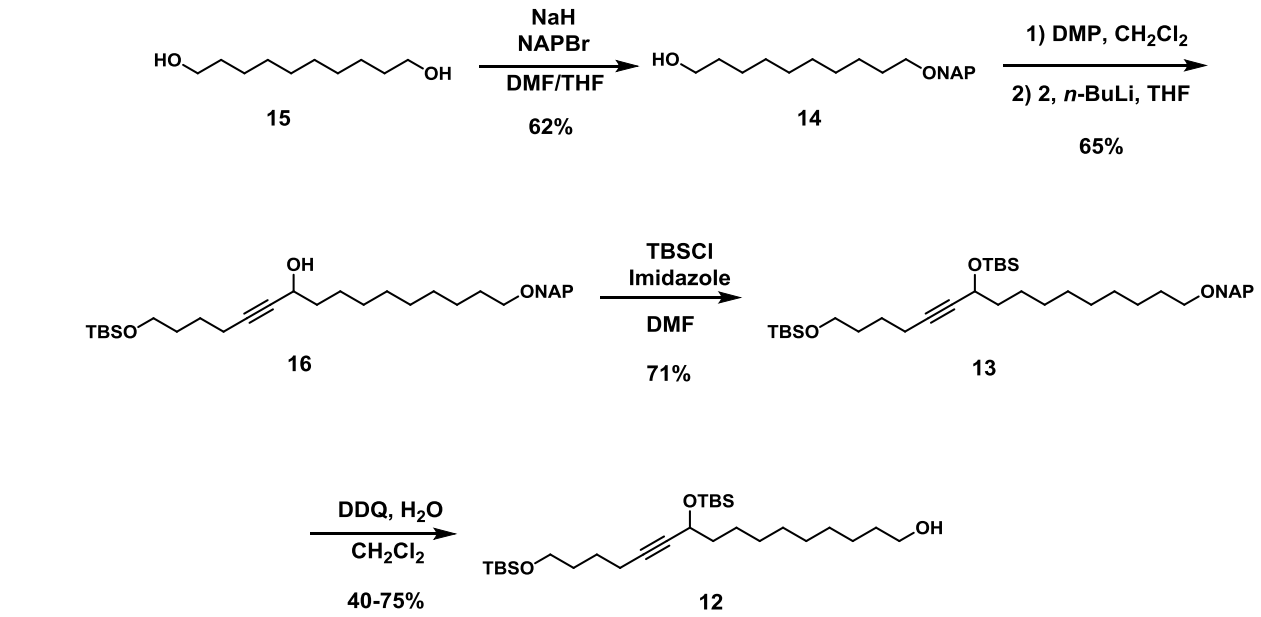

Scheme 2.3. Synthesis of the primary alcohol **12**

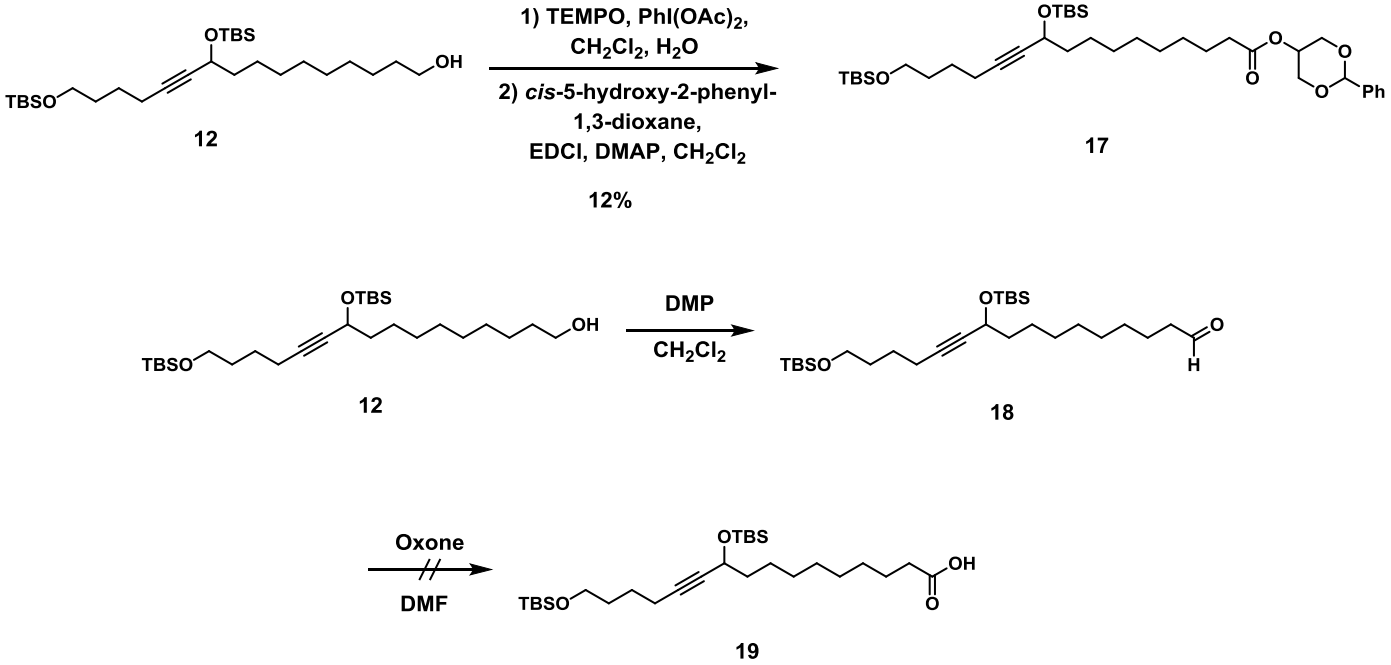

Scheme 2.4 Attempted synthesis of the intermediate ester **17**

Further oxidation of the primary alcohol **12** to the corresponding carboxylic acid with 2,2,6,6-tetramethylpiperidine 1-oxy (TEMPO) and $PhI(OAc)_2$ in CH_2Cl_2 and H_2O, followed by an esterification with the 1,3-protected glycerol *cis*-5-hydroxy-2-phenyl-1,3-dioxane by Steglich esterification with *N*-(3-dimethylaminopropyl)-*N´*-ethylcarbodiimide hydrochloride (EDCl) and 4-dimethylaminopyridine (DMAP) in CH_2Cl_2 only produced ester **17** in very low yields (12%) (Scheme 2.4). In order to overcome this, a new strategy was attempted, consisting on a two-step oxidation process, from the alcohol to the aldehyde by Dess-Martin oxidation followed by oxidation to the carboxylic acid with Oxone ($2KHSO_5 \cdot KHSO_4 \cdot K_2SO_4$) in DMF according to the procedure by Travis *et al.*[170], but no product was recovered. A plausible explanation is that the treatment with HCl during work-up caused the removal of the TBS groups, despite that diluted HCl (1%) was used as an attempt to avoid this issue. A new strategy for the oxidation to the carboxylic acid was attempted by the Pinnick process, with $NaClO_2$, NaH_2PO_4 and 2-methyl-2-butene in *t*-BuOH and H_2O,[171] as can be seen in Scheme 2.5. The resulting carboxylic acid was was reacted with *cis*-5-hydroxy-2-phenyl-1,3-dioxane by Steglich esterification to obtain **17** in 40% yield. Both TBS groups were deprotected with 20% aq. HF at 0 °C for 4 h, producing diol **11** in a 55% yield.

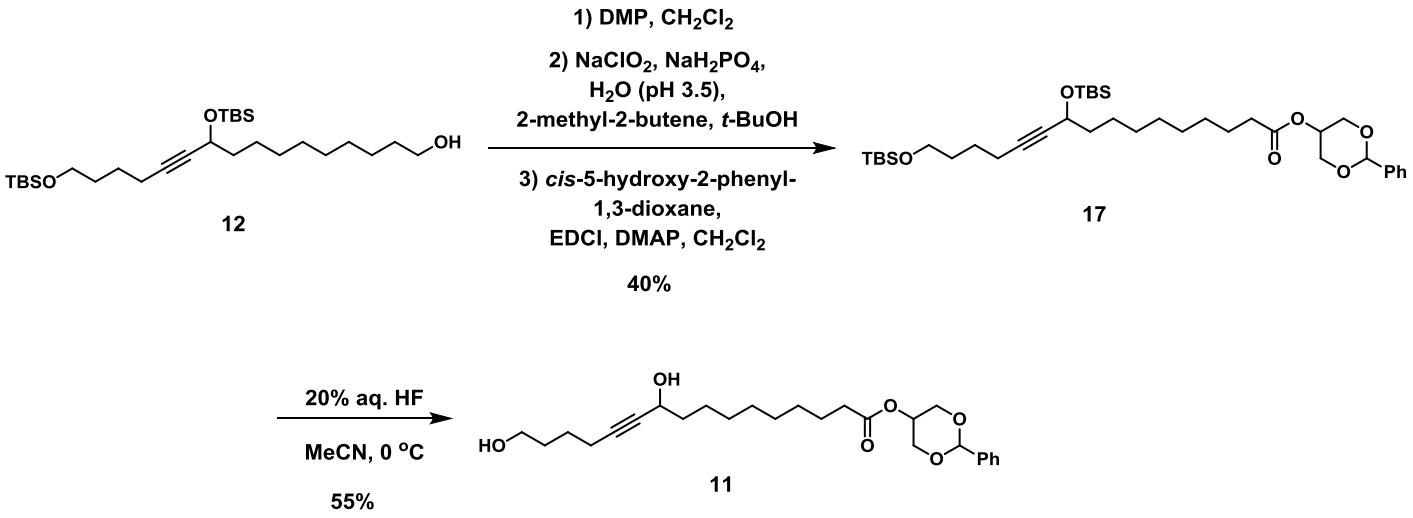

Scheme 2.5. Last steps in the synthesis of the deuterated produvt **9**

The last step for the synthesis of deuterium-labelled 10-hydroxy 2-MHG was the reduction of the triple bond of compound **11** with deuterium gas and the concomitant cleavage of the benzylidene group. As in the original 2-MHG synthesis, Pearlman´s catalyst[172] was used to ensure mild reaction conditions and mitigate the possibility of migration of the acyl group to one of its primary alcohols. Extreme care was taken during the recrystallization of the product due to its tendency of migration.

^{1}H NMR of the product revealed a small triplet at 2.46 ppm, next to the signal corresponding to the ester, which integrates to 0.4 as can be seen in Figure 2.1. This was initially attributed to migration of the glyceryl moiety, but no signals of a primary glyceryl ester were appreciable and HPLC-ELS analysis did not show presence of the migrated product. A possible explanation for this is that Pd(II) act as a Lewis acid, promoting a Meyer-Schuster rearrangement of the propargylic alcohol, and forming an α,β-unsaturated ketone.[173] The unsaturation of the product would then be readily reduced by deuteration, leading to 1,3-dihydroxypropan-2-yl 16-hydroxy-12-oxohexadecanoate-10,11-d_2, as is depicted in Scheme 2.6.

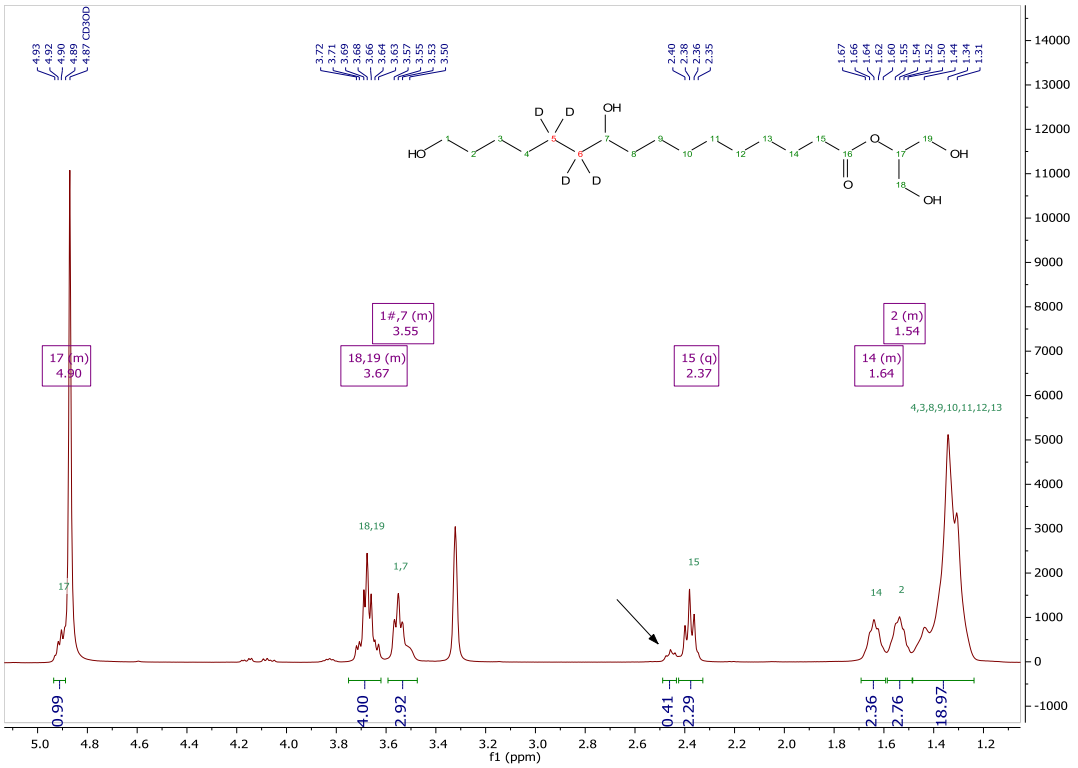

Figure 2.1. ^{1}H NMR spectrum of compound **9**

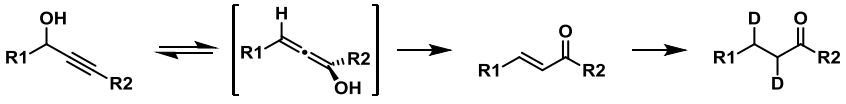

Scheme 2.6. Meyer-Schulter rearrangement and deuteration of the product

Another problem with the deuteration arose when HRMS of the product was conducted. The mass spectra showed a peak at 389 m/z, which corresponds to the sodium adduct of the desired product. However, it also showed the presence of 388, 387, 386 and 385 m/z peaks, which correspond with the incorporation of 3, 2, 1 and 0 deuterium atoms, respectively (Scheme 2.7). This result implies the presence of an alternative source of hydrogen that was incorporated together with deuterium. This source of hydrogen was not identified, but it was speculated that it could come from the C-H bonds on the surface of the carbon catalyst support.

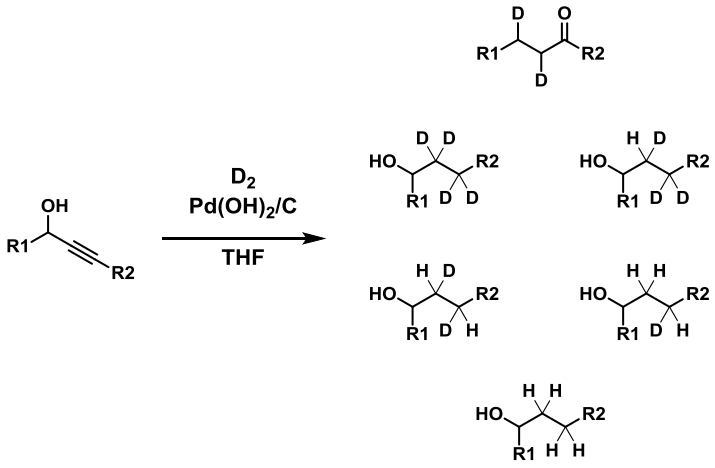

Scheme 2.7. Attempted synthesis of d_4-labelled 10-hydroxy 2-MHG

Given that this deuterization produced an inseparable mixture of deuterium-labelled products, it could not be used to study CUS1 specificity, as the polymerization with 9-hydroxy 2-MHG would produce a mixture of oligomers with an inapprehensible pattern of masses.

Due to the lack of facilities to handle radioactive materials at DTU, tritium labelling of diol **11** was performed by a specialized company, Quotient Bioresearch. The radioactivity of tritium makes manual handling of the product impossible, and therefore purification by recrystallization is inadvisable. Instead, an automated method of purification, such as HPLC, is preferred. The sensitivity of 2-MHG towards migration cast doubts about the feasibility of such method, and thus it was tested prior to the reaction. After several attempts, a HPLC method with enough resolution to separate 2-MHG from its migrated derivative (which will be referred to as 1-MHG hereafter) was developed (see Section 6.1). To test the feasibility of the method, pure 1-MHG was prepared by dissolving 2-MHG in methanol and letting it stand at 20 °C for 24 h, and pure 1- and 2-MHG and a 1:1 mixture of the two were analysed. As can be seen in Figure 2.2, the mixture of isomers was separated with very good resolution, and the amount of migration of pure 2-MHG resultant from passing through the column was neglectable.

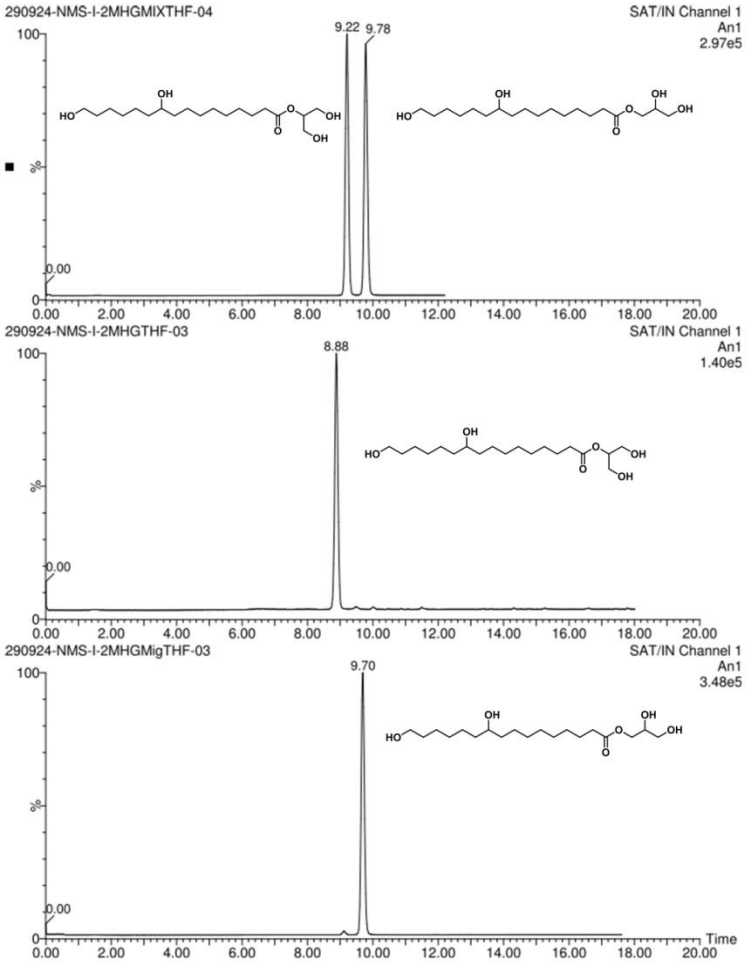

Figure 2.2. HPLC chromatograms of a mixture of 1- and 2-MHG (top), pure 2-MHG (middle), pure 1-MHG (below)

With the assurance of having a suitable method to purify the radioactive material, tritium labelling of diol **11** was performed by Quotient Bioresearch. The reported radiochemical purity of the product by HPLC was 91.6%, yet HRMS showed once more a mixture of labelled products with various degrees of incorporation of tritium. Nevertheless, the tritiated product can still be useful in the study of monomer transport *in planta*, by monitoring its movement due to its radioactivity.

A new synthetic strategy based on the original synthesis of 2-MHG was developed. Dr. Hélène Viart reported in her PhD thesis that treatment of the ester **6** with tetrabutylammonium (TBAF) only resulted in the cleavage of the terminal TBS group.[174] This selective deprotection allows the controlled labelling with a single deuterium atom by oxidizing the free alcohol *via* Dess-Martin oxidation, followed by reduction of the aldehyde with sodium borodeuteride. The final part of the synthesis is analogous to the

original, with deprotection of the secondary TBS group with 20% HF and final hydrogenolysis of the benzylidene acetal.

The synthesis of intermediate **6** was performed following the already mentioned procedure, starting from the protection of one hydroxyl of 1,10-decanediol by benzylation in 51% yield. The other hydroxyl was oxidised with Dess-Martin periodinane (DMP) in CH_2Cl_2 and the resultant aldehyde was reacted with the terminal alkyne **2** and *n*-BuLi to produce the propargylic alcohol **3** in 53% yield. The protection of the free hydroxyl with TBSCl and imidazole and the hydrogenolysis of the benzyl ether and reduction of the triple bond by palladium-catalysed hydrogenolysis/hydrogenation were achieved in excellent yields. The resulting alcohol was oxidised with $PhI(OAc)_2$ and TEMPO in CH_2Cl_2 to the carboxylic acid and it was then esterified with *cis*-5-hydroxy-2-phenyl-1,3-dioxane by Steglich esterification to produce **6** in a 44% yield. The selective deprotection of the terminal TBS group with TBAF in THF was performed in excellent yield. The free alcohol of compound **21** was oxidised to the aldehyde by means of Dess-Martin oxidation, and the product was reduced again with sodium borodeuteride in very good yield to produce the deuterium-labelled alcohol **22,** as can be seen in Scheme 2.8. ^{1}H and ^{13}C NMR spectra indicated the presence of deuterium. The peak corresponding to carbon 16 in the ^{13}C NMR spectrum had a much lower intensity and was split in three. The presence of the deuterium atom was furthermore confirmed by HRMS. The synthesis was finalised by the removal of the secondary TBS group of **22** with 20% aq. HF in MeCN to form compound **23** and the hydrogenolysis of the benzylidene acetal of the diol to form the final product **24**, which were achieved in 66% and 44% yield, respectively.

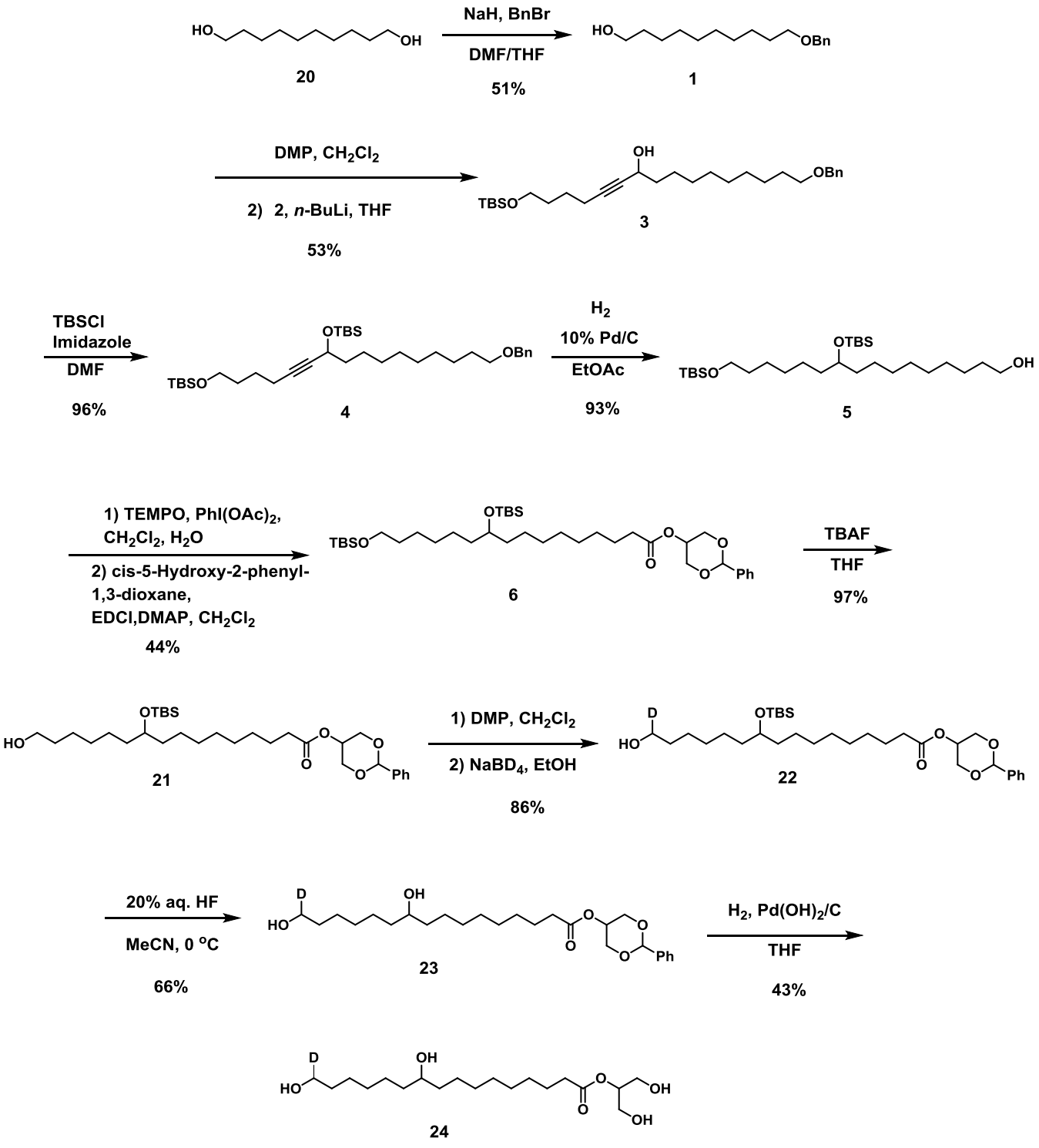

Scheme 2.8. Synthesis of deuterium-labelled 10-hydroxy 2-MHG (**23**)

2.3 Study of CUS1 specificity

The specificity of CUS1 towards the position of the mid-chain hydroxyl was tested by performing a series of enzymatic experiments in the same conditions as the reported 10-hydroxy 2-MHG oligomerization. A summary of the enzymatic experiments and the compounds used as substrates is displayed in Table 2.1.
9-Hydroxy 2-MHG and its respective deuterium-labelled derivative were synthesized by other member of the group, Gauthier Scavée, following an analogous procedure to the one for 10-hydroxy 2-MHG. The negative controls were performed in the absence of enzyme in order to prove that the polymerization in the corresponding assays is due to CUS1 activity and not due to spontaneous polymerization of the substrates. All positive tests that included a deuterated substrate were performed in triplicates, and all the others in duplicate. Figure 2.3 shows the molecules used in these experiments.

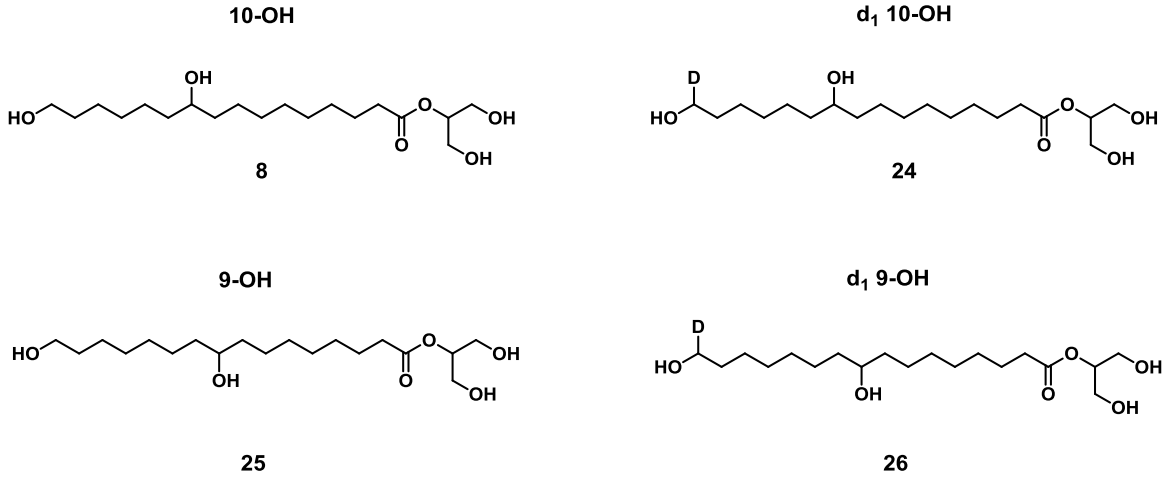

Figure 2.3. Deuterated and non-deuterated 10- and 9-hydroxy 2-MHG used in the enzymatic experiments

Table 2.1. Experiments for the study of CUS1 specificity towards the position of the mid-chain alcohol of dihydroxyhexadecanoic acid. All experiments were performed accordingAbbreviations: 10-H, 10-hydroxy 2-MHG; 9-H, 9-hydroxy 2-MHG; d_1 10-H, deuterium-labelled 10-hydroxy 2-MHG; d_1 9-H, deuterium-labelled 9-hydroxy 2-MHG

Experiment	**1**	**2**	**3**	**4**	**5**	**6**	**7**	**8**	**9**	**10**
CUS1	+	-	+	-	+	+	+	+	-	***-e***
Substrate	10-H	10-H	9-H	9-H	d_1 10-H	d_1 9-H	d_1 10-H + 9-H	10-H + d_1 9-H	d_1 10-H + 9-H	10-H + d_1 9-H

The products of all assays were analysed by MALDI-TOF. The results show that 9-hydroxy 2-MHG is a substrate of CUS1 and form oligomers of up to six monomeric units. In fact, the mass spectrum presents the same pattern as the one for the 10-hydroxy 2-MHG experiment, which suggests that CUS1 does not take into account the position of the mid-chain hydroxyl group. Deuterium-labelled 9- and 10- hydroxy 2-MHG were also successfully oligomerized, and presented the same pattern in their mass spectra (Figure 2.4), suggesting that the presence of deuterium in the terminal hydroxyl does not have an effect on the polymerization.

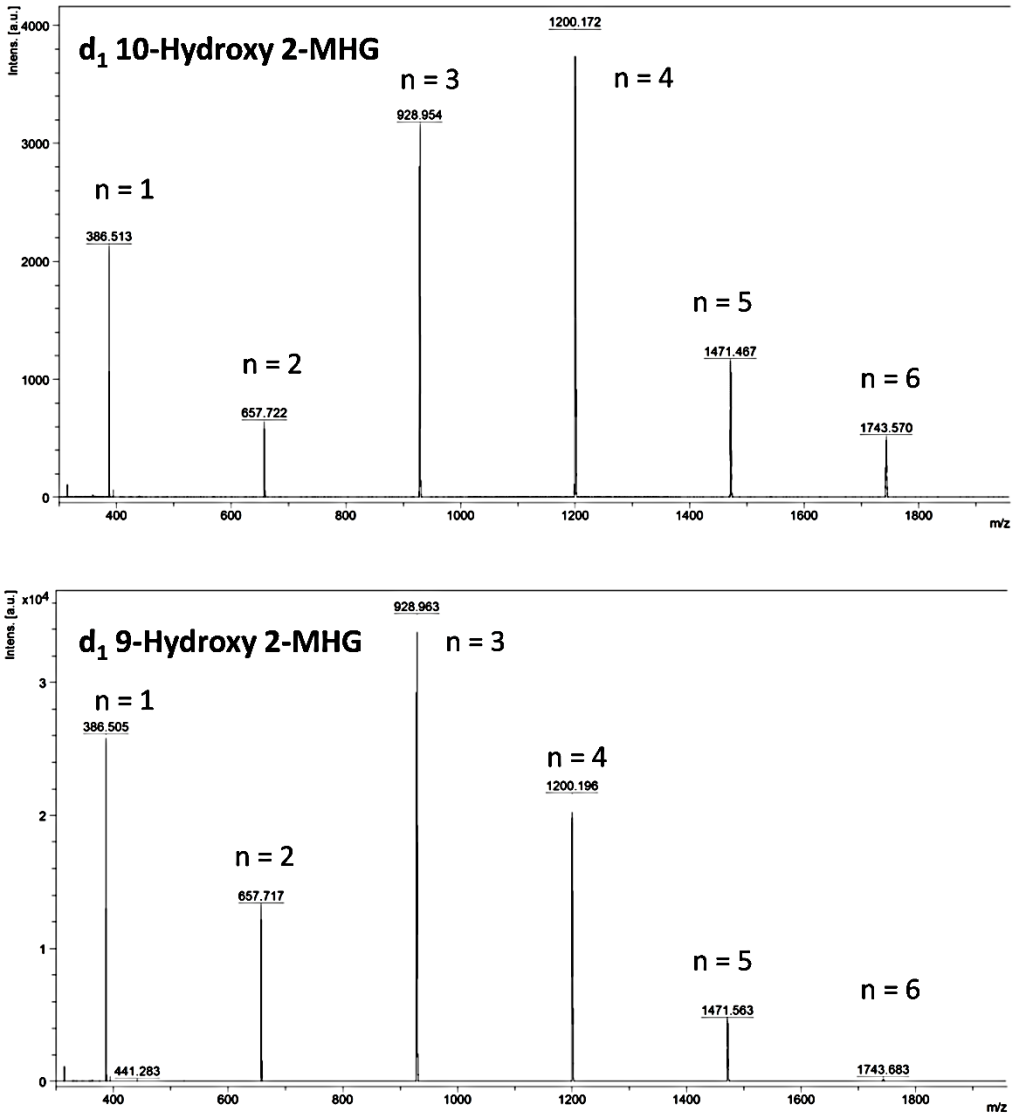

Figure 2.4 MALDI-TOF mass spectra of oligomers from *in vitro* assays of deuterium-labelled 10-hydroxy 2-MHG (above) and deuterium-labelled 9-hydroxy 2-MHG (below) as substrates for CUS1. n = degree of polymerization

Oligomers with three or more units present a split pattern in their peaks which is characteristic of compounds with a large number of carbon atoms. This is due to the presence of ^{13}C, which constitutes approximately 1.1% of the carbon atoms. Compounds with a large number of carbon atoms present a larger probability of having one or more ^{13}C atoms, which is reflected in the mass spectrum as the aforementioned split pattern. For example, the trimer of 2-MHG has 51 carbon atoms, which confers it approximately a 57% chance of not having any ^{13}C, a 25% of having a single ^{13}C and a 18% of having two or more ^{13}C. However, its corresponding region in the mass spectrum presents only two peaks, which correspond to the molecules with zero or one ^{13}C atoms. Trimers with a higher amount of ^{13}C atoms were not present in quantities large enough to be detected. The pattern of those peaks only provides a rough indication of the relative abundance of each adduct, as MALDI-TOF is not sensitive enough to be used as a quantitative method.

The enzymatic oligomerizations combining 9- and 10-hydroxy 2-MHG were set to determine which one, if any, is preferred by CUS1. In order to know how many units of each monomer are present in the oligomers, one of them was labelled with deuterium while the other was maintained in its natural form. Two experiments were prepared, with either 9- or 10-hydroxy 2-MHG as the deuterated species, in order to assess any influence that the deuterium could have in the reaction rate.

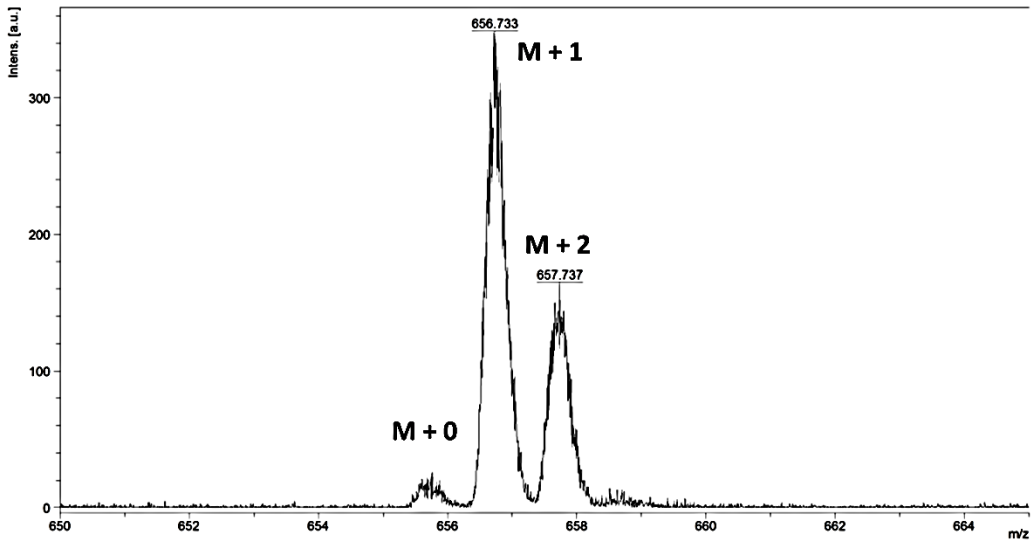

Figure 2.5. Zoom in the dimer region of the MALDI-TOF-mass spectrum of Experiment 8 (see Table 2.1).

The mass spectra of both mixtures of oligomers present the same pattern. The split pattern of each peak was more complex for the mixtures than for the pure compounds, as it does not only reflect the relative amount of ^{13}C isotopes in each oligomer, but the relative amount of deuterated and non-deuterated

monomers. For example, the region corresponding to the dimer in Experiment 8, in which the deuterated species was 9-hydroxy 2-MHG, was split in three as is seen in Figure 2.5. The first peak, which corresponds to M + 0 dimers (that is, dimers that do not contain any ^{13}C or deuterium atom), is barely noticeable, while the other two (corresponding to M + 1 and M + 2 dimers, respectively) are much more intense. The M + 1 peak is the most intense and the M + 2 peak is roughly half of its size. The M + 0 peak corresponds exclusively to homo-dimers of 10-hydroxy 2-MHG, the M + 1 peak corresponds to either hetero-dimers or homo-dimers of 10-hydroxy 2-MHG with a single ^{13}C and the M + 2 peak can correspond to homo-dimers of 9-hydroxy 2-MHG, hetero-dimers with a single ^{13}C or homo-dimers of 10-hydroxy 2-MHG with two ^{13}C atoms.

Assuming that CUS1 does not differentiate between both substrates, a random distribution of dimers is to be expected. In this case, and taking into account that 1.1% of the carbon atoms would be ^{13}C isotopes, approximately 17% of dimers would be M + 0, 39% would be M + 1, 30% would be M + 2 and 14% would be M + 3 or higher. The intensity of M + 1 and M + 2 peaks in experiment 8 is higher than would be expected in a random distribution, which could suggest that CUS1 presents a certain preference towards 9-hydroxy 2-MHG. However, if that were the case, the peak corresponding to M + 3 dimers would also be more intense. Furthermore, the mass spectrum of the dimer in experiment 7, in which the 10-hydroxy was the deuterated species, presents exactly the same pattern. It is likely that the distribution is in fact random, and that MALDI-TOF is simply not sensitive enough to detect the dimers occurring in lesser amounts.

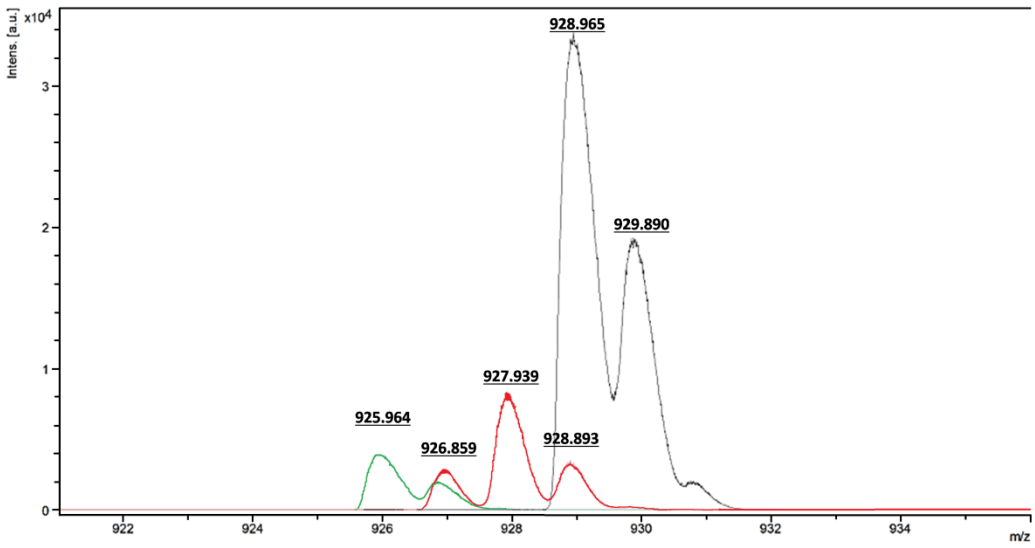

Figure 2.6 Comparison of the trimer region of the MALDI-TOF-mass spectra between experiments 1 (green), 7 (red) and 6 (black)

A close analysis of the pattern of the triplet peaks support the idea that CUS1 does not differentiate between the two substrates. Figure 2.6 shows a comparison of the mass spectra in the trimer region of experiments 1 (green), 7 (red) and 6 (black). In this occasion, the peak corresponding to the M + 0 trimer does not appear in the experiment with combined substrates, the M + 1 and M + 3 peaks are roughly equal in size and the most intense peak corresponds to the M + 2 adduct. This result matches what would be expected if both monomers would be assembled randomly. In that case, the M + 1 and M + 3 adducts would constitute approximately 24 and 22% of the total amount of trimers, respectively, and the M + 2 adduct would be the most common, constituting 32% of the total. The M + 0 and M + 4 would be present in 7 and 10%, respectively, and would probably not be detected. The mass spectra of oligomers with more than three units present more complex patterns, as the probability of finding ^{13}C atoms and the possible combinations increase, but it consistently presented the same pattern in both monomeric mixtures. The negative controls did not present any trace of oligomerization, which proves that ester formation in the positive experiments was due to the action of CUS1. This results suggest that CUS1 does not differentiate between 9- and 10-hydroxy 2-MHG, and is likely to be responsible for the polymerization of both substrates.

2.4 Conclusions

Two new routes for the synthesis of isotopically-labelled 10-hydroxy 2-MHG, based on the previous synthesis of the non-labelled product, have been developed. The first synthesis relayed on the introduction of hydrogen isotopes *via* reduction of a triple bond, and yielded a mixture of products with a diverse number of isotopes. Thus, this route was not feasible for the synthesis of deuterium-labelled 10-hydroxy 2-MHG used for the study of CUS1 specificity. Nonetheless, it is successful for the synthesis tritium-labelled 10-hydroxy 2-MHG, as its potential use for the study of 2-MHG transport *in planta* would likely not be affected by the presence of a mixture of deuterium-labelled species. The second synthetic route produced 10-hydroxy 2-MHG labelled with a single deuterium atom by selectively removing the terminal TBS group of compound **6**, oxidizing the resultant free alcohol to the corresponding aldehyde and reducing back the aldehyde to the alcohol by use of sodium borodeuteride.

A series of *in vitro* enzymatic oligomerizations using 9- and 10-hydroxy 2-MHG and their respective deuterium-labelled derivatives as substrates for CUS1 were performed and their products were analysed by MALDI-TOF. CUS1 showed activity both with 9- and 10-hydroxy 2-MHG and their labelled derivatives. Two different oligomerizations, combining 9- and 10-hydroxy 2-MHG as substrates, in which one of the two monomers was in its deuterium-labelled form, were performed.

Both oligomerizations showed the same pattern in their mass spectra, which resembles what would be expected from a random monomer distribution among the oligomers. This result suggest that CUS1 is equally active towards 9- and 10-hydroxy 2-MHG and is likely to participate in the polymerization of both monomers in cutin.

3. Synthesis of suberin monomers as CUS1 substrates

3.1 Goals and scope of the project

The mechanism and enzymes involved in suberin biopolymerization are largely unknown. However, there are obvious similarities in the composition and monomer synthesis of the aliphatic domain of suberin and cutin, which open the door to question whether the polymerization mechanism is also similar. It has been proven that the biosynthesis of both polymers require the presence of GPAT enzymes, which produce 2-MAGs of the fatty acids used as monomers. In cutin biosynthesis, 2-MAGs are polymerized by the recently discovered family of enzymes, CUS. This enzyme family, or a similar undiscovered one, might be involved in suberin biopolymerization.

The goal of the present project is the synthesis of three 2-MAG derivatives of fatty acids typically found as suberin monomers (see section 1.3.2). These monomers (Figure 3.1.) can be a useful tool for studying and discovering synthases. In the present project, they are used as substrates for CUS1 in *in vitro* polymerization assays. The formation of oligomers in those assays would support the hypothesis that CUS enzymes are involved in suberin biopolymerization.

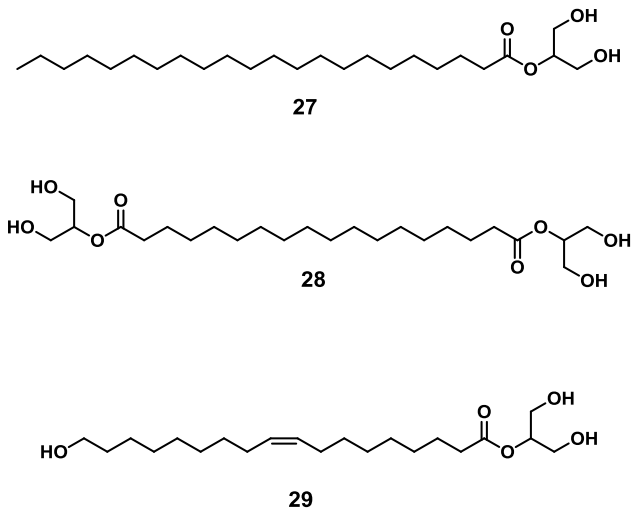

Figure 3.1. Target 2-MAG derivatives of three common suberin monomers.

3.2 Synthesis of suberin monomers

The synthesis of the first two target molecules, **27** and **28**, presented no difficulties, as their respective fatty acid starting materials, behenic acid and 1,18-octadecanedioic acid, are commercially available. Both synthesis were performed in two steps: a Steglich esterification of the fatty acids with 1,3-benzylidene-protected glycerol (double esterification in the case of 1,18 octadecanediol), followed by a cleavage of the benzylidene acetal by hydrogenolysis to yield the 2-MAG **27** and the bis-2-MAG **28** as shown in Scheme 3.1.

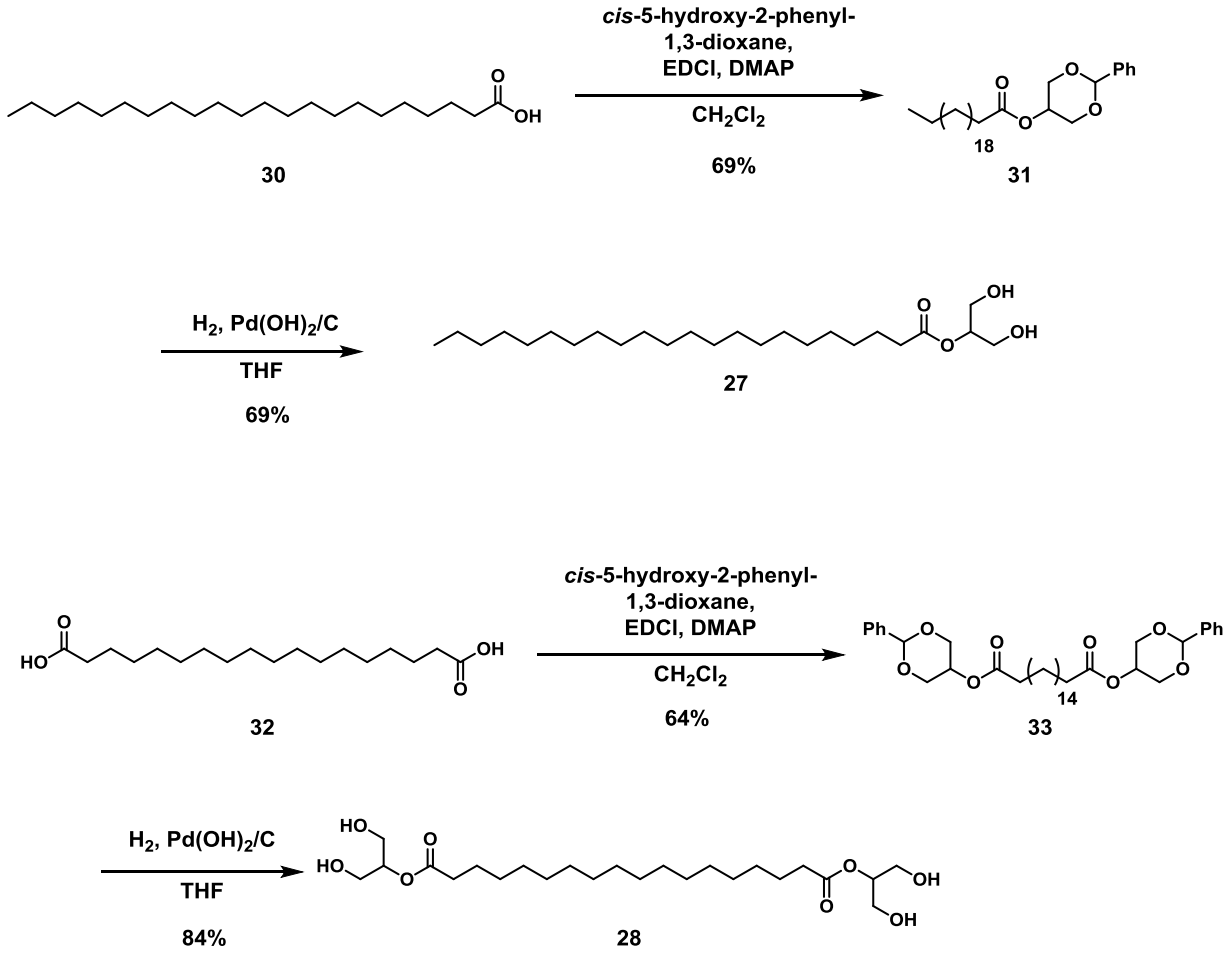

Scheme 3.1. Synthesis of the 2-MAG **27** and bis-2-MAG **28**

The synthesis of the 2-MAG derivative of (*Z*)-18-hydroxyoctadec-9-enoic acid, on the other hand, turned out to be more challenging. The first attempted synthetic strategy is retrosynthetically displayed in Figure 3.2. The desired 2-MAG **29** would be produced by the deprotection of the ester **34**, which in turn would come from the alkyne **35** by deprotection of the NAP group, oxidation of the free alcohol to the carboxylic acid, esterification with 1,3-protected glycerol, deprotection of the TBS group and Lindlar hydrogenation of the alkyne. The C18 carbon chain would be produced by alkylation of the terminal alkyne **36** and the iodoalkane **37**.

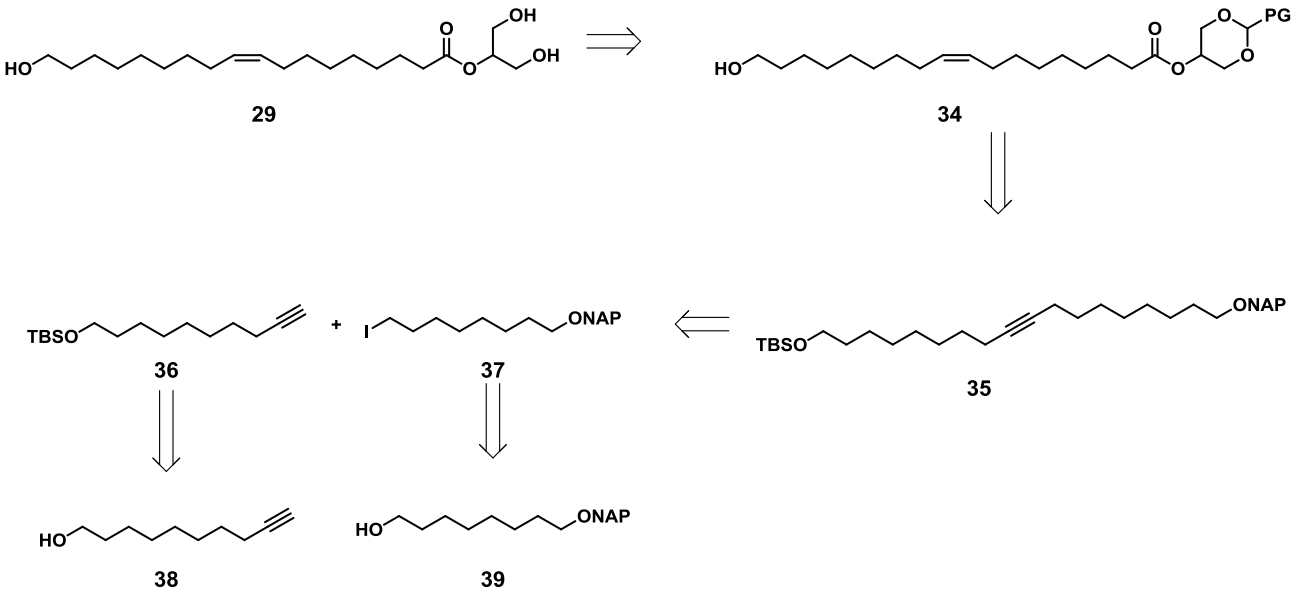

Figure 3.2. Retrosynthetic analysis for 1,3-dihydroxypropan-2-yl (*Z*)-18-hydroxyoctadec-9-enoate (**29**)

The first question that needed to be considered for this synthesis was the nature of the protecting group in the glycerol moiety. The use of a benzylidene acetal was preferred, because *cis*-5-hydroxy-2-phenyl-1,3-dioxane in commercially available. However, the necessity of maintaining the double bond forbids the use of standard hydrogenolysis for the removal of the benzylidene acetal, and it was unclear whether the Lindar catalyst would be active enough to produce the required hydrogenolysis. In order to test the deprotection of the benzylidene acetal, ester **41** was synthesized in good yield from oleic acid by means of a Steglich esterification with 1,3 benzylidene-protected glycerol as shown in Scheme 3.2. The subsequent attempt to remove the acetal by hydrogenolysis with Lindlar catalyst had no effect. An alternative deprotection *via* catalytic-transfer hydrogenolysis with ammonium formate and 10% palladium on carbon in methanol was attempted, but once again, no reaction was observed. Other deprotection methods, such as hydrolysis of the acetal under acid conditions, were discarded due to the

risk of promoting the migration of the deprotected glyceryl moiety to one of the primary alcohols. Thus, the use of benzylidene acetal as a protective group was discarded.

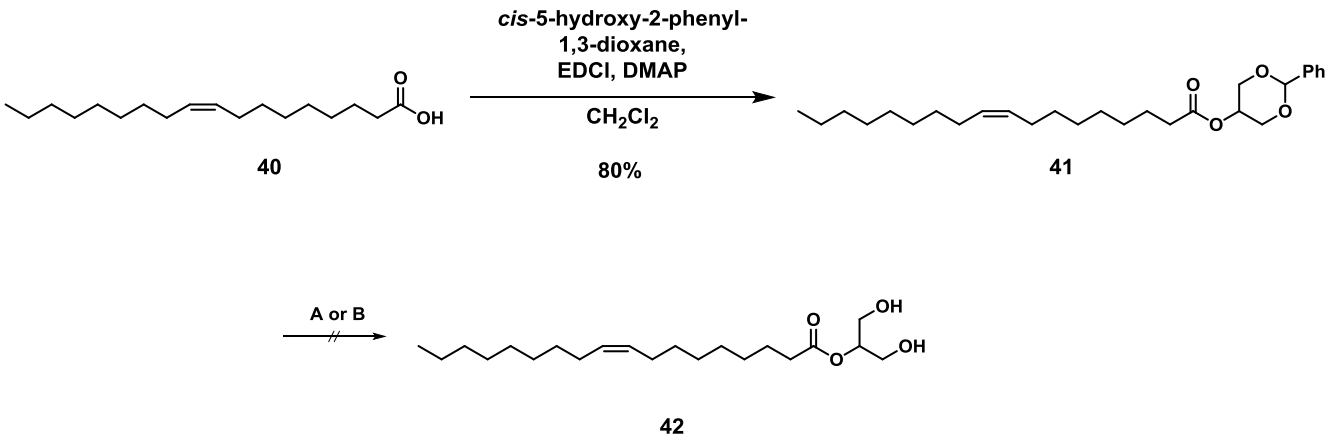

Scheme 3.2. Synthesis of 2-phenyl-1,3-dioxan-5-yl oleate (**41**) and attempted deprotection of the benzylidene acetal. **A**: H_2, Lindlar catalyst in THF; **B**: Ammonium formate, 10% Pd/C in MeOH

A new protecting group for the 1,3-positions of the glyceryl moiety was needed. The limitations imposed by the target molecule (i. e. respect the integrity of the double bond and prevent migration of the unprotected glyceryl moiety) prevented the use of hydrogenolysis, as well as acid or basic conditions in the deprotection step. Two protecting groups, which according to literature[168] could be removed under oxidative conditions with DDQ, were selected: *p*-methoxybenzylidene acetal and naphthylidene acetal. Unfortunately, neither 1,3-protected glycerols were commercially available, and therefore had to be synthesized, as is shown in Scheme 3.3.

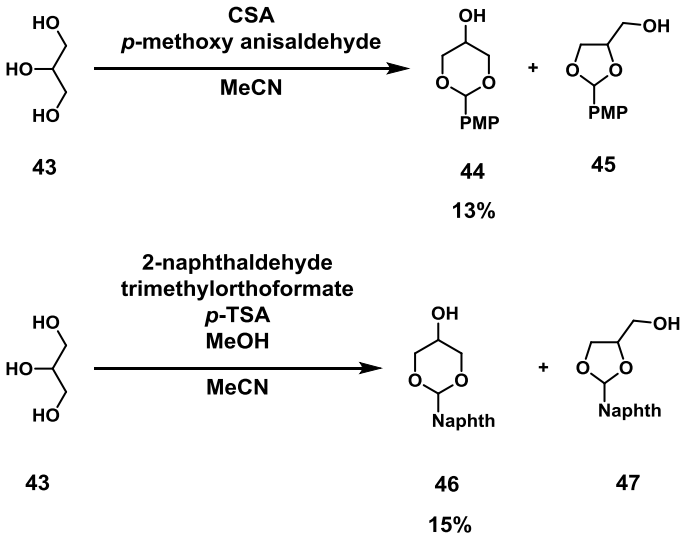

Scheme 3.3. Synthesis of 1,3-protected glycerol with *p*-methoxy benzylidene (**44**) and 2-naphthylidene (**46**) acetals

The synthesis of both 1,3-protected glycerols produced a significant amount of the 1,2-isomers, which was difficult to separate. At least four consecutive flash chromatography separations were necessary to obtain the products **44** and **46** in acceptable purity, significantly reducing the yield of the reactions.

Once they were isolated, the protected glycerols **44** and **46** were reacted with oleic acid to form the corresponding esters **48** and **49** *via* Steglich esterification, as shown in Scheme 3.4. The deprotection of both acetals was tested in the same conditions used for the deprotection of the NAP group during the synthesis of isotopically labelled 2-MHG (See section 2.2). After 16 hour, no deprotection of the naphthylidene acetal from compound **49** was observed. Maintaining the reaction for longer time did not produce any result, and it was finally discarded after 100 hours. Ester **48**, on the other hand, showed full conversion after 16 hours. The product of this reaction could not be crystallized, and had to be purified by reverse-phase flash column chromatography while trying to avoid the migration of the glyceryl moiety, which is catalysed by the acidity of the silica. Despite that precaution, the recovered product was fully migrated, perhaps due to the formation of acidic products during the decomposition of DDQ in water. To avoid this issue, the reaction was repeated using a phosphate aqueous buffer of pH 7.5 instead of water. In this case the reaction was successful, forming product **42**.

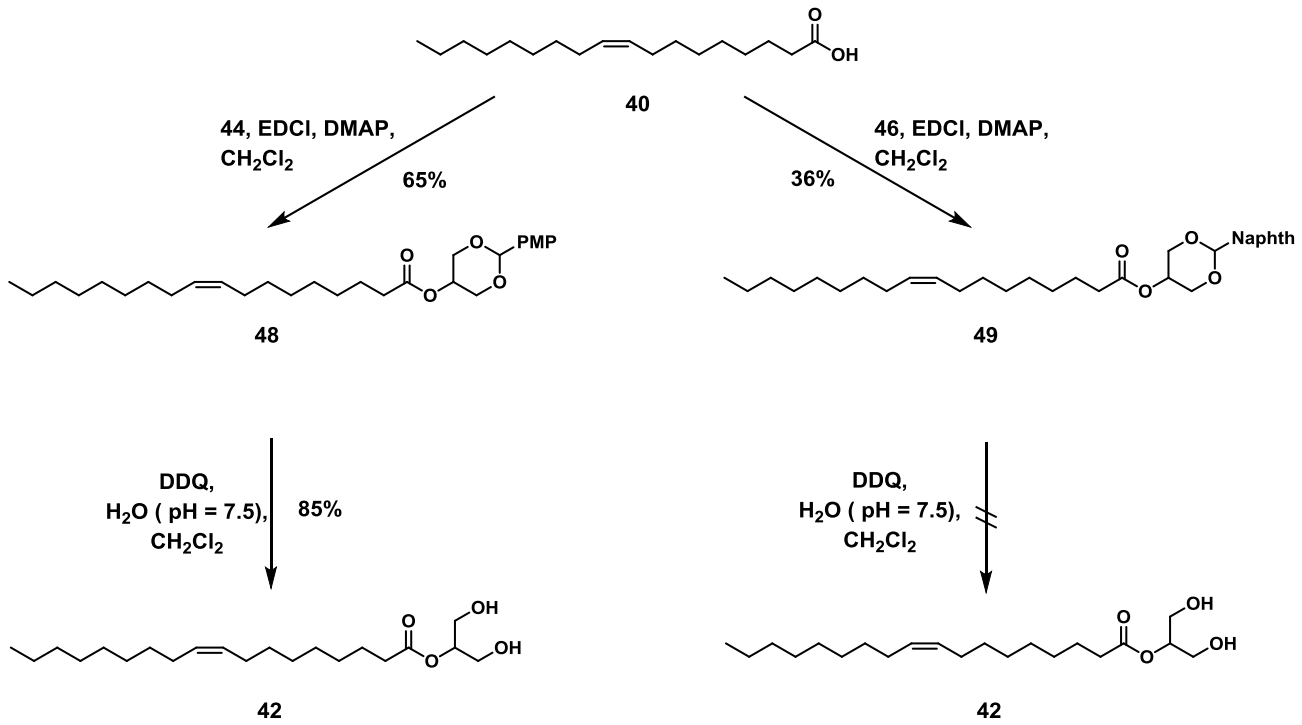

Scheme 3.4. Synthesis of oleic esters with 1,3-protected glycerol and deprotection tests with DDQ

Once a suitable protecting group for the glyceryl moiety was found, the synthesis of ω-hydroxy oleate 2-MAG (**29**) could commence. The first steps of the synthesis consist on the protection of the hydroxyl group of dec-9-yn-1-ol (**38**) with TBS chloride and the protection of one of the hydroxyls of 1,8-octanediol (**50**) with 2-(bromomethyl)naphthalene to form products **36** and **39**, respectively. This step was achieved in good yields as is shown in Scheme 3.5. The free hydroxyl group of the alcohol **39** was tosylated to form product **51** in 92% yield, which was then treated with sodium iodide leading to product **52** in 64% yield, as can be seen in Scheme 3.6.

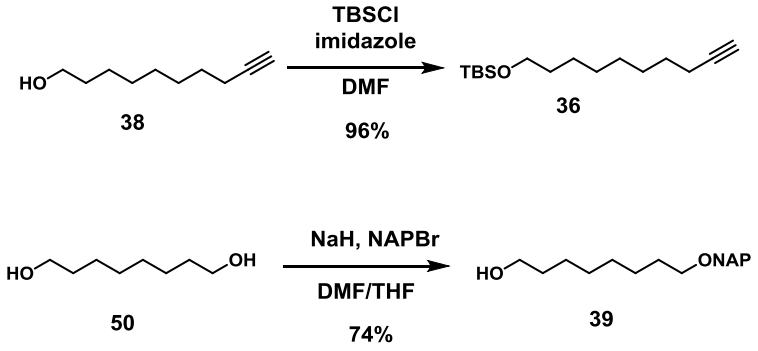

Scheme 3.5. Protection of the starting materials

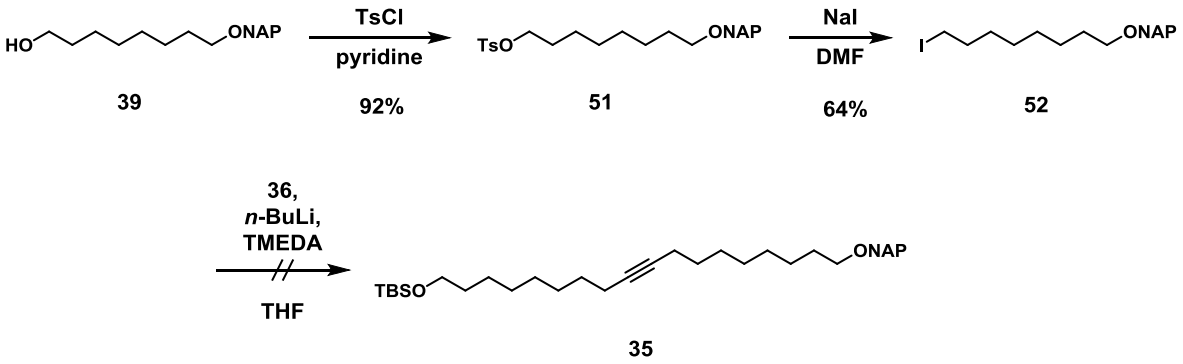

Scheme 3.6. Attempted synthesis of the alkyne **35**

The alkylation of very similar iodoalkanes and terminal alkynes with *n*-BuLi has been reported in the literature in very good yields,[175] and therefore it was expected to work without incident. However, that optimism turned out to be unfounded, as the alkylation of **36** failed, forming no product. The reaction was repeated several times taking extreme care in ensuring dry conditions and adding *N,N,N',N'*-tetramethylethylenediamine (TMEDA) to coordinate to the lithium ions, but the efforts were in vain. No reaction was observed and all the starting material was recovered. In order to understand if the problem was related to the deprotonation of the alkyne, two different alkylation reactions with product **36** were tested, using methyl iodide and benzaldehyde, respectively, as electrophiles. Both reactions produced the expected products in 70% and 52% yield, respectively, as is shown in Scheme 3.7. This showed that under the tested conditions the deprotonation of the alkyne **36** was in fact taking place, but the reaction was not moving forward possibly due to lack of electrophilic reactivity of compound **52**.

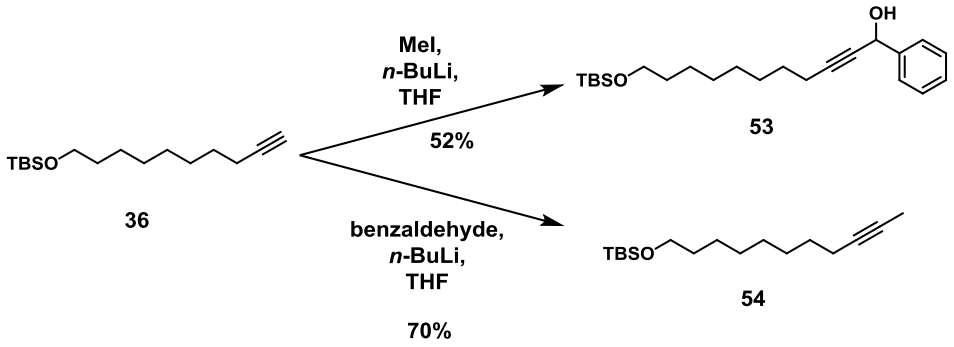

Scheme 3.7. Alkylation tests of *tert*-butyl(dec-9-yn-1-yloxy)dimethylsilane (**36**)

As a consequence of the failed attempts to form compounds **35** from the reaction between compounds **36** and **52**, a new synthetic strategy was developed, based on the previous synthesis of 2-MHG as shown in Figure 3.3. Alkyne **35** would be synthesized from the deoxygenation of the propargylic alcohol **55**, which could be formed by the coupling of alkyne **36** with the aldehyde resulting from the oxidation of the alcohol **39**.

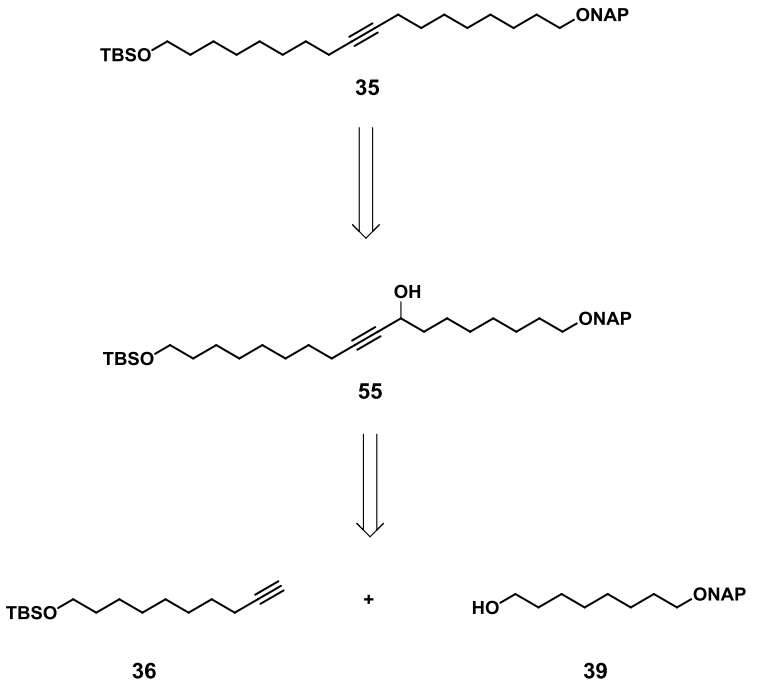

Figure 3.3 Alternative retrosynthetic analysis for the synthesis of the alkyne **35**

The free alcohol of product **39** was oxidized to the aldehyde *via* Dess-Martin oxidation and then reacted with **36** in an overall yield of 76%, further confirming that the deprotonation of the alkyne under these conditions is efficient. The subsequent deoxygenation of the propargylic alcohol was attempted by following a recently published procedure, using triethylsilane as a hydride source and phosphotungstic acid hydrate as a catalyst,[176] as can be seen in Scheme 3.8. The reaction was kept at room temperature overnight, but the only product that could be recovered apart from the starting material was the triethylsilyl ether derivative of the alcohol. Several reaction conditions were tried, such as changing the solvent, the temperature and the amount of catalyst, but none of them produced the desired material. The use of 2,2,2-trifluoroethanol as solvent and increasing the temperature had no effect on the outcome of the reaction, whereas increasing drastically the amount of catalyst only had the additional effect of cleaving the acid-sensitive TBS protecting group. With these results in hand, it

was decided to abandon this strategy. A summary of the reaction conditions attempted and their outcome is displayed in Table 3.1.

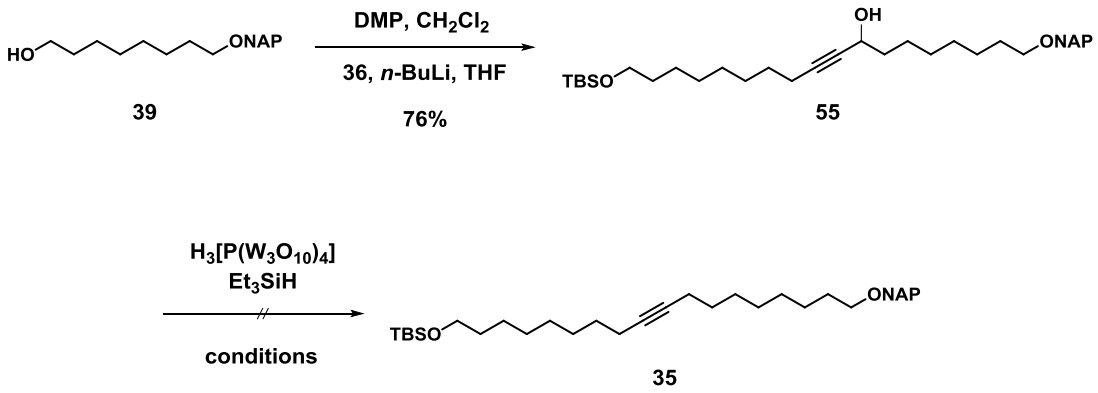

Scheme 3.8. Synthesis of the propargylic alcohol **55** and attempted deoxygenation with triethylsilane and phosphotungstic acid hydrate

Table 3.1. Summary of the conditions tried for the deoxygenation of the propargylic alcohol **35** with triethylsilane with $H_3[P(W_3O_{10})_4]$ as catalyst

Reaction	Catalyst (mol %)	Solvent	Temperature (°C)	Outcome
1	1	CH_2Cl_2	20	Silylation of the alcohol
2	1	CF_3CH_2OH	20	Silylation of the alcohol
3	1	CH_2Cl_2	50	Silylation of the alcohol
4	15	$Cl(CH_2)_2Cl$	20	Silylation of the alcohol, TBS group removal

A common method to remove secondary alcohols proceeds through the Barton-McCombie deoxygenation, which consists of two steps. In the first step, the alcohol is converted to a thioxoester or xanthate derivative, which is then removed through a radical reaction with tributyltin and 2,2'-azobis(2-methylpropionitrile) (AIBN).[177] Despite no literature source describing this technique for the deoxygenation of propargylic alcohols could be found, it was believed to be a suitable option.

The propargylic alcohol of product **55** was attempted to be converted to the corresponding methyl xanthate by means of reaction with sodium hydride, carbon disulfide, imidazole and methyl iodide,

according to a standard procedure.[178] After one hour under reflux TLC showed total conversion of the starting material and the formation of a single product with a higher R_f value, as it would be expected from the formation of the xanthate.

However, NMR analysis of the only product revealed a surprising result, as it did not correspond to the expected methyl xanthate (see Figure 3.4). The ^{13}C NMR spectrum showed two peaks above 180 ppm, which normally indicate the presence of carbonyl compounds, although the target molecule only has one. Furthermore, the peaks that should correspond to the carbons in the triple bond had an unexpectedly high value, 93.15 and 95.15 ppm, respectively. A careful analysis of the correlations in the heteronuclear 2D spectra of the product led to the conclusion that the obtained product was an allene, which could be formed through a 3,3 sigmatropic rearrangement of the xanthate, as is illustrated in Scheme 3.9. Some examples of this type of rearrangements of propargylic xanthates and thionocarbonates forming allenes could be found in the literature.[179,180]

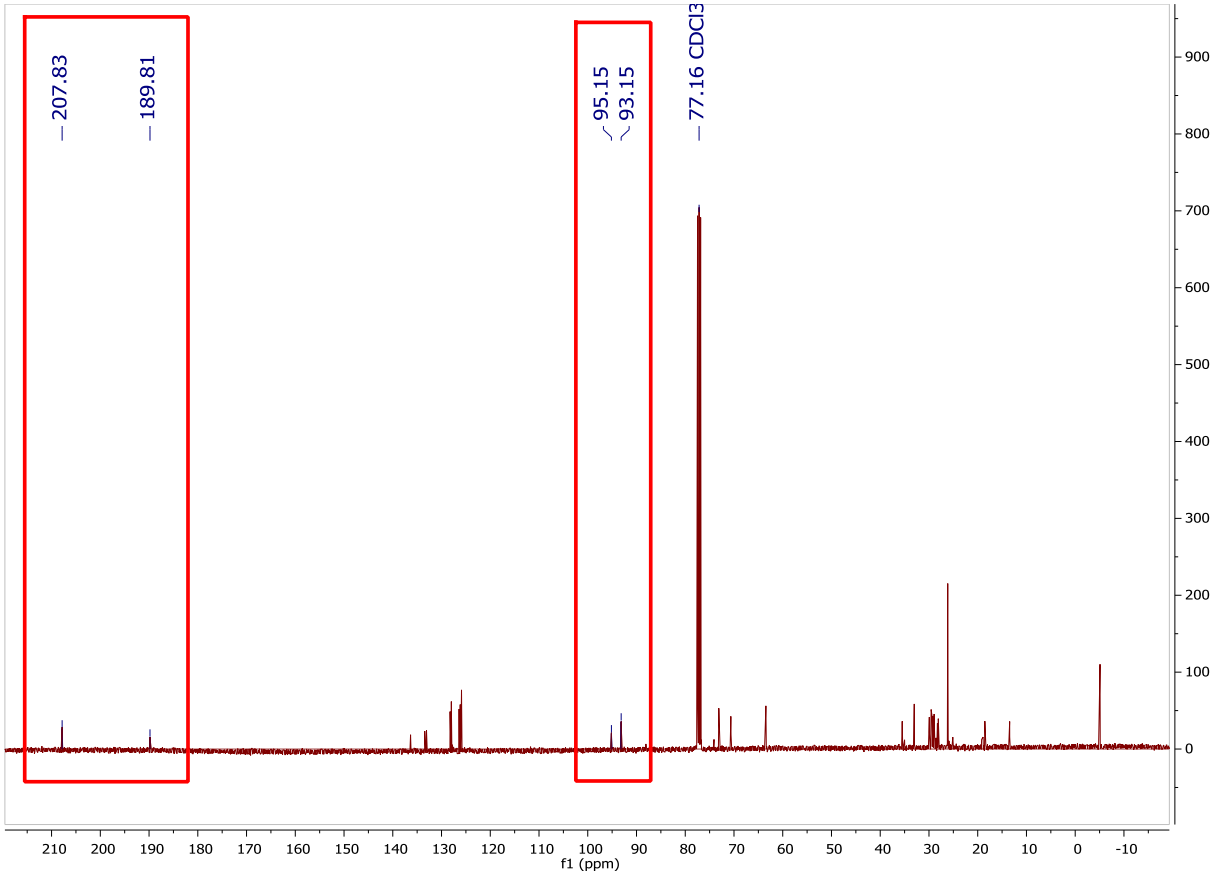

Figure 3.4. ^{13}C NMR spectrum of the allene **57**

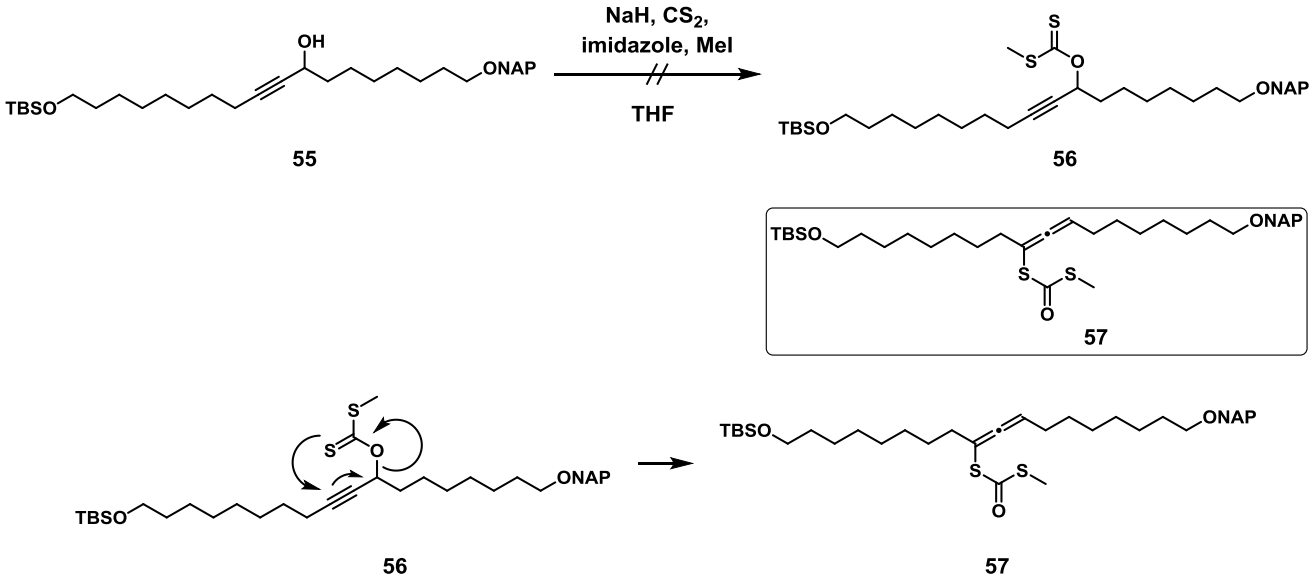

Scheme 3.9 Attempted synthesis of the xanthate **56** and possible reaction mechanism for the formation of the allene **57**

Despite the tendency of this type of compounds to form allenes, the synthesis of other thiocarbonyl derivatives was attempted. Reaction of the alcohol **55** with 1,1´-thiocarbonyldiimidazole (TCDI) and DMAP did not yield the desired thionocarbamate **58**, but instead it produced the rearrangement product **59** (Scheme 3.10).

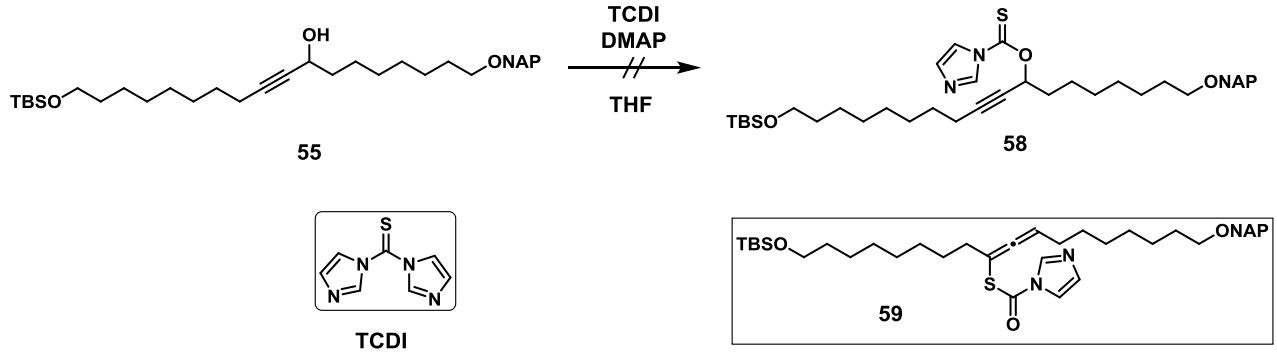

Scheme 3.10. Attempted synthesis of the thionocarbamate **58**

A new attempt to synthesize a thiocarbonyl derivative of compound **55** was made by reacting it with *O*-phenyl chlorothionoformate and DMAP in dichloromethane as is seen in Scheme 3.11. This time, NMR analysis of the product showed a mixture of the desired thionocarbonate **60** and the allene **61**, in

which the latter was present in minor amounts. By reducing the reaction time from four to three hours, only a negligible amount of the allene was formed (≈ 4%) and the desired product was isolated in excellent yield.

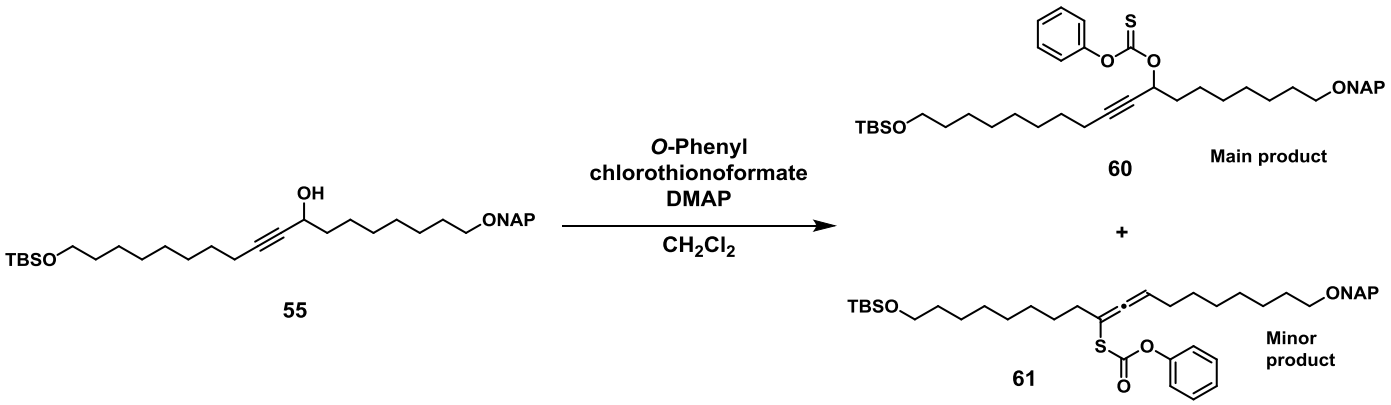

Scheme 3.11. Synthesis of the thionocarbonate **60**

The next step of the deoxygenation consisted on the replacement of the thionocarbonate by a hydrogen atom to give an alkyl group. The reaction follows a radical mechanism with tributyltin as the reactant radical species and AIBN as the radical initiator. However, the first attempts to perform this reaction were unfructuous, and the starting material was recovered intact. In order to investigate whether the failure of this reaction was specific to our substrate or there were other issues (e.g. degraded reagents), the deoxygenation of a simpler alcohol using two different thiocarbonyl derivatives was attempted. The free alcohol of compound **39** was converted to the corresponding phenyl thionocarbonate and the methyl xanthate in 70 and 77% yield, respectively as is depicted in Scheme 3.12. The radical deoxygenation of those compounds did not produced any results, signaling that there was a problem either with the reagents used or with the way the reaction was conducted. A new batch of tributyltin was acquired and used to repeat the deoxygenation of the xanthate **63**, which this time resulted in the formation of product **62**. Despite an initial attempt to purify it, NMR of the product showed a large amount of tributyltin. No further attempt of purifying it was deemed necessary, as NMR showed that the deoxygenation had taken place.

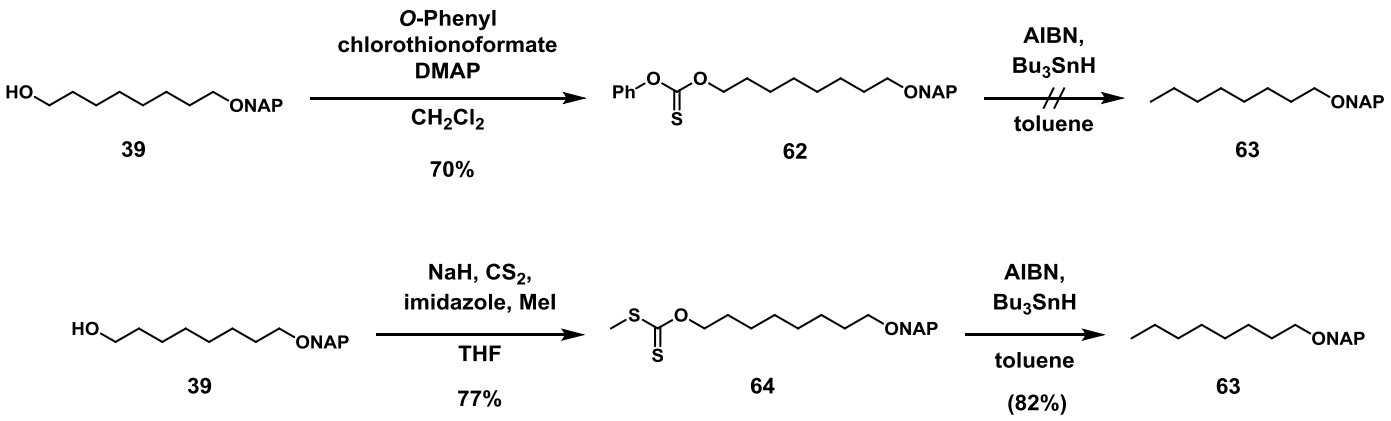

Scheme 3.12. Initial tests of the Barton-McCombie deoxygenation of the alcohol **39** using phenyl thionocarbonate and methyl xanthate as thiocarbonyl derivatives. When a new batch of tributyltin was used, the deoxygenation of the methyl xanthate was completed in 82% yield.

Using the new batch of tributyltin, the deoxygenation of compound **60** was performed producing the alkyne **35** in a excellent yield as is shown in Scheme 3.13. The NAP group of this compound was then removed by use of DDQ and water in dichloromethane, producing compound **65** in 44% yield. The free alcohol of this product was oxidized to the carboxylic acid by sequentially submit it to a Dess-Martin and a Pinnick oxidations. The carboxylic acid was then reacted with the 1,3-protected glycerol **44** together with EDCl and DMAP in dichloromethane to obtain the ester **66**. Despite leading to the desired product, the overall yield of these reactions was only 23%. In order to try to improve the yield of the ester formation two other esterification methods, shown in Scheme 3.14, were attempted. The first one, which uses *p*-toluenesulfonyl chloride and *N*-methylimidazole in acetonitrile,[181] only improved the yield compared to the Steglich esterification, producing the desired ester in 27% yield. The other esterification method, consisting on the use of 1-(2-mesitylenesulfonyl)-3-nitro-1H-1,2,3-triazole (MSNT) and methylimidazole in THF, proved to be more effective, and produced the ester **66** in 55% yield.

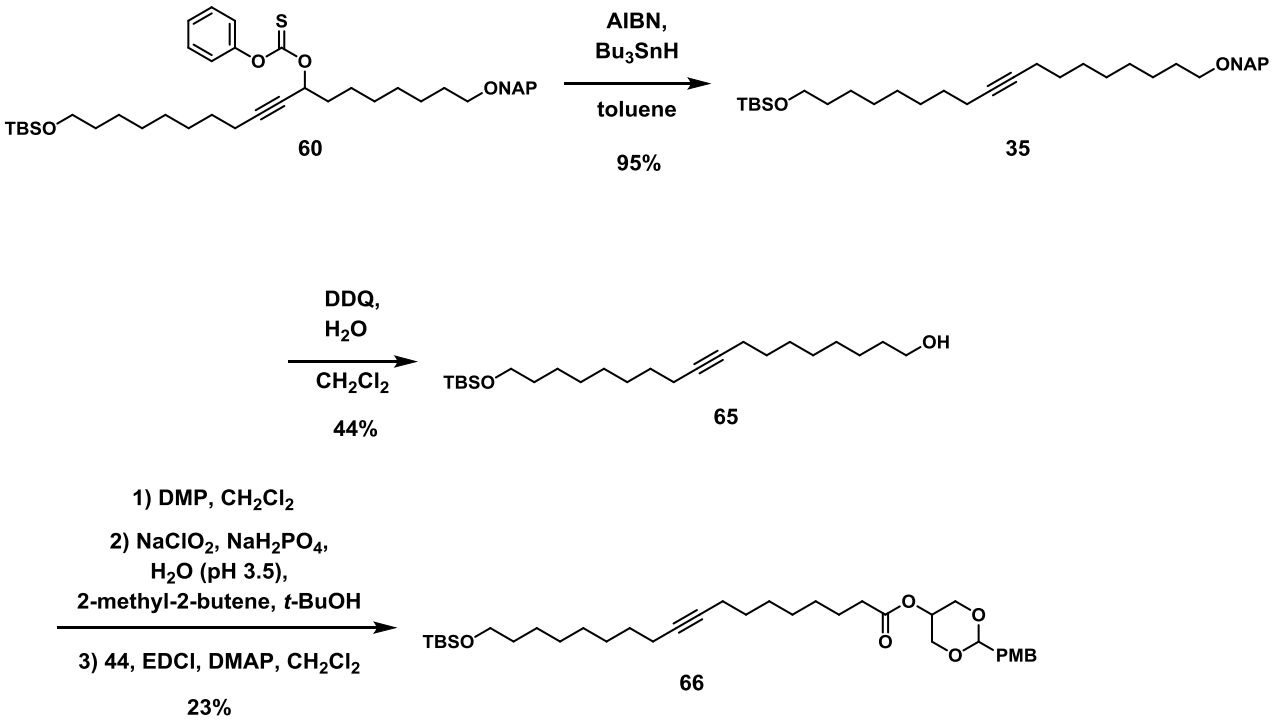

Scheme 3.13. Synthesis of the alcohol **65** and subsequent esterification with the protected glycerol **44** by *via* Steglich esterification to form ester **66**

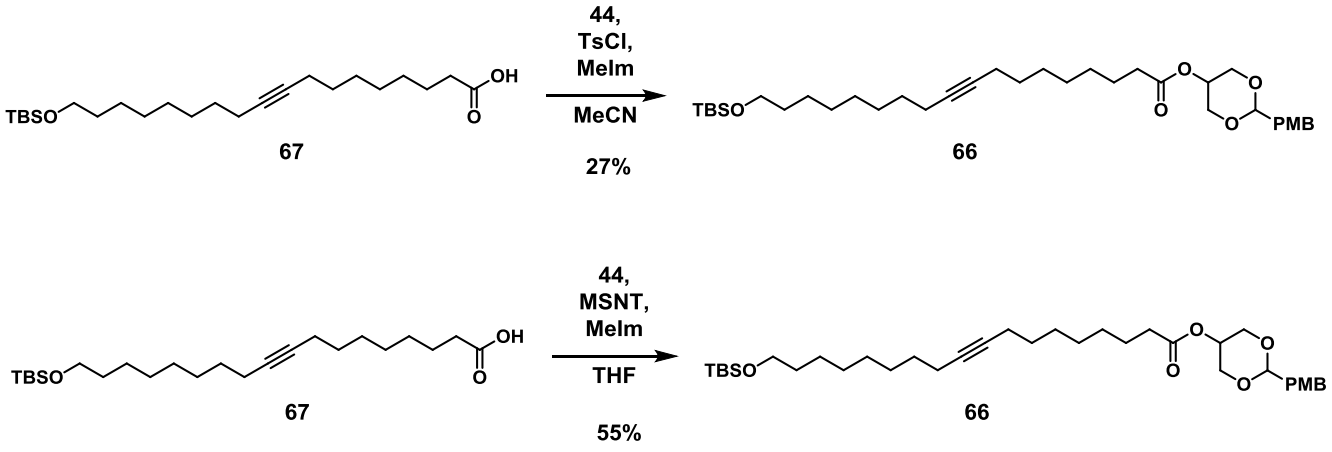

Scheme 3.14. Alternative esterification reactions for the synthesis of **66**. The yields are combined for the previous oxidation steps.

The next two steps, showed in Scheme 3.15, consisted on the deprotection of the terminal alcohol of compound **66** by use of TBAF, which was accomplished in 62% yield and the Lindlar hydrogenation of the alkyne of compound **68** to produce a double bond with *cis* configuration. This reaction proceeded without incident and produced the desired product **34** in excellent yield. Finally, the synthesis was completed with the deprotection of the PMB acetal by oxidation with DDQ and a phosphate aqueous buffer of pH 7.5. As it was expected, the product could not be recrystallized and had to be purified by reverse-phase dry-column chromatography. Due to the tendency of the glyceryl moiety to migrate to the primary position in the presence of protonated solvents, the purification was attempted using pure acetonitrile as the mobile phase. However, no separation was achieved, and the purification was repeated using a 7:3 acetonitrile:water mixture as the eluent in the first fraction, and increasing the amount of acetonitrile by 10% in successive fractions. The product started eluting at the fraction with 9:1 acetonitrile:water, and continued in the successive fractions with pure acetonitrile. The only fraction with water was concentrated separately from the rest and it showed complete migration, while the other fractions only showed minor amounts of it. The non-migrated product, however, was not pure. The purification had to be repeated three more times, using the same gradient in the eluent mixture. The amount of impurities decreased in each iteration, but the amount of migration increased. After the fourth purification, the impurities had been successfully removed, but approximately 25% of the product had succumbed to migration. Unfortunately, no more of compound **66** was available, and due to time constrains, it was not possible to repeat the synthesis to try to achieve a purer product.

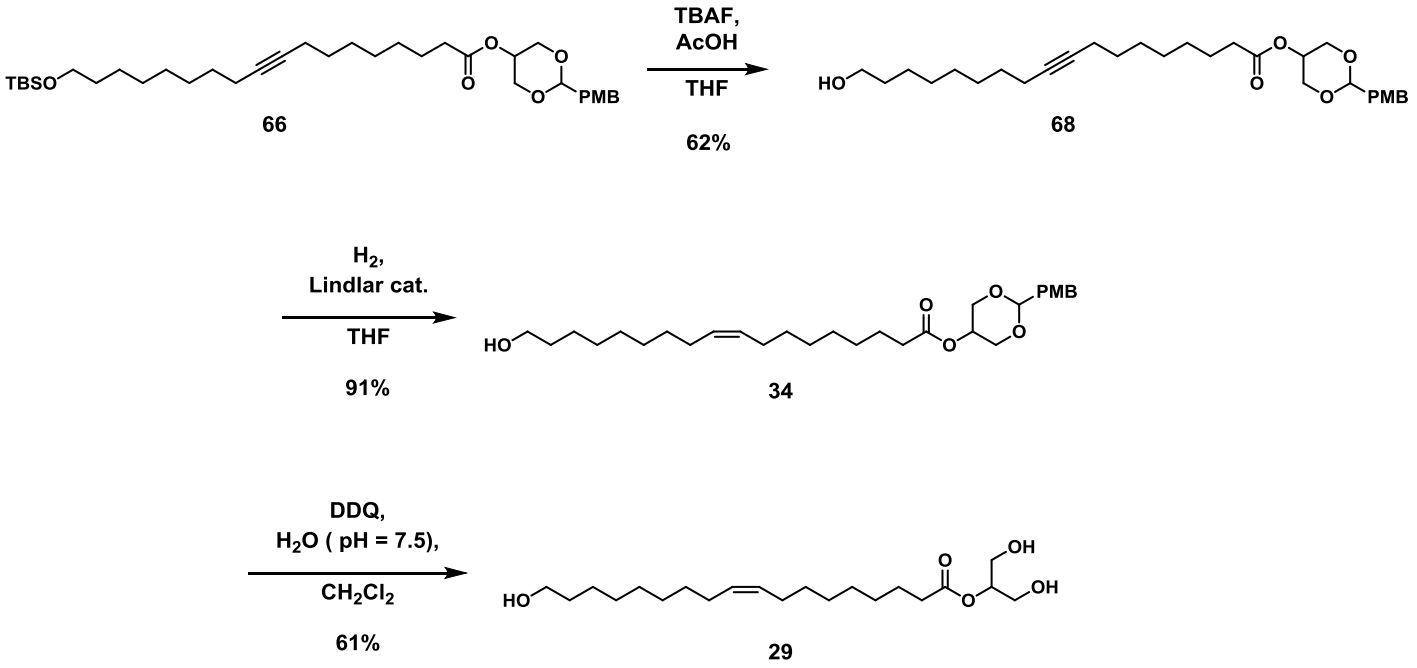

Scheme 3.15. Final steps in the synthesis of the 2-MAG **29**

3.3 Enzymatic oligomerization of suberin monomers with CUS1

The enzymatic oligomerization of the 2-MAG **29** was performed following an analogous procedure to the enzymatic oligomerization of 2-MHG (See section 0). The other two suberin monomers, **27** and **28**, cannot polymerize by themselves, as they lack a hydroxyl functionality which can participate in the transesterification. They can, however, form ester bonds with other hydroxy fatty acids. Therefore, the enzymatic tests involving the 2-MAG **27** and the bis-2-MAG **28** were performed using an equimolar mixture of the corresponding suberin monomer and 2-MHG. Negative controls were run in parallel. All tests were performed in triplicate and products were analysed by MALDI-TOF. A summary of the enzymatic experiments is displayed in Table 3.2

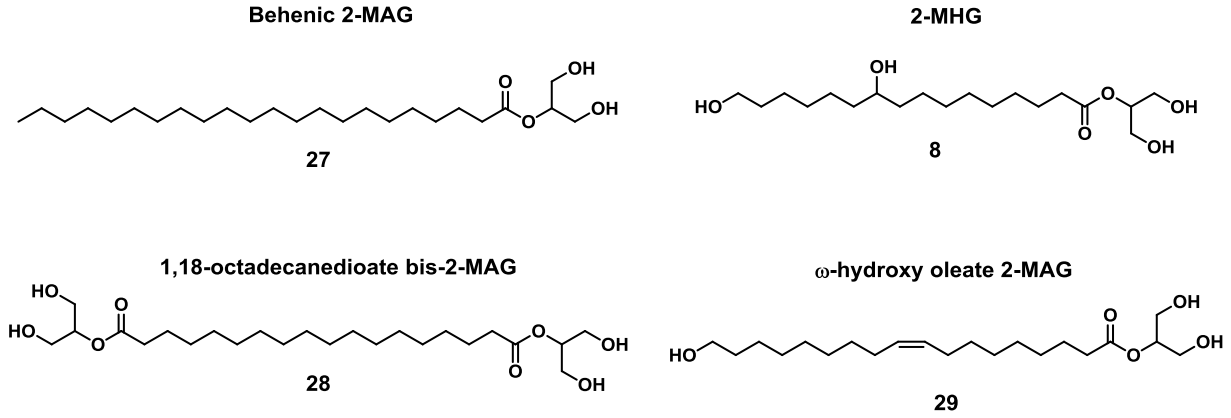

Figure 3.5. Compounds used in the enzymatic experiments

Table 3.2. Enzymatic oligomerization tests with suberin monomers

Experiment	**1**	**2**	**3**	**4**	**5**	**6**	**7**	**8**
CUS1	+	-	+	-	+	-	+	-
Substrate	**28** + 2-MHG	**28** + 2-MHG	**27** + 2-MHG	**27** + 2-MHG	**29**	**29**	2-MHG	2-MHG

The mass spectrum of experiment 1, found in Figure 3.6, shows the regular pattern for 2-MHG oligomerization, in which oligomers with up to six units were discernible. In addition, a series of peaks with much lower intensity could be detected. Those signals correspond to the incorporation of one unit

of the dicarboxylic acid in a 2-MHG dimer, trimer and tetramer, respectively. Despite their low intensity, these peaks appeared in all the three triplicates. The corresponding negative control did not produce any ester products. This exiting result implies that CUS1 is indeed capable of performing transesterification reactions with monomers other than 2-MAGs of dihydroxyhexadecanoic acid, and can accept a typical suberin monomer as substrate, albeit with poor selectivity over 2-MHG.

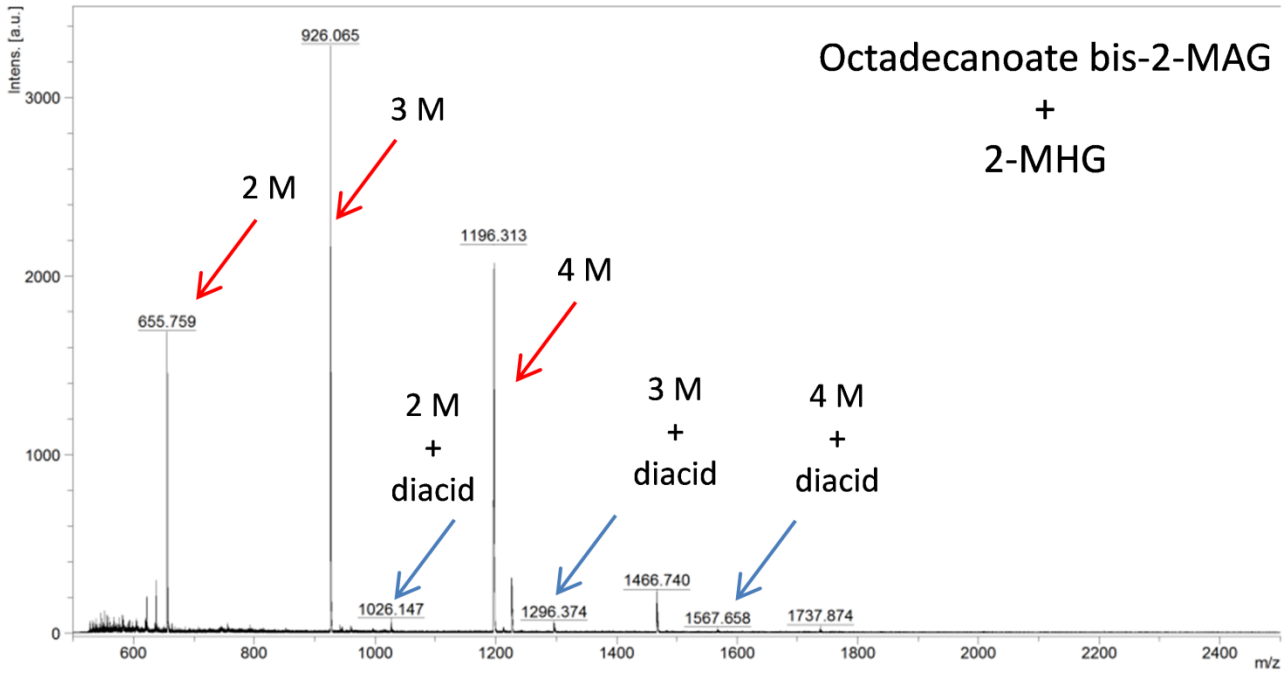

Figure 3.6. MALDI-TOF mass spectrum experiment 1, with 2-MHG and the bis-2-MAG **28** as CUS1 substrates. M = units of 10,16-dihydroxyhexadecanoic acid

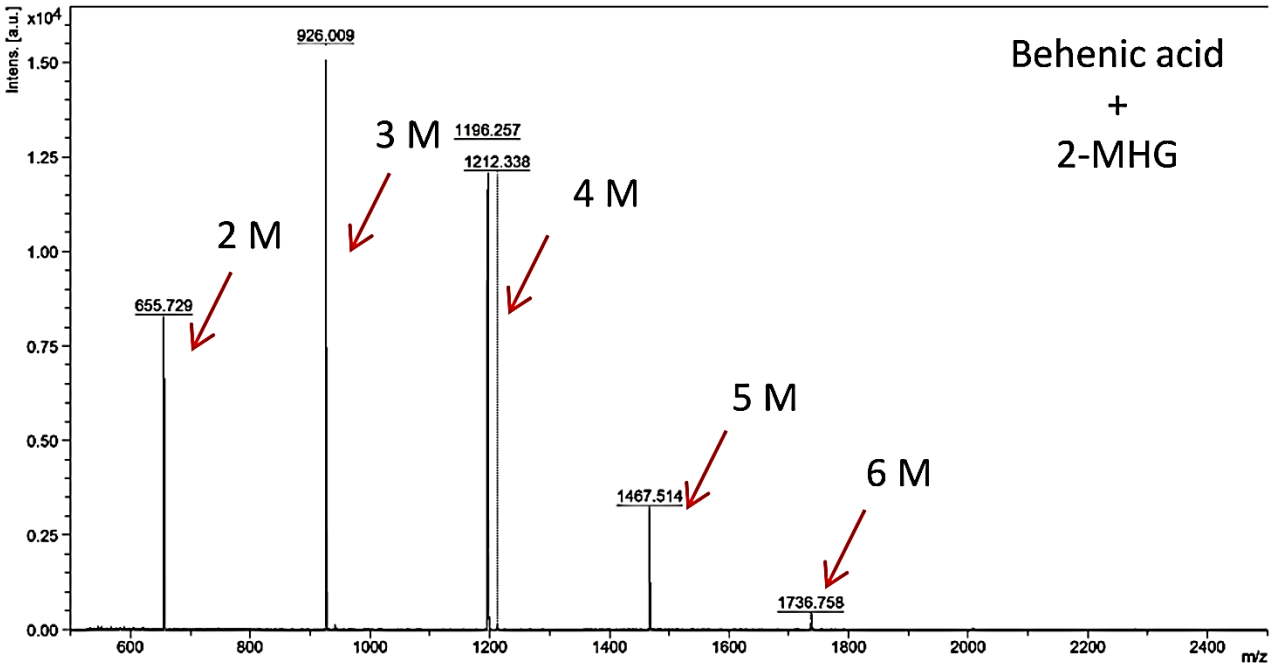

Figure 3.7. MALDI-TOF mass spectrum experiment 3, with 2-MHG and the –MAG **27** as CUS1 substrates. M = units of 10,16-dihydroxyhexadecanoic acid

Experiment 3, on the other hand, did not result in the formation of any hetero-oligomers. In this case, the only products formed were homo-oligomers of 2-MHG, as can be seen in Figure 3.7. This shows that CUS1 does not accept behenic 2-MAG (**27**) as a substrate, suggesting that there are other enzymes responsible for the incorporation of very long fatty acids into suberin.

The mass spectrum of the triplicate experiments of experiment 5 is displayed in Figure 3.8. As it can be seen, no product formation was appreciable in one of the experiments, while the other two show the formation of the ω-hydroxy oleic acid dimer, but not of longer oligomers. None of the negative controls resulted in the formation of any ester product, which shows that the formation of the dimer was due to enzymatic activity. This shows that CUS1 is capable of accepting ω-hydroxy oleic acid as a substrate, although it does not seem to present high activity towards its polymerization. It is necessary to acknowledge that the purity of the substrate was rather low (≈ 75%). However, the only impurity present in the sample was the product of migration of the glyceryl moiety, which, although it is not expected to be reactive under these conditions, it is likely that its presence would not hamper the polymerization.

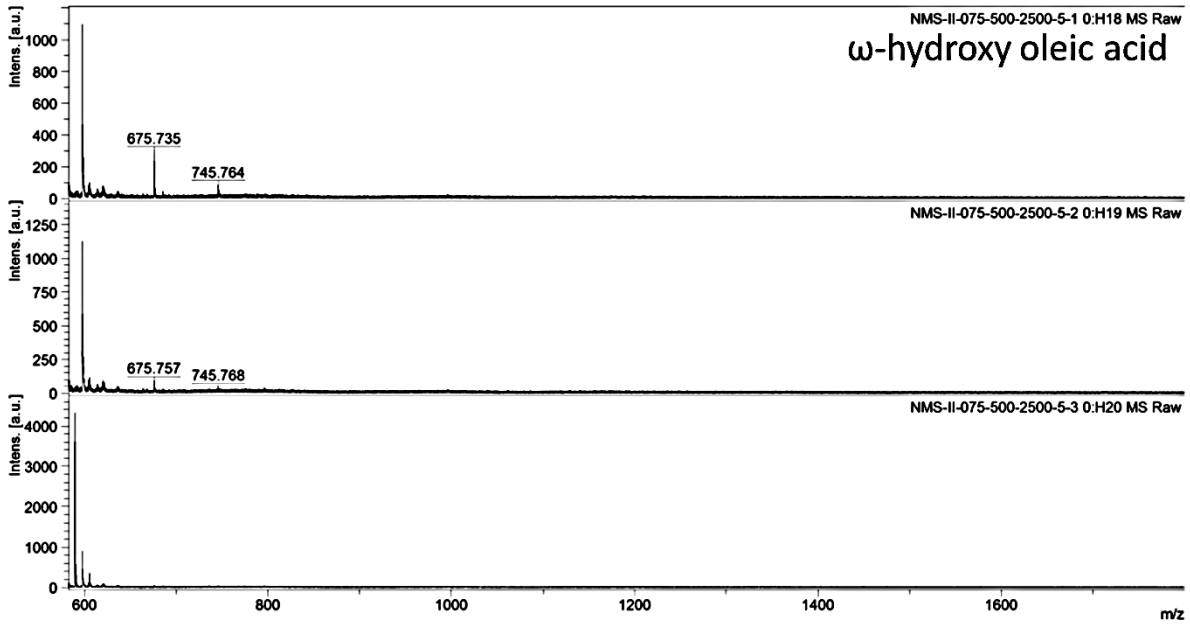

Figure 3.8. MALDI-TOF mass spectra of the triplicate experiments of experiment 5.

3.4 Conclusions

The 2-MAG derivatives of three common suberin monomers, behenic acid, 1,18-octadecanedioic acid and ω-hydroxy oleic acid, were synthesized in this project. The synthesis of the first two monomers was trivial and could be completed in two steps with good overall yield. The synthesis of the oleic acid derivative **29** proved to be more challenging, and the synthetic strategy had to be modified at various points. Difficulties during the purification of the final product led to a significant formation of the migrated product, which could not be separated, reducing the purity of the product to approximately 75%.

Enzymatic oligomerizations of the three 2-MAGs with CUS1 were attempted. Compounds **24** and **25** lack the necessary hydroxyl group to form homo-oligomers, and were tested as part of an equimolar mixture with 2-MHG. The oligomerization of 2-MHG with the bis-2-MAG **28** produced a small amount of 2-MHG hetero-oligomers with a single unit of the diacid. The negative control did not result in the formation of any ester product, thus confirming that CUS1 was responsible for the incorporation of the diacids into the 2-MHG oligomers. The oligomerization of the 2-MAG **27** with 2-MHG, on the other hand, did not produce any hetero-oligomers, and the only product were regular 2-MHG

oligomers. Finally, the enzymatic test with the 2-MAG **29** only resulted in the formation of the dimer in two out of three repetitions of the experiment. Once again, the corresponding negative control did not result in the formation of any ester products, which confirms that the dimer was formed due to enzymatic activity.

This results show that CUS1 presents some activity towards dihydroxyhexadecanoate 2-MAGs. In fact, it has shown a remarkable promiscuity by accepting two C18 2-MAG monomers characteristically found in suberin. However, CUS1 only showed moderate activity towards the C18 monomers, and none at all towards the C22 behenic acid 2-MAG. These results contribute to the hypothesis that enzymes from the CUS or another undiscovered similar family also could be involved in the polymerization of the aliphatic domain of suberin, although it is likely that other suberin-specific enzymes participate in this process, particularly in the incorporation of very long fatty acid monomers.

4. Synthesis and oligomerization of 2-MHG derivatives with different head-groups

4.1 Goals and scope of the project

One of the characteristics of the biosynthesis of cutin is the requirement of the formation of 2-MAG derivatives of the fatty acid monomers. Moreover, members of the CUS family of enzymes have shown *in vitro* activity towards this type of monomers for the formation of oligomers. However, as it has been commented previously, *sn*-2 glyceryl esters are not thermodynamically stable and present a tendency to migrate, forming the more stable *sn*-1 esters, particularly in the presence of protonated solvents. This information suggests that CUS enzymes have a strong preference for 2-MAG fatty acids. Nevertheless, this hypothesis has not been tested, and it is reasonable to question whether these enzymes could polymerize monomers with different ester functionalities.

The goal of this project is to synthesize four 2-MHG derivatives in which the *sn*-2 glyceryl moiety has been substituted for other similar ester groups, including the thermodynamically more table *sn*-1 glyceryl and to perform enzymatic oligomerization tests of the synthesized esters with CUS1. For this purpose, 1,3-methoxy-2-propanol, ethylene glycol, 2-propanol and *sn*-1 glycerol were selected based on their resemblance to *sn*-2 glycerol. The target molecules are displayed in Figure 4.1

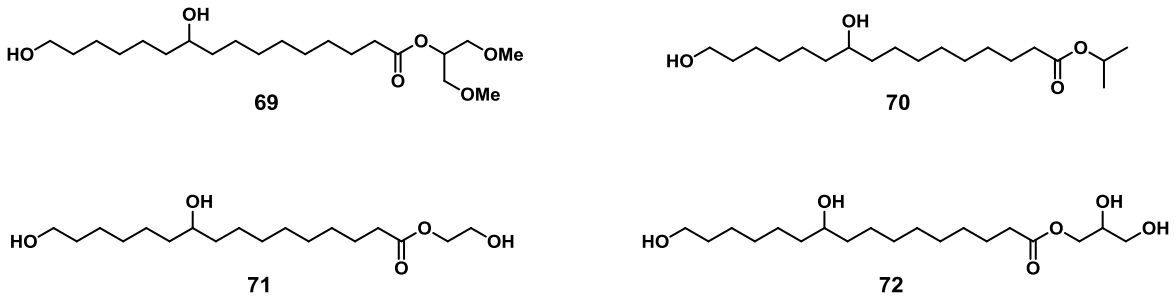

Figure 4.1. Target 2-MHG derivatives

4.2 Synthesis of 2-MHG derivatives

All 2-MHG derivatives were synthesized from the intermediate **5** (see Section 2.2). The free alcohol of **5** was oxidized to the carboxylic acid either by use of TEMPO $PhI(OAc)_2$ or by a two-step procedure, in which it was first oxidized to the aldehyde by use of DMP in CH_2Cl_2, and further oxidized to the acid by means of Pinnick oxidation. The carboxylic acid **73** was divided in four fractions, and each one of them was subjected to a Steglich esterification with a different alcohol, forming products **74**–**77** in yields ranging from 58 to 80%, as can be seen in Scheme 4.1.

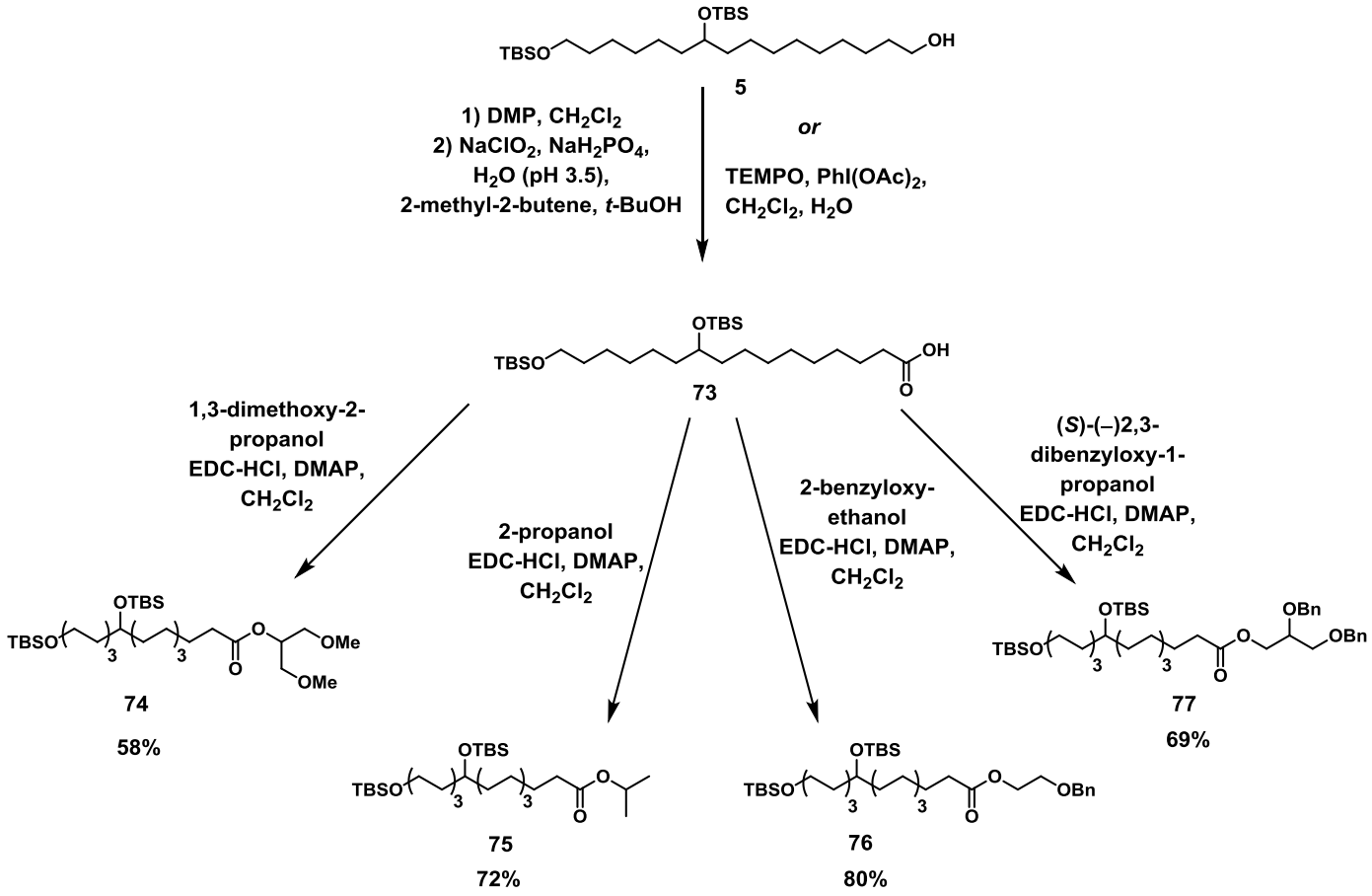

Scheme 4.1. Formation of the carboxylic acid **73** and its esterification with different alcohols to form the products **74**–**77**

The next step in all syntheses was the removal of the TBS groups with aqueous HF in MeCN, which was achieved in good to excellent yields, as is shown in Scheme 4.2. With this deprotection step, the synthesis of the final products **69** and **70** was completed. Additionally, the synthesis of compounds **71** and **72** required the cleavage of their respective benzyl ethers by hydrogenolysis, which was accomplished in 78 and 80% yield, respectively.

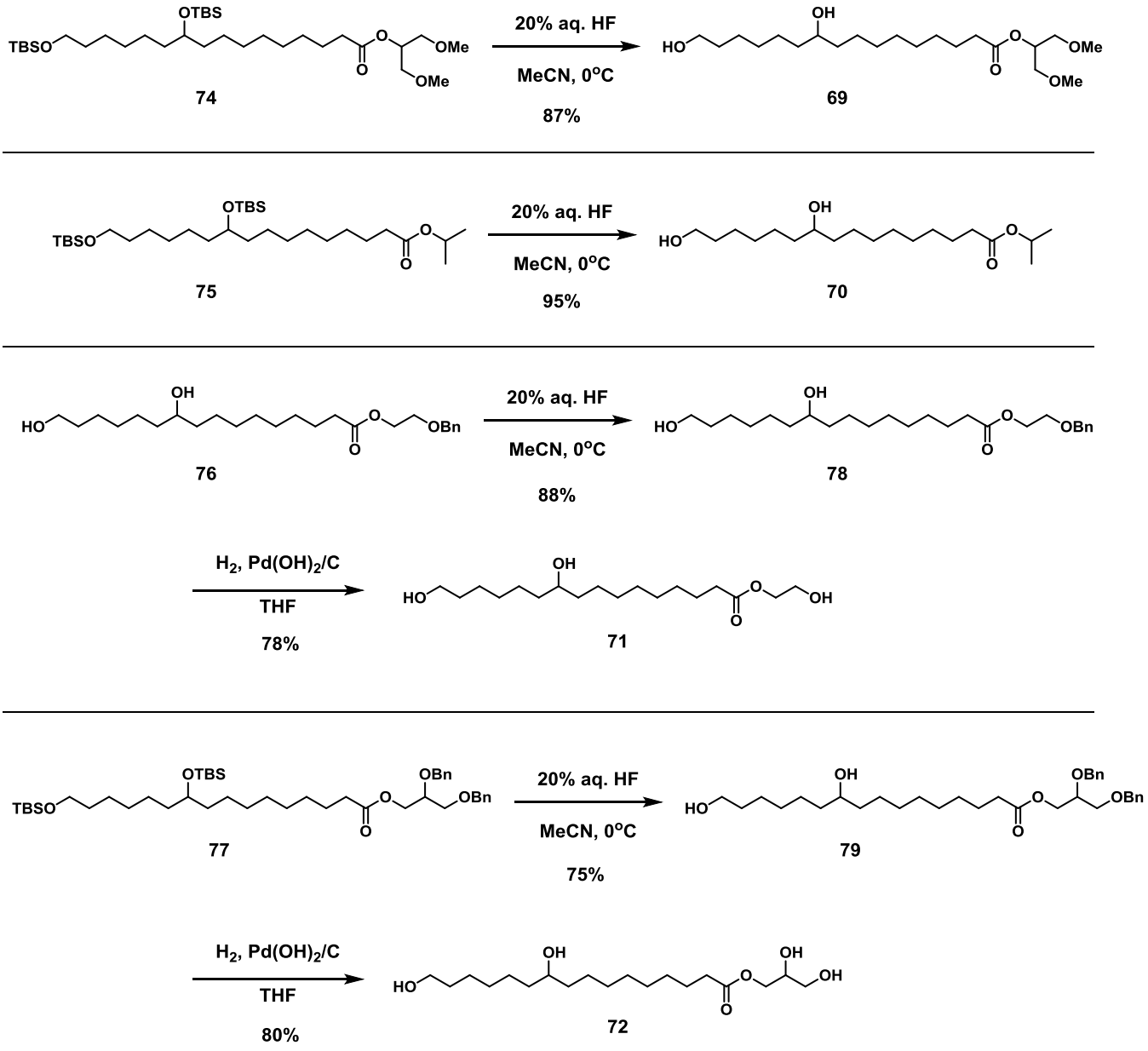

Scheme 4.2. Final steps in the synthesis of compounds **69–72**

4.3 Enzymatic oligomerization of 2-MHG derivatives

The *in vitro* oligomerization experiments of compounds **69**–**72** were performed by our collaborators at Cornell University, following the same procedure to the oligomerization of 2-MHG. The products of the oligomerizations were analysed by MALDI-TOF. Negative controls were also performed to account for any non-catalysed self-esterification process. Surprisingly, CUS1 displayed some activity towards all the compounds, as can be seen in Figure 4.2 and Figure 4.3, which show the mass spectra for all the experiments, including the negative controls.

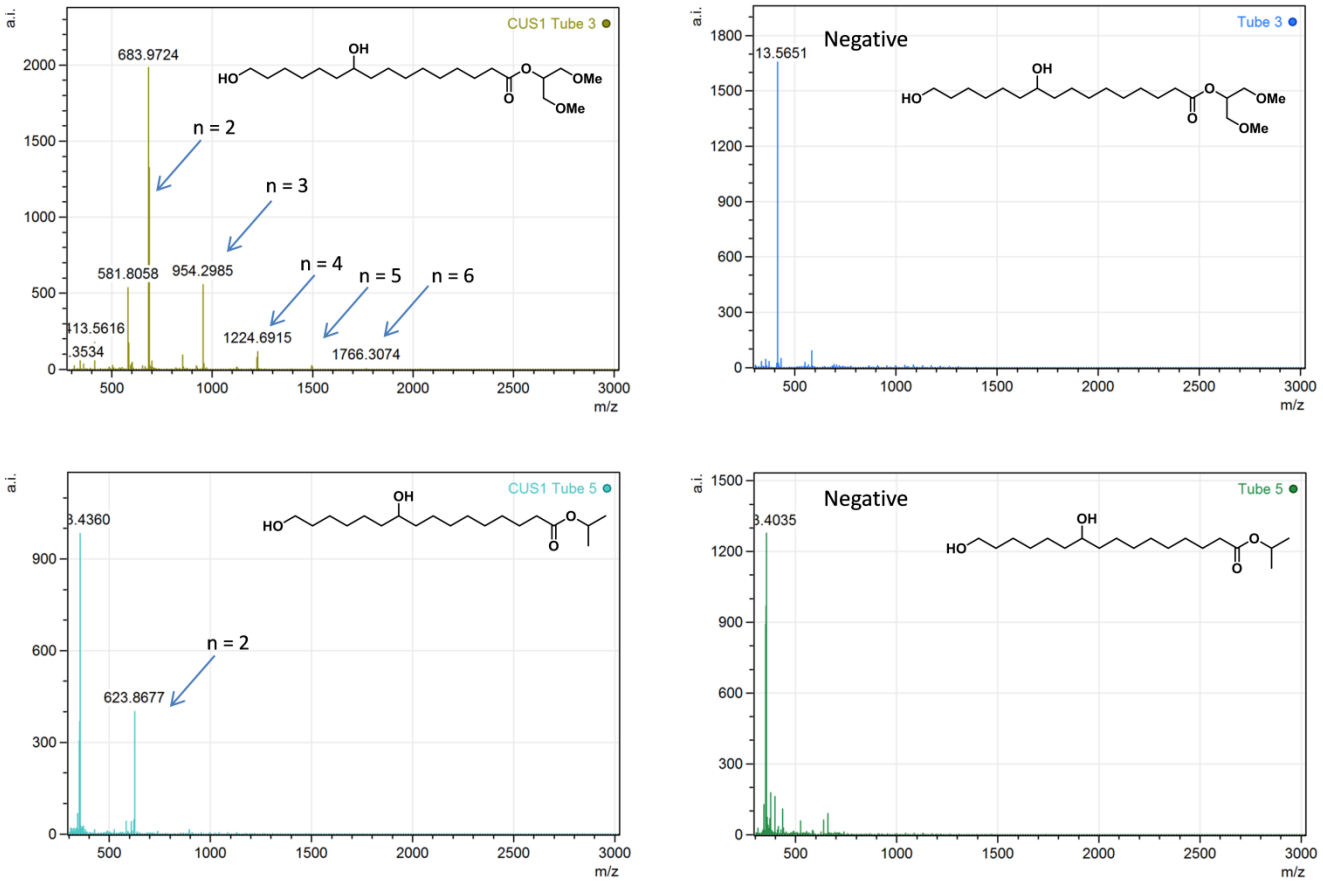

Figure 4.2. MALDI-TOF mass spectra of the oligomerization tests with the esters **69** and **70** (above and below, respectively), and their corresponding negative controls (right). n = degree of polymerization

The mass spectrum of the experiment with 1,3-methoxy glyceryl ester **69** shows a series of peaks which corresponds to its oligomers with up to six monomeric units. The negative control, on the other

hand, did not produce any oligomer, proving that the esterification reactions were produced due to enzymatic activity. Moreover, the enzymatic experiment of products **71** and **72** also produced oligomers with up to six monomeric units, while the experiment with compound **70** only produced the dimer. None of mass spectra of the negative controls, however, showed the formation of any polymerization products. This surprising result shows that CUS1 is a much more promiscuous enzyme than it was initially believed, and that the *sn*-2 glyceryl moiety is not essential for the formation of the polymer. It is also remarkable that CUS1 accepted the *sn*-1glyceryl ester **72** as a substrate, as it undermines the hypothesis that *sn*-2 glyceryl esters of fatty acids are essential for the biopolymerization of cutin.

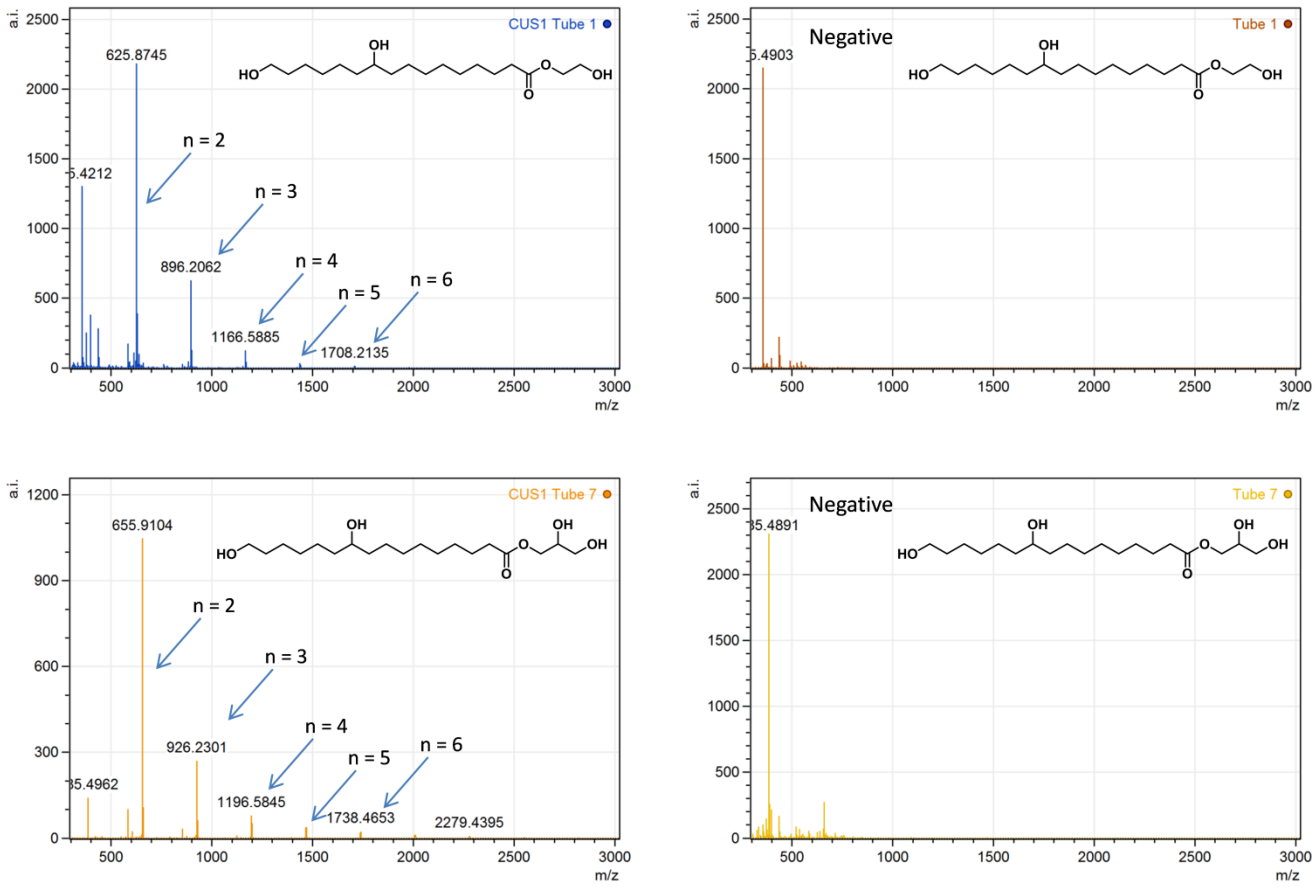

Figure 4.3. MALDI-TOF mass spectra of the oligomerization tests with the esters **71** and **72** (above and below, respectively), and their corresponding negative controls (right). n = degree of polymerization

4.4 Conclusions

Four derivative compounds of 2-MHG with different head-groups (**69**–**72**), were synthesized from intermediate **5.** All products were tested as substrates of CUS1 for the formation of 10,16-dihydroxyhexadecanoic acid oligomers. Oligomers with up to six monomeric units were formed from the esters **69**, **71** and **72**, while ester **70** only formed the dimer. Negative controls confirmed that the products formed are a result of enzymatic activity.

These results confirm that CUS1 presents activity towards fatty acid esters different than 2-MAGs *in vitro*. Moreover, CUS1 also showed activity towards 1-MHG, the thermodynamically more stable migration product of the glyceryl moiety of 2-MHG. This result is particularly interesting, as it was assumed that the migrated glyceryl moiety would prevent the enzymatic reaction, due to the essential role that GPAT enzymes, which selectively form 2-MAG esters, play in the biosynthesis of cutin. Moreover, this opens the door to the enzymatic production of cutin-like polymeric materials whose monomers could be obtained from transesterification of cutin with some simple alcohols. Further enzymatic assays with these substrates will be conducted at DTU.

5. Polyester synthesis with Candida Antarctica Lipase B (CALB)

The projects carried during the external stay at the Rensselar Polytechnic Institute (RPI), USA, under the supervision of Prof. Gross are presented in this chapter. Two different projects, involving the synthesis of polyesters with the enzyme *Candida Antarctica* Lipase B (CALB) were performed. One of them consisted on the synthesis of polypentadecalactone (PPDL) by enzymatic reactive extrusion (eREX) for its use as scaffold to direct axonal extension in spinal cord injury models, whereas the other consisted in the synthesis of branched polyol polyesters with pendant alkyne groups, which allow further modifications by copper-catalysed azide-alkyne cycloadditions ("click" chemistry).

5.1 Introduction

Polymeric materials can be found almost everywhere in the modern world. Their range of applications seems to be endless, covering from everyday usages, to industry, medicine or transportation. They are so embedded in our lives that it is impossible to imagine the current society without such materials. Polymerization reactions often require the use of catalysts or initiators to take place. In the early days of polymer science, nearly a century ago, anionic, cationic or radical catalysts (or initiators) were the only ones used. This changed in the decade of the 50´s, when the famous Zieggler-Nata catalyst[182,183] was discovered, opening the door for transition metal catalysts, which was followed by the use of metathesis catalysts.[184,185] In these cases, the development of new catalyst allowed the creation of a variety of polymeric materials that had a big impact in society and are still commonly used nowadays.

In the last decades there have been significant changes in the approach chemists take to solve problems, having a greater consideration of the environmental impact of their practices. Thus, the concept of "green chemistry" emerged,[186,187] in which factors such as toxicity of reactants and catalysts, use of solvents, reaction temperature and source of the starting materials (i.e. from renewable sources as opposed to fossil ones) are given a special attention.[188] In the field of polymer science, the concept of "green polymer chemistry" appeared for the first time in 1999.[189] In this context, the use of enzymes for polymerization reactions has gained a great interest.

Enzymes are macromolecules found in al living organisms that catalyse metabolic reactions *in vivo* necessary to maintain life. The first enzyme to be discovered was noted as diastase (amylase) by the

French chemists A. Payen and J. Persoz in 1833. From that moment, the study of enzymes and their mechanism of reaction have been one of the central topics of study in fields as biology, biochemistry, organic chemistry and pharmaceutical chemistry.[190] The relationship between enzyme and substrate was early described by the "lock and key" model by E. Fisher[191] in 1894. According to this idea, the enzyme acts as a lock and only recognizes a specific substrate, the key. However, the actual relationship between enzyme and substrate is not so strict and allows a certain degree of flexibility.[187] This means that enzymes can recognize not only natural products as substrates, but also artificial ones. This flexibility makes enzymes a useful tool to catalyse reactions *in vitro*, including polymerization reactions.

The term enzymatic polymerization is defined as a chemical polymer synthesis *in vitro* via non-biosynthetic pathways which is catalysed by an isolated enzyme.[189] Enzyme-catalysed polymerizations present a series of advantages over their chemically-catalysed counterparts, such as the mild reaction conditions, the possibility to synthesize polymers with well-defined structure and the fact that enzymes are derived from renewable resources.[187]

Lipases are one of the types of enzymes most commonly used in enzymatic polymerizations. Lipases are a ubiquitous class of esterases found in most plans and animals, which can hydrolyse triglycerides at the interface between oil and water.[192] They are amongst the most versatile types of biocatalysts for the synthesis of organic compounds due to the wide variety of synthetic substrates that are capable of accommodating. Furthermore, lipases can be used in non-aqueous media to perform ester syntheses or transesterifications.[193]

5.1.2 Lipases as catalysts for ring opening polymerization

The use of lipases in ring opening polymerization (ROP) of lactones was first reported in 1993 independently by Kobayashi *et al.*[194] and Knaki *et al*.[195] Lactones with a ring size ranging from 4 to 17 have been successfully polymerized using lipases from various sources. The mechanism for this type of enzymatic reactions was first proposed by Uyama *et al.* (Figure 5.1). [196] The key step in the process is the formation of an acyl-enzyme intermediate (enzyme-activated monomer, EM) through the ring opening of the lactone. The initiation stage occurs by the nucleophilic attack of water, presumably contained within the enzyme, on the acyl carbon of the EM intermediate, yielding a ω-hydroxycarboxylic acid. Another EM suffers the nucleophilic attack of the terminal hydroxy group of the growing polymer species, thus forming an one-unit elongated chain.[197]

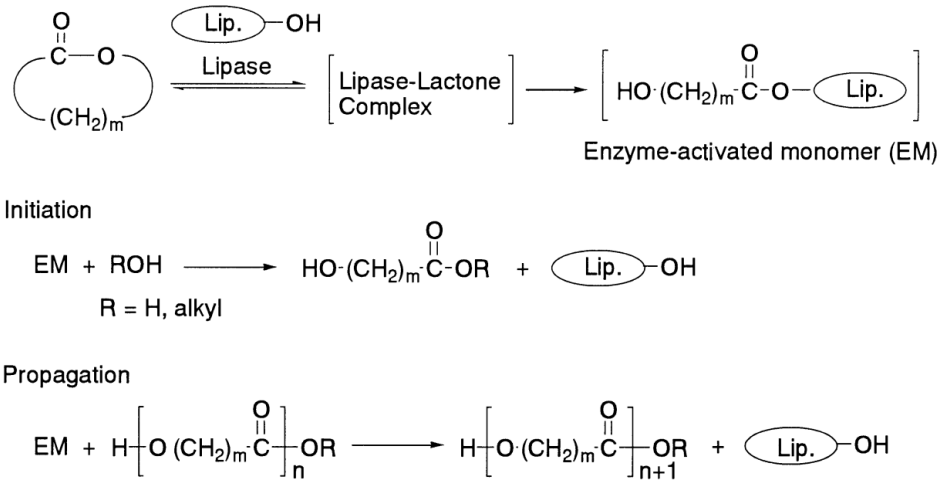

Figure 5.1. Proposed reaction mechanism for the lipase-catalysed polymerization of lactones[197]

The ROP of macrolides (lactones with ring size ≥ 12 atoms) by conventional catalysts require long reaction times and only low molecular weight products are obtained. Lipase-catalysed ROP of macrolides, on the other hand, proceeds efficiently. In fact, the ease of polymerization of lactones using lipases is directly related to their ring size.[198] The study of chemical ROP of lactones revealed that it depends strongly on the strain on the ring, and as a result, small lactones polymerize faster. On the other hand, lipase catalysed ROP depends mainly on the conformation of the lactone. A transoid conformation (see Figure 5.2), which can only be adopted by lactones with a ring size of ten or more, is preferred over the cisoid conformation, typical of small lactones.[198,199] Among the various lipases studied for ROP of lactones, CALB has been the most often used, due to its high activity.[190]

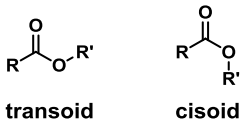

Figure 5.2. Cisoid and transoid conformations of an ester bond

The synthesis of high molecular weight (number average molecular weight (M_n) > 50000 g/mol) polyesters by ROP usually encounters diffusion problems due to the high viscosity of the polyester products. This issue is commonly overcome by increasing the reaction temperature or by use of solvent. The increase of temperature is not feasible for enzymatic reactions, and the use of solvent reduces the volumetric productivity of the reaction and requires solvent recycling. An alternative

solution is the use of reactive extrusion (REX), in which the formation of the polymer is produced simultaneously to its extrusion.[200] A recent study demonstrated that the immobilised CALB Novozyme 435 (N435) is able to withstand the rough conditions used in the REX of ω-pentadecalactone (PDL), yielding very a high molecular weight (M_n = 90000 g/mol) polyester. This supposes a great improvement compared to enzymatic bulk polymerization in a batch reactor, whose products did not exceed M_n values of about 20000 g/mol. Furthermore, REX shortens reaction time and increases monomer conversion, so the product does not require additional purification.[200]

5.1.3 Lipases as catalysts for polycondensation reactions

Lipases can also be used as catalysts for polycondensation reactions of diols and dicarboxylic acids or their esters.[201] The enzymatic synthesis of aliphatic polyesters from dicarboxylic acids and diols in a solvent-free system was first reported in 1998, using CALB as the catalyst.[202] Shortly after, CALB was used in a bulk polymerization of adipic acid and sorbitol (1:1 mixture), which resulted in polyester products with M_n = 17,000 g/mol and a polydispersity index (Đ) of 1.6.[203] The molecular weight could be increased to 117,000 g/mol by using a 50:35:15 mixture of adipic acid, 1,8-octanediol and sorbitol, respectively. CALB presents a significant regioselectivity (95%) towards the primary alcohols of sorbitol, producing linear polymers with unsubstituted hydroxyl groups, which can potentially be used as anchoring points to further modify the material. Moreover, an increase in the ratio of glycerol or sorbitol to 1,8-octanediol produces a decrease in the degree of crystallinity, melting point and glass-transition temperature. Furthermore, the susceptibility of the copolymer to suffer hydrolytic degradation increases with the amount of sorbitol/glycerol, which can be exploited to produce materials with adjustable bioresorption rates.[204] However, when glycerol was used instead of sorbitol, the selectivity towards the primary alcohols was reduced to 66%, yielding highly branched polymers.[203] The degree of branching of copolyesters of 1,8-octanediol, glycerol and adipic acid could be adjusted by varying the reaction time.[205] During the first 18 hours of reaction, the products were mostly linear, but the degree of branching increased after that point. After 42 hours, hyperbranched polymers with dendritic glycerol units and broad weight distributions were produced.

The lipase-catalysed synthesis of polyesters with pendant groups that could allow further modifications of the polymers has been explored. For instance, Kulshrestha *et al.* reported the synthesis of polyesters with pendant carboxylic acid groups using CALB as catalyst without the need of protection-deprotection steps.[206] CALB has also been used for the synthesis of other aliphatic polyesters bearing functional groups such as mercapto,[207] vinyl,[208] tertiary amine,[209] hydroxy[210] and epoxy.[211] The incorporation of azido groups in aliphatic polymer chains is of particular interest, as it allows a wide range of modifications, such as the incorporation of small functional groups,[212,213] macromolecules[214,215] and pharmacologically active molecules.[216,217]

5.2 Synthesis of PPDL and a poly-L-lactic acid/poly(pentadecalactone) (PLLA-PPDL) blend by eREX

5.2.1 Goals and scope of the project

Electrospun polymer fibres have potential uses as scaffolds for tissue engineering purposes, particularly in spinal cord injury applications.[218,219] Aligned electrospun fibers provide anisotropic guidance for the growing neurons, which tend to mimic the topography of the polymer matrix.[220,221] To date, it has not been reported the influence of surface topography of electrospun fibres on neural growth. Nonetheless, it has been found to be an important factor in other types of cells.[222] The tensile properties of the scaffold also have an influence in neural growth, as it has been proved that a lower tensile modulus is beneficial in neuronal differentiation and adhesion.[223,224] Poly-L-lactic acid (PLLA) fibres have demonstrated efficacy in promoting spinal cord injury regeneration,[220] despite their high tensile modulus. Moreover, a study by Spinella *et al*. previously demonstrated that the reactive blending of PLLA with poly(ω-hydroxytetradecanoic acid) by reactive extrusion results in a decrease in the Young´s modulus of the blend.[225]

The goal of the present project is to synthesize high molecular weight PPDL by eREX using CALB as the biocatalyst, and use the produced polyester to prepare a PLLA/PPDL blend using the method developed by Spinella *et al.*[225] Electrospun fibres of the PPDL/PLLA blend will later be produced and characterised for their use as scaffold to direct neural growth.

5.2.2 Results and discussion

High molecular weight PPDL was first attempted to be synthesized by eREX following the procedure developed by Spinella *et al.* (Scheme 5.1).[200] The reaction was monitored indirectly by measuring the force required to rotate the screws of the reactive extruder. This axial force is proportional to the viscosity of the polymer, which in turn provides an indication of the degree of polymerization. According to the literature, the polymerization is considered to be finished when a force of 10,000 N, the maximum allowed by the instrument, is reached. However, when the reaction was attempted, the maximum axial force registered was 1700 N, which remained constant thereafter. Furthermore, the obtained product was stiff and brittle, which is an indication of low molecular weight. This was believed to be due to the presence of water, which would lead to the hydrolysis of the polymer chains, and thus prevent the formation of high molecular weight products. Several attempts of repeating the reaction were made taking different measures to avoid the presence of water inside the extruder (e.g.

using newly acquired enzyme and/or drying the enzyme and the monomer under vacuum), with identical results.

Finally, by increasing the temperature inside the extruder to 150 °C and flushing it with nitrogen for 15 minutes prior to the start of the reaction, an axial force of 10,000 N was reached and the polymer product was flexible. The obtained PPDL presented a M_n of 106,000 g/mol, which is significantly higher than the one reported in the literature (M_n = 90,000 g/mol), and a Đ of 1.55.

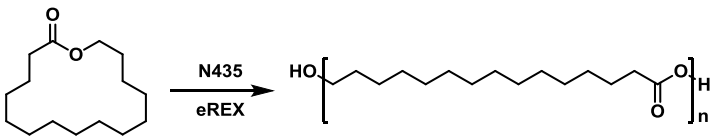

Scheme 5.1. Synthesis of PPDL by enzymatic reactive extrusion of PDL

The synthesized PPDL, together with commercially available PLLA (Mn = 113,000 g/mol, Đ = 1.45), were used to form a PLLA/PPDL (9/1 w/w) blend following the procedure developed by Spinella *et al*. using the reactive extruder to achieve an homogeneous mixing and $Ti(OBu)_4$ as catalyst.[225] PLLA and PPDL are thermodynamically immiscible due to the low polarity of the aliphatic chain of PDL, which leads to phase separation. The purpose of the reactive blending is to increase the adhesion of the two polymers by forming block-like copolymers at the interface of the two phases (Figure 5.3). The resulting blend presented a lower M_n of 83,000 g/mol, which is attributed to mechanical degradation caused by the torque generated by the screws, while Đ remained similar, with a value of 1.53.

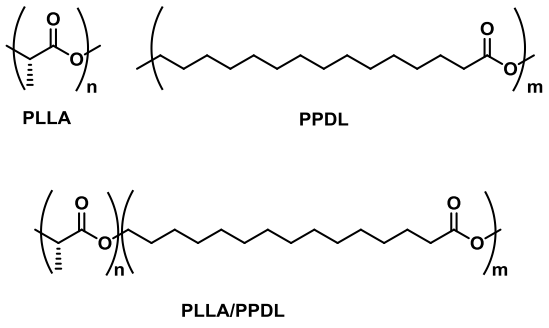

Figure 5.3. PLLA/PPDL blend. Block PLLA-PPDL copolymers form in the interface between the two polymers.

^{1}H NMR of the PLLA/PPDL blend (Figure 5.4) shows two intense signals, a quadruplet at 5.17 ppm and a duplet at 1.58 ppm which correspond to the single proton at the α position to the carbonyl and the methyl group of PLLA, respectively. Two triplets at 4.05 and 2.28 ppm, which correspond to the protons at the α position to the carbonyl and the ester of PPDL, respectively, are also visible. The signals corresponding to PPDL showed an integration of 0.06, which corresponds to a 9:1 ratio once the different degree of polymerization of both materials.

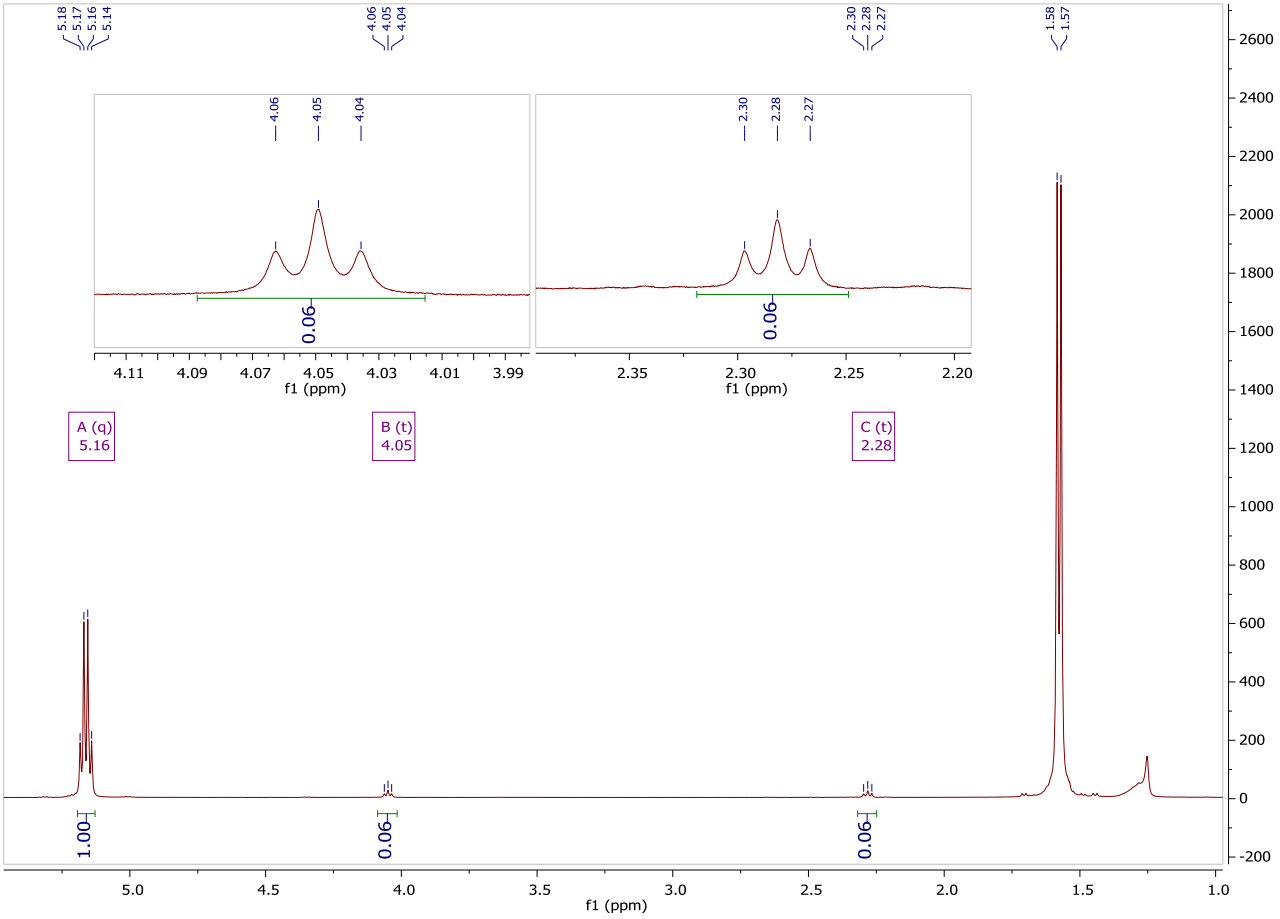

Figure 5.4. ^{1}H NMR of the PLLA/PPDL blend

5.2.3 Conclusions and future perspectives

High molecular weight PPDL was successfully synthesized by eREX using CALB as the catalyst. The initial low molecular weights obtained were attributed to the presence of traces of humidity in the system. This problem could be overcome by pre-heating the extruder and flushing it with nitrogen prior to the reaction, which suggests that this procedure is more sensitive to humidity than it was initially believed. A PLLA/PPDL (9/1 w/w) blend was formed by reactive blending using $Ti(OBu)_4$ as catalyst to promote transesterification reactions, forming block copolymers at the interface of the two polyesters.

Production and characterization of polymer fibres by electrospinning was carried by other member of the group. These fibres were used as scaffolds to direct neural growth, as part of a study in spinal cord injury models, pendant of publication.

5.3 Enzymatic polycondensation of polyols with terminal alkyne groups

5.3.1 Goals and scope of the project

CALB has proven to be an effective catalyst for the formation of polyesters with polyols, diols and dicarboxylic acids in solvent-free conditions. It has been found that both the molecular weight of the products and their degree of branching depend to a great extent on the polyol used.[226] Polyesters with higher molecular weights and degrees of branching have been obtained by the use of mannitol as the polyol. It is hypothesized that by adjusting the ratio of the reactants, hyperbranched polymers could be synthesized by this method. Furthermore, it is possible that those hyperbranched polyesters could be able to form stable unimolecular micelles in aqueous media, provided that a sufficiently hydrophobic dicarboxylic acid is used. Additionally, pendant terminal alkyne groups, which would allow further modifications of the material by "click" chemistry, could be incorporated into the polymer.

The goal of the present project is to synthesize branched polyesters with dodecanedioic acid (DDDA), mannitol, 1,6-hexanediol (HD) and 5-hexynoic acid (HA) (Figure 5.5) by enzymatic polymerization with CALB in a solvent-free system. The influence of the ratio diol/polyol and alkyne/polyol in the molecular weight and thermal properties of the final polymers will be explored, and unimolecular micelles of the materials would be attempted to form in aqueous medium.

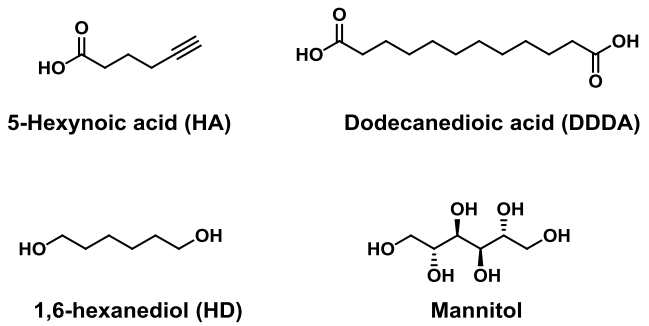

Figure 5.5. Monomers used in the enzymatic polycondensation reactions

5.3.2 Results and discussion

All polymers were synthesized following the procedure developed by Hu *et al*,[226] using a variety of proportions of the different monomers, DDDA, HD, HA and mannitol. In all cases, the number of moles of DDDA was equal to the sum of HD and mannitol, and therefore, the amount of dicarboxylic acids of DDDA is equal to the total amount of primary hydroxyl groups. All those monomers are bifunctional, and therefore could constitute the backbone of the final polymer. HA, on the other hand, only has one group that can form ester linkages, and therefore is a terminal monomer. The addition of a certain amount of HA implies that there are more carboxylic acid groups than primary hydroxyl groups. Hence, in the case of achieving total monomer conversion, a certain degree of secondary esters would necessarily be formed.

Polyesters (PE) with eight different monomeric compositions were synthesized, in order to assess the influence of the molar ratios of diol/polyol and alkyne/polyol (Table 5.1). It has been reported that this type of reactions are very sensitive to small variations in the applied vacuum, having a noticeable impact on the molecular weight of the products. Hence, a vacuum regulator was used. Furthermore, each reaction was performed in triplicate.

Table 5.1. Molar ratio of HD/mannitol and HA/mannitol of the synthesized polyesters.

Polymer	HD/mannitol ratio	HA/mannitol ratio
PE-1	0.5	1
PE-2	1	1
PE-3	3	1
PE-4	5	1
PE-5	3	0.5
PE-6	3	1.3
PE-7	3	1.6
PE-8	3	2

Figure 5.6 displays the influence of the molar ratio of HD/mannitol and HA/mannitol on M_n and Đ and the correspondent values are listed in Table 5.2. The ratio HD/mannitol did not appear to have a significant effect on the molecular weight of the products, which had a M_n of approximately 10000 g/mol, with the exception of polymers with a ratio of HD/mannitol of 0.5, whose M_n was significantly lower than the rest, at around 3000 g/mol. The ratio HA/mannitol, on the other hand, appeared to have a small effect on the molecular weight, which tends to decrease as the ratio increases. However, this is a slight trend, which is mainly noticeable at the highest and lowest values of the HA/mannitol ratio. It was indeed expected that increasing the relative amount of a terminal monomer would result in lower molecular weights, as its inclusion in the polymer occupies a hydroxyl position, blocking any further polymer growth in it.

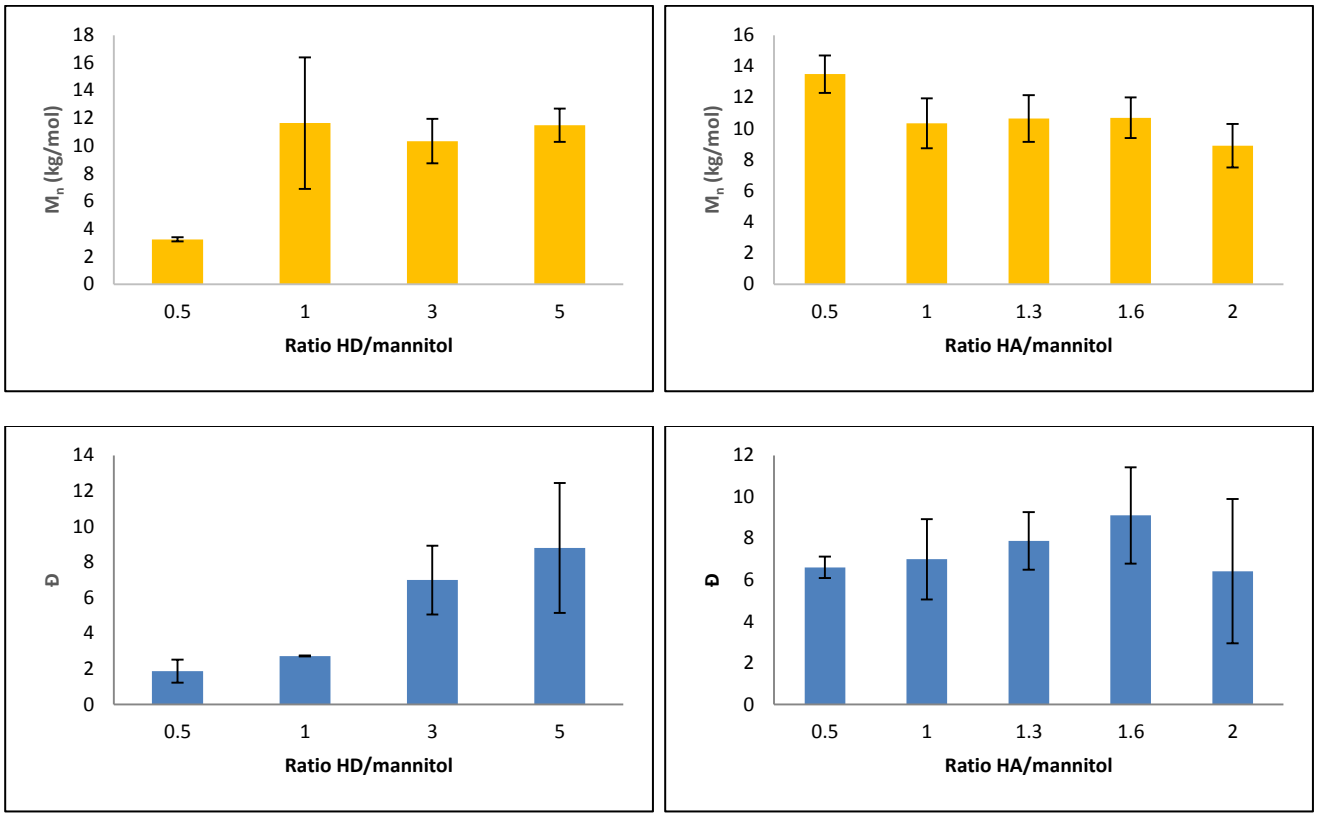

Figure 5.6. Effect of the molar ratio of HD/mannitol (left) and HA/mannitol (right) on M_n (above) and Đ (below)

All synthesized polymers presented broad polydispersity indexes, ranging from 1.9 to 9.7. The ratio of HD/mannitol had a significant effect on Đ, which was higher in polymers with a higher HD content. Moreover, Đ values varied significantly between the triplicates, particularly in samples with higher HD contents. Đ also seemed to increase with the ratio HA/mannitol, except in the material with a HA/mannitol ratio of 2. However, the high standard deviation of these values prevents to reach any conclusion.

DSC analysis of the products did not show any glass transition in the measured range of temperatures (-80–225 °C). However, all materials showed crystallization and melting temperatures (T_c and T_m, respectively), evidence of the presence of crystalline regions in the polyesters. T_c and T_m presented a significant variation with the different HD/mannitol ratios, ranging from 41 to 0.5 °C and from 30 to 56 °C, respectively (Figure 5.7). T_c and T_m appear have the tendency to increase with the HD/mannitol ratio, except for the material with a ratio equal to 1, which presented significantly lower values. However, it is difficult to reach a conclusion with such low number of data points. Moreover, T_c and T_m show a clearer tendency to decrease with increasing HA/mannitol ratios, ranging from 21 to 27 °C and from 39 to 53 °C, respectively.

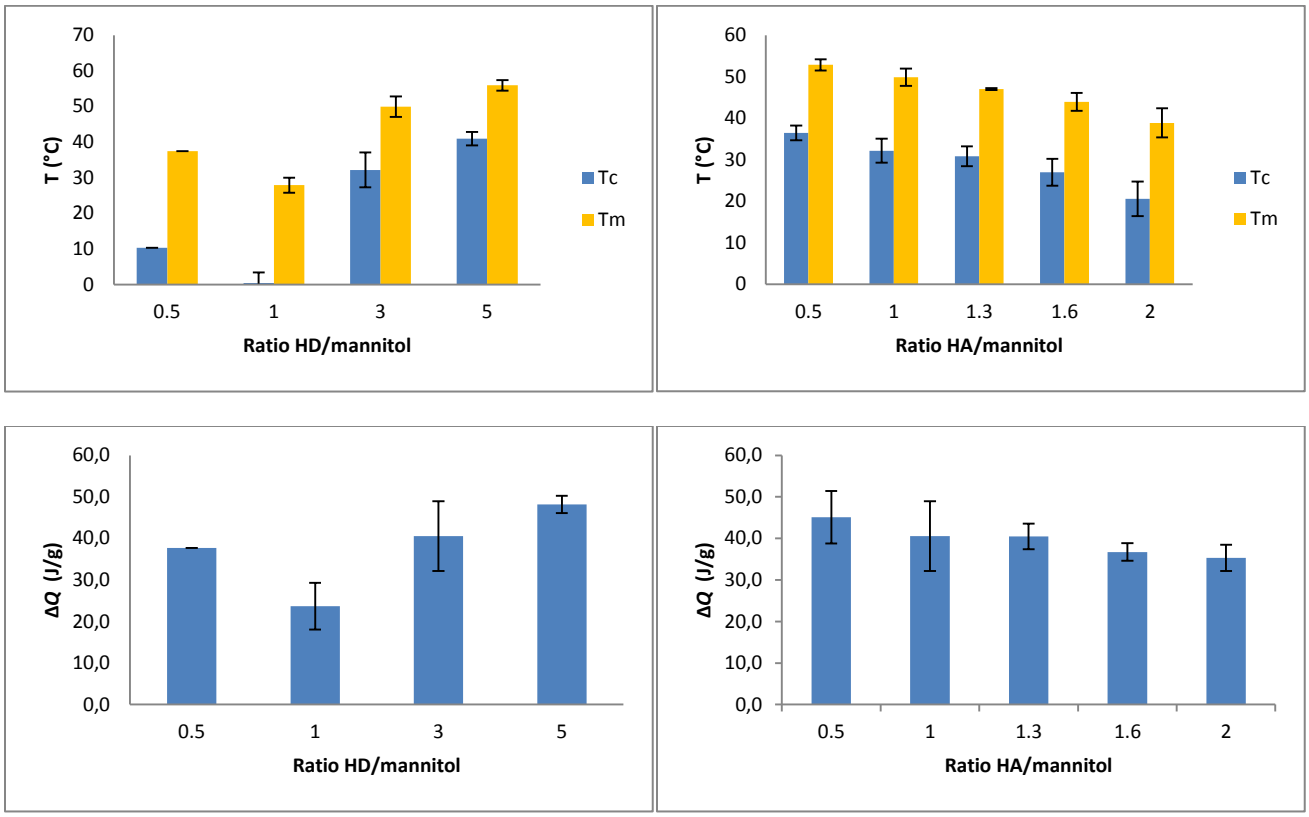

Figure 5.7. Effect of the molar ratio of HD/mannitol (left) and HA/mannitol (right) on T_c and T_m (above) and ΔQ (below)

The heat of fusion (ΔQ) of the polymers provides an indication of their degree of crystallinity. ΔQ tended to increase with the ratio HD/mannitol, with the exception of the polymer with a ratio equal to one, which again presented a lower value than expected. This result was expected, as it has been reported that the degree of crystallinity of aliphatic polyesters decreases with the content of polyols.[204] A small reduction of ΔQ with increasing AH/mannitol ratios was also observed. It is likely that the crystallinity of the polyesters is largely due to the presence of long aliphatic chains of DDDA. The use of larger amounts of HA would reduce the total amount of DDDA, and thus the crystallinity of the final polymer. A summary of the values of T_c, T_m and ΔQ is displayed in Table 5.2.

Table 5.2. Average M_n, Đ, T_c, T_m and ΔQ of the synthesized polyesters

Polymer	M_n (kg/mol)		Đ		T_c (°C)		T_m (°C)		ΔQ (J/g)	
	Average	±	Average	±	Average	±	Average	±	Average	±
PE-1	3.3	0.2	1.9	0.6	10.3	-	37.5	-	37.7	-
PE-2	11.7	4.8	2.7	0.0	0.5	2.9	27.9	2.09	23.7	5.63
PE-3	10.4	1.6	7.0	1.9	32.2	4.9	49.9	2.87	40.6	8.38
PE-4	11.5	1.2	8.8	3.6	41.0	1.9	55.9	1.47	48.2	2.09
PE-5	13.5	1.2	6.6	0.5	36.5	1.8	52.9	1.36	45.1	6.32
PE-6	10.7	1.5	7.9	1.4	30.9	2.4	47.0	0.25	40.5	3.08
PE-7	10.7	1.3	9.1	2.3	27.0	3.3	43.9	2.18	36.7	2.13
PE-8	8.9	1.4	6.4	3.5	20.6	4.2	38.9	3.50	35.3	3.16

The formation of unimolecular micelles was first attempted with PE-5, which was selected due to its high molecular weight, by the following procedure: 25 μl of a rhodamine solution in THF (5mg/ml) were added to a solution of PE-5 (150 mg) in THF (1 ml). The resulting mixture was added to H_2O (5ml) while stirring in a vortex mixer (1200 rpm) at a pace of 10 μl per 30 seconds. The emulsification was a failure, as the polymer precipitated. Due to time constrains, it was not possible to optimize the conditions or to make further attempts with other polyesters. Additional work on the direction will be carried out by other members of the group.

5.3.3 Conclusions and future perspectives

In the present project, a series of polyesters with eight different monomeric compositions were synthesized, using DDDA, HA, HD and mannitol as monomers and CALB as the catalyst in a solvent-free system. The influence of the HD/mannitol and HA/mannitol ratios on the molecular weight, polydispersity, crystallization and melting temperatures and the heat of fusion of the different polymers were analysed. No strong correlation could be observed between the HD/mannitol and HA/mannitol ratios and the molecular weight of the products. However, M_n seemed decrease at higher HA/mannitol ratios. T_c, T_m and ΔQ do not show a clear correlation with the HD/mannitol ratio either. However, T_c, T_m and ΔQ show a tendency to decrease in polymers with higher HA/mannitol ratios.

The first attempt to form unimolecular micelles with material PE-5 in an aqueous medium resulted in the precipitation of the polyester. No further attempts of optimizing the conditions of the emulsification were made due to time limitations. Future stages of the project, including formation and characterization of unimolecular micelles and their further modification by “click” chemistry will be undertaken by other members of prof. Gross´s group.

6. Experimental

6.1 General considerations

All reagents, solvents and materials were purchased from commercial sources and used without further purification. All solvents were of HPLC grade. All reactions in which anhydrous conditions were necessary were performed in flame-dried glassware under inert atmosphere of either argon or nitrogen. Anhydrous solvents were obtained from an Innovative Technology PS-MD-7 Pure-solv solvent purification system. All reactions were monitored by thin-layer chromatography (TLC) performed on Merck aluminium coated with silica gel C-60 F_{254}. The plates were visualised by UV radiation (254 nm) and/or by applying heat after dipping in a developing solution [$KMnO_4$ (3 g) in water (300 ml) together with K_2CO_3 (20 g) and 5% aqueous NaOH (5 ml)]. Eluent systems and R_f values are specified for each compound and the eluent system is given as volume ratio. Solvents were removed under reduced pressure (*in vacuo*) using a Heidolph Laborota 400 system at a temperature range of 20–40 °C. Traces of solvents were removed *in vacuo* by means of a membrane pump operating at 0.27 mbar. Gerudan silicagel 60 (40-63 µm) was used as the stationary phase for flash column chromatography following the general method developed by Still *et al.*[227] Reverse–phase chromatography was performed using a C18 silica gel as stationary phase by the general procedure for dry column vacuum chromatography described in the literature.[228] The eluent system is specified for each synthesis, indicating the ratio as volume ratio. Nuclear Magnetic Resonance Spectroscopy (NMR) spectra were recorded with a Bruker Ascend 400 spectrometer with a Prodigy cryoprobe, operating at 400 MHz for ^{1}H and at 101 MHz for ^{13}C. Chemical shifts (δ) are reported in parts per million (ppm) downfield from tetramethylsilane (δ = 0 ppm) using the solvent resonance as the internal standard ($CDCl_3$, ^{1}H: 7.26 ppm, ^{13}C: 77.16 ppm; MeOD, ^{1}H: 4.87 ppm, ^{13}C: 49.00 ppm; benzene, ^{1}H: 7.16 ppm, ^{13}C: 128.06 ppm) and coupling constants (*J*) are reported in Hz. Multiplicities are reported as singlet (s), broad singlet (br. s), doublet (d), doublet of doublets (dd), doublet of triplets (dt), triplet (t), triplet of doublets (td), triplets of triplets (tt), quadruplet (q), pentet (p) and multiplet (m). All compounds were characterized by NMR using 1D and 2D experiments and all peaks have been assigned except the ones corresponding to free hydroxyl groups as it can be seen in the supporting information. HPLC-ELS analysis were performed using a Waters e2695 module, equipped with a 1260 Infinity ELS detector (evaporation temperature: 50 °C, Nebulization temperature: 50 °C) with a C8 column (length: 7.5 cm, particle size 3 µm, flow: 1 ml/min). Elution was carried out combining eluent A (5 mM NH_4Ac in H_2O) and eluent B (5 mM NH_4Ac in 90% aq. MeCN) in the following fashion: 20% B for 1 minute, gradual increment of B to 30% for 4 minutes, gradual increment of B to 40% for 15 minutes, then sudden reduction of B to 20% and hold for 3 minutes. Total run time: 23 min. HRMS was performed either with a MALDI-TOF (Bruker Solarix XR 7T ESI/MALDI-FT-ICR-MS run in MALDI+ mode, externally calibrated with NaTFA cluster ions and using dithranol as the matrix) or with a UHPLC-

QTOF system (Dionex ultimate 3000 and Bruker Maxis) with an electrospray ionization (ESI) and controlled using DataAnalysis v4.2 software. Melting points were measured in a Stuart melting point SMP30 and reported in °C uncorrected. Fourier Transformation Infra-Red (FT-IR) spectroscopy was conducted on a Bruker Alpha-P FT-IR instrument. The enzymatic assays were conducted in an Eppendorf ThermoMixer C. MALDI-MS was conducted in a UltraFlex run in MALDI+ mode, externally calibrated with a proprietary mixture of polyhexose using super DHB (9:1 (w/w) mixture of 2,5-DHB and 2-hydroxy-5-methoxybenzoic acid, respectively) as matrix. Polycondensation reactions were performed in an Argonaut Advantage Series 2050 personal synthesizer, which allows running five different reactions in parallel with independent temperature control and magnetic stirring. Pressure was controlled by a digital vacuum regulator J-KEM Schientific, model 200. Molecular weight of the products was measured in a Viscotek THF-GPCmax model 302. Enzymatic reactive extrusions (eREX) were performed in a Xplore Microcompounder MC15. M_n and Đ were determined by a Waters 515 Chloroform GPC. The synthesis of 1,3-dihydroxypropan-2-yl 10,16-dihydroxyhexadecanoate-11,11,12,12-t_4 from **7** was performed by Quotient Bioresearch following the same procedure as the synthesis of **8**, but substituting deuterium for tritium. The final product was purified by HPLC using the method stated above. 91.6% radiochemical purity (RCP).

6.2 General procedure for the enzymatic oligomerization of cutin and suberin monomers

In an Eppendorf tube were mixed 0.5 µl of stock solution of the monomer (5 µmol of monomer in 50 µl of dry DMSO) with 1.25 µl of CUS1 solution (0.4 µg/µl) and a buffer solution (NH_4Ac, 50 mmolar, pH = 5) up to a total volume of 50 µl. In the case of the experiments involving two monomers, 0.5 µl of a premix solution (prepared by mixing 10 µl of each of the stock solutions of the monomers) was added. The negative controls were prepared without CUS1 solution. The mixture was kept at 37 °C for 24 h and then it was quenched with MeOH (150 µl).

6.3 General procedure for the synthesis of polyol-polyesters *via* enzymatic polycondensation

All polymerizations were performed according to literature protocols.[226] Dodecanedioic acid (DDDA), 1,6-hexanediol, 5-hexynoic acid and mannitol, with a total weight of 2 g, were placed in a glass vessel. The reactants were heated to 130 °C for one hour, allowing them to melt and form a homogeneous liquid. Temperature was reduced to 90 °C and N435 (200 mg) was added. The reactions were kept at

90 °C for 46 h while stirring. The pressure was reduced in accordance to the following schedule: 760 torr for 2 h, 100 torr for 4 h, 75 torr for 12 h, 50 torr for 12 h, and 25 torr for 16 h. The reaction mixture was then dissolved in chloroform (10 ml), filtered through Celite and concentrated. The resulting polyesters were dissolved in chloroform (2 ml), fractionated in cold MeOH (15 ml, -78 °C), filtered and dried in a vacuum oven.

6.4 Experimental procedures

10-(Benzyloxy)decan-1-ol (**1**)

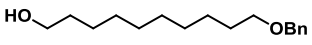

To a suspension of NaH (60% in oil, 1.38 g, 0.0574 mol) in dry DMF (25 ml) at 0 °C under an atmosphere of nitrogen was slowly added a solution of 1,10-decanediol (10.00 g, 0.057 mol) in a mixture of THF and DMF (20 and 25 ml, respectively). The resulting mixture was let to warm slowly to 20 °C. After 2 h, BnBr (9.52 g, 0.043 mol) was added dropwise. The reaction was stirred for 16 h and excess reagent was quenched by addition of ice until bubbling ceased. The mixture was extracted with Et_2O (3 × 100 ml). The combined organic phases were washed with sat. aq. NaCl (100 ml), dried with $MgSO_4$, filtered, concentrated and purified by flash chromatography (EtOAc/heptane 1:4) affording **1** as a white solid (3.83 g, 51%); $\mathbf{R_f}$ (EtOAc/heptane 1:4) = 0.16; **^{1}H NMR** (400 MHz, $CDCl_3$) δ 7.40–7.24 (m, 5H), 4.50 (s, 2H), 3.63 (t, *J* = 6.6 Hz, 2H), 3.46 (t, *J* = 6.6 Hz, 2H), 1.67–1.52 (m, 4H), 1.42–1.25 (m, 12H); **^{13}C NMR** (101 MHz, $CDCl_3$) δ 138.83, 128.47 (2C), 127.75 (2C), 127.60, 72.99, 70.66, 63.21, 32.92, 29.90, 29.67, 29.65, 29.59, 29.54, 26.32, 25.86; **HRMS (MALDI+)** $C_{17}H_{28}O_2$, m/z [M+Na+] 287.1982, found 287.1982

tert-Butyl(hex-5-yn-1-yloxy)dimethylsilane (**2**)

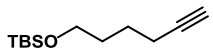

To a solution of 5-hexyn-1-ol (9.00 g, 91.7 mmol) in dry DMF (45 ml) under an atmosphere of nitrogen was added imidazole (9.37 g, 137.6 mmol) and TBSCl (18.02 g, 119.2 mmol). The reaction mixture was stirred for 4 h, and then poured on sat. aq. NH_4Cl (250 ml) and extracted with CH_2Cl_2 (3 × 250 ml). The combined organic phases were washed with sat. aq. NH_4Cl (250 ml), dried with $MgSO_4$, filtered, concentrated and purified by flash chromatography (EtOAc/heptane 1:19) affording **2** as a colourless oil (19.30 g, 99%); $\mathbf{R_f}$ (EtOAc/heptane 1:19) = 0.77; **^{1}H NMR** (400 MHz, $CDCl_3$) δ 3.63 (t, *J* = 6.0 Hz, 2H), 2.21 (td, *J* = 6.8, 2.6 Hz, 2H), 1.94 (t, *J* = 2.6 Hz, 1H), 1.66–1.57 (m, 4H), 0.89 (s, 9H), 0.05 (s, 6H); **^{13}C NMR** (101 MHz, $CDCl_3$) δ 84.69, 68.39, 62.74, 31.96, 26.10 (3C), 25.10, 18.49, 18.37, -5.1 (2C); **HRMS (MALDI+)** $C_{12}H_{24}OSi$, m/z [M+Na+] 235.1489, found 235.1500.

16-(Benzyloxy)-1-((*tert*-butyldimethylsilyl)oxy)hexadec-5-yn-7-ol (**3**)

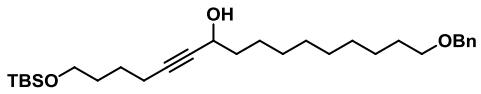

To a mixture of DMP (12.512 g, 29.50 mmol) in CH_2Cl_2 (50 ml) was added slowly a solution of **1** (6.00 g, 22.69 mmol) in CH_2Cl_2 (40 ml). The resulting mixture was stirred for 1.5 h and poured into an aqueous solution of $Na_2S_2O_3 \cdot 5H_2O$ (70 g in 300 ml). The mixture was stirred vigorously for 5 min and was extracted with Et_2O (300 ml). The organic phase was washed with sat. aq. $NaHCO_3$ (300 ml), dried with $MgSO_4$ concentrated, and used in the subsequent reaction without further purification. To a solution of **2** (6.26 g, 29.497 mmol) in dry THF (10 ml) at -78 °C under an atmosphere of nitrogen was added dropwise *n*-BuLi (12.6 ml, 2.7 M in pentane, 34.035 mmol). The resulting mixture was allowed to warm slowly to 20 °C and a solution of the crude aldehyde (5.95 g, 22.69 mmol) in dry THF (15 ml) was added. The resulting mixture was stirred for 16 h, poured into sat. aq. NH_4Cl (200 ml) and extracted with CH_2Cl_2 (3 × 200 ml). The combined organic phases were dried with $MgSO_4$, filtered, concentrated and purified by flash chromatography (EtOAc/heptane 1:9) affording **3** as a yellow oil (5.74 g, 53%); $\mathbf{R}_f$ (EtOAc/heptane 1:5) = 0.33; **^{1}H NMR** (400 MHz, $CDCl_3$) δ 7.37–7.27 (m, 5H), 4.50 (s, 2H), 4.33 (tt, *J* = 6.6, 2.0 Hz, 1H), 3.62 (t, *J* = 6.0 Hz, 2H), 3.46 (t, *J* = 6.7 Hz, 2H), 2.23 (td, *J* = 6.8, 2.0 Hz, 2H), 1.78–1.51 (m, 8H), 1.48–1.24 (m, 12H), 0.89 (s, 9H), 0.05 (s, 6H); **^{13}C NMR** (101 MHz, $CDCl_3$) δ 138.83, 128.46 (2C), 127.75 (2C), 127.59, 85.38, 81.69, 72.99, 70.64, 62.88, 62.78, 38.34, 32.06, 29.91, 29.65, 29.63, 29.60, 29.42, 26.33, 26.10 (3C), 25.36, 25.27, 18.64, 18.48, -5.14 (2C); **HRMS (MALDI+)**[22]

16-(Benzyloxy)-1,7-bis((*tert*-butyldimethylsilyl)oxy)hexadec-5-yn (**4**)

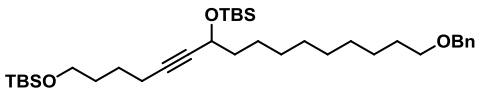

To a solution of **3** (5.73 g, 12.086 mmol) in dry DMF (30 ml) under an atmosphere of nitrogen was added imidazole (1.23 g, 18.13 mmol) and TBSCl (2.37 g, 15.712 mmol). The reaction mixture was stirred for 18 h, and then it was poured into sat. aq. NH_4Cl (200 ml) and was extracted with CH_2Cl_2 (3 × 200 ml). The combined organic phases were dried with $MgSO_4$, filtered, concentrated and purified by flash chromatography (EtOAc/heptane 1:19) affording **4** as a colourless oil (6.83 g, 96%); $\mathbf{R_f}$ (EtOAc/heptane 1:19) = 0.62; **^{1}H NMR** (400 MHz, $CDCl_3$) δ 7.36–7.27 (m, 5H), 4.50 (s, 2H), 4.31 (tt, *J* = 6.6, 2.0 Hz, 1H), 3.62 (t, *J* = 6.0 Hz, 2H), 3.46 (t, *J* = 6.7 Hz, 2H), 2.21 (td, *J* = 6.9, 2.0 Hz, 2H), 1.66–1.51 (m, 8H), 1.47–1.24 (m, 12H), 0.90 (s, 9H), 0.89 (s, 9H), 0.12 (s, 3H), 0.11 (s, 3H), 0.05 (s, 6H); **^{13}C NMR** (101 MHz, $CDCl_3$) δ 138.86, 128.48 (2C), 127.76 (2C), 127.60, 84.29, 82.37, 73.00, 70.68, 63.37, 62.81, 39.19, 32.11, 29.93, 29.70, 29.69, 29.63, 29.43, 26.35, 26.11 (3C), 26.02 (3C), 25.51, 25.33, 18.67, 18.49, 18.45, -4.27, -4.80, -5.14 (2C); **HRMS (MALDI+)**[22]

10,16-Bis((*tert*-butyldimethylsilyl)oxy)hexadecan-1-ol (**5**)

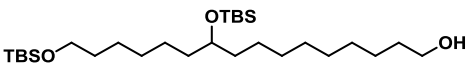

To a solution of **4** (6.75 g, 11.471 mmol) in dry EtOAc (120 ml) under an atmosphere of nitrogen was added 10% Pd/C (1.22 mg). A hydrogen atmosphere was installed by bubbling H_2 through the solution for 10 minutes. The reaction mixture was stirred under an atmosphere of hydrogen for 15 h, filtered through Celite and concentrated, affording **5** as a colourless oil (5.37 mg, 93%); $\mathbf{R_f}$ (EtOAc/heptane 1:9) = 0.16; **^{1}H NMR** (400 MHz, $CDCl_3$) δ 3.67–3.55 (m, 5H), 1.62–1.46 (m, 4H), 1.44–1.19 (m, 22H), 0.89 (s, 9H), 0.88 (s, 9H), 0.05 (s, 6H), 0.03 (s, 6H); **^{13}C NMR** (101 MHz, $CDCl_3$) δ 72.52, 63.47, 63.24, 37.28, 37.25, 33.01, 32.97, 30.00, 29.83, 29.73, 29.72, 29.57, 26.14 (3C), 26.10 (3C), 25.99, 25.89, 25.48 (2C), 18.54, 18.32, -4.24 (2C), -5.09 (2C); **HRMS (MALDI+)**[22]

2-Phenyl-1,3-dioxan-5-yl 10,16-bis((*tert*-butyldimethylsilyl)oxy)hexadecanoate (**6**)

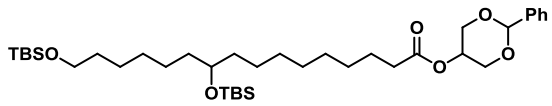

To a solution of **5** (2.05 g, 3.972 mmol) in CH_2Cl_2 (20 ml) and water (3 ml) was added $PhI(OAc)_2$ (3.20 g, 9.932 mmol) and TEMPO (125 mg, 0.794 mmol). The resulting mixture was stirred vigorously for 3 h, poured into 10%. aq. $Na_2S_2O_3$ (100 ml) and extracted with EtOAc (3 × 100 ml). The combined organic phases were dried with Na_2SO_4, filtered, concentrated and taken up in CH_2Cl_2 (100 ml). To this solution was added *cis*-5-hydroxy-2-phenyl-1,3-dioxane (0.930 g, 5.164 mmol), DMAP (0.825 g, 6.752 mmol) and EDCI (1.142 g, 5.958 mmol). After 17 h, the reaction was concentrated, taken on silica and purified by flash chromatography (EtOAc/heptane 1: 9) affording **6** as a colourless oil (1.19 g, 44%); $\mathbf{R_f}$ (EtOAc/heptane 1:9) = 0.25; **^{1}H NMR** (400 MHz, $CDCl_3$) δ 7.55–7.48 (m, 2H), 7.37 (m, 3H), 5.56 (s, 1H), 4.72 (s, 1H), 4.29 (d, *J* = 12.0 Hz, 2H), 4.17 (d, *J* = 11.8 Hz, 2H), 3.65–3.56 (m, 3H), 2.44 (t, *J* = 7.6 Hz, 2H), 1.67 (p, *J* = 7.4 Hz, 2H), 1.57–1.45 (m, 2H), 1.45–1.22 (m, 20H), 0.90 (s, 9H), 0.88 (s, 9H), 0.05 (s, 6H), 0.03 (s, 6H); **^{13}C NMR** (101 MHz, $CDCl_3$) δ 173.97, 137.95, 129.18, 128.40 (2C), 126.14 (2C), 101.34, 72.47, 69.25 (2C), 65.81, 63.43, 37.26, 37.22, 34.52, 32.98, 29.96, 29.79, 29.62, 29.40, 29.24, 26.12 (3C), 26.08 (3C), 25.95, 25.45 (2C), 25.07, 18.50, 18.28, -4.27 (2C), -5.12 (2C); **HRMS (MALDI+)**[22]

2-Phenyl-1,3-dioxan-5-yl 10,16-dihydroxyhexadecanoate (**7**)

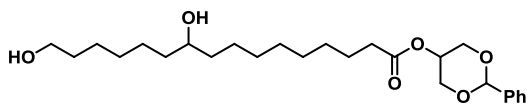

To a solution of **36** (1.19 g, 1.752 mmol) in MeCN (200 ml) at 0 °C was added 20% aq. HF (5 ml). The resulting mixture was stirred at 0 °C for 4 h. TMSOMe (20 ml) was added, and the mixture was stirred for 30 minutes, poured into sat. aq. NH_4Cl (200 ml) and extracted with CH_2Cl_2 (3 × 200 ml). The combined organic phases were dried with Na_2SO_4, filtered,

concentrated and purified by flash chromatography (EtOAc/hetane 7:3), affording **7** as a white solid (0.500 g, 63%); $\mathbf{R_f}$ (EtOAc/heptane 6:4) = 0.18; **mp**: 70–72 °C **^{1}H NMR** (400 MHz, $CDCl_3$) δ 7.56–7.45 (m, 2H), 7.43–7.30 (m, 3H), 5.56 (s, 1H), 4.72 (p, *J* = 1.6 Hz, 1H), 4.28 (dd, *J* = 13.1, 1.6 Hz, 2H), 4.17 (dd, *J* = 13.0, 1.6 Hz, 2H), 3.63 (t, *J* = 6.6 Hz, 2H), 3.62–3.51 (m, 1H), 2.43 (t, *J* = 7.5 Hz, 2H), 1.67 (p, *J* = 7.4 Hz, 2H), 1.57 (p, *J* = 6.7 Hz, 2H), 1.50–1.23 (m, 20H); **^{13}C NMR** (101 MHz, $CDCl_3$) δ 174.02, 137.96, 129.22, 128.44 (2C), 126.17 (2C), 101.39, 72.06, 69.28 (2C), 65.85, 63.14, 37.61, 37.48, 34.53, 32.84, 29.73, 29.59, 29.52, 29.32, 29.20, 25.85, 25.73, 25.72, 25.05; **HRMS (MALDI+)**[22]

1,3-Dihydroxypropan-2-yl 10,16-dihydroxyhexadecanoate (**8**)

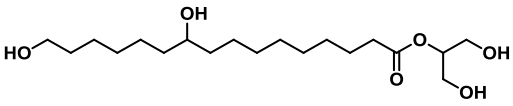

To a solution of **37** (0.250 g, 0.555 mmol) in dry THF (25 ml) under an atmosphere of nitrogen was added 20% $Pd(OH)_2/C$ (40 mg). A hydrogen atmosphere was installed by bubbling H_2 through the solution for 5 minutes. The reaction mixture was stirred under an atmosphere of hydrogen for 16 h, filtered through Celite, concentrated and recrystallized from EtOAc and heptane, affording **8** as a white solid (160 mg, 80%); $\mathbf{R_f}$ (CH_2Cl_2/MeOH 9:1) = 0.24; **mp**: 59–62 °C; **^{1}H NMR** (400 MHz, MeOD) δ 4.93–4.88 (m, 1H), 3.72–3.62 (m, 4H), 3.55 (t, *J* = 6.6 Hz, 2H), 3.53–3.48 (m, 1H), 2.38 (t, *J* = 7.5 Hz, 2H), 1.69–1.59 (m, 2H), 1.59–1.51 (m, 2H), 1.51–1.27 (m, 20H); **^{13}C NMR** (101 MHz, MeOD) δ 175.34, 76.53, 72.42, 62.99, 61.70 (2C), 38.43, 38.38, 35.15, 33.63, 30.78, 30.68, 30.59, 30.37, 30.17, 26.96, 26.80, 26.78, 25.98; **HRMS (MALDI+)**[22]

10-(Naphthalene-2-ylmethoxy)decan-1-ol (**14**)

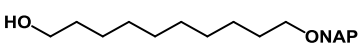

To a suspension of NaH (60% in oil, 3.44 g, 0.086 mol) in dry DMF (40 ml) at 0 °C under an atmosphere of argon was added slowly a solution of 1,10-decanediol (15.00 g, 0.086 mol) in a mixture of THF and DMF (30 and 40 ml respectively). The resulting mixture was let to warm slowly to 20 °C. After 2 h, a solution of NAPBr (9.52 g, 0.043 mol) in dry DMF (30 ml) was added dropwise. The reaction was stirred for 16 h and excess reagent was quenched by addition of ice until bubbling ceased. The mixture was extracted with Et_2O (3 × 200 ml). The combined organic phases were washed with sat. aq. NaCl (200 ml), dried with $MgSO_4$, filtered, concentrated and purified by flash chromatography (EtOAc/heptane 1:4) affording **14** as a white solid (8.44 g, 62%). $\mathbf{R_f}$ (EtOAc/heptane 1:4) = 0.16; **mp**: 60–62 °C; **^{1}H NMR** (400 MHz, $CDCl_3$) δ 7.86–7.80 (m, 3H), 7.78 (s, 1H), 7.51–7.43 (m, 3H), 4.67 (s, 2H), 3.63 (t, *J* = 6.6 Hz, 2H), 3.51 (t, *J* = 6.7 Hz, 2H), 1.69–1.60 (m, 2H), 1.60–1.51 (m, 2H), 1.44–1.23 (m, 12H); **^{13}C NMR** (101 MHz, $CDCl_3$) δ 136.4, 133.4, 133.1, 128.2, 128.0, 127.8, 126.4, 126.2, 125.9, 125.9, 73.1, 70.7, 63.2,

32.9, 29.9, 29.7, 29.7, 29.6, 29.5, 26.3, 25.9; **HRMS (MALDI+)** $C_{21}H_{30}O_2$, m/z [M+Na^+] 337.2138, found 337.2140.

1-((*tert*-Butyldimethylsilyl)oxy)-16-(napththalene-2-ylmethoxy)hexadec-5-yn-7-ol (**16**)

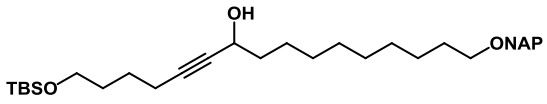

To a mixture of DMP (6.63 g, 15.63 mmol) in CH_2Cl_2 (25 ml) was added slowly a solution of **14** (3.78 g, 12.02 mmol) in CH_2Cl_2 (20 ml). The resulting mixture was stirred for 1.5 h and poured into an aqueous solution of $Na_2S_2O_3$ (35 g in 200 ml). The mixture was stirred vigorously for 5 min and extracted with Et_2O (200 ml). The organic phase was washed with sat. aq. $NaHCO_3$ (200 ml), dried with $MgSO_4$ and concentrated, and used in the subsequent reaction without further purification.

To a solution of **2** (3.32 g, 15.64 mmol) in THF (15 ml) at -78 °C under an atmosphere of nitrogen was added dropwise *n*-BuLi (6.7 ml, 2.7 M in pentane, 18.05 mmol). The resulting mixture was allowed to warm slowly to 20 °C and a solution of the crude aldehyde (3.760 g, 12.0 mmol) in dry THF (15 ml) was added. The resulting mixture was stirred for 16 h, poured into sat. aq. NH_4Cl (100 ml) and extracted with CH_2Cl_2 (3 × 100 ml). The combined organic phases were dried with $MgSO_4$, filtered, concentrated and purified by flash chromatography (EtOAc/heptane 1:9) affording **16** as a yellow oil (4.12 g, 65%); $\mathbf{R_f}$ (EtOAc/heptane 1:9) = 0.17; **^{1}H NMR** (400 MHz, $CDCl_3$) δ 7.86–7.80 (m, 3H), 7.78 (s, 1H), 7.51–7.45 (m, 3H), 4.67 (s, 2H), 4.34 (tt, *J* = 8.9, 4.1 Hz, 1H), 3.62 (t, *J* = 6.0 Hz, 2H), 3.51 (t, *J* = 6.7 Hz, 2H), 2.23 (td, *J* = 6.7, 1.7 Hz, 2H), 1.72–1.53 (m, 8H), 1.48–1.25 (m, 12H), 0.91 (s, 9H), 0.05 (s, 6H); **^{13}C NMR** (101 MHz, $CDCl_3$) δ 136.36, 133.44, 133.08, 128.24, 127.99, 127.82, 126.40, 126.16, 125.91, 125.88, 85.41, 81.69, 73.09, 70.67, 62.90, 62.79, 38.35, 32.06, 29.94, 29.66, 29.64, 29.61, 29.42, 26.35, 26.10 (3C), 25.36, 25.27, 18.64, 18.48, -5.14 (2C); **HRMS (MALDI+)** $C_{33}H_{52}O_3Si$, m/z [M+H+] 525.3578, found 525.3593.

1,7-Bis((*tert*-Butyldimethylsilyl)oxy)-16-(naphthalen-2-ylmethoxy)hexadec-5-yne (**13**)

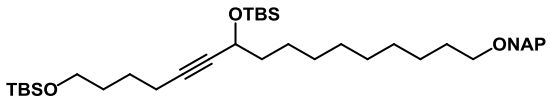

To a solution of **16** (4.12 g, 7.86 mmol) in dry DMF (20 ml) under an atmosphere of nitrogen was added imidazole (0.803 g, 11.80 mmol) and TBSCl (1.54 g, 10.22 mmol). The reaction mixture was stirred for 18 h, poured into sat. aq. NH_4Cl (100 ml) and was extracted with CH_2Cl_2 (3 × 100 ml). The combined organic phases were dried with $MgSO_4$, filtered, concentrated and purified by flash chromatography (EtOAc/heptane 1:19) affording **13** as a colourless oil (3.54 g, 71%); $\mathbf{R_f}$ (EtOAc/heptane 1:19) = 0.33; **^{1}H NMR (400 MHz, $CDCl_3$)** δ 7.85–7.80 (m, 3H), 7.78 (s, 1H), 7.50–7.43 (m, 3H), 4.67 (s, 2H), 4.31 (tt, *J* = 6.6, 1.9 Hz, 1H), 3.61 (t, *J* = 6.0 Hz, 2H), 3.51 (t, *J* = 6.6 Hz, 2H), 2.21 (td, *J* = 6.9, 1.9 Hz, 2H), 1.68–1.50 (m, 8H), 1.37 (m, 4H), 1.28 (d, *J* = 2.9 Hz, 8H), 0.90

(s, 9H), 0.89 (s, 9H), 0.12 (s, 2H), 0.10 (s, 3H), 0.04 (s, 6H); **^{13}C NMR (101 MHz, $CDCl_3$)** δ 136.36, 133.44, 133.08, 128.22, 127.98, 127.81, 126.38, 126.14, 125.89, 125.86, 84.27, 82.37, 73.08, 70.67, 63.36, 62.78, 39.17, 32.09, 29.95, 29.69, 29.67, 29.62, 29.42, 26.36, 26.10 (3C), 26.01 (3C), 25.49, 25.31, 18.65, 18.46, 18.43, -4.28, -4.81, -5.16 (2C); **HRMS (MALDI+)** $C_{39}H_{66}O_3Si_2$, m/z [M+Na^+] 661.4443, found 661.4445.

10,16-Bis((*tert*-butyldimethylsilyl)oxy)hexadec-11-yn-1-ol (**12**)

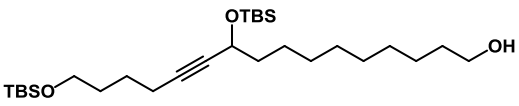

To a solution of **13** (3.47 g, 5.431 mmol) in CH_2Cl_2 (85 ml) was added DDQ (1.85 g, 8.15 mmol) and H_2O (20 ml). After 16 h, the mixture was poured into sat. aq. $NaHCO_3$ (100 ml), and was extracted with CH_2Cl_2 (3 × 100 ml). The combined organic phases were dried with MgSO4, filtered, concentrated and purified by flash chromatography (EtOAc/heptane 1:9) affording **12** as a colourless oil (1.95 g, 72%); **R_f** (EtOAc/heptane 1:4) = 0.29; **^{1}H NMR** (400 MHz, $CDCl_3$) δ 4.31 (tt, *J* = 6.6, 2.0 Hz, 1H), 3.66–3.58 (m, 4H), 2.21 (td, *J* = 6.9, 2.0 Hz, 2H), 1.67–1.50 (m, 8H), 1.45–1.24 (m, 12H), 0.90 (s, 8H), 0.89 (s, 9H), 0.11 (s, 3H), 0.09 (s, 3H), 0.04 (s, 6H); **^{13}C NMR** (101 MHz, $CDCl_3$) δ 84.30, 82.36, 63.36, 63.23, 62.81, 39.17, 32.96, 32.11, 29.68, 29.64, 29.56, 29.41, 26.11 (3C), 26.02 (3C), 25.88, 25.48, 25.32, 18.67, 18.48, 18.45, -4.28, -4.81, -5.15 (2C); **HRMS (MALDI+)** $C_{28}H_{58}O_3Si_2$, *m/z* [M+Na^+] 521.3817, found 521.3825.

cis-2-Phenyl-1,3-dioxan-5-yl 10,16-bis((*tert*-butyldimethylsilyl)oxy)hexadec-11-ynoate (**17**)

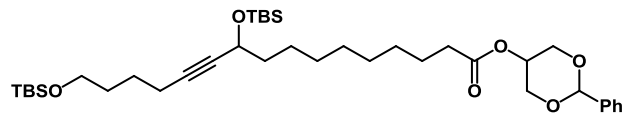

To a mixture of DMP (1.25 g, 2.95 mmol) in CH_2Cl_2 (30 ml) was added slowly a solution of **12** (1.13 g, 2.27 mmol) in CH_2Cl_2 (30 ml). The resulting mixture was stirred for 2.5 h and poured into a solution of $Na_2S_2O_3$ (45 g) in sat. aq. $NaHCO_3$ (250 ml). The mixture was stirred vigorously for 5 min and then extracted with Et_2O (200 ml). The organic phase was washed with sat. aq. $NaHCO_3$ (200 ml), dried with $MgSO_4$, concentrated and used in the subsequent reaction without further purification.

To a solution of the crude aldehyde (1.24 g) in *t*-BuOH (100 ml) was added 2-methyl-2-butene (3.180 g, 4.8 ml, 45.34 mmol) and an aqueous solution (27 ml) of NaH_2PO_4 (2.18 g, 18.14 mmol) and $NaClO_2$ (0.267 g, 2.95 mmol). After 15 h, a buffer aqueous solution of NaH_2PO_4 was added (0.66 M, 100 ml) and the mixture was extracted with CH_2Cl_2 (3 × 150 ml). The combined organic phases were washed with sat. aq. NaCl (200 ml), dried with Na_2SO_4, filtered, concentrated, and used in the subsequent reaction without further purification.

To a solution of the crude carboxylic acid (1.47 g) in dry CH_2Cl_2 (100 ml) under an atmosphere of nitrogen was added *cis*-5-hydroxy-2-phenyl-1,3-dioxane (0.531 g, 2.946 mmol), DMAP (0.472 g, 3.852 mmol) and EDCI (0.660 g, 3.399 mmol). After 15 h, the reaction mixture was concentrated, taken on silica and purified by flash chromatography (EtOAc/hetane 1:9), affording **17** as a transparent oil (0.609 g, 40%); $\mathbf{R_f}$ (EtOAc/heptane 1:9) = 0.22; **^{1}H NMR** (400 MHz, $CDCl_3$) δ 7.55–7.47 (m, 2H), 7.41–7.32 (m, 3H), 5.56 (s, 1H), 4.74–4.69 (m, 1H), 4.34–4.13 (m, 5H), 3.61 (t, *J* = 6.1 Hz, 2H), 2.43 (t, *J* = 7.6 Hz, 2H), 2.21 (td, *J* = 6.8, 1.8 Hz, 2H), 1.73–1.50 (m, 8H), 1.47–1.21 (m, 10H), 0.90 (s, 9H), 0.89 (s, 9H), 0.11 (s, 3H), 0.10 (s, 3H), 0.06–0.03 (m, 6H); **^{13}C NMR** (101 MHz, $CDCl_3$) δ 173.99, 137.97, 129.19, 128.41 (2C), 126.16 (2C), 101.35, 84.27, 82.33, 69.26 (2C), 65.83, 63.33, 62.78, 39.14, 34.52, 32.08, 29.53, 29.37 (2C), 29.24, 26.08 (3C), 26.00 (3C), 25.47, 25.29, 25.06, 18.64, 18.45, 18.42, -4.30, -4.82, -5.17 (2C); **HRMS (MALDI+)** $C_{38}H_{66}O_6Si_2$, m/z [M+Na$^+$] 697.4290, found 697.4243.

<u>*cis*-2-Phenyl-1,3-dioxan-5-yl 10,16-dihydroxyhexadec-11-ynoate (**11**)</u>

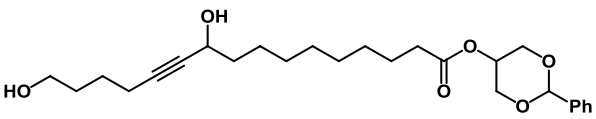

To a solution of **17** (0.975 g, 1.445 mmol) in MeCN (145 ml) at 0 °C was added 20% aq. HF (6 ml, 69 mmol). The resulting mixture was stirred at 0 °C for 4 h. TMSOEt (33 ml) was added, and the mixture was stirred for 30 minutes, poured into sat. aq. NH_4Cl (200 ml) and extracted with CH_2Cl_2 (3 × 200 ml). The combined organic phases were dried with $MgSO_4$, filtered, concentrated and purified by flash chromatography (EtOAc/hetane 6:4), affording **11** as a white solid (0.354 g, 55%); $\mathbf{R_f}$ (EtOAc/heptane 6:4) = 0.16; **mp**: 50–52 °C; **^{1}H NMR** (400 MHz, $CDCl_3$) δ 7.58–7.46 (m, 2H), 7.45–7.31 (m, 3H), 5.56 (s, 1H), 4.72 (s, 1H), 4.38–4.25 (m, 3H), 4.17 (d, *J* = 13.2, 2H), 3.65 (t, *J* = 6.3 Hz, 2H), 2.43 (t, *J* = 7.5 Hz, 2H), 2.25 (td, *J* = 6.8, 2.0 Hz, 2H), 1.74–1.54 (m, 10H), 1.50–1.24 (m, 10H); **^{13}C NMR** (101 MHz, $CDCl_3$) δ 174.04, 137.94, 129.23, 128.44 (2C), 126.17 (2C), 101.38, 85.16, 81.89, 69.28 (2C), 65.87, 62.84, 62.47, 38.27, 34.52, 31.91, 29.43, 29.29, 29.24, 29.19, 25.26, 25.06, 25.05, 18.62; **HRMS (MALDI+)** $C_{26}H_{38}O_6$, m/z [M+Na$^+$] 469.2561, found 469.2563.

<u>1,3-Dihydroxypropan-2-yl 10,16-dihydroxyhexadecanoate-11,11,12,12-d_4 (**9**)</u>

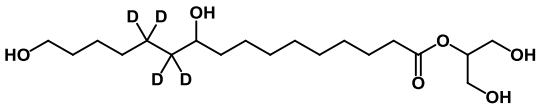

To a solution of **11** (0.169 g, 0.378 mmol) in dry THF (20 ml) under an atmosphere of nitrogen was added 20% $Pd(OH)_2/C$ (40 mg). A deuterium atmosphere was installed by bubbling D_2 through the solution for 5 minutes. The reaction mixture was stirred under a D_2 atmosphere for 15 h filtered through Celite, concentrated and recrystallized from EtOAc and heptane, affording **9** as a white solid (96 mg, 69%); **mp**: 56–58 °C; **^{1}H NMR** (400 MHz, MeOD) δ 4.94–4.88 (m, 1H), 3.70 (dd, *J* = 12.4, 5.3 Hz, 2H), 3.65 (dd, *J* = 12.0, 6.0 Hz, 2H), 3.55 (t, *J* = 6.6 Hz, 2H), 3.52–3.48 (m, 1H), 2.38 (t, *J* = 7.4 Hz, 2H), 1.68–1.59 (m, 2H), 1.58–1.49 (m, 2H), 1.48–1.24 (m,

16H); **^{13}C NMR** (101 MHz, MeOD) δ 175.34, 76.53, 62.99, 61.70 (2C), 38.38, 35.15, 33.64, 30.79, 30.59, 30.37, 30.17, 26.78, 25.98; **HRMS (MALDI+)** $C_{19}H_{34}D_4O_6$, m/z [M+Na$^+$] 389.2812, found 389.2827

2-Phenyl-1,3-dioxan-5-yl 10-((*tert*-butyldimethylsilyl)oxy)-16-hydroxyhexadecanoate (**21**)

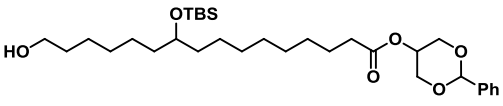

To a solution of **6** (250 mg, 0.368 mmol) in dry THF (25 ml) under an atmosphere of nitrogen was added TBAF (480 µl, 1M in THF, 0.478 mmol). After 2 h, the reaction mixture was diluted in CH_2Cl_2 (50 ml) and washed with sat. aq NH_4Cl (50 ml). The organic phase was dried with Na_2SO_4, filtered, concentrated and purified by flash chromatography (EtOAc/heptane 3:7) affording **21** as transparent oil (200 mg, 97%); $\mathbf{R_f}$ (EtOAc/heptane 3:7) = 0.19; **^{1}H NMR** (400 MHz, $CDCl_3$) δ 7.55–7.47 (m, 2H), 7.43–7.31 (m, 3H), 5.56 (s, 1H), 4.72 (p, *J* = 1.6 Hz, 1H), 4.29 (dd, *J* = 13.0, 1.6 Hz, 2H), 4.17 (dd, *J* = 12.9, 1.6 Hz, 2H), 3.67–3.56 (m, 3H), 2.44 (t, *J* = 7.5 Hz, 2H), 1.67 (p, *J* = 7.5 Hz, 2H), 1.60–1.52 (m, 2H), 1.47–1.20 (m, 21H), 0.88 (s, 9H), 0.03 (s, 6H); **^{13}C NMR** (101 MHz, $CDCl_3$) δ 174.04, 137.97, 129.22, 128.44 (2C), 126.17 (2C), 101.39, 72.46, 69.29 (2C), 65.85, 63.20, 37.28, 37.18, 34.55, 32.92, 29.95, 29.82, 29.61, 29.40, 29.26, 26.09 (3C), 25.91, 25.44 (2C), 25.09, 18.31, -4.24, -4.26; **HRMS (MALDI+)** $C_{32}H_{56}O_6Si$, m/z [M+Na$^+$] 587.3738, found 587.3748

2-Phenyl-1,3-dioxan-5-yl 10-((*tert*-butyldimethylsilyl)oxy)-16-hydroxyhexadecanoate-16-*d* (**22**)

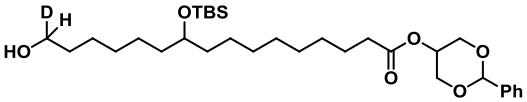

To a solution of **21** (148 mg, 0.262 mmol) in CH_2Cl_2 (6 ml) was added DMP (155 mg, 0.366 mmol). After 4 h stirring, a 10% aq solution of $Na_2S_2O_4$ (20 ml) was added and the mixture was stirred vigorously for 10 more minutes. The phases were separated, and the aqueous phase was extracted with CH_2Cl_2 (3 × 15 ml). The combined organic phases were dried with Na_2SO_4, filtered, concentrated and used in the next step without further purification.

To a solution of the crude aldehyde in EtOH (5 ml) was added $NaBD_4$ (13.16 mg, 0.314 mmol). After 10 minutes, TLC showed completion. The reaction mixture was poured into sat. aq. NH_4Cl (20 ml) and extracted with CH_2Cl_2 (3 × 20 ml). The combined organic phases were dried with Na_2SO_4, filtered and concentrated, affording **22** as a transparent oil (128 mg, 86%); $\mathbf{R_f}$ (EtOAc/heptane 3:7) = 0.19; **^{1}H NMR** (400 MHz, $CDCl_3$) δ 7.55–7.47 (m, 2H), 7.43–7.32 (m, 3H), 5.56 (s, 1H), 4.72 (p, *J* = 1.7 Hz, 1H), 4.29 (dd, *J* = 13.0, 1.6 Hz, 2H), 4.17 (dd, *J* = 13.0, 1.6 Hz, 2H), 3.66–3.57 (m, 2H), 2.44 (t, *J* = 7.6 Hz, 2H), 2.07 (br. s, 1H), 1.67 (p, *J* = 7.5 Hz, 2H), 1.61–1.50 (m, 2H), 1.44–1.20 (m, 20H), 0.88 (s, 9H), 0.03 (s, 6H); **^{13}C NMR** (101 MHz, $CDCl_3$) δ 174.04, 137.96, 129.22, 128.43 (2C), 126.17 (2C),

101.39, 72.46, 69.29 (2C), 65.85, 62.82 (t, *J* = 21.7 Hz), 37.27, 37.17, 34.55, 32.80, 29.95, 29.82, 29.60, 29.40, 29.26, 26.09 (3C), 25.88, 25.43 (2C), 25.08, 18.31, -4.24, -4.26;

2-Phenyl-1,3-dioxan-5-yl 10,16-dihydroxyhexadecanoate-16-*d* (**23**)

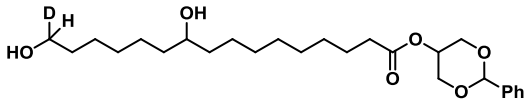

To a solution of **22** (120 mg, 0.2122 mmol) in MeCN (15 ml) at 0 °C was added 20% aq. HF (0.5 ml). The resulting mixture was stirred at 0 °C for 4 h. TMSOMe (2 ml) was added, and the mixture was stirred for 30 minutes, poured into sat. aq. NH_4Cl (20 ml) and extracted with CH_2Cl_2 (3 × 15 ml). The combined organic phases were dried with Na_2SO_4, filtered, concentrated and purified by flash chromatography (EtOAc/heptane 7:3), affording **23** as a white solid (63 mg, 66%); $\mathbf{R_f}$ (EtOAc/heptane 6:4) = 0.18; **^{1}H NMR** (400 MHz, $CDCl_3$) δ 7.54–7.46 (m, 2H), 7.42–7.32 (m, 3H), 5.56 (s, 1H), 4.72 (s, 1H), 4.28 (dd, *J* = 13.0, 1.8 Hz, 2H), 4.17 (dd, *J* = 13.0, 1.8 Hz, 2H), 3.67–3.51 (m, 2H), 2.43 (t, *J* = 7.5 Hz, 2H), 1.67 (p, *J* = 7.4 Hz, 2H), 1.59–1.23 (m, 22H); **^{13}C NMR** (101 MHz, $CDCl_3$) δ 174.02, 137.95, 129.21, 128.42 (2C), 126.16 (2C), 101.38, 72.04, 69.27 (2C), 65.85, 62.74 (t, *J* = 21.7 Hz), 37.60, 37.46, 34.52, 32.72, 29.72, 29.58, 29.51, 29.31, 29.19, 25.82, 25.72, 25.71, 25.04; **HRMS (MALDI+)** $C_{26}H_{41}DO_6$, m/z [M+Na$^+$] 474.2936, found 474.2944

1,3-Dihydroxypropan-2-yl 10,16-dihydroxyhexadecanoate-16-*d* (**24**)

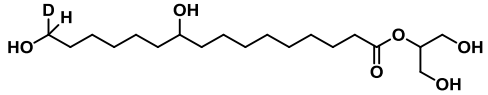

To a solution of **23** (60 mg, 0.137 mmol) in dry THF (5 ml) under an atmosphere of nitrogen was added 20% $Pd(OH)_2/C$ (10 mg). A hydrogen atmosphere was installed by bubbling H_2 through the solution for 5 minutes. The reaction mixture was stirred under an atmosphere of hydrogen for 16 h, filtered through Celite, concentrated and recrystallized from EtOAc and heptane, affording **24** as a white solid (21 mg, 43%); $\mathbf{R_f}$ (CH_2Cl_2/MeOH 9:1) = 0.24; **mp**: 47–49 °C **^{1}H NMR** (400 MHz, MeOD) δ 4.95–4.86 (m, 1H), 3.74–3.60 (m, 4H), 3.59–3.46 (m, 2H), 2.38 (t, *J* = 7.4 Hz, 2H), 1.70–1.58 (m, 2H), 1.59–1.49 (m, 2H), 1.50–1.27 (m, 20H); **^{13}C NMR** (101 MHz, MeOD) δ 175.34, 76.53, 72.42, 62.62 (t, *J* = 21.1 Hz), 61.70 (2C), 38.43, 38.38, 35.15, 33.53, 30.78, 30.69, 30.59, 30.37, 30.18, 26.93, 26.81, 26.79, 25.98; **HRMS (MALDI+)** $C_{19}H_{37}DO_6$, m/z [M+Na$^+$] 386.2623, found 386.2626

2-Phenyl-1,3-dioxan-5-yl docosanoate (**31**)

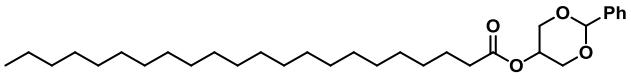

To a solution of behenic acid (1.067 g, 3.13 mmol) in dry CH_2Cl_2 (50 ml) under Ar atmosphere was added *cis*-5-hydroxy-2-phenyl-1,3-dioxane (0.686 g, 3.81 mmol), DMAP (0.609 g, 4.98 mmol) and EDCI (0.846 g, 4.41 mmol). After 16 h, the reaction mixture was concentrated, taken on silica and purified by flash chromatography (EtOAc/heptane 1:9) affording **31** as white solid (1.023 g, 69%); $\mathbf{R_f}$ (EtOAc/heptane 1:9) = 0.24; **mp**: 64–66 °C; **^{1}H NMR** (400 MHz, $CHCl_3$) δ 7.55–7.47 (m, 2H), 7.43–7.30 (m, 3H), 5.56 (s, 1H), 4.72 (p, *J* = 1.6 Hz, 1H), 4.29 (dd, *J* = 13.0, 1.6 Hz, 2H), 4.17 (dd, *J* = 13.0, 1.6 Hz, 2H), 2.44 (t, *J* = 7.6 Hz, 2H), 1.67 (p, *J* = 7.5 Hz, 2H), 1.25 (d, *J* = 1.9 Hz, 36H), 0.87 (t, *J* = 7.0 Hz 3H); **^{13}C NMR** (101 MHz, $CDCl_3$) δ 174.04, 137.98, 129.22, 128.44 (2C), 126.18 (2C), 101.39, 69.29 (2C), 65.84, 34.56, 32.08, 29.85 (10C), 29.81, 29.77, 29.63, 29.52, 29.44, 29.28, 25.10, 22.85, 14.28; **HRMS (MALDI+)** $C_{32}H_{54}O_4$, m/z [M+Na^+] 525.3914, found 525.3909

‘

1,3-Dihydroxypropan-2-yl docosanoate (**27**)

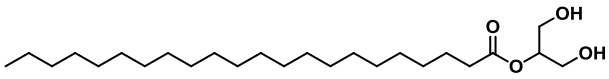

To a solution of **31** (0.897 g, 1.785 mmol) in dry THF (100 ml) under an atmosphere of nitrogen was added 20% $Pd(OH)_2/C$ (250 mg). A hydrogen atmosphere was installed by bubbling H_2 through the solution for 10 minutes. The reaction mixture was stirred under an atmosphere of hydrogen for 16 h, filtered through Celite, concentrated and recrystallized from EtOAc and heptane, affording **27** as a white solid (509 mg, 69%); **mp**: 74–76 °C; **^{1}H NMR** (400 MHz, $CDCl_3$) δ 4.92 (p, *J* = 4.7 Hz, 1H), 3.83 (d, *J* = 4.7 Hz, 4H), 2.37 (t, *J* = 7.6 Hz, 2H), 1.97 (s, 2H), 1.64 (p, *J* = 7.4 Hz, 2H), 1.37–1.18 (m, 36H), 0.88 (t, *J* = 6.7 Hz, 3H); **^{13}C NMR** (101 MHz, $CDCl_3$) δ 174.24, 75.19, 62.70 (2C), 34.51, 32.08, 29.86 (10C), 29.81, 29.76, 29.62, 29.52, 29.41, 29.27, 25.12, 22.85, 14.28; **HRMS (MALDI+)**[229]

bis(2-Phenyl-1,3-dioxan-5-yl) octadecanedioate (**33**)

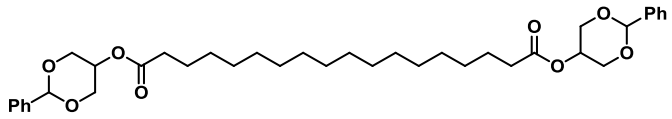

To a solution of octadecanedioic acid (600 mg. 0.488 mmol) in dry DMF (50 ml) under an atmosphere of nitrogen was added DMAP (583 mg, 4.77 mmol), EDCI (952 mg, 0.733 mmol) and *cis*-5-hydroxy-2-phenyl-1,3-dioxane (826 mg, 4.58 mmol). After 16 h, the reaction mixture was poured into sat. aq. NH_4Cl (250 ml) and extracted with CH_2Cl_2 (250 ml). The organic phase was washed with NH_4Cl (3 × 250 ml), H_2O (250 ml) and brine (250 ml), dried with $MgSO_4$, filtered, concentrated and purified by flash chromatography (EtOAc/heptane 1:2) affording **33** as white solid

(685 mg, 64%); $\mathbf{R_f}$ (EtOAc/heptane 1:2) = 0.25. **mp**: 109–110 °C; **^{1}H NMR** (400 MHz, $CDCl_3$) δ 7.55–7.47 (m, 4H), 7.43–7.32 (m, 6H), 5.56 (s, 2H), 4.72 (p, *J* = 1.6 Hz, 2H), 4.28 (dd, *J* = 13.1, 1.6 Hz, 4H), 4.17 (dd, *J* = 12.9, 1.6 Hz, 4H), 2.43 (t, *J* = 7.6 Hz, 4H), 1.67 (p, *J* = 7.5 Hz, 4H), 1.40–1.21 (m, 24H); **^{13}C NMR** (101 MHz, $CDCl_3$) δ 174.04 (2C), 137.98 (2C), 129.22 (2C), 128.44 (4C), 126.17 (4C), 101.38 (2C), 69.29 (4C), 65.83 (2C), 34.56 (2C), 29.82 (2C), 29.80 (2C), 29.76 (2C), 29.62 (2C), 29.44 (2C), 29.27 (2C), 25.10 (2C). **HRMS (MALDI+)** $C_{38}H_{54}O_8$, m/z [M+Na^+] 661.3711, found 661.3718

bis(1,3-Dihydroxypropan-2-yl) octadecanedioate (**28**)

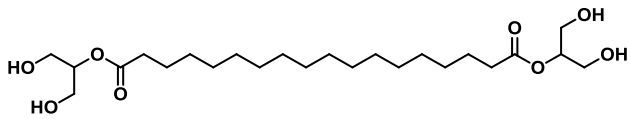

To a solution of **33** (0.530 g, 0.830 mmol) in dry THF (50 ml) under an atmosphere of nitrogen was added 20% $Pd(OH)_2/C$ (200 mg). A hydrogen atmosphere was installed by bubbling H_2 through the solution for 5 minutes. The reaction mixture was stirred under an atmosphere of hydrogen for 16 h, filtered through Celite, concentrated and recrystallized from EtOAc and heptane, affording **28** as a white solid (321 mg, 84%); **mp**: 104–106 °C; **^{1}H NMR** (400 MHz, MeOD) δ 4.94–4.89 (m, 2H), 3.75–3.61 (m, 8H), 2.38 (t, *J* = 7.4 Hz, 4H), 1.64 (p, *J* = 7.2 Hz, 4H), 1.32 (d, *J* = 9.9 Hz, 24H); **^{13}C NMR** (101 MHz, MeOD) δ 175.33 (2C), 76.52 (2C), 61.70 (4C), 35.15 (2C), 30.78 (2C), 30.77 (2C), 30.72 (2C), 30.61 (2C), 30.43 (2C), 30.20 (2C), 25.99 (2C); **HRMS (MALDI+)** $C_{24}H_{46}O_8$, m/z [M+Na^+] 485.3085, found 485.3085

2-(4-Methoxyphenyl)-1,3-dioxan-5-ol (**44**)

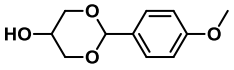

To a solution of glycerol (3.0 g, 32.58 mmol) in MeCN (50 ml) under an atmosphere of nitrogen with 3 Å molecular sieves were added CSA (2.27 g, 9.77 mmol) and *p*-methoxy anisaldehyde (8.9 g, 48.86 mmol). The reaction was refluxed for 17 h, filtered, poured into sat. aq. $NaHCO_3$ (100 ml), and extracted with Et_2O (3 × 100 ml). The combined organic phases were dried with Na_2SO_4, filtered, concentrated and purified repeatedly by flash chromatography (EtOAc/heptane, 1:1, 0.4% Et_3N) affording **44** as a white solid (0.9 g, 13.1%); $\mathbf{R_f}$ (EtOAc/heptane 1:1) = 0.13; **^{1}H NMR** (400 MHz, Benzene-*d6*) δ 7.53 (d, *J* = 8.5 Hz, 2H), 6.82 (d, *J* = 8.8 Hz, 2H), 5.21 (s, 1H), 3.85 (d, *J* = 10.8 Hz, 2H), 3.43 (d, *J* = 11.7 Hz, 2H), 3.27 (s, 3H), 3.01–2.93 (m, 1H); **^{13}C NMR** (101 MHz, Benzene-*d6*) δ 160.52, 131.47, 127.75 (2C), 113.81 (2C), 101.59, 72.20 (2C), 64.02, 54.79; **HRMS (MALDI+)** $C_{11}H_{14}O_4$, m/z [M+Na^+] 233.0784, found 233.0780

2-(Naphthalen-2-yl)-1,3-dioxan-5-ol (**46**)

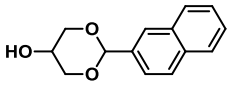

To a solution of 2-naphthaldehyde (7.63 g, 48.86 mmol) in MeOH (60 ml) were added trimethyl orthoformate (8.64 g, 8.93 ml, 81.44 mmol) and toluene sulfonic acid monohydrate (0.62 g, 3.6 mmol). The reaction mixture was stirred for 2 h, evaporated *in vacuo* and added to a solution of glycerol (3 g, 32.58 mmol) in MeCN (50 ml). The reaction mixture was refluxed for 16 h, neutralized with Et_3N (3 ml), poured into sat. aq. $NaHCO_3$ (100 ml), extracted with Et_2O (3 × 100 ml). The combined organic phases were dried with Na_2SO_4, filtered, concentrated and purified repeatedly by flash chromatography (EtOAC: heptane, 1:1, 0.4% Et_3N) affording **46** as a white solid (1.1 g, 14.6%); $\mathbf{R_f}$ (EtOAc/heptane 1:1) = 0.22; **mp**: 132–133 °C; **^{1}H NMR** (400 MHz, Benzene-*d6*) δ 8.11–8.04 (m, 1H), 7.74–7.58 (m, 4H), 7.29–7.20 (m, 2H), 5.31 (s, 1H), 3.89 (dd, *J* = 11.8, 1.6 Hz, 2H), 3.46 (dd, *J* = 11.8, 1.6 Hz, 2H), 3.02 (p, *J* = 1.6 Hz, 1H), 2.99 (p, *J* = 1.6 Hz, 1H), 2.95 (s, 1H), 2.92 (s, 1H); **^{13}C NMR** (101 MHz, Benzene-*d6*) δ 136.38, 134.11, 133.54, 128.72, 128.23 (2C), 126.55, 126.41, 125.85, 124.31, 101.57, 72.29 (2C), 64.04; **HRMS (MALDI+)** $C_{14}H_{14}O_3$, m/z [M+Na$^+$] 253.0835, found 253.0831

2-(4-Methoxyphenyl)-1,3-dioxan-5-yl oleate (**48**)

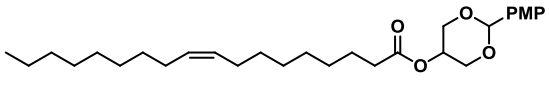

To a solution of oleic acid (50 mg, 0.177 mmol) was dissolved in dry CH_2Cl_2 (10 ml) under an atmosphere of nitrogen was added **44** (48 mg, 0.230 mmol), DMAP (37 mg, 0.300 mmol) and EDCI (51 mg, 0.266 mmol). After 16 h, the reaction mixture was concentrated, taken on silica and purified by flash chromatography (EtOAc: heptane 1:9, 0.4% Et_3N) affording **48** as an oil (55 mg, 65%); $\mathbf{R_f}$ (EtOAc/heptane 1:9) = 0.16; **mp**: 36–37 °C; **^{1}H NMR** (400 MHz, Benzene-*d6*) δ 7.60 (d, *J* = 8.7 Hz, 2H), 6.80 (d, *J* = 8.8 Hz, 2H), 5.49 (m, 2H), 5.24 (s, 1H), 4.34 (p, *J* = 1.6 Hz, 1H), 4.12 (dd, *J* = 12.9, 1.6 Hz, 2H), 3.54 (dd, *J* = 12.9, 1.6 Hz, 2H), 3.23 (s, 3H), 2.18 (t, *J* = 7.5 Hz, 2H), 2.15–2.02 (m, 4H), 1.65–1.52 (m, 2H), 1.44–1.13 (m, 20H), 0.96–0.85 (m, 3H); **^{13}C NMR** (101 MHz, Benzene-*d6*) δ 173.27, 160.52, 131.56, 130.23 (2C), 127.94 (2C), 113.76 (2C), 101.30, 68.94 (2C), 66.20, 54.74, 34.49, 32.33, 30.27, 30.16, 30.01, 29.79, 29.77, 29.59, 29.55, 29.41, 27.73, 27.70, 25.31, 23.13, 14.39; **HRMS (MALDI+)** $C_{29}H_{46}O_5$, m/z [M+Na+] 479.3237, found 497.3234

1,3-Dihydroxypropan-2-yl oleate (**42**)

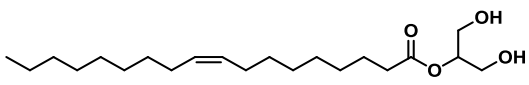

To a solution of **48** (78 mg, 0.164 mmol) in CH_2Cl_2 (4 ml) was added DDQ (93 mg, 0.411 mmol) and an aqueous phosphate buffer (0.5 ml, pH 7.5). After 16 h, the reaction mixture was poured into $NaHCO_3$, (5 ml), extracted with CH_2Cl_2 (3 × 5 ml), dried with Na_2SO_4,

filtered, concentrated and purified by reverse phase chromatography (C18 silica, MeCN:H_2O 7:3 → 1:0) affording **42** as a colourless oil (50 mg, 85%); $\mathbf{R_f}$ (EtOAc/heptane 1:1) = 0.25; **^{1}H NMR** (400 MHz, $CDCl_3$) δ 5.40–5.29 (m, 2H), 4.93 (p, *J* = 4.7 Hz, 1H), 3.83 (d, *J* = 4.7 Hz, 4H), 2.37 (t, *J* = 7.6 Hz, 2H), 2.01 (q, *J* = 6.1 Hz, 4H), 1.71–1.58 (m, 2H), 1.29 (dd, *J* = 16.4, 4.0 Hz, 20H), 0.92–0.83 (m, 3H); **^{13}C NMR** (101 MHz, $CDCl_3$) δ 174.19, 130.19, 129.85, 75.19, 62.71 (2C), 34.49, 32.06, 29.92, 29.84, 29.67, 29.47 (2C), 29.31, 29.24, 29.22, 27.37, 27.31, 25.10, 22.83, 14.27; **HRMS** (MALDI+)[229]

2-(Naphthalen-2-yl)-1,3-dioxan-5-yl oleate (**49**)

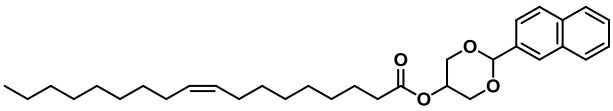

To a solution of oleic acid (140 mg. 0.488 mmol) in dry CH_2Cl_2 (20 ml) under an atmosphere of nitrogen was added DMAP (102 mg, 0.835 mmol), EDCI (141 mg, 0.733 mmol) and **46** (135 mg, 0.586 mmol). After 4 h, the reaction mixture was concentrated, taken on silica and purified by flash chromatography (EtOAc/heptane 1:4) affording **49** as an oil (86 mg, 36%); $\mathbf{R_f}$ (EtOAc/heptane 1:4) = 0.39; **^{1}H NMR** (400 MHz, Benzene-*d6*) δ 8.10 (d, *J* = 1.6 Hz, 1H), 7.79 (dd, *J* = 8.6, 1.7 Hz, 1H), 7.71–7.55 (m, 3H), 7.27–7.17 (m, 2H), 5.55–5.40 (m, 2H), 5.36 (s, 1H), 4.38 (p, *J* = 1.6 Hz, 1H), 4.16 (dd, *J* = 13.0, 1.6 Hz, 2H), 3.58 (dd, *J* = 12.9, 1.6 Hz, 2H), 2.20 (t, *J* = 7.5 Hz, 2H), 2.14–2.00 (m, 4H), 1.60 (p, *J* = 7.4 Hz, 2H), 1.43–1.12 (m, 20H), 0.95–0.86 (m, 3H); **^{13}C NMR** (101 MHz, Benzene-*d6*) δ 173.29, 136.44, 134.14, 133.52, 130.22 (2C), 128.68, 128.18, 127.94, 126.46, 126.31, 126.09, 124.51, 101.33, 69.03 (2C), 66.21, 34.50, 32.33, 30.27, 30.15, 30.01, 29.79, 29.76, 29.58, 29.53, 29.41, 27.72, 27.67, 25.32, 23.12, 14.39; **HRMS (MALDI+)** $C_{32}H_{46}O_4$, m/z [M+Na^+] 517.3288, found 517.3299

8-(Naphthalen-2-ylmethoxy)octan-1-ol (**39**)

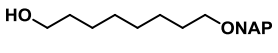

To a suspension of NaH (60% in oil, 4.31g, 0.107 mol) in dry DMF (36 ml) at 0 °C under an atmosphere of nitrogen was added slowly a solution of 1,8-octanediol (15.00 g, 0.1026 mol) in a mixture of THF and DMF (30 and 36 ml, respectively). The resulting mixture was let to warm slowly to 20 °C. After 2 h, a solution of NAPBr (9.89 g, 0.045 mol) in dry THF (20 ml) was added dropwise. The reaction was stirred for 16 h and excess reagent was quenched by addition of ice until bubbling ceased. The mixture was extracted with Et_2O (3 × 200 ml). The combined organic phases were washed with sat. aq. NH_4Cl (200 ml), dried with Na_2SO_4, filtered, concentrated and purified by flash chromatography (EtOAc/heptane 1:4) affording 3**9** as a white solid (9.50 g, 74%). $\mathbf{R_f}$ (EtOAc/heptane 1:4) = 0.19; **mp**: 51–52 °C; **^{1}H NMR** (400 MHz, $CDCl_3$) δ 7.87–7.79 (m, 3H), 7.78 (s, 1H), 7.53–7.41 (m, 3H), 4.67 (s, 2H), 3.62 (t, *J* = 6.6 Hz, 2H), 3.51 (t, *J* = 6.6 Hz, 2H), 1.70–1.58 (m, 2H), 1.61–1.49 (m, 2H), 1.45–1.27 (m, 8H); **^{13}C NMR** (101 MHz, $CDCl_3$) δ 136.3,

133.4, 133.1, 128.2, 128.0, 127.8, 126.4, 126.2, 125.9, 125.9, 73.1, 70.6, 63.2, 32.9, 29.9, 29.6, 29.5, 26.3, 25.8; **HRMS (MALDI+)** $C_{19}H_{26}O_2$, *m/z* [M+Na^+] 309.1825, found 309.1824

tert-Butyl(dec-9-yn-1-yloxy)dimethylsilane (**36**)

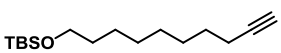

To a solution of 9-decyn-1-ol (2.11 g, 13.71 mmol) in dry DMF (10 ml) under an atmosphere of nitrogen was added imidazole (1.40 g, 20.56 mmol) and TBSCl (2.69 g, 17.82 mmol). The reaction mixture was stirred for 3 h, poured into sat. aq. NH_4Cl (50 ml) and extracted with CH_2Cl_2 (3 × 50 ml). The combined organic phases were washed with sat. aq. NH_4Cl (50 ml), dried with $MgSO_4$, filtered, concentrated and purified by flash chromatography (EtOAc/heptane 1:19) affording **36** as a colourless oil (3.53 g, 96%); $\mathbf{R_f}$ (EtOAc/heptane 1:19) = 0.77; **^{1}H NMR** (400 MHz, $CDCl_3$) δ 3.59 (t, *J* = 6.6 Hz, 2H), 2.18 (td, *J* = 7.1, 2.7 Hz, 2H), 1.93 (t, *J* = 2.6 Hz, 1H), 1.58–1.46 (m, 4H), 1.45–1.35 (m, 2H), 1.35–1.26 (m, 6H), 0.89 (s, 9H), 0.05 (s, 6H; **^{13}C NMR** (101 MHz, $CDCl_3$) δ 84.9, 68.2, 63.5, 33.0, 29.4, 29.2, 28.9, 28.6, 26.1 (3C), 25.9, 18.6 (2C), -5.1 (2C)M; **HRMS (MALDI+)** $C_{16}H_{32}OSi$, *m/z* [M+Na^+] 269.2295, found 269.2293

18-((*tert*-Butyldimethylsilyl)oxy)-1-(naphthalen-2-ylmethoxy)octadec-9-yn-8-ol (**55**)

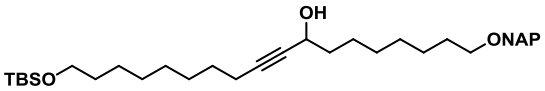

To a mixture of DMP (9.79 g, 23.04 mmol) in CH_2Cl_2 (40 ml) was added slowly a solution of **39** (5.50 g, 19.20 mmol) in CH_2Cl_2 (20 ml). The resulting mixture was stirred for 2 h and poured into an aqueous solution of $Na_2S_2O_3 \cdot 5\ H_2O$ (50 g in 300 ml). The mixture was stirred vigorously for 5 min and extracted with Et_2O (200 ml). The organic phase was washed with sat. aq. $NaHCO_3$ (200 ml), dried with $MgSO_4$, concentrated and used in the subsequent reaction without further purification. To a solution of **36** (4.40 g, 16.39mmol) in THF (25 ml) at -78 °C under an atmosphere of nitrogen was added dropwise *n*-BuLi (8.6 ml, 2.7 M in pentane, 19.66 mmol). The resulting mixture was allowed to slowly warm to 20 °C and a solution of the crude aldehyde (5.45 g, 19.20 mmol) in dry THF (20 ml) was added dropwise. The resulting mixture was stirred for 16 h, poured into sat. aq. NH_4Cl (250 ml) and extracted with CH_2Cl_2 (3 × 200 ml). The combined organic phases were dried with Na_2SO_4, filtered, concentrated and purified by flash chromatography (EtOAc/heptane 1:9) affording **55** as a yellow oil (8.11 g, 76%); $\mathbf{R_f}$ (EtOAc/heptane 1:9) = 0.17; **^{1}H NMR** (400 MHz, $CDCl_3$) δ 7.86–7.80 (m, 3H), 7.78 (s, 1H), 7.50–7.44 (m, 3H), 4.66 (s, 2H), 4.33 (tt, *J* = 6.5, 2.0 Hz, 1H), 3.59 (t, *J* = 6.6 Hz, 2H), 3.50 (t, *J* = 6.6 Hz, 2H), 2.19 (td, *J* = 7.1, 2.0 Hz, 2H), 1.70–1.59 (m, 6H), 1.55–1.25 (m, 18H), 0.89 (s, 9H), 0.04 (s, 6H); **^{13}C NMR** (101 MHz, $CDCl_3$) δ 136.34, 133.44, 133.08, 128.24, 127.99, 127.82, 126.40, 126.16, 125.90, 125.88, 85.66, 81.47, 73.11, 70.64, 63.46, 62.88, 38.34, 32.99, 29.92, 29.54, 29.45, 29.39, 29.23, 28.93,

28.80, 26.28, 26.14 (3 C), 25.91, 25.31, 18.81, 18.54, -5.09 (2C); **HRMS (MALDI+)** $C_{35}H_{56}O_3Si$, *m/z* [M+H$^+$] 553.4071, found 553.4059

18-((*tert*-Butyldimethylsilyl)oxy)-1-(naphthalen-2-ylmethoxy)octadec-9-yn-8-yl) *O*-phenyl carbonothioate (**60**)

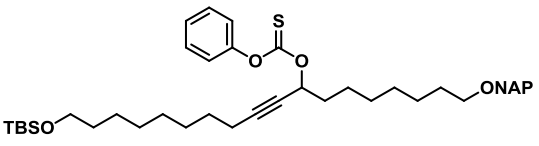

To a solution of **55** (1.70 g, 3.07 mmol) and DMAP (0.56 g, 4.59 mmol) in CH_2Cl_2 (80 ml) at 0 °C under an atmosphere of nitrogen was added PCTF (0.55 ml, 4.61 mmol). The reaction was allowed to warm up to 20 °C. After 3 h, the reaction mixture was poured into sat. aq. $NaHCO_3$ (250 ml) and extracted with CH_2Cl_2 (3 × 120 ml). The combined organic phases were dried with Na_2SO_4, filtered, concentrated and purified by flash chromatography (EtOAc/heptane 1:9) affording **60** as a yellow oil (2.08 g, 95%); $\mathbf{R_f}$ (EtOAc/heptane 1:9) = 0.48; **^{1}H NMR** (400 MHz, $CDCl_3$) δ 7.87–7.78 (m, 3H), 7.81–7.75 (s, 1H), 7.52–7.25 (m, 6H), 7.16–7.07 (m, 2H), 5.84–5.74 (m, 1H), 4.67 (s, 2H), 3.59 (t, *J* = 6.6 Hz, 2H), 3.52 (t, *J* = 6.6 Hz, 2H), 2.24 (td, *J* = 7.1, 2.0 Hz, 2H), 2.01–1.82 (m, 2H), 1.71–1.60 (m, 2H), 1.58–1.45 (m, 6H), 1.47–1.22 (m, 14H), 0.89 (s, 9H), 0.05 (s, 6H); **^{13}C NMR** (101 MHz, $CDCl_3$) δ 194.41, 153.61, 136.32, 133.44, 133.08, 129.61 (2C), 128.26, 127.99, 127.82, 126.65, 126.41, 126.17, 125.89 (2C), 122.14 (2C), 88.53, 76.32, 75.49, 73.13, 70.61, 63.45, 34.94, 33.02, 29.92, 29.49, 29.46, 29.25, 29.23, 28.94, 28.55, 26.28, 26.15 (3C), 25.94, 25.06, 18.92, 18.53, -5.09 (2C); **HRMS (MALDI+)** $C_{42}H_{60}O_4SSi$, *m/z* [M+Na$^+$] 711.3874, found 711.3882

tert-Butyldimethyl((18-(naphthalen-2-ylmethoxy)octadec-9-yn-1-yl)oxy)silane (**35**)

To a solution of **60** (1.84 g, 2.67 mmol) and AIBN (66 mg, 0.40 mmol) in toluene (30 ml) under an atmosphere of nitrogen in a round bottom flask equipped with a condenser was added Bu_3SnH (1.44 ml, 5.34 mmol). The reaction was refluxed for 1.5 h, poured into sat. aq. $NaHCO_3$ (200 ml) and extracted with CH_2Cl_2 (3 × 200 ml). The combined organic phases were dried with Na_2SO_4, filtered, concentrated and purified by flash chromatography (EtOAc/heptane 1:19) affording **35** as an oil (1.36 g, 95%); **Rf** (EtOAc/heptane 1:19) = 0.38; **^{1}H NMR** (400 MHz, $CDCl_3$) δ 7.86–7.78 (m, 3H), 7.81–7.75 (m, 1H), 7.52–7.41 (m, 3H), 4.67 (s, 2H), 3.59 (t, *J* = 6.6 Hz, 2H), 3.51 (t, *J* = 6.7 Hz, 2H), 2.18–2.08 (m, 4H), 1.70–1.58 (m, 2H), 1.48 (m, 6H), 1.43–1.24 (m, 16H), 0.89 (s, 9H), 0.05 (s, 6H); **^{13}C NMR** (101 MHz, $CDCl_3$) δ 136.36, 133.44, 133.08, 128.24, 127.99, 127.82, 126.40, 126.16, 125.90, 125.88, 80.38, 80.35, 77.16, 73.11, 70.68, 63.48, 33.03, 29.94, 29.54, 29.50, 29.31 (3C), 29.27, 28.99, 28.97, 26.33, 26.14 (3C), 25.93, 18.91, 18.54, -5.09 (2C); **HRMS (MALDI+)** $C_{35}H_{56}O_2Si$, m/z [M+Na$^+$], 559.3942, found. 559.3978

18-((*tert*-Butyldimethylsilyl)oxy)octadec-9-yn-1-ol (**65**)

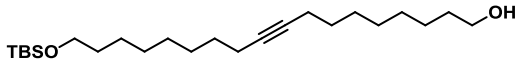

To a solution of **35** (1.35 g, 2.59 mmol) in CH_2Cl_2 (40 ml) was added DDQ (0.882 g, 3.89 mmol) and H_2O (5 ml). The resulting mixture was stirred vigorously for 16 h, poured into sat. aq. $NaHCO_3$ (250 ml) and extracted with CH_2Cl_2 (3 × 100 ml). The combined organic phases were dried with $MgSO_4$, filtered, concentrated and purified by flash chromatography (EtOAc/heptane 1:9) affording **65** as a colourless oil (0.456 g, 44%); $\mathbf{R_f}$ (EtOAc/heptane 1:9) = 0.13; **^{1}H NMR** (400 MHz, $CDCl_3$) δ 3.66–3.57 (m, 4H), 2.13 (t, *J* = 6.9 Hz, 4H), 1.62–1.42 (m, 8H), 1.42–1.24 (m, 16H), 0.89 (s, 9H), 0.04 (s, 6H); **^{13}C NMR** (101 MHz, $CDCl_3$) δ 80.41, 80.33, 63.49, 63.20, 33.02, 32.94, 29.51, 29.48, 29.31 (2C), 29.28 (2C), 28.98, 28.93, 26.14 (3C), 25.93, 25.85, 18.90 (2C), 18.54, -5.10 (2C); **HRMS (MALDI+)** $C_{24}H_{48}O_2Si$, *m/z* [M+H$^+$] 397.3496, found. 397.3494

2-(4-Methoxyphenyl)-1,3-dioxan-5-yl 18-((*tert*-butyldimethylsilyl)oxy)octadec-9-ynoate (**66**)

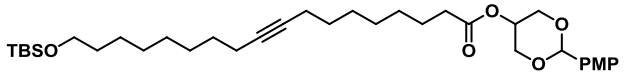

To a mixture of DMP (449 mg, 1.06 mmol) in CH_2Cl_2 (5 ml) was added slowly a solution of **65** (440 mg, 1.11 mmol) in CH_2Cl_2 (5 ml). The resulting mixture was stirred for 2.5 h and poured into an aqueous solution of $Na_2S_2O_3 \cdot 5H_2O$ (5 g in 50 ml). The mixture was stirred vigorously for 5 min and was extracted with Et_2O (50 ml). The organic phase was washed with sat. aq. $NaHCO_3$ (50 ml), dried with Na_2SO_4, concentrated, and used in the subsequent reaction without further purification.

To a solution of the crude aldehyde (278 mg, 0.706vmmol) in *t*-BuOH (30 ml) was added 2-methyl-2-butene (0.989 g, 1.5 ml, 14.11 mmol) and an aqueous solution of NaH_2PO_4 (0.677 g, 5.64 mmol) and $NaClO_2$ (89 mg, 0.988 mmol in 7.5 ml). After 16 h, an aqueous buffer solution of NaH_2PO_4 was added (0.66 M, 20 ml). The mixture was extracted with CH_2Cl_2 (3 × 30 ml), and the combined organic phaseswere washed with sat. aq. NaCl (30 ml), dried with Na_2SO_4, filtered, concentrated, and used in the subsequent reaction without further purification.

To a solution of the crude carboxylic acid (144 mg) in dry THF (10 ml) under an atmosphere of nitrogen was added MeIm (87 mg, 1.054 mmol), MSNT (125 mg, 0.421 mmol) and **44** (81 mg, 0.386 mmol). After 16 h, the reaction was poured into H_2O (50 ml) and extracted with Et_2O (2 × 50 ml). The combined organic phases were dried with Na_2SO_4, filtered, concentrated and purified by flash chromatography (EtOAc/heptane 1:9, 0.4% Et_3N) affording **66** as an oil (115 mg, 55%); $\mathbf{R_f}$ (EtOAc/heptane 1:9) = 0.25; **^{1}H NMR** (400 MHz, Benzene-*d6*) δ 7.60 (m, 2H), 6.80 (m, 2H), 5.24 (s, 1H), 4.33 (p, *J* = 1.6 Hz, 1H), 4.11 (dd, *J* = 13.0, 1.6 Hz, 2H), 3.61–3.49 (m, 4H), 3.24 (s, 3H), 2.21–

2.09 (m, 6H), 1.61–1.06 (m, 22H), 1.00 (s, 9H), 0.08 (s, 6H); **^{13}C NMR** (101 MHz, Benzene-*d6*) δ 173.27, 160.52, 131.55, 127.93 (2C), 113.76 (2C), 101.29, 80.52 (2C), 68.94 (2C), 66.19, 63.36, 54.74, 34.46, 33.31, 29.79, 29.66, 29.62, 29.57, 29.30, 29.27, 29.13, 29.05, 26.28, 26.21 (3C), 25.24, 19.28, 19.23, 18.56, -5.09 (2C); **HRMS (MALDI+)** $C_{35}H_{58}O_6Si$, m/z [M+Na$^+$] 625.3895, found 625.3886

2-(4-Methoxyphenyl)-1,3-dioxan-5-yl 18-hydroxyoctadec-9-ynoate (**68**)

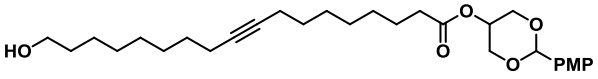

To a solution of **66** (100 mg, 0.166 mmol) in dry THF (2.5 ml) at 0 °C under an atmosphere of nitrogen was added TBAF (200 µl, 1M in THF, 0.200 mmol) and AcOH (2 µl, 0.033 mmol). The reaction was allowed to warm up to 20 °C. After 18 h, the reaction mixture was diluted in CH_2Cl_2 (50 ml) and washed with sat. aq. NH_4Cl (50 ml). The organic phase was dried with Na_2SO_4, filtered, concentrated and purified by flash chromatography (EtOAc/heptane 1:9, 0.4% Et_3N) affording **68** as a white solid (50 mg, 62%); $\mathbf{R_f}$ (EtOAc/heptane 3:7) = 0.10; **mp**: 55–57 °C; **^{1}H NMR** (400 MHz, Benzene-*d6*) δ 7.60 (d, *J* = 8.7 Hz, 2H), 6.81 (d, *J* = 8.8 Hz, 2H), 5.24 (s, 1H), 4.33 (p, *J* = 1.7 Hz, 1H), 4.11 (d, *J* = 11.5 Hz, 2H), 3.54 (d, *J* = 11.3 Hz, 2H), 3.36 (t, *J* = 6.5 Hz, 2H), 3.24 (s, 3H), 2.21–2.07 (m, 6H), 1.62–1.06 (m, 22H); **^{13}C NMR** (101 MHz, Benzene-*d6*) δ 173.34, 160.53, 131.52, 127.93 (2C), 113.78 (2C), 101.29, 80.58, 80.55, 68.94 (2C), 66.21, 62.72, 54.75, 34.47, 33.23, 29.79, 29.61, 29.56, 29.53, 29.32, 29.18, 29.13, 29.02, 26.14, 25.24, 19.25, 19.21; **HRMS (MALDI+)** $C_{29}H_{44}O_6$, m/z [M+Na$^+$] 511.3030, found 511.3026

2-(4-Methoxyphenyl)-1,3-dioxan-5-yl (Z)-18-hydroxyoctadec-9-enoate (**34**)

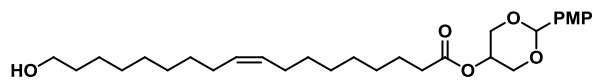

To a solution of **68** (70 mg, 0.143 mmol) in dry THF (5 ml) under an atmosphere of nitrogen was added Lindlar catalyst (5% Pd in $CaCO_3$ poisoned with Pb, 28 mg). A hydrogen atmosphere was installed by bubbling H_2 through the solution for 5 minutes. The reaction mixture was stirred under an atmosphere of hydrogen for 16 h, filtered through Celite and concentrated, affording **34** as a white solid (64 mg, 91%); $\mathbf{R_f}$ (EtOAc/heptane 3:7) = 0.10; **^{1}H NMR** (400 MHz, Benzene-*d6*) δ 7.60 (d, *J* = 8.8 Hz, 2H), 6.80 (d, *J* = 8.8 Hz, 2H), 5.60–5.40 (m, 2H), 5.24 (s, 1H), 4.34 (t, *J* = 1.8 Hz, 1H), 4.11 (d, *J* = 11.4 Hz, 2H), 3.54 (d, *J* = 11.1 Hz, 2H), 3.38 (t, *J* = 6.5 Hz, 2H), 3.24 (s, 3H), 2.19 (t, *J* = 7.5 Hz, 2H), 2.16–1.98 (m, 4H), 1.59 (p, *J* = 7.3 Hz, 2H), 1.49–1.12 (m, 20H); **^{13}C NMR** (101 MHz, Benzene-*d6*) δ 173.36, 160.53, 131.52, 130.26, 130.22, 127.93 (2C), 113.77 (2C), 101.30, 68.94 (2C), 66.22, 62.74, 54.74, 34.49, 33.26, 30.21, 30.14, 29.97, 29.88, 29.64, 29.56, 29.51, 29.41, 27.67 (2C), 26.22, 25.30; **HRMS (MALDI+)** $C_{29}H_{46}O_6$, m/z [M+Na$^+$] 513.3187, found 513.3183

1,3-Dihydroxypropan-2-yl (Z)-18-hydroxyoctadec-9-enoate (**29**)

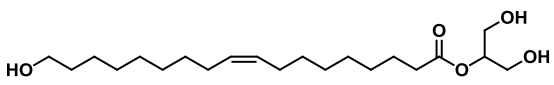

To a solution of **34** (43 mg, 0.0869 mmol) in CH_2Cl_2 (4 ml) was added DDQ (49 mg, 0.2172 mmol) and an aqueous phosphate buffer (0.5 ml, pH 7.5). After 16 h, the reaction mixture was poured into $NaHCO_3$, (20 ml), extracted with CH_2Cl_2 (3 × 10 ml), dried with Na_2SO_4, filtered, concentrated and purified by reverse phase chromatography (C18 silica, MeCN:H_2O 7:3 → 1:0) affording **29** as a colourless oil (26 mg, 75% purity, 61%); $\mathbf{R_f}$ (EtOAc/heptane 1:1) = 0.2; **^{1}H NMR** (400 MHz, $CDCl_3$) δ 5.39–5.29 (m, 2H), 4.92 (p, *J* = 4.7 Hz, 1H), 3.83 (d, *J* = 4.7 Hz, 4H), 3.64 (t, *J* = 6.7 Hz, 2H), 2.37 (t, *J* = 7.6 Hz, 2H), 2.01 (m, 4H), 1.70–1.50 (m, 4H), 1.40–1.23 (m, 18H); **^{13}C NMR** (101 MHz, $CDCl_3$) δ 174.21, 130.12, 129.94, 75.17, 63.23, 62.65 (2C), 34.49, 32.91, 29.82, 29.77, 29.59, 29.54, 29.31, 29.26, 29.22, 29.17, 27.29, 27.26, 25.87, 25.09; **HRMS (MALDI+)** $C_{21}H_{40}O_5$, m/z [M+Na^+] 395.2768, found 395.2772

8-(Naphthalen-2-ylmethoxy)octyl 4-methylbenzenesulfonate (**51**)

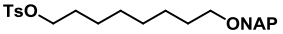

To a solution of **39** (1.451 g, 5.067 mmol) in pyridine (8 ml) at 0 °C was added TsCl (1.448 g, 7.600 mmol) portion wise. After 3 h, TLC showed completion. The reaction mixture was poured into H_2O (50 ml) and extracted with Et_2O (2 × 50 ml). The combined organic phases were washed with a solution of $CuSO_4 \cdot 5H_2O$ (0.5 g in 50 ml of H_2O), H_2O (50 ml), sat. aq. $NaHCO_3$ (50 ml) and brine (50 ml). The organic phase was dried with Na_2SO_4, filtered, concentrated and purified by flash chromatography (EtOAc/heptane 1:4) affording **51** as an oil (2.05 g, 92%); $\mathbf{R_f}$ (EtOAc/heptane 1:4) = 0.27; **^{1}H NMR** (400 MHz, $CDCl_3$) δ 7.34–7.25 (m, 6H), 6.98–6.92 (m, 3H), 6.82 (d, *J* = 8.0 Hz, 2H), 4.15 (s, 2H), 3.49 (t, *J* = 6.5 Hz, 2H), 2.98 (t, *J* = 6.6 Hz, 2H), 1.92 (s, 3H), 1.10 (m, 4H), 0.87–0.68 (m, 8H); **^{13}C NMR** (101 MHz, $CDCl_3$) δ 144.75, 136.29, 133.42, 133.36, 133.07, 129.92 (2C), 128.25, 128.01 (2C), 127.97, 127.82, 126.42, 126.18, 125.90 (2C), 73.12, 70.79, 70.54, 29.86, 29.33, 29.00, 28.92, 26.20, 25.40, 21.76; **HRMS (MALDI+)** $C_{26}H_{32}O_4S$, m/z [M+Na^+] 463.1914, found 463.1911

2-(((8-Iodooctyl)oxy)methyl)naphthalene (**52**)

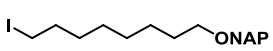

To a solution of **51** (1.582 g, 3.591 mmol) in DMF (20 ml) was added NaI (1.246 g, 8.973 mmol) and the reaction mixture was warmed up to 80 °C. After 1.5 h, TLC showed completion. The reaction mixture was poured into H_2O (100 ml) and extracted with Et_2O (3 × 100 ml). The combined organic phases were washed with sat. aq. $NaHCO_3$ (100 ml) and brine (100 ml), dried with Na_2SO_4, filtered, concentrated and purified by flash chromatography (EtOAc/heptane 1:9) affording **52** as a white solid (0.91 g, 64%); $\mathbf{R_f}$ (EtOAc/heptane 1:4) = 0.61; **mp**:

42–43 °C; **^{1}H NMR** (400 MHz, $CDCl_3$) δ 7.78–7.73 (m, 3H), 7.71 (s, 1H), 7.43–7.37 (m, 3H), 4.59 (s, 2H), 3.43 (t, *J* = 6.6 Hz, 2H), 3.10 (t, *J* = 7.0 Hz, 2H), 1.73 (p, *J* = 7.0 Hz, 2H), 1.56 (p, *J* = 8.1, 6.6 Hz, 2H), 1.36–1.20 (m, 8H); **^{13}C NMR** (101 MHz, $CDCl_3$) δ 136.32, 133.43, 133.08, 128.25, 127.99, 127.82, 126.42, 126.17, 125.90 (2C), 73.12, 70.57, 33.66, 30.58, 29.88, 29.38, 28.63, 26.26, 7.45; **HRMS (MALDI+)** $C_{19}H_{25}IO$, m/z [M+Na^+] 419.0842, found 419.0839

11-((*tert*-Butyldimethylsilyl)oxy)-1-phenylundec-2-yn-1-ol (**53**)

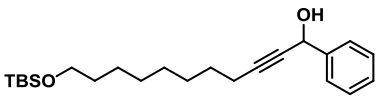

To a solution of **36** (55 mg, 0.205 mmol) in THF (4 ml) at -78 °C under an atmosphere of nitrogen was added dropwise *n*-BuLi (90 µl, 2.7 M in pentane, 0.239 mmol). The resulting mixture was allowed to slowly warm to 20 °C and benzaldehyde (33 mg, 34 µl, 0.310 mmol) was added dropwise. The resulting mixture was stirred for 16 h, poured into sat. aq. NH_4Cl (20 ml) and extracted with CH_2Cl_2 (3 × 20 ml). The combined organic phases were dried with Na_2SO_4, filtered, concentrated and purified by flash chromatography (EtOAc/heptane 1:9) affording **53** as an oil (40 mg, 52%); **R_f** (EtOAc/heptane 1:9) = 0.23; **^{1}H NMR** (400 MHz, $CDCl_3$) δ 7.59–7.28 (m, 5H), 5.45 (s, 1H), 3.59 (t, *J* = 6.7 Hz, 2H), 2.27 (td, *J* = 7.1, 2.0 Hz, 2H), 1.64–1.21 (m, 12H), 0.89 (d, *J* = 1.9 Hz, 9H), 0.04 (d, *J* = 2.8 Hz, 6H); **^{13}C NMR** (101 MHz, $CDCl_3$) δ 141.42, 128.66 (2C), 128.33, 126.77 (2C), 87.86, 80.08, 64.99, 63.46, 32.98, 29.43, 29.20, 28.96, 28.68, 26.14 (3C), 25.88, 18.95, 18.53, -5.10 (2C); **HRMS (MALDI+)** $C_{23}H_{38}O_2Si$, m/z [M+Na^+] 397.2533, found 397.2533

tert-Butyldimethyl(undec-9-yn-1-yloxy)silane (**54**)

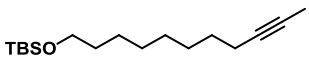

To a solution of **36** (54 mg, 0.199 mmol) in THF (4 ml) at -78 °C under an atmosphere of nitrogen was added dropwise *n*-BuLi (90 µl, 2.7 M in pentane, 0.239 mmol). The resulting mixture was allowed to slowly warm to 20 °C and MeI (57 mg, 25 µl, 0.399 mmol) was added dropwise. The resulting mixture was stirred for 16 h, poured into sat. aq. NH_4Cl (20 ml) and extracted with CH_2Cl_2 (3 × 20 ml). The combined organic phases were dried with Na_2SO_4, filtered, concentrated and purified by flash chromatography (EtOAc/heptane 1:39) affording **54** as an oil (39 mg, 70%); **R_f** (EtOAc/heptane 1:19) = 0.64; **^{1}H NMR** (400 MHz, $CDCl_3$) δ 3.59 (t, *J* = 6.6 Hz, 2H), 2.11 (m, 2H), 1.78 (t, *J* = 2.6 Hz, 3H), 1.54–1.43 (m, 4H), 1.41–1.24 (m, 8H), 0.89 (s, 9H), 0.04 (s, 6H); **^{13}C NMR** (101 MHz, $CDCl_3$) δ 79.54, 75.46, 63.47, 33.02, 29.49, 29.32, 29.23, 29.01, 26.14 (3C), 25.92, 18.87, 18.54, 3.62, -5.10 (2C); **HRMS (MALDI+)** $C_{17}H_{34}OSi$, m/z [M+H^+] 283.2452, found 283.2446.

O-(8-(naphthalen-2-ylmethoxy)octyl) O-phenyl carbonothioate (**62**)

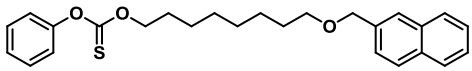

To a solution of **39** (70 mg, 0.244 mmol) and DMAP (63 mg, 0.366 mmol) in CH_2Cl_2 (5 ml) at 0 °C under an atmosphere of nitrogen was added PCTF (50 µl, 0.366 mmol). The reaction was allowed to warm up to 20 °C. After 20 h, the reaction mixture was poured into sat. aq. $NaHCO_3$ (50 ml) and extracted with CH_2Cl_2 (3 × 50 ml). The combined organic phases were dried with Na_2SO_4, filtered, concentrated and purified by flash chromatography (EtOAc/heptane 1:9) affording **62** as a yellow oil (72 mg, 70%); **^{1}H NMR** (400 MHz, $CDCl_3$) δ 7.87 – 7.79 (m, 3H), 7.79 (d, *J* = 1.7 Hz, 1H), 7.52 – 7.26 (m, 6H), 7.15 – 7.07 (m, 2H), 4.67 (s, 2H), 4.51 (t, *J* = 6.7 Hz, 2H), 3.52 (t, *J* = 6.6 Hz, 2H), 1.88 – 1.75 (m, 2H), 1.71 – 1.58 (m, 2H), 1.48 – 1.20 (m, 8H). **^{13}C NMR** (101 MHz, $CDCl_3$) δ 195.42, 153.70, 153.53, 136.32, 133.44, 133.08, 129.80, 129.64, 128.26, 127.99, 127.83, 126.96, 126.64, 126.43, 126.18, 125.91, 122.13, 121.97, 77.16, 74.76, 73.13, 70.58, 29.91, 29.44, 29.30, 28.31, 26.27, 25.88.

S-methyl *O*-(8-(naphthalen-2-ylmethoxy)octyl) carbonodithioate (**64**)

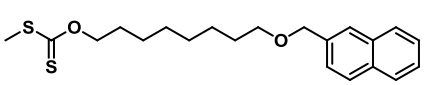

To a suspension of NaH (14 mg, 0.55 mmol) and imidazole (1.3 mg, 0.018 mmol) in dry THF (2 ml) was added a solution of 3**9** in dry THF (5 ml). The mixture was stirred for 2.5 h, and then CS_2 (110 µl, 1.84 mmol) was added. The reaction was refluxed for 50 minutes, and then MeI (114 µl, 1.84 mmol) was added. The reaction was refluxed for 1.5 h and it was poured into sat. aq. $NaHCO_3$ (20 ml) and extracted with CH_2Cl_2 (3 × 20 ml). The combined organic phases were dried with Na_2SO_4, filtered, concentrated and purified by flash chromatography (EtOAc/heptane 8:2), affording **64** as an oil (103 mg, 77%). **R_f** (EtOAc/heptane 8:2) = 0.52. **^{1}H NMR** (400 MHz, $CDCl_3$) δ 7.87 – 7.78 (m, 3H), 7.78 (s, 1H), 7.52 – 7.42 (m, 3H), 4.67 (s, 2H), 4.58 (t, *J* = 6.7 Hz, 2H), 3.51 (t, *J* = 6.6 Hz, 2H), 2.55 (s, 3H), 1.85 – 1.73 (m, 2H), 1.70 – 1.59 (m, 2H), 1.47 – 1.19 (m, 8H). **^{13}C NMR** (101 MHz, $CDCl_3$) δ 216.13, 136.32, 133.43, 133.08, 128.25, 127.98, 127.82, 126.42, 126.17, 125.91, 77.16, 74.39, 73.12, 70.57, 29.90, 29.43, 29.30, 28.36, 26.26, 25.97, 19.05.

1,3-Dimethoxypropan-2-yl 10,16-bis((tert-butyldimethylsilyl)oxy)hexadecanoate (**74**)

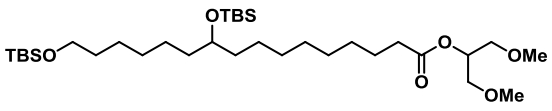

To a solution of **5** (506 mg, 0.99 mmol) in CH_2Cl_2 (4 ml) and water (2 ml) was added $PhI(OAc)_2$ (834 mg, 2.58 mmol) and TEMPO (34 mg, 0.20 mmol). The resulting mixture was stirred vigorously for 6 hours, poured into 10% aq. $Na_2S_2O_3$ (10 ml) and extracted with EtOAc (3 × 20 ml). The combined organic phases were dried with $MgSO_4$, filtered, concentrated and used in the subsequent reaction without further purification.

To a solution of the crude aldehyde (1.49 g) in *t*-BuOH (150 ml) was added 2-methyl-2-butene (4.2 g, 6.4 ml, 60 mmol) and an aqueous solution (37 ml) of NaH_2PO_4 (2.93 g, 24.4 mmol) and $NaClO_2$ (0.35 g, 3.9 mmol). After 15 h, a buffer aqueous solution of NaH_2PO_4 was added (0.66 M, 150 ml) and the mixture was extracted with CH_2Cl_2 (3 × 100 ml). The combined organic phases were washed with sat. aq. NaCl (100 ml), dried with $MgSO_4$, filtered, concentrated, and used in the subsequent reaction without further purification

To a solution of the crude carboxylic acid (514 mg, 0.99 mmol) in CH_2Cl_2 (10 mL) was added 1,3-dimethoxy-2-propanol (159 mg, 1.3 mmol), DMAP (206 mg, 1.7 mmol) and EDCI (287 mg, 1.5 mmol). The reaction was stirred for 16 hours, taken on silica, concentrated and purified by flash chromatography (EtOAc:heptane 1:19) affording **74** as a colorless oil (357 mg, 58%). $\mathbf{R_f}$ (EtOAc:heptane 1:19) = 0.10. **^{1}H NMR** (400 MHz, $CDCl_3$) δ 5.14 (p, *J* = 5.1 Hz, 1H), 3.62 – 3.57 (m, 3H), 3.53 (d, *J* = 5.1 Hz, 4H), 3.36 (s, 6H), 2.34 (t, *J* = 7.4 Hz, 2H), 1.63 (p, *J* = 7.4 Hz, 2H), 1.50 (p, *J* = 6.6 Hz, 2H), 1.44 – 1.34 (m, 4H), 1.35 – 1.17 (m, 16H), 0.89 (s, 9H), 0.88 (s, 9H), 0.04 (s, 6H), 0.03 (s, 6H). **^{13}C NMR** (101 MHz, $CDCl_3$) δ 173.5, 72.5, 71.4 (2C), 71.1, 63.5, 59.4 (2C), 37.3, 37.3, 34.6, 33.0, 30.0, 29.8, 29.7, 29.4, 29.2, 26.1 (3C), 26.1 (3C), 26.0, 25.5 (2C), 25.1, 18.5, 18.3, -4.3 (2C), -5.1 (2C). **HRjMS (MALDI+)** $C_{33}H_{70}O_6Si_2$, *m/z* [M+Na$^+$] 641.4603, found 641.4617

1,3-Dimethoxypropan-2-yl 10,16-dihydroxyhexadecanoate (**69**)

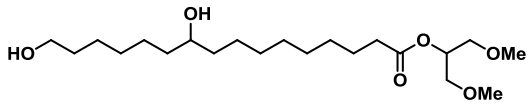

To a solution of **74** (192 mg, 0.31 mmol) in MeCN (15 ml) at 0 °C was added 20% aq. HF (1.5 ml). The resulting mixture was stirred at 0 °C for 4 h. TMSOMe (5.6 ml) was added, and the mixture was stirred for 30 minutes, poured into sat. aq. NH_4Cl (45 ml) and extracted with CH_2Cl_2 (3 × 45 ml). The combined organic phases were dried with $MgSO_4$, filtered, concentrated and purified by flash chromatography (EtOAc/heptane 3:2), affording **69** as a white solid (110 mg, 87%); **m.p**. 52–53 °C $\mathbf{R_f}$ (EtOAc/heptane 3:2) = 0.1; **^{1}H NMR** (400 MHz, $CDCl_3$) δ 5.14 (p, *J* = 5.0 Hz, 1H), 3.64 (t, *J* = 6.6 Hz, 2H), 3.60 – 3.55 (m, 1H), 3.53 (d, *J* = 5.0 Hz, 4H), 3.36 (s, 6H), 2.34 (t, *J* = 7.5 Hz, 2H), 1.68 – 1.51 (m, 4H), 1.47 – 1.26 (m, 20H). **^{13}C NMR** (101 MHz, $CDCl_3$) δ 173.5, 72.1, 71.4 (2C), 71.0, 63.1, 59.4 (2C), 37.6, 37.5, 34.5, 32.8, 29.7, 29.6, 29.5, 29.3, 29.2, 25.9, 25.7 (2C), 25.1. **HRMS (MALDI+)** $C_{21}H_{42}O_6$, *m/z* [M+Na$^+$] 413.2874, found 413.2884.

Isopropyl 10,16-bis((tert-butyldimethylsilyl)oxy)hexadecanoate (**75**)

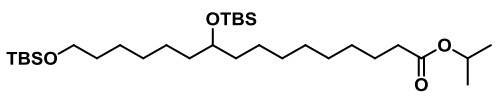

To a mixture of DMP (1.77 g, 4.2 mmol) in CH_2Cl_2 (20 ml) was added slowly a solution of **5** (1.51 g, 3.0 mmol) in CH_2Cl_2 (20 ml). The resulting mixture was stirred for 2 h and poured into a solution of $Na_2S_2O_3$ (25 g) in sat. aq. $NaHCO_3$ (100 ml). The mixture was stirred vigorously for 5 min and then extracted with Et_2O (100 ml). The organic phase was washed with sat. aq. $NaHCO_3$ (100 ml), dried with $MgSO_4$, concentrated and used in the subsequent reaction without further purification.

To a solution of the crude aldehyde (1.49 g) in *t*-BuOH (150 ml) was added 2-methyl-2-butene (4.2 g, 6.4 ml, 60 mmol) and an aqueous solution (37 ml) of NaH_2PO_4 (2.93 g, 24.4 mmol) and $NaClO_2$ (0.35 g, 3.9 mmol). After 15 h, a buffer aqueous solution of NaH_2PO_4 was added (0.66 M, 150 ml) and the mixture was extracted with CH_2Cl_2 (3 × 100 ml). The combined organic phases were washed with sat. aq. NaCl (100 ml), dried with $MgSO_4$, filtered, concentrated, and used in the subsequent reaction without further purification

To a solution of the crude carboxylic acid (514 mg, 0.99 mmol) in CH_2Cl_2 (10 mL) was added 2-propanol (80 mg, 1.3 mmol), DMAP (212 mg, 1.7 mmol) and EDCI (285 mg, 1.5 mmol). The reaction was stirred for 16 hours, taken on silica, concentrated and purified by flash chromatography (EtOAc:heptane 3:97) affording **75** as a colorless oil (400 mg, 72%). $\mathbf{R_f}$ (EtOAc:heptane 3:97) = 0.14; $^{\mathbf{1}}$**H NMR** (400 MHz, $CDCl_3$) δ 5.00 (m, 1H), 3.65 – 3.55 (m, 3H), 2.25 (t, *J* = 7.4 Hz, 2H), 1.59 (p, *J* = 7.4 Hz, 2H), 1.51 (p, *J* = 6.7 Hz, 2H), 1.45 – 1.35 (m, 4H), 1.35 – 1.23 (m, 16H), 1.22 (d, *J* = 6.3 Hz, 6H), 0.89 (s, 9H), 0.88 (s, 9H), 0.04 (s, 6H), 0.03 (s, 6H). $^{\mathbf{13}}$**C NMR** (101 MHz, $CDCl_3$) δ 173.6, 72.5, 67.5, 63.5, 37.3, 37.3, 34.9, 33.0, 30.0, 29.8, 29.6, 29.4, 29.3, 26.1 (3C), 26.1 (3C), 26.0, 25.5, 25.5, 25.2, 22.0 (2C), 18.5, 18.3, -4.3 (2C), -5.1 (2C). **HRMS (MALDI+)** $C_{31}H_{66}O_4Si_2$, *m/z* [$M+Na^+$] 581.4392, found 581.4405.

Isopropyl 10,16-dihydroxyhexadecanoate (**70**)

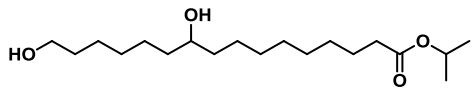

To a solution of **75** (196 mg, 0.30 mmol) in MeCN (37 ml) at 0 °C was added 20% aq. HF (1.5 ml). The resulting mixture was stirred at 0 °C for 4 h. TMSOMe (6.1 ml) was added, and the mixture was stirred for 30 minutes, poured into sat. aq. NH_4Cl (40 ml) and extracted with CH_2Cl_2 (3 × 40 ml). The combined organic phases were dried with $MgSO_4$, filtered, concentrated and purified by flash chromatography (EtOAc/heptane 1:1), affording **70** as a white solid (113 mg, 95%); **m.p**. 46–47 ^{o}C $\mathbf{R_f}$ (EtOAc/heptane 3:2) = 0.1; $^{\mathbf{1}}$**H NMR** (400 MHz, $CDCl_3$) δ 5.00 (m, 1H), 3.64 (t, *J* = 6.6 Hz, 2H), 3.61 – 3.53 (m, 1H), 2.25 (t, *J* = 7.5 Hz, 2H), 1.65 – 1.52 (m, 4H), 1.45 – 1.25 (m, 20H), 1.22 (d, *J* = 6.3 Hz, 6H). $^{\mathbf{13}}$**C NMR** (101 MHz, $CDCl_3$) δ 173.6, 72.1, 67.5, 63.1, 37.6, 37.5, 34.9, 32.8, 29.7, 29.6,

29.5, 29.3, 29.2, 25.9, 25.7 (2C), 25.2, 22.0 (2C). **HRMS (MALDI+)** $C_{19}H_{38}O_4$, *m/z* [M+Na^+] 353.2662, found 353.2671.

2-(Benzyloxy)ethyl 10,16-bis((tert-butyldimethylsilyl)oxy)hexadecanoate (**76**)

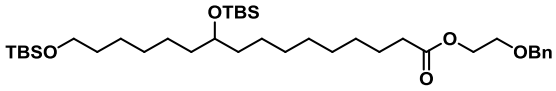

To a mixture of DMP (1.77 g, 4.2 mmol) in CH_2Cl_2 (20 ml) was added slowly a solution of **5** (1.51 g, 3.0 mmol) in CH_2Cl_2 (20 ml). The resulting mixture was stirred for 2 h and poured into a solution of $Na_2S_2O_3$ (25 g) in sat. aq. $NaHCO_3$ (100 ml). The mixture was stirred vigorously for 5 min and then extracted with Et_2O (100 ml). The organic phase was washed with sat. aq. $NaHCO_3$ (100 ml), dried with $MgSO_4$, concentrated and used in the subsequent reaction without further purification.

To a solution of the crude aldehyde (1.49 g) in *t*-BuOH (150 ml) was added 2-methyl-2-butene (4.2 g, 6.4 ml, 60 mmol) and an aqueous solution (37 ml) of NaH_2PO_4 (2.93 g, 24.4 mmol) and $NaClO_2$ (0.35 g, 3.9 mmol). After 15 h, a buffer aqueous solution of NaH_2PO_4 was added (0.66 M, 150 ml) and the mixture was extracted with CH_2Cl_2 (3 × 100 ml). The combined organic phases were washed with sat. aq. NaCl (100 ml), dried with $MgSO_4$, filtered, concentrated, and used in the subsequent reaction without further purification

To a solution of the crude carboxylic acid (514 mg, 0.99 mmol) in CH_2Cl_2 (10 mL) was added 2-benzyloxyethanol (200 mg, 1.3 mmol), DMAP (209 mg, 1.7 mmol) and EDCI (290 mg, 1.5 mmol). The reaction was stirred for 16 hours, taken on silica, concentrated and purified by flash chromatography (EtOAc:heptane 1:19) affording **76** as a colorless oil (519 mg, 80%). $\mathbf{R_f}$ (EtOAc:heptane 1:19) = 0.12; **^{1}H NMR** (400 MHz, $CDCl_3$) δ 7.38 – 7.27 (m, 5H), 4.57 (s, 2H), 4.25 (t, *J* = 4.7 Hz, 2H), 3.67 (t, *J* = 4.7 Hz, 2H), 3.63 – 3.56 (m, 3H), 2.33 (t, *J* = 7.5 Hz, 2H), 1.61 (p, *J* = 7.5 Hz, 2H), 1.51 (p, *J* = 7.0 Hz, 2H), 1.44 – 1.35 (m, 4H), 1.35 – 1.21 (m, 16H), 0.89 (s, 9H), 0.88 (s, 9H), 0.05 (s, 6H), 0.03 (s, 6H). **^{13}C NMR** (101 MHz, $CDCl_3$) δ 174.0, 138.0, 128.6 (2C), 127.9, 127.9 (2C), 73.3, 72.5, 68.1, 63.5, 63.5, 37.3, 37.3, 34.4, 33.0, 30.0, 29.8, 29.6, 29.4, 29.3, 26.1 (3C), 26.1 (3C), 26.0, 25.5 (2C), 25.1, 18.5, 18.3, -4.2 (2C), -5.1 (2C). **HRMS (MALDI+)** $C_{37}H_{70}O_5Si_2$, *m/z* [M+Na^+] 673.4654, found 673.4669

2-(Benzyloxy)ethyl 10,16-dihydroxyhexadecanoate (**78**)

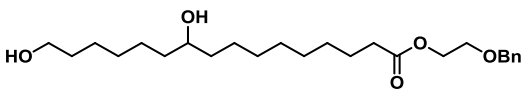

To a solution of **76** (353 mg, 0.50 mmol) in MeCN (58 ml) at 0 °C was added 20% aq. HF (2 ml). The resulting mixture was stirred at 0 °C for 4 h. TMSOMe (9.5 ml) was added, and the mixture was stirred for 30 minutes, poured into sat. aq. NH_4Cl (60 ml) and extracted with

CH_2Cl_2 (3 × 60 ml). The combined organic phases were dried with $MgSO_4$, filtered, concentrated and purified by flash chromatography (EtOAc/heptane 1:1), affording **78** as a white solid (202 mg, 88%); **m.p**. 64–65 °C **R_f** (EtOAc/heptane 1:1) = 0.11; **^{1}H NMR** (400 MHz, $CDCl_3$) δ 7.38 – 7.27 (m, 5H), 4.57 (s, 2H), 4.25 (t, *J* = 4.7 Hz, 2H), 3.67 (t, *J* = 4.7 Hz, 2H), 3.63 (t, *J* = 6.6 Hz, 2H), 3.61 – 3.54 (m, 1H), 2.33 (t, *J* = 7.5 Hz, 2H), 1.68 – 1.52 (m, 4H), 1.47 – 1.24 (m, 20H). **^{13}C NMR** (101 MHz, $CDCl_3$) δ 174.0, 138.0, 128.6 (2C), 127.9, 127.9 (2C), 73.3, 72.1, 68.1, 63.5, 63.1, 37.6, 37.5, 34.4, 32.8, 29.7, 29.6, 29.5, 29.3, 29.2, 25.9, 25.7 (2C), 25.0. **HRMS (MALDI+)** $C_{25}H_{42}O_5$, *m/z* [M+Na^+] 445.2924, found 445.2935.

2-Hydroxyethyl 10,16-dihydroxyhexadecanoate (**71**)

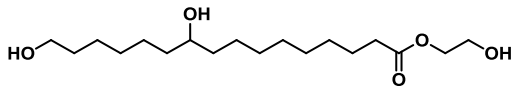

To a solution of **78** (147 mg, 0.35 mmol) in dry THF (15 ml) under an atmosphere of nitrogen was added 20% $Pd(OH)_2$/C (27 mg). A hydrogen atmosphere was installed by bubbling H_2 through the solution for 5 minutes. The reaction mixture was stirred under an atmosphere of hydrogen for 16 h, filtered through Celite, concentrated and recrystallized from EtOAc and heptane, affording **71** as a white solid (92 mg, 78%); **m.p**. 61.9–63.7 °C; **R_f** (EtOAc/heptane 7:3) = 0.07; **^{1}H NMR** (400 MHz, $CDCl_3$) δ 4.25 – 4.17 (m, 2H), 3.86 – 3.79 (m, 2H), 3.64 (t, *J* = 6.6 Hz, 2H), 3.63 – 3.53 (m, 1H), 2.35 (t, *J* = 7.5 Hz, 2H), 1.72 – 1.51 (m, 4H), 1.50 – 1.24 (m, 20H). **^{13}C NMR** (101 MHz, $CDCl_3$) δ 174.4, 72.1, 66.1, 63.1, 61.5, 37.6, 37.5, 34.3, 32.8, 29.7, 29.6, 29.5, 29.2, 29.2, 25.9, 25.7, 25.7, 25.0. **HRMS (MALDI+)** $C_{18}H_{36}O_5$, *m/z* [M+Na^+] 355.2455, found 355.2464.

2,3-bis(Benzyloxy)propyl 10,16-bis((tert-butyldimethylsilyl)oxy)hexadecanoate (**77**)

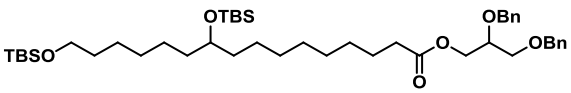

To a mixture of DMP (1.77 g, 4.2 mmol) in CH_2Cl_2 (20 ml) was added slowly a solution of **5** (1.51 g, 3.0 mmol) in CH_2Cl_2 (20 ml). The resulting mixture was stirred for 2 h and poured into a solution of $Na_2S_2O_3$ (25 g) in sat. aq. $NaHCO_3$ (100 ml). The mixture was stirred vigorously for 5 min and then extracted with Et_2O (100 ml). The organic phase was washed with sat. aq. $NaHCO_3$ (100 ml), dried with $MgSO_4$, concentrated and used in the subsequent reaction without further purification.

To a solution of the crude aldehyde (1.49 g) in *t*-BuOH (150 ml) was added 2-methyl-2-butene (4.2 g, 6.4 ml, 60 mmol) and an aqueous solution (37 ml) of NaH_2PO_4 (2.93 g, 24.4 mmol) and $NaClO_2$ (0.35 g, 3.9 mmol). After 15 h, a buffer aqueous solution of NaH_2PO_4 was added (0.66 M, 150 ml) and the mixture was extracted with CH_2Cl_2 (3 × 100 ml). The combined organic phases were washed with sat.

aq. NaCl (100 ml), dried with $MgSO_4$, filtered, concentrated, and used in the subsequent reaction without further purification

To a solution of the crude carboxylic acid (514 mg, 0.99 mmol) in CH_2Cl_2 (10 mL) was added (*S*)-(-)-2,3-dibenzyloxy-1-propanol (360 mg, 1.3 mmol), DMAP (206 mg, 1.7 mmol) and EDCI (285 mg, 1.5 mmol). The reaction was stirred for 16 hours, taken on silica, concentrated and purified by flash chromatography (EtOAc:heptane 1:19) affording **77** as a colorless oil (530 mg, 69%). $\mathbf{R_f}$ (EtOAc:heptane 1:19) = 0.13; **^{1}H NMR** (400 MHz, $CDCl_3$) δ 7.37 – 7.26 (m, 10H), 4.67 (s, 2H), 4.54 (s, 2H), 4.31 (dd, *J* = 11.6, 4.2 Hz, 1H), 4.17 (dd, *J* = 11.6, 5.6 Hz, 1H), 3.86–3.76 (m, 1H), 3.64 – 3.55 (m, 5H), 2.28 (t, *J* = 7.4 Hz, 2H), 1.66–1.53 (m, 2H), 1.53–1.45 (m, 2H), 1.45 – 1.36 (m, 4H), 1.36 – 1.21 (m, 16H), 0.90 (s, 9H), 0.88 (s, 9H), 0.05 (s, 6H), 0.03 (s, 6H). **^{13}C NMR** (101 MHz, $CDCl_3$) δ 173.8, 138.4, 138.2, 128.5 (2C), 128.5 (2C), 127.9 (2C), 127.8 (2C), 127.8 (2C), 76.0, 73.6, 72.5, 72.3, 69.8, 63.8, 63.5, 37.3, 37.3, 34.4, 33.0, 30.0, 29.8, 29.7, 29.4, 29.3, 26.2 (3C), 26.1 (3C), 26.0, 25.5 (2C), 25.1, 18.5, 18.3, -4.2 (2C), -5.1 (2C). **HRMS (MALDI+)** $C_{45}H_{78}O_6Si_2$, *m/z* [M+Na$^+$] 793.5229, found 793.5245

2,3-bis(Benzyloxy)propyl 10,16-dihydroxyhexadecanoate (**79**)

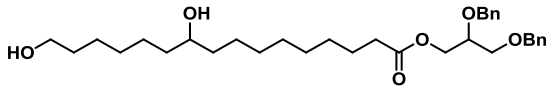

To a solution of **77** (341 mg, 0.44 mmol) in MeCN (48 ml) at 0 °C was added 20% aq. HF (2 ml). The resulting mixture was stirred at 0 °C for 4 h. TMSOMe (7.7 ml) was added, and the mixture was stirred for 30 minutes, poured into sat. aq. NH_4Cl (50 ml) and extracted with CH_2Cl_2 (3 × 50 ml). The combined organic phases were dried with $MgSO_4$, filtered, concentrated and purified by flash chromatography (EtOAc/heptane 1:1), affording **79** as a white solid (224 mg, 75%); **m.p**. 34–35 ^{o}C; $\mathbf{R_f}$ (EtOAc/heptane 1:1) = 0.15**; ^{1}H NMR** (400 MHz, $CDCl_3$) δ 7.39 – 7.25 (m, 10H), 4.67 (s, 2H), 4.54 (s, 2H), 4.30 (dd, *J* = 11.7, 4.2 Hz, 1H), 4.17 (dd, *J* = 11.7, 5.6 Hz, 1H), 3.81 (m, 1H), 3.64 (t, *J* = 6.6 Hz, 2H), 3.61 – 3.54 (m, 3H), 2.28 (t, *J* = 7.5 Hz, 2H), 1.64 – 1.51 (m, 4H), 1.49 – 1.24 (m, 20H). **^{13}C NMR** (101 MHz, $CDCl_3$) δ 173.8, 138.4, 138.2, 128.5 (2C), 128.5 (2C), 127.9 (2C), 127.8 (2C), 127.8 (2C), 76.0, 73.6, 72.3, 72.1, 69.8, 63.8, 63.1, 37.6, 37.5, 34.4, 32.8, 29.8, 29.6, 29.5, 29.3, 29.3, 25.9, 25.7 (2C), 25.0. **HRMS (MALDI+)** $C_{33}H_{50}O_6$, *m/z* [M+Na$^+$] 565.3500, found 565.3513.

2,3-dihydroxypropyl 10,16-dihydroxyhexadecanoate (**72**)

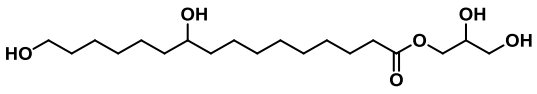

To a solution of **79** (166 mg, 0.30 mmol) in dry THF (15 ml) under an atmosphere of nitrogen was added 20% $Pd(OH)_2/C$ (24 mg). A hydrogen atmosphere was installed by bubbling H_2 through the solution for 5 minutes. The reaction mixture was stirred under an atmosphere of hydrogen for 16 h, filtered through Celite, concentrated and recrystallized from EtOAc and heptane, affording **72** as a white solid (89 mg, 80%); **m.p**. 64.9–66.0°C; $\mathbf{R_f}$ (CH_2Cl_2/MeOH 9:1) = 0.24; **^{1}H NMR** (400 MHz, $(CD_2)_4O$) δ 4.09–3.95 (m, 3 H), 3.75 – 3.64 (m, 2H), 3.51 – 3.36 (m, 5H), 3.33–3.24 (m, 2H), 2.28 (t, *J* = 7.2 Hz, 2H), 1.59 (p, *J* = 7.2 Hz, 2H), 1.52 – 1.41 (m, 4H), 1.43 – 1.23 (m, 18H). **^{13}C NMR** (101 MHz, $(CD_2)_4O$) δ 173.5, 71.4, 71.0, 66.4, 64.4, 62.6, 38.9 (2C), 34.7, 34.2, 30.8 (2C), 30.6, 30.3, 30.1, 27.1, 26.9, 26.8, 25.9. **HRMS (MALDI+)** $C_{19}H_{38}O_6$, *m/z* [$M+Na^+$] 385.2561, found 385.2571.

PPDL synthesis by REX

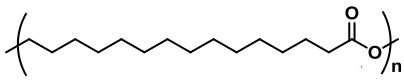

The reactive extruder was preheated at 150 °C and flashed with nitrogen for 15 minutes. PDL (13.5 g) and N435 (1.35 g), previously dried (40 °C and 20 torr overnight) were injected into the extruder at 90 °C and 30 rpm. Rotation was increased to 60 rpm. The polymerization continued until the instrument reached its maximum allowed force, 10000 N, and the extruder was stopped and the product collected. M_n = 106000, Đ = 1.55.

^{1}H NMR (500 MHz, $CDCl_3$) δ 4.05 (t, *J* = 6.8 Hz, 2H), 2.28 (t, *J* = 7.6 Hz, 2H), 1.65–1.58 (m, 4H), 1.27 (m, 20H).

Preparation of a 10% PPDL-PLLA blend by REX

$Ti(OBu)_4$ (2.6 mg) was added to a solution of PPDL (1.3 g, M_n = 106000, Đ = 1.55) in chloroform (18 ml) at 50 °C and the mixture was stirred vigorously for 5 minutes. Films of the mixture were prepared by solvent casting. Solvent was removed by gently blowing Ar for 15 minutes, followed by 18 h resting. Films were cut into small pieces (approximately 1 mm × 1mm) and were introduced into the reactive extruder together with PLLA (13 g, M_n = 113000, Đ = 1.45). The mixture was kept at 200 °C and 30 rpm for 5 minutes. Rotation speed was increased to 150 rpm and the reaction was maintained for 30 more minutes. PPDL-PLLA blend: M_n = 83000; Đ = 1.53.

^{1}H NMR (500 MHz, $CDCl_3$) δ 5.16 (q, *J* = 7.1 Hz, 1H), 4.05 (t, *J* = 6.7 Hz, 2H), 2.28 (t, *J* = 7.6 Hz, 2H), 1.58 (d, *J* = 7.1 Hz, 3H), 1.33–1.24 (m, 20H).

7. Bibliography

1. Waters, E. R. Molecular adaptation and the origin of land plants. *Mol. Phylogenet. Evol.* **29,** 456–463 (2003).

2. Rydz, J., Sikorska, W., Kyulavska, M. & Christova, D. Polyester-based (bio)degradable polymers as environmentally friendly materials for sustainable development. *Int. J. Mol. Sci.* **16,** 564–596 (2015).

3. Geyer, R., Jambeck, J. R. & Law, K. L. Production, use, and fate of all plastics ever made. *Sci. Adv.* **3,** (2017).

4. Vert, M. Aliphatic polyesters: Great degradable polymers that cannot do everything. *Biomacromolecules* **6,** 538–546 (2005).

5. Heredia-Guerrero, J. A. *et al.* Cutin from agro-waste as a raw material for the production of bioplastics. *J. Exp. Bot.* **68,** 5401–5410 (2017).

6. Franke, R. *et al.* Apoplastic polyesters in Arabidopsis surface tissues - A typical suberin and a particular cutin. *Phytochemistry* **66,** 2643–2658 (2005).

7. Kolattukudy, P. E. Biopolyester Membranes of Plants : Cutin and Suberin. **208,** 990–1000 (1980).

8. Leliaert, F., Verbruggen, H. & Zechman, F. W. Into the deep: New discoveries at the base of the green plant phylogeny. *BioEssays* **33,** 683–692 (2011).

9. Edwards, D. Cells and tissues in the vegetative sporophytes of early land plants. *New Phytol.* **125,** 225–247 (1993).

10. Isaacson, T. *et al.* Cutin deficiency in the tomato fruit cuticle consistently affects resistance to microbial infection and biomechanical properties, but not transpirational water loss. *Plant J.* **60,** 363–377 (2009).

11. Yeats, T. H. & Rose, J. K. C. The Formation and Function of Plant Cuticles. *Plant Physiol.* **163,** 5–20 (2013).

12. Sorensen, I., Domozych, D. & Willats, W. G. T. How Have Plant Cell Walls Evolved? *Plant Physiol.* **153,** 366–372 (2010).

13. P. Albersheim, A. Darvill, K. Roberts, R. S. *Plant Cells Walls*. (Garland Science, 2011).

14. Adapted from https://studyforce.com/index.php?action=gallery;sa=view;id=5421. (2016).

15. Heredia, A. & Dominguez, E. The plant cuticle: A complex lipid barrier between the plant and the environment. An overview. *NATO Sci. Peace Secur. Ser. A Chem. Biol.* **2,** 109–116 (2009).

16. Suh, M. C. *et al.* Cuticular lipid composition , surface structure , and gene expression in arabidopsis stem epidermis. **139,** 1649–1665 (2005).

17. Sabater, M. J. & Ródenas, T. H. A. in *Handbook of Biopolymer-Based Materials: From Blends and*

Composites to Gels and Complex Networks 37–86 (2013).

18. Luque, P. & Heredia, A. Glassy State in Plant Cuticles during Growth. *Zeitschrift fur Naturforsch. - Sect. C J. Biosci.* **49,** 273–275 (1994).

19. Dominguez, E., Heredia-Guerrero, J. A. & Heredia, A. The biophysical design of plant cuticles: An overview. *New Phytol.* **189,** 938–949 (2011).

20. Baker E. A. Martin J. T. Cutin from plant cuticles. *Nature* **199,** (1963).

21. Heredia-Guerrero, J. a. *et al.* Infrared and Raman spectroscopic features of plant cuticles: a review. *Front. Plant Sci.* **5,** 1–14 (2014).

22. Yeats, T. H. *et al.* The identification of cutin synthase: formation of the plant polyester cutin. *Nat. Chem. Biol.* **8,** 609–611 (2012).

23. Pollard, M., Beisson, F., Li, Y. & Ohlrogge, J. B. Building lipid barriers: biosynthesis of cutin and suberin. *Trends Plant Sci.* **13,** 236–246 (2008).

24. P. E. Kolattukudy. in *Advances in Biochemical Engineering/Biotechnology* (ed. Springer-Verlag) 1–49 (2001).

25. Heredia, A. Biophysical and biochemical characteristics of cutin, a plant barrier biopolymer. *Biochim. Biophys. Acta - Gen. Subj.* **1620,** 1–7 (2003).

26. Stark, R. E. & Tian, S. The Cutin Biopolymer Matrix. *Biol. Plant Cuticle* 126–144 (2006).

27. Fich, E. A., Segerson, N. A. & Rose, J. K. C. The Plant Polyester Cutin: Biosynthesis, Structure, and Biological Roles. *Annu. Rev. Plant Biol.* **67,** 207–233 (2016).

28. Gupta, N. S., Collinson, M. E., Briggs, D. E. G., Evershed, R. P. & Pancost, R. D. Reinvestigation of the occurrence of cutan in plants: implications for the leaf fossil record. *Paleobiology* **32,** 432–449 (2006).

29. Nawrath, C. Unraveling the complex network of cuticular structure and function. *Curr. Opin. Plant Biol.* **9,** 281–287 (2006).

30. Guzmán, P. *et al.* Localization of polysaccharides in isolated and intact cuticles of eucalypt, poplar and pear leaves by enzyme-gold labelling. *Plant Physiol. Biochem.* **76,** 1–6 (2014).

31. España, L. *et al.* Biomechanical properties of the tomato (Solanum lycopersicum) fruit cuticle during development are modulated by changes in the relative amounts of its components. *New Phytol.* **202,** 790–802 (2014).

32. Tsubaki, S., Sugimura, K., Teramoto, Y., Yonemori, K. & Azuma, J. ichi. Cuticular Membrane of Fuyu Persimmon Fruit Is Strengthened by Triterpenoid Nano-Fillers. *PLoS One* **8,** 1–13 (2013).

33. Martin, L. B. B. & Rose, J. K. C. There's more than one way to skin a fruit: Formation and functions of fruit cuticles. *J. Exp. Bot.* **65,** 4639–4651 (2014).

34. Kallio, H., Nieminen, R., Tuomasjukka, S. & Hakala, M. Cutin composition of five finnish berries. *J. Agric.*

Food Chem. **54,** 457–462 (2006).

35. Holloway, P. J. Cutins of Malus pumila fruits and leaves. *Phytochemistry* **12,** 2913–2920 (1973).

36. Bonaventure, G., Beisson, F., Ohlrogge, J. & Pollard, M. Analysis of the aliphatic monomer composition of polyesters associated with Arabidopsis epidermis: Occurrence of octadeca-cis-6, cis-9-diene-1,18-dioate as the major component. *Plant J.* **40,** 920–930 (2004).

37. Jeffree, C. E. The fine structure of the plant cuticle. *Annu. Plant Rev. Vol. 23 Biol. Plant Cuticle* 11–125 (2006).

38. Kosma, D. K. *et al.* Fruit cuticle lipid composition during development in tomato ripening mutants. *Physiol. Plant.* **139,** 107–117 (2010).

39. Ju, Z. & Bramlage, W. J. Developmental changes of cuticular constituents and their association with ethylene during fruit ripening in 'Delicious' apples. *Postharvest Biol. Technol.* **21,** 257–263 (2001).

40. Bauer, S., Schulte, E. & Thier, H. P. Composition of the surface wax from tomatoes : I. Identification of the components by GC/MS. *Eur. Food Res. Technol.* **219,** 223–228 (2004).

41. Goodwin, S. M. & Jenks, M. A. Plant Cuticle Function as a Barrier to Water Loss. *Plant Abiotic Stress* 14–36 (2007). doi:10.1002/9780470988503.ch2

42. Schreiber, L. & Riederer, M. Ecophysiology of cuticular transpiration: comparative investigation of cuticular water permeability of plant species from different habitats. *Oecologia* **107,** 426–432 (1996).

43. Knoche, M., Peschel, S., Hinz, M. & Bukovac, M. J. Studies on water transport through the sweet cherry fruit surface: II. Conductance of the cuticle in relation to fruit development. *Planta* **213,** 927–936 (2001).

44. Riederer, M. & Schreiber, L. Protecting against water loss: analysis of the barrier properties of plant cuticles. *J. Exp. Bot.* **52,** 2023–2032 (2001).

45. Becker, M., Kerstiens, G. & Schönherr, J. Water permeability of plant cuticles: permeance, diffusion and partition coefficients. *Trees* **1,** 54–60 (1986).

46. Lee, D. R. Vasculature of abscission zone of tomato fruit: implications for transport. *Can. J. Bot. Can. Bot.* **67,** 1898–1902 (1989).

47. Parsons, E. P. *et al.* Fruit cuticle lipid composition and fruit post-harvest water loss in an advanced backcross generation of pepper (Capsicum sp.). *Physiol. Plant.* **146,** 15–25 (2012).

48. Kosma, D. K. & Jenks, M. A. in *Advances in Molecular Breeding Toward Drought and Salt Tolerant Crops* (eds. Jenks, M. A., Hasegawa, P. M. & Jain, S. M.) 91–120 (Springer Netherlands, 2007).

49. Manandhar, J., Hartman, G. & Wang, T. Anthracnos development on pepper fruits inoculated with Colletotrichum gloeosporoides. *Plant Disease* **79,** 380–383 (1995).

50. Gomes, S., Bacelar, E., Martins-Lopes, P., Carvalho, T. & Guedes-Pinto, H. Infection Process of Olive Fruits by Colletotrichum acutatum and the Protective Role of the Cuticle and Epidermis. *J. Agric. Sci.* **4,** 101–110 (2012).

51. Vidhyasekaran, P. *Fungal pathogenesis in plants and crops: molecular biology and hoste defense mechanisms*. *Fungal pathogenesis in plants and crops: molecular biology and hoste defense mechanisms* (Elsevier Science, 1997).

52. Longhi, S. & Cambillau, C. Structure-activity of cutinase, a small lipolytic enzyme. *Biochim. Biophys. Acta - Mol. Cell Biol. Lipids* **1441,** 185–196 (1999).

53. Kauss, H., Fauth, M., Merten, A. & Jeblick, W. Cucumber Hypocotyls Respond to Cutin Monomers via Both an Inducible and a Constitutive H_2O_2-Generating System1. *Plant Physiol.* **120,** 1175–1182 (1999).

54. P. Schweizer, G. Felix, A. Buchala, C. Müller, J. P. M. Perception of free cutin monomers by plant cells. *Plant J.* **10,** 331–334 (1996).

55. Boller, T. & Felix, G. A Renaissance of Elicitors: Perception of Microbe-Associated Molecular Patterns and Danger Signals by Pattern-Recognition Receptors. *Annu. Rev. Plant Biol.* **60,** 379–406 (2009).

56. Bessire, M. *et al.* A permeable cuticle in Arabidopsis leads to a strong resistance to Botrytis cinerea. *EMBO J.* **26,** 2158–2168 (2007).

57. Krauss, P., Markstadter, C. & Riederer, M. Attenuation of UV radiation by plant cuticles from woody species. *Plant Cell Environ.* **20,** 1079–1085 (1997).

58. Mulroy, T. W. Spectral Properties of Heavily Glaucous and Non-Glaucous leaves of a Suculent Rosette-Plant. *Oecologia* **38,** 349–357 (1979).

59. Pfündel, E. E., Agati, G. & Cerovic, Z. G. Optical properties of plant surfaces. *Biol. Plant Cuticle* 216–249 (2006).

60. Holmes, M. G. & Keiller, D. R. Effects of pubescence and waxes on the reflectance of leaves in the ultraviolet and photosynthetic wavebands: A comparison of a range of species. *Plant, Cell Environ.* **25,** 85–93 (2002).

61. Matas, A. J., Cobb, E. D., Bartsch, J. A., Paolillo, D. J. & Niklas, K. J. Biomechanics and anatomy of Lycopersicon esculentum fruit peels and enzyme-treated samples. *Am. J. Bot.* **91,** 352–360 (2004).

62. Javelle, M., Vernoud, V., Rogowsky, P. M. & Ingram, G. C. Epidermis: The formation and functions of a fundamental plant tissue. *New Phytol.* **189,** 17–39 (2011).

63. Yephremov, A. Characterization of the FIDDLEHEAD Gene of Arabidopsis Reveals a Link between Adhesion Response and Cell Differentiation in the Epidermis. *Plant Cell Online* **11,** 2187–2202 (1999).

64. Wellesen, K. *et al.* Functional analysis of the LACERATA gene of Arabidopsis provides evidence for different roles of fatty acid ω-hydroxylation in development. *Proc. Natl. Acad. Sci. U. S. A.* **98,** 9694–9699 (2001).

65. Kurdyukov, S. The Epidermis-Specific Extracellular BODYGUARD Controls Cuticle Development and Morphogenesis in Arabidopsis. *Plant Cell Online* **18,** 321–339 (2006).

66. Smirnova, A., Leide, J. & Riederer, M. Deficiency in a Very-Long-Chain Fatty Acid -Ketoacyl-Coenzyme A Synthase of Tomato Impairs Microgametogenesis and Causes Floral Organ Fusion. *Plant Physiol.* **161,**

196–209 (2013).

67. Barthlott, W. & Neinhuis, C. Purity of the sacred lotus, or escape from contamination in biological surfaces. *Planta* **202,** 1–8 (1997).

68. Yeats, T. H. *et al.* The fruit cuticles of wild tomato species exhibit architectural and chemical diversity, providing a new model for studying the evolution of cuticle function. *Plant J.* **69,** 655–666 (2012).

69. Buda, G. J., Isaacson, T., Matas, A. J., Paolillo, D. J. & Rose, J. K. C. Three-dimensional imaging of plant cuticle architecture using confocal scanning laser microscopy. *Plant J.* **60,** 378–385 (2009).

70. Espelie, K. E., Davis, R. W. & Kolattukudy, P. E. Composition, ultrastructure and function of the cutin and suberin containing layers in the leaf, fruit peel, juice-sac and Inner Seed Coat of Grapefruit (Citrus paradisi). *Planta* **511,** 498–511 (1980).

71. Riederer, M. & Schönherr, J. Development of plant cuticles: fine structure and cutin composition of Clivia miniata Reg. leaves. *Planta* **174,** 127–138 (1988).

72. Velcheva, M. P., Espelie, K. E. & Ivanov, C. P. Aliphatic composition of cutin from inner seed coat of apple. *Phytochemistry* **20,** 2225–2227 (1981).

73. Matzke, K. & Riederer, M. The composition of the cutin of the caryopses and leaves of Triticum aestivum L. *Planta* **182,** 461–466 (1990).

74. Graça, J., Schreiber, L., Rodrigues, J. & Pereira, H. Glycerol and glyceryl esters of ω-hydroxyacids in cutins. *Phytochemistry* **61,** 205–215 (2002).

75. Goodwin, S. M., Edwards, C. J., Jenks, M. A. & Wood, K. V. Leaf cutin monomers, cuticular waxes, and blackspot resistance in rose. *HortScience* **42,** 1631–1635 (2007).

76. Petit, J. *et al.* Analyses of Tomato Fruit Brightness Mutants Uncover Both Cutin-Deficient and Cutin-Abundant Mutants and a New Hypomorphic Allele of GDSL Lipase. *Plant Physiol.* **164,** 888–906 (2013).

77. Järvinen, R., Kaimainen, M. & Kallio, H. Cutin composition of selected northern berries and seeds. *Food Chem.* **122,** 137–144 (2010).

78. Osman, S. F., Irwin, P., Fett, W. F., O'Connor, J. V. & Parris, N. Preparation, isolation, and characterization of cutin monomers and oligomers from tomato peels. *J. Agric. Food Chem.* **47,** 799–802 (1999).

79. Han, J. *et al.* The cytochrome P450 CYP86A22 is a fatty acyl-CoA ω-hydroxylase essential for estolide synthesis in the stigma of Petunia hybrida. *J. Biol. Chem.* **285,** 3986–3996 (2010).

80. Li-Beisson, Y. *et al.* Nanoridges that characterize the surface morphology of flowers require the synthesis of cutin polyester. *Proc. Natl. Acad. Sci.* **106,** 22008–22013 (2009).

81. Lü, S. *et al.* Arabidopsis CER8 encodes LONG-CHAIN ACYL-COA SYNTHETASE 1 (LACS1) that has overlapping functions with LACS2 in plant wax and cutin synthesis. *Plant J.* **59,** 553–564 (2009).

82. Beisson, F., Li-Beisson, Y. & Pollard, M. Solving the puzzles of cutin and suberin polymer biosynthesis.

Curr. Opin. Plant Biol. **15,** 329–337 (2012).

83. Xiao, F. *et al.* Arabidopsis CYP86A2 represses Pseudomonas syringae type III genes and is required for cuticle development. *EMBO J.* **23,** 2903–2913 (2004).

84. Molina, I., Ohlrogge, J. B. & Pollard, M. Deposition and localization of lipid polyester in developing seeds of Brassica napus and Arabidopsis thaliana. *Plant J.* **53,** 437–449 (2008).

85. Kurdyukov, S. *et al.* Genetic and biochemical evidence for involvement of HOTHEAD in the biosynthesis of long-chain α-,ω-dicarboxylic fatty acids and formation of extracellular matrix. *Planta* **224,** 315–329 (2006).

86. Yang, W. *et al.* A distinct type of glycerol-3-phosphate acyltransferase with sn-2 preference and phosphatase activity producing 2-monoacylglycerol. *Proc. Natl. Acad. Sci. U. S. A.* **107,** 12040–12045 (2010).

87. Yang, W. *et al.* A Land-Plant-Specific Glycerol-3-Phosphate Acyltransferase Family in Arabidopsis: Substrate Specificity, sn-2 Preference, and Evolution. *Plant Physiol.* **160,** 638–652 (2012).

88. Pighin, J. A., Zheng, H., Balakshin, L. J., Goodman, I. P., Western, T. L., Jetter, R., Kunst, L., Samuels, A. L. Plant Cuticular Lipid Export Requires an ABC Transporter. *Science* **306,** 702–704 (2004).

89. Bird, D. *et al.* Characterization of Arabidopsis ABCG11/WBC11, an ATP binding cassette (ABC) transporter that is required for cuticular lipid secretion. *Plant J.* **52,** 485–498 (2007).

90. McFarlane, H. E., Shin, J. J. H., Bird, D. A. & Samuels, A. L. *Arabidopsis* ABCG Transporters, Which Are Required for Export of Diverse Cuticular Lipids, Dimerize in Different Combinations. *Plant Cell* **22,** 3066–3075 (2010).

91. Bessire, M. *et al.* A Member of the PLEIOTROPIC DRUG RESISTANCE Family of ATP Binding Cassette Transporters Is Required for the Formation of a Functional Cuticle in *Arabidopsis*. *Plant Cell* **23,** 1958–1970 (2011).

92. Yeats, T. H. & Rose, J. K. The biochemistry and biology of extracellular plant lipid-transfer proteins (LTPs). *Protein Sci* **17,** 191–198 (2008).

93. Kim, H. *et al.* Characterization of glycosylphosphatidylinositol-anchored lipid transfer protein 2 (LTPG2) and overlapping function between LTPG/LTPG1 and LTPG2 in cuticular wax export or accumulation in arabidopsis thaliana. *Plant Cell Physiol.* **53,** 1391–1403 (2012).

94. Heredia, A., Heredia-Guerrero, J. a, Domínguez, E. & Benítez, J. J. Cutin synthesis: A slippery paradigm. *Biointerphases* **4,** P1–P3 (2009).

95. Heredia-Guerrero, J. A., Benítez, J. J. & Heredia, A. Self-assembled polyhydroxy fatty acids vesicles: A mechanism for plant cutin synthesis. *BioEssays* **30,** 273–277 (2008).

96. Domínguez, E., Heredia-Guerrero, J. A., Benítez, J. J. & Heredia, A. Self-assembly of supramolecular lipid nanoparticles in the formation of plant biopolyester cutin. *Mol. Biosyst.* **6,** 948–950 (2010).

97. Domínguez, E., Heredia-Guerrero, J. a. & Heredia, A. Plant cutin genesis: unanswered questions. *Trends*

Plant Sci. **20,** 1–8 (2015).

98. Girard, A.-L. *et al.* Tomato GDSL1 Is Required for Cutin Deposition in the Fruit Cuticle. *Plant Cell* **24,** 3119–3134 (2012).

99. Yeats, T. H. *et al.* Tomato Cutin Deficient 1 (CD1) and putative orthologs comprise an ancient family of cutin synthase-like (CUS) proteins that are conserved among land plants. *Plant J.* **77,** 667–675 (2014).

100. Jiang, Y., Morley, K. L., Schrag, J. D. & Kazlauskas, R. J. Different Active-Site Loop Orientation in Serine Hydrolases versus Acyltransferases. *ChemBioChem* **12,** 768–776 (2011).

101. Rautengarten, C. *et al.* Arabidopsis Deficient in Cutin Ferulate Encodes a Transferase Required for Feruloylation of -Hydroxy Fatty Acids in Cutin Polyester. *Plant Physiol.* **158,** 654–665 (2012).

102. Serra, O., Chatterjee, S., Huang, W. & Stark, R. E. Mini-review: What nuclear magnetic resonance can tell us about protective tissues. *Plant Sci.* **195,** 120–124 (2012).

103. Fried, J. R. *Polymer Science and Technology, second edition*. (2009).

104. Domínguez, E., Cuartero, J. & Heredia, A. An overview on plant cuticle biomechanics. *Plant Sci.* **181,** 77–84 (2011).

105. López-Casado, G., Matas, A. J., Domínguez, E., Cuartero, J. & Heredia, A. Biomechanics of isolated tomato (Solanum lycopersicum L.) fruit cuticles: The role of the cutin matrix and polysaccharides. *J. Exp. Bot.* **58,** 3875–3883 (2007).

106. Casado, C. G. & Heredia, A. Specific heat determination of plant barrier lipophilic components: Biological implications. *Biochim. Biophys. Acta - Biomembr.* **1511,** 291–296 (2001).

107. Boraston, A. B. The interaction of carbohydrate-binding modules with insoluble non-crystalline cellulose is enthalpically driven. *Biochem. J.* **385,** 479–484 (2005).

108. Matas, A. J., Cuartero, J. & Heredia, A. Phase transitions in the biopolyester cutin isolated from tomato fruit cuticles. *Thermochim. Acta* **409,** 165–168 (2004).

109. Graça, J. & Santos, S. Suberin: A biopolyester of plants' skin. *Macromol. Biosci.* **7,** 128–135 (2007).

110. Ranathunge, K., Schreiber, L. & Franke, R. Suberin research in the genomics era-New interest for an old polymer. *Plant Sci.* **180,** 339–413 (2011).

111. Pereira, H. Chemical composition and variability of cork from Quercus suber L. *Wood Sci. Technol.* **22,** 211–218 (1988).

112. Bernards, M. a. Demystifying suberin. *Can. J. Bot.* **80,** 227–240 (2002).

113. Hooke, R. *Micrographia*. (The Royal Society, 1665).

114. Steudle, E. & Peterson, C. A. How does water get through roots? *J. Exp. Bot.* **49,** 775–788 (1998).

115. Schreiber, L. Chemical composition of Casparian strips isolated from Clivia miniata Reg. roots: evidence

for lignin. *Planta* **49,** 596–601 (1996).

116. Enstone, D. E., Peterson, C. A. & Ma, F. Root endodermis and exodermis: Structure, function, and responses to the environment. *J. Plant Growth Regul.* **21,** 335–351 (2002).

117. Dean, B. B. & Kolattukudy, P. E. Synthesis of Suberin during Wound-healing in Jade Leaves, Tomato Fruit, and Bean Pods. *Plant Physiol.* **58,** 411–416 (1976).

118. Schreiber, L. Transport barriers made of cutin, suberin and associated waxes. *Trends Plant Sci.* **15,** 546–553 (2010).

119. Serra, O. *et al.* Silencing of StKCS6 in potato periderm leads to reduced chain lengths of suberin and wax compounds and increased peridermal transpiration. *J. Exp. Bot.* **60,** 697–707 (2009).

120. Franke, R. & Schreiber, L. Suberin - a biopolyester forming apoplastic plant interfaces. *Curr. Opin. Plant Biol.* **10,** 252–259 (2007).

121. Barrowclough, D. E., Peterson, C. a & Steudle, E. Radial hydraulic conductivity along developing onion roots. *J. Exp. Bot.* **51,** 547–557 (2000).

122. Soukup, A., Votrubová, O. & Čížková, H. Development of anatomical structure of roots of Phragmites australis. *New Phytol.* **153,** 277–287 (2002).

123. Clarkson, D. T., Robards, A. W., Stephens, J. E. & Stark, M. Suberin lamellae in the hypodermis of maize (Zea mays) roots; development and factors affecting the permeability of hypodermal layers. *Plant. Cell Environ.* **10,** 83–93 (1987).

124. Schreiber, L., Franke, R. & Hartmann, K. Effects of NO3 deficiency and NaCl stress on suberin deposition in rhizo- and hypodermal (RHCW) and endodermal cell walls (ECW) of castor bean (Ricinus communis L.) roots. *Plant Soil* **269,** 333–339 (2005).

125. Foster, K. J. & Miklavcic, S. J. A Comprehensive Biophysical Model of Ion and Water Transport in Plant Roots. I. Clarifying the Roles of Endodermal Barriers in the Salt Stress Response. *Front. Plant Sci.* **8,** 1–18 (2017).

126. Lulai, E. C. & Corsini, D. L. Differential deposition of suberin phenolic and aliphatic domains and their roles in resistance to infection during potato tuber (Solanum tuberosum L.) wound-healing. *Physiol. Mol. Plant Pathol.* **53,** 209–222 (1998).

127. North, G. B. & Nobel, P. S. Changes in root hydraulic conductivity for two tropical epiphytic cacti as soil moisture varies. *Am. J. Bot.* **81,** 46–53 (1994).

128. Visser, E. J. W., Colmer, T. D., Blom, C. W. P. M. & Voesenek, L. A. C. J. Changes in growth, porosity, and radial oxygen loss from adventitious roots of selected mono- and dicotyledonous wetland species with contrasting types of aerenchyma. *Plant, Cell Environ.* **23,** 1237–1245 (2000).

129. Garthwaite, A. J., Armstrong, W. & Colmer, T. D. Assessment of O_2 diffusivity across the barrier to radial O_2 loss in adventitious roots of Hordeum marinum. *New Phytol.* **179,** 405–416 (2008).

130. De Simone, O. *et al.* Apoplasmic barriers and oxygen transport properties of hypodermal cell walls in

roots from four amazonian tree species. *Plant Physiol.* **132,** 206–217 (2003).

131. Santos, S. & Graça, J. Stereochemistry of C18 monounsaturated cork suberin acids determined by spectroscopic techniques including 1H-NMR multiplet analysis of olefinic protons. *Phytochem. Anal.* **25,** 192–200 (2014).

132. Graça, J. & Pereira, H. Methanolysis of bark suberins: Analysis of glycerol and acid monomers. *Phytochem. Anal.* **11,** 45–51 (2000).

133. Graça, J. & Pereira, H. Cork Suberin: A Glyceryl Based Polyester. *Holzforschung* **51,** 225–234 (1997).

134. Moire, L. *et al.* Glycerol Is a Suberin Monomer. New Experimental Evidence for an Old Hypothesis1. *Plant Physiol.* **119,** 1137–1146 (1999).

135. Matzke, K. & Riederer, M. A comparative study into the chemical constitution of cutins and suberins from Picea abies (L.) Karst., Quercus robur L., and Fagus sylvatica L. *Planta* **185,** 233–245 (1991).

136. Holloway, P. J. The suberin composition of the cork layers from some ribes species. *Chem. Phys. Lipids* **9,** 171–179 (1972).

137. Schreiber, L., Hartmann, K., Skrabs, M. & Zeier, J. Apoplastic barriers in roots: chemical composition of endodermal and hypodermal cell walls. *J. Exp. Bot.* **50,** 1267–1280 (1999).

138. Holloway, P. J. Some variations in the composition of suberin from the cork layers of higher plants. *Phytochemistry* **22,** 495–502 (1983).

139. Composition, C. & Cell, E. Chemical Composition of Hypodermal and Endodermal Cell Walls and Xylem Vessels Isolated from Clivia miniata. 1223–1231 (2014).

140. Zeier, J. & Schreiber, L. Comparative investigation of primary and tertiary endodermal cell walls isolated from the roots of five monocotyledoneous species: Chemical composition in relation to fine structure. *Planta* **206,** 349–361 (1998).

141. Lu, F. & Ralph, J. Derivatization Followed by Reductive Cleavage (DFRC Method), a New Method for Lignin Analysis: Protocol for Analysis of DFRC Monomers. *J. Agric. Food Chem.* **45,** 2590–2592 (1997).

142. Franke, R. *et al.* The DAISY gene from Arabidopsis encodes a fatty acid elongase condensing enzyme involved in the biosynthesis of aliphatic suberin in roots and the chalaza-micropyle region of seeds. *Plant J.* **57,** 80–95 (2009).

143. Lee, S. B. *et al.* Two Arabidopsis 3-ketoacyl CoA synthase genes, KCS20 and KCS2/DAISY, are functionally redundant in cuticular wax and root suberin biosynthesis, but differentially controlled by osmotic stress. *Plant J.* **60,** 462–475 (2009).

144. Yang, W. L. & Bernards, M. A. Metabolite profiling of potato (Solanum tuberosum L.) tubers during wound-induced suberization. *Metabolomics* **3,** 147–159 (2007).

145. Li, Y. *et al.* Identification of acyltransferases required for cutin biosynthesis and production of cutin with suberin-like monomers. *Proc. Natl. Acad. Sci. U. S. A.* **104,** 18339–18344 (2007).

146. Höfer, R. *et al.* The Arabidopsis cytochrome P450 CYP86A1 encodes a fatty acid ω-hydroxylase involved in suberin monomer biosynthesis. *J. Exp. Bot.* **59,** 2347–2360 (2008).

147. Benveniste, I. *et al.* CYP86A1 from *Arabidopsis thaliana* encodes a cytochrome P450-dependent fatty acid omega-hydroxylase. *Biochem. Biophys. Res. Commun.* **243,** 688–93 (1998).

148. Serra, O. *et al.* CYP86A33-Targeted Gene Silencing in Potato Tuber Alters Suberin Composition, Distorts Suberin Lamellae, and Impairs the Periderm's Water Barrier Function. *Plant Physiol.* **149,** 1050–1060 (2008).

149. Millar, a a & Kunst, L. Very-long-chain fatty acid biosynthesis is controlled through the expression and specificity of the condensing enzyme. *Plant J.* **12,** 121–131 (1997).

150. Trenkamp, S., Martin, W. & Tietjen, K. Specific and differential inhibition of very-long-chain fatty acid elongases from Arabidopsis thaliana by different herbicides. *Proc. Natl. Acad. Sci. U. S. A.* **101,** 11903–8 (2004).

151. Paul, S. *et al.* Members of the arabidopsis FAE1-like 3-ketoacyl-CoA synthase gene family substitute for the elop proteins of Saccharomyces cerevisiae. *J. Biol. Chem.* **281,** 9018–9029 (2006).

152. Denic, V. & Weissman, J. S. A Molecular Caliper Mechanism for Determining Very Long-Chain Fatty Acid Length. *Cell* **130,** 663–677 (2007).

153. D'Auria, J. C. Acyltransferases in plants: a good time to be BAHD. *Curr. Opin. Plant Biol.* **9,** 331–340 (2006).

154. Gou, J.-Y., Yu, X.-H. & Liu, C.-J. A hydroxycinnamoyltransferase responsible for synthesizing suberin aromatics in Arabidopsis. *Proc. Natl. Acad. Sci.* **106,** 18855–18860 (2009).

155. Molina, I., Li-Beisson, Y., Beisson, F., Ohlrogge, J. B. & Pollard, M. Identification of an Arabidopsis feruloyl-coenzyme a transferase required for suberin synthesis. *Plant Physiol.* **151,** 1317–1328 (2009).

156. Serra, O. *et al.* A feruloyl transferase involved in the biosynthesis of suberin and suberin-associated wax is required for maturation and sealing properties of potato periderm. *Plant J.* **62,** 277–290 (2010).

157. Soler, M. *et al.* A Genomic Approach to Suberin Biosynthesis and Cork Differentiation. *Plant Physiol.* **144,** 419–431 (2007).

158. Panikashvili, D. *et al.* The arabidopsis DSO/ABCG11 transporter affects cutin metabolism in reproductive organs and suberin in roots. *Mol. Plant* **3,** 563–575 (2010).

159. Graça, J. Suberin: the biopolyester at the frontier of plants. *Front. Chem.* **3,** 1–11 (2015).

160. Graça, J. & Santos, S. Glycerol-derived ester oligomers from cork suberin. *Chem. Phys. Lipids* **144,** 96–107 (2006).

161. Graça, J. & Pereira, H. Suberin structure in potato periderm: Glycerol, long-chain monomers, and glyceryl and feruloyl dimers. *J. Agric. Food Chem.* **48,** 5476–5483 (2000).

162. Graça, J. & Pereira, H. Cork suberin: A glyceryl based polyester. *Holzforschung* **51,** 225–234 (1997).

163. Cordeiro, N., Belgacem, M. N., Silvestre, A. J. D., Pascoal Neto, C. & Gandini, A. Cork suberin as a new source of chemicals. 1. Isolation and chemical characterization of its composition. *Int. J. Biol. Macromol.* **22,** 71–80 (1998).

164. Cordeiro, N., Belgacem, N. M., Gandini, A. & Neto, C. P. Cork suberin as a new source of chemicals: 2. Crystallinity, thermal and rheological properties. *Bioresour. Technol.* **63,** 153–158 (1998).

165. Cordeiro, N., Aurenty, P., Belgacem, M. N., Gandini, A. & Pascoal Neto, C. Surface properties of suberin. *J. Colloid Interface Sci.* **187,** 498–508 (1997).

166. Fernandes, E. M., Aroso, I. M., Mano, J. F., Covas, J. A. & Reis, R. L. Functionalized cork-polymer composites (CPC) by reactive extrusion using suberin and lignin from cork as coupling agents. *Compos. Part B Eng.* **67,** 371–380 (2014).

167. Gandini, A., Pascoal Neto, C. & Silvestre, A. J. D. Suberin: A promising renewable resource for novel macromolecular materials. *Prog. Polym. Sci.* **31,** 878–892 (2006).

168. Greene, T. W. *Greene´s Protective Groups in Organic Synthesis*. (John Wiley & Sons, Inc, 2007).

169. Dess, D. B. & Martin, J. C. A useful 12-I-5 triacetoxyperiodinane (the Dess-Martin periodinane) for the selective oxidation of primary or secondary alcohols and a variety of related 12-I-5 species. *J. Am. Chem. Soc.* **113,** 7277–7287 (1991).

170. Travis, B. R., Sivakumar, M., Hollist, G. O. & Borhan, B. Facile oxidation of aldehydes to acids and esters with Oxone. *Org. Lett.* **5,** 1031–1034 (2003).

171. Lindgren, B. O. & Nilsson, T. Preparation of Carboxylic-Acids From Aldehydes (Including Hydroxylated Benzaldehydes) by Oxidation with Chlorite. *Acta Chemica Scandinavica* **27,** 888–890 (1973).

172. Pearlman, W. M. Noble metal hydroxides on carbon nonpyrophoric dry catalysts. *Tetrahedron Lett.* **8,** 1663–1664 (1967).

173. Engel, D. A. & Dudley, G. B. The Meyer–Schuster rearrangement for the synthesis of α,β-unsaturated carbonyl compounds. *Org. Biomol. Chem.* **7,** 4149 (2009).

174. April, V. Organic synthesis - applications in enzymatic studies , catalysis and surface modification Organic synthesis - applications in enzymatic studies , catalysis and surface modification. (2013).

175. Mori, K., Shikichi, Y., Shankar, S. & Yew, J. Y. Pheromone synthesis. Part 244: Synthesis of the racemate and enantiomers of (11Z,19Z)-CH503 (3-acetoxy-11,19-octacosadien-1-ol), a new sex pheromone of male Drosophila melanogaster to show its (S)-isomer and racemate as bioactive. *Tetrahedron* **66,** 7161–7168 (2010).

176. Egi, M., Kawai, T., Umemura, M. & Akai, S. Heteropolyacid-catalyzed direct deoxygenation of propargyl and allyl alcohols. *J. Org. Chem.* **77,** 7092–7097 (2012).

177. D. K. Barton, S. W. M. A new method for the Deoxygenation of Secondary Alcohols. *J. Chem. Soc. Perkin Trans.* 1574–1585 (1975).

178. Binkley, R. W. B. and E. R. in *Radical reactions of carbohydrates. Volume II: Radical Reactions in*

Carbohydrate Synthesis (2014).

179. K. Tomita, M. N. Studies on Organo Sulfur Compounds III. The Reaction of Sodium prim-α-Acetylenyl Xanthates and Alkyl Halide. *Chem. Pharm. Bull* **16,** 1907–1910 (1968).

180. Banert, K. New Functionalized Allenes: Synthesis Using Sigmatropic Rearrangements and Unusual Reactivity. *Liebigs Ann* 2005–2018 (1997).

181. Wakasugi, K., Iida, A., Misaki, T., Nishii, Y. & Tanabe, Y. Simple, Mild, and Practical Esterification, Thioesterification, and Amide Formation Utilizing p-Toluenesulfonyl Chloride and N-Methylimidazole. *Adv. Synth. Catal.* **345,** 1209–1214 (2003).

182. Ziegler, K., Holzkamp, E., Breil, H. & Martin, H. Das Mülheimer Normaldruck-Polyäthylen-Verfahren. *Angew. Chemie* **67,** 541–547 (1955).

183. Natta, G. *et al.* Crystalline High Polymers of A-Olefins. *J. Am. Chem. Soc.* **77,** 1708–1710 (1955).

184. Trnka, T. M. & Grubbs, R. H. The development of L2X2RU=CHR olefin metathesis catalysts: An organometallic success story. *Acc. Chem. Res.* **34,** 18–29 (2001).

185. Schrock, R. R. High oxidation state multiple metal-carbon bonds. *Chem. Rev.* **102,** 145–179 (2002).

186. Anastas, P. T. & Warner, J. C. *Green Chemistry: Theory and Practice*. (Oxford University Press, 1998).

187. Shoda, S., Uyama, H., Kadokawa, J., Kimura, S. & Kobayashi, S. Enzymes as Green Catalysts for Precision Macromolecular Synthesis. *Chem. Rev.* **116,** 2307–2413 (2016).

188. Horváth, I. T. & Anastas, P. T. Innovations and green chemistry. *Chem. Rev.* **107,** 2169–2173 (2007).

189. Kobayashi, S. Enzymatic polymerization: a new method of polymer synthesis. *J. Polym. Sci. Part A Polym. Chem.* **37,** 3041–3056 (1999).

190. Kobayashi, S. & Makino, A. Enzymatic polymer synthesis: an opportunity for green polymer chemistry. *Chem. Rev.* **109,** 5288–5353 (2009).

191. Fischer, E. Einfluss der Configuration auf die Wirkung der Enzyme. *Berichte der Dtsch. Chem. Gesellschaft* **27,** 2985–2993 (1894).

192. Schmid, R. D. & Verger, R. Lipases: Interfacial Enzymes with Attractive Applications. *Angew. Chemie Int. Ed.* **37,** 1608–1633 (1998).

193. Albertsson, A. C. & Srivastava, R. K. Recent developments in enzyme-catalyzed ring-opening polymerization. *Adv. Drug Deliv. Rev.* **60,** 1077–1093 (2008).

194. Uyama, H. & Kobayashi, S. Enzymatic Ring-Opening Polymerization of Lactones Catalyzed by Lipase. *Chem. Lett.* **22,** 1149–1150 (1993).

195. Knani, D., Gutman, A. L. & Kohn, D. H. Enzymatic polyesterification in organic media. Enzyme-catalyzed synthesis of linear polyesters. I. Condensation polymerization of linear hydroxyesters. II. Ring-opening polymerization of ϵ-caprolactone. *J. Polym. Sci. Part A Polym. Chem.* **31,** 1221–1232 (1993).

196. Uyama, H., Namekawa, S. & Kobayashi, S. Mechanistic Studies on the Lipase-Catalyzed Ring-Opening Polymerization of Lactones. *Polymer Journal* **29,** 299–301 (1997).

197. Matsumura, S. Enzymatic Synthesis of Polyesters via Ring-Opening Polymerization. **194,** 95–132 (2006).

198. Van Der Mee, L. *et al.* Investigation of lipase-catalyzed ring-opening polymerizations of lactones with various ring sizes: Kinetic evaluation. *Macromolecules* **39,** 5021–5027 (2006).

199. Veld, M. A. J., Fransson, L., Palmans, A. R. A., Meijer, E. W. & Hult, K. Lactone size dependent reactivity in Candida antarctica lipase B: A molecular dynamics and docking study. *ChemBioChem* **10,** 1330–1334 (2009).

200. Spinella, S. *et al.* Enzymatic reactive extrusion: moving towards continuous enzyme-catalysed polyester polymerisation and processing. *Green Chem.* **17,** 4146–4150 (2015).

201. Uyama, H. & Kobayashi, S. Enzymatic synthesis of polyesters via polycondensation. *Adv. Polym. Sci.* **194,** 133–158 (2006).

202. Binns, F., Harffey, P., Roberts, S. & Taylor, a. Studies of lipase-catalyzed polyesterification of an unactivated diacid/diol system. *J. Polym. Sci. Part A Polym. Chem.* **36,** 2069–2080 (1998).

203. Kumar, A., Kulshrestha, A. S., Gao, W. & Gross, R. A. Versatile route to polyol polyesters by lipase catalysis. *Macromolecules* **36,** 8219–8221 (2003).

204. Fu, H. *et al.* Physical characterization of sorbitol or glycerol containing aliphatic copolyesters synthesized by lipase-catalyzed polymerization. *Macromolecules* **36,** 9804–9808 (2003).

205. Kulshrestha, A. S., Gao, W. & Gross, R. A. Glycerol copolyesters: Control of branching and molecular weight using a lipase catalyst. *Macromolecules* **38,** 3193–3204 (2005).

206. Kulshrestha, A. S., Sahoo, B., Gao, W., Fu, H. & Gross, R. A. Lipase catalysis. A direct route to linear aliphatic copolyesters of bis(hydroxymethyl)butyric acid with pendant carboxylic acid groups. *Macromolecules* **38,** 3205–3213 (2005).

207. Kato, M., Toshima, K. & Matsumura, S. Direct enzymatic synthesis of a polyester with free pendant mercapto groups. *Biomacromolecules* **10,** 366–373 (2009).

208. Van Der Meulen, I. *et al.* Copolymers from unsaturated macrolactones: Toward the design of cross-linked biodegradable polyesters. *Biomacromolecules* **12,** 837–843 (2011).

209. Jiang, Z. Lipase-Catalyzed Synthesis of Poly (amine-co-esters) via Copolymerization of Diester with Amino-Substituted Diol. *Society* 1089–1093 (2010).

210. Kline, B. J., Beckman, E. J. & Russell, A. J. One-step biocatalytic synthesis of linear polyesters with pendant hydroxyl groups. *J. Am. Chem. Soc.* **120,** 9475–9480 (1998).

211. Olsson, A., Lindström, M. & Iversen, T. Lipase-catalyzed synthesis of an epoxy-functionalized polyester from the suberin monomer cis-9,10-epoxy-18-hydroxyoctadecanoic acid. *Biomacromolecules* **8,** 757–760 (2007).

212. Yao, K., Tang, C., Zhang, J. & Bunyard, C. Degradable and salt-responsive random copolymers. *Polym. Chem.* **4,** 528–535 (2013).

213. Riva, R. *et al.* Contribution of 'click chemistry' to the synthesis of antimicrobial aliphatic copolyester. *Polymer (Guildf).* **49,** 2023–2028 (2008).

214. Freichels, H., Alaimo, D., Auzély-Velty, R. & Jérôme, C. α-Acetal, ω-alkyne Poly(ethylene oxide) as a versatile building block for the synthesis of glycoconjugated graft-copolymers suited for targeted drug delivery. *Bioconjug. Chem.* **23,** 1740–1752 (2012).

215. Naolou, T., Busse, K. & Kressler, J. Synthesis of well-defined graft copolymers by combination of enzymatic polycondensation and 'Click' chemistry. *Biomacromolecules* **11,** 3660–3667 (2010).

216. Suksiriworapong, J., Sripha, K. & Junyaprasert, V. B. Synthesis and characterization of bioactive molecules grafted on poly(e{open}-caprolactone) by ' click' chemistry. *Polymer (Guildf).* **51,** 2286–2295 (2010).

217. Wang, J. *et al.* Robust antimicrobial compounds and polymers derived from natural resin acids. *Chem. Commun.* **48,** 916–918 (2012).

218. Pham, Q. P., Sharma, U. & Mikos, A. G. Electrospinning of Polymeric Nanofibers for Tissue Engineering Applications: A Review. *Tissue Eng.* **12,** 1197–1211 (2006).

219. Ziemba, A. M. & Gilbert, R. J. Biomaterials for local, controlled drug delivery to the injured spinal cord. *Front. Pharmacol.* **8,** 1–20 (2017).

220. A. Hurtado, J. M. Cregg, H. B. Wang, D. F. Wendell, M. Oudega, R. J. Gilbert, J. M. Robust CNS regeneration after complete spinal chord transection using aligned poly-L-lactic acid microfibers. **32,** 6068–6079 (2011).

221. Xie, J., Macewan, M. R., Li, X., Sakiyama-elbert, S. E. & Xia, Y. Neurite Outgrowth on Nanofiber Scaffolds with Different Orders,.pdf. **3,** 1151–1159 (2009).

222. Fozdar, D. Y., Lee, J. Y., E Schmidt, C. & Chen, S. Selective axonal growth of embryonic hippocampal neurons according to topographic features of various sizes and shapes. *Int. J. Nanomedicine* **6,** 45–57 (2011).

223. Leipzig, N. D. & Shoichet, M. S. The effect of substrate stiffness on adult neural stem cell behavior. *Biomaterials* **30,** 6867–6878 (2009).

224. Georges, P. C., Miller, W. J., Meaney, D. F., Sawyer, E. S. & Janmey, P. A. Matrices with compliance comparable to that of brain tissue select neuronal over glial growth in mixed cortical cultures. *Biophys. J.* **90,** 3012–3018 (2006).

225. Spinella, S. *et al.* Polylactide/poly(ω-hydroxytetradecanoic acid) reactive blending: A green renewable approach to improving polylactide properties. *Biomacromolecules* **16,** 1818–1826 (2015).

226. Hu, J., Gao, W., Kulshrestha, A. & Gross, R. A. 'Sweet Polyesters': Lipase-Catalyzed Condensation−Polymerizations of Alditols. *Macromolecules* **39,** 6789–6792 (2006).

227. W. C. Still, M. Khan, A. M. Rapid Chromatographic Technique for Preparative Separations with Moderate Resolution. *J. Org. Chem* **43,** 2923–2925 (1978).

228. Pedersen, D. & Rosenbohm, C. Dry Column Vacuum Chromatography. *Synthesis (Stuttg).* **2001,** 2431–2434 (2004).

229. Whitten, K. M., Makriyannis, A. & Vadivel, S. K. Application of chemoenzymatic hydrolysis in the synthesis of 2-monoacylglycerols. *Tetrahedron* **68,** 5422–5428 (2012).